

BRNO UNIVERSITY OF TECHNOLOGY
FACULTY OF CIVIL ENGINEERING



Institute of Structural Mechanics

Stochastic fracture mechanics and size effect

by

Miroslav Vořechovský

A dissertation
submitted in partial fulfillment
of the requirements for the degree
Doctor of Philosophy in *Theory of Structures*

Supervisor: Prof. Ing. Drahomír Novák, DrSc.

July 2004

Extensive copying of this thesis, including all its input files and macro package (electronic version), is allowable for scholarly purposes, consistent with “fair use” and with accordance to Copyright Laws. Requests for copying or reproduction of this thesis may be sent via the author’s web site at

<http://www.fce.vutbr.cz/STM/vorechovsky.m>

or via the author’s email address

vorechovsky.m@fce.vutbr.cz

ISBN 80-214-2695-0

KEYWORDS: Probabilistic-based assessment, failure probability, reliability, reliability software, Latin Hypercube Sampling, sensitivity analysis, quasibrittle materials, concrete, multi-filament yarn, fiber bundle models, delayed activation, nonlinear fracture mechanics, cohesive crack, size effect, theory of extreme values, Weibull theory, random field simulation, stochastic finite element method

© Copyright by Miroslav Vořechovský
July 2004
All rights reserved

Typeset by L^AT_EX 2_ε

Approvals

This dissertation is submitted in partial fulfillment of the requirements for the degree of
Doctor of Philosophy
36-06-9 – Theory of Structures

Ing. Miroslav Vořechovský

This is to certify that I have examined this copy of a doctoral dissertation by

Miroslav Vořechovský

and have found that it is complete and satisfactory in all respects,
and that any and all revisions required by the final
examining committee have been made.

Approved:

Prof. Ing. Drahomír Novák, DrSc.
(Supervisor)

Prof. Ing. Jindřich Melcher, DrSc.
(Chair)

Prof. Ing. Zdeněk Bittnar, DrSc.
(Reading committee)

Ing. Jiří Náprstek, DrSc.
(Reading committee)

Ing. Vladimír Červenka, Ph.D.
(Reading committee)

Accepted by the Brno University of Technology, Faculty of Civil Engineering:

Prof. Ing. RNDr. Petr Štěpánek, CSc.
(Dean)

July 2004

Abstract

Quasibrittle materials such as concrete, fiber composites, rocks, tough ceramics, sea ice, dry snow slabs, wood and some biomaterials, fail at different nominal strengths with respect to their structural size. Smaller structures fail in a ductile manner which usually involves distributed cracking with strain-softening. The stress redistribution that is caused by fracture and distributed cracking engenders an energetic size effect, i.e., decrease of the nominal strength of structures with increasing structure size. A structure far larger than the fracture process zone (FPZ) fails in an almost perfectly brittle manner and, if the failure occurs right at the crack initiation, the failure load is governed by the statistically weakest point in the structure, which gives a basis to the statistical size effect.

Strategies for capturing the statistical size effect using the stochastic finite element method in the sense of extreme value statistics are presented. They combine feasible types of Monte Carlo simulation based on nonlinear fracture mechanics. This is exemplified by various cases of size effect in plain concrete structures. A special attention is devoted to size effects of concrete reinforcement in the form of yarns made of glass fibers (a new composite material called textile reinforced concrete).

The interdisciplinary field of stochastic fracture mechanics is accessed by utilizing new advanced software developments which progress beyond the traditional approach and attempt to treat in a combined manner the reliability theory with fracture nonlinearity. This approach automatically yields not only the statistical part of size effect at crack initiation, but also the energetic part of size effect. Examples of statistical simulations of size effect with nonlinear fracture mechanics software ATENA combined with probabilistic software FREET are presented. Capturing the statistical size effect is made possible by (1) incorporating the analytical results of extreme value statistics into the stochastic finite element calculations, (2) implementing an efficient random field generation, and (3) exploiting small-sample Monte-Carlo type simulation called Latin Hypercube Sampling.

The necessary steps towards the results were the development of mathematical tools and algorithms (with their theoretical and numerical validation) and finally software development (FREET). Next, the applications of the methods and software follow aiming at study of size effects in various materials and loading conditions.

Acknowledgments

This thesis features latest results of my work but partially also work of my collaborators is reflected. I would like to acknowledge and to extend my sincere appreciation to many individuals with whom I had the pleasure to collaborate in the course of my research work on Stochastic Fracture Mechanics.

First and foremost, I wish to express my deepest gratitude to Professor Drahomír Novák my supervisor, for his continuous guidance, encouragement and support during my study and research in pursuing my PhD degree at Brno University of Technology. I feel that I am privileged to work with him since 1997. I learned a great deal through participation in collaborative research with his research group and I became motivated in methodological research through his sharp insight.

The whole group at the Institute of Structural Mechanics with focus on probabilistic aspect of computational mechanics established by Prof. Břetislav Teplý has formed good working environment for professional growth of all members. I want express my appreciation to Dr. Zbyněk Keršner for many valuable discussions during my study.

This work also consists of results obtained during my long-term stays at RWTH Aachen (Aachen University of Technology, Germany) and Northwestern University in Evanston, USA. Dr. Rostislav Chudoba, my colleague and friend from Aachen University shares my passion for probabilistic mechanics. The fruitful cooperation with him was a real pleasure. Professor Zdeněk P. Bažant, my advisor at Northwestern University, has been a source of inspiration for me in so many ways. His persistence in solving difficult problems, his insight and imagination to come up with some of the most unique ideas, his trust in science and his extremely competitive spirit never ceased to amaze me.

I am also indebted in many other people for cooperation with me resulting in professional publications and who however, are not mentioned here by name.

Last but not least, my thanks are due to my girlfriend Dita Matesová who shares the everyday life with me for several years and is a source of support and inspiration for me.

This work would not be possible without a financial support of grants, scholarships and projects listed bellow. The financial support by grants of the Grant Agency of Czech Republic (GAČR) No. 103/02/1030, 103/00/0603 and by project No. CEZ:J22/98:261100007 of the Ministry of Education of Czech Republic are greatly appreciated. The work was partially supported by the German Science Foundation (DFG) in the framework of the Collaborative Research Center 532. The support during the stay at Aachen University of Technology, Germany is gratefully acknowledged. The work was partially supported by the U.S. National Science Foundation under grant CMS-9713944 to Northwestern University. The support during the stay at Northwestern University, USA is gratefully acknowledged.

Fulbright Foundation is thanked for supporting my research at Northwestern University, USA. The foundation *Nadace Josefa, Marie a Zdeňky Hlávkových* (Hlavka's foundation) is thanked for a financial support through Doctoral scholarship during the difficult first year of my doctoral study. The foundation is also thanked for financial support for my participation at the International Congress on Challenges of Concrete Construction in Dundee, Scotland. The Massachusetts Institute of Technology in Cambridge, USA is acknowledged for awarding me a travel fellowships for the Second M.I.T. conference on Computational Fluid and Solid Mechanics. The Electricité de France (EDF) company is thanked for awarding me the Stipend of Excellence for the fourth FraMCoS conference on fracture mechanics of Concrete and Concrete Structures in Paris. The *Cerra* association (Civil Engineering Risk and Reliability Association) is acknowledged for awarding me the conference fellowship at the ICASP International Conference on Applications of Statistics and Probability in Civil Engineering held in San Francisco, USA.

Contents

Abstract	iv
Acknowledgements	vi
Contents	viii
List of figures	xii
1 Introduction	1
1.1 Aims and general concept of the thesis	1
1.2 Thesis structure	3
I SMALL-SAMPLE SIMULATION METHODS AND APPROACHES TO STOCHASTIC MECHANICS	7
2 Probabilistic assessment of computationally intensive problems	9
2.1 Reliability theory	9
2.1.1 Fundamental concept of structural reliability	10
2.1.2 Response and limit state function	10
2.1.3 Reliability index	11
2.1.4 Failure probability	11
2.2 Stochastic analysis software	13
2.3 LHS: the small-sample stochastic technique	14
2.4 LHS: sensitivity analysis (nonparametric rank-order)	15
2.5 LHS: reliability estimation based on curve fitting	16
3 Random variables: sampling and statistical correlation	19
3.1 Introduction	19
3.2 LHS: Sampling and statistical correlation	19
3.3 Stochastic optimization method Simulated Annealing	26
3.4 Numerical examples	28
3.4.1 Correlated properties of concrete	28
3.4.2 Non-positive definite prescribed correlation matrix?	29
3.5 Concluding remarks	30
4 Simulation of random fields and error assessment	33
4.1 Introduction	33
4.2 Orthogonal transformation of covariance matrix	34
4.3 Latin Hypercube Sampling utilization	35
4.4 Error assessment of random field simulation	36
4.4.1 Reduction of spurious correlation	37
4.4.2 Classification of sampling schemes	39
4.5 Conclusions	41

II STOCHASTIC MODELING OF MULTI-FILAMENT YARNS FOR TEXTILE REINFORCED CONCRETE 43

5	Micromechanical model and random properties within the yarn cross section	45
5.1	Introduction	45
5.2	Effects included in the tensile test	46
5.3	Deterministic model	49
5.4	Parametric studies	51
5.4.1	Different filament lengths	51
5.4.2	Differences in filament diameters	52
5.4.3	Delayed activation of filaments	54
5.5	Correspondence between the delayed activation and waviness	54
5.6	Identification of the parameter distributions	57
5.7	Conclusions	59

6	Random properties over the length and size effect	61
6.1	Introduction	61
6.2	Random strength along the filament	62
6.2.1	Spatial strength randomization using IID	63
6.2.2	Spatial strength randomization using stationary random process	64
6.3	Random strength along filaments within the bundle	66
6.3.1	Comparison with Daniels's numerical recursion	66
6.3.2	Comparison with Daniels's and Smith's asymptotic result	68
6.3.3	Size effect of bundles for increasing number of filaments n_f	69
6.4	Random stiffness along the bundle	70
6.4.1	Asymptotic behavior with random stiffness	70
6.4.2	Comparison between the effect of random strength and stiffness	72
6.5	Application to the experiment	75
6.5.1	Testing of single filament	75
6.5.2	Tensile test on a bundle	75
6.5.3	Systematic identification of the distribution parameters	78
6.6	Conclusions	78

III STOCHASTIC MODELING OF QUASIBRITTLE MATERIALS 81

7	Size effect on modulus of rupture of concrete structures: state of the art	83
7.1	Introduction	83
7.2	Nonlinear fracture mechanics and deterministic size effect of concrete structures	84
7.3	Stochastic nonlinear fracture mechanics and complex size effect	85
7.3.1	Statistical size effect and Nonlocal Weibull theory	85
8	Connections of fiber bundles models and size effect of concrete structures	89
8.1	General size effect theory	89
8.1.1	Energetic size effect	89
8.1.2	Probabilistic size effect	89
8.2	Asymptotics of size effect	90
8.2.1	Small-size asymptotes	90
8.2.2	Large-size asymptotes	91
8.3	Transition between small and large size asymptotes	92
8.3.1	Chain of bundles model	92
8.3.2	Nonlinear stochastic finite element method	93
8.4	Concluding remarks	93

9	Computational modeling of statistical size effect: extreme value approach	95
9.1	Introduction	95
9.2	Weakest link concept and theory of extreme values	96
9.2.1	Limiting forms of distribution of minimum	99
9.3	Implications for finite element method	100
9.4	Numerical example: size effect of span in four-point bending tests	101
9.4.1	Experiment and attempt at deterministic simulation	101
9.4.2	Statistical size effect	102
9.5	Conclusions	104
9.6	Further discussion	105
10	Combined deterministic-energetic and statistical size effect in quasibrittle failure	107
10.1	Introduction	107
10.2	Deterministic-energetic size effect formula	108
10.3	Energetic-statistical size effect formula	109
10.4	Superimposition of FEM deterministic-energetic and statistical size effects	112
10.5	Numerical example	115
10.5.1	Tool of deterministic NLFEM modeling	115
10.5.2	Superimposition modeling	116
10.5.3	Statistical size effect and formula verification	118
10.6	Concluding remarks	119
11	Overall conclusions and recommendations for future research	121
A	Software FREET	125
A.1	Introduction	125
A.2	Main program tree	126
A.3	Stochastic model	126
A.3.1	Random variables	126
A.3.2	Statistical correlation	128
A.4	Response or limit state function definition	129
A.4.1	FREET M-version	129
A.4.2	FREET A-version	129
A.5	Sampling	130
A.5.1	General data	130
A.5.2	Check of the samples	131
A.5.3	Model analysis	131
A.6	Simulation results assessment	133
A.6.1	Histograms	133
A.6.2	Limit state function definition	134
A.6.3	Sensitivity analysis	134
A.6.4	Reliability analysis	135
A.7	Software ATENA	136
A.8	Conclusions	138
A.9	Available probability distributions in FREET	139
	Bibliography	144
	Vita	158
	Author's papers	160

List of Figures

1.1	Illustration of size effect on nominal strength and the range of structural sizes of interest in the thesis	2
2.1	Normal distribution of safety margin as a subtraction of two normal random variables and the meaning of the safety index β	10
2.2	FORM and SORM methods for reliability estimation	12
2.3	Multiple design point	12
2.4	Geometrical interpretation of failure probability p_f (Eqs. 2.6 and 2.8) in case of two-variate joint probability density $f_{\mathbf{X}}(x_1, x_2)$	13
2.5	Parallel co-ordinates representations.	17
2.6	a) Best CDF obtained as a fit to computed histogram of results; b) Examples of fits (using estimated statistical moments for analytical PDF) and the uncertainty in estimation in the failure probability p_f	17
3.1	Samples as the probabilistic means of intervals	21
3.2	Top: Example of statistically independent samples representing two-dimensional PDF; Bottom: Example of strong positive statistical dependence between samples from random vector	24
3.3	Top: Another example of statistically independent samples; Bottom: Example of negative statistical dependence between samples representing random vector	25
3.4	Energy landscape - problem of local and global minimum	27
3.5	Sketch of Simulated Annealing algorithm implementation in C	28
3.6	The norm E (error) vs. number of random changes; see Fig. A.9 for the image as implemented in FREET software	29
4.1	Random field realizations for correlation length a) $d = 0.1$ m; and b) $d = 1$ m. Means and \pm standard deviations are plotted.	37
4.2	Reduction of number of random variables based on normalized variability.	38
4.3	Scatterband of autocorrelation function $C_{aa}(\xi)$ for $N_{Sim} = 32$: a) LHS-mean-SC; b) LHS-mean-SCD; and $N_{Sim} = 64$: c) LHS-mean-SC; d) LHS-mean-SCD	38
4.4	Statistics of mean and standard deviation ($d = 1$ m): a) mean of mean; b) standard deviation of mean; c) mean of standard deviation; d) standard deviation of standard deviation	41
4.5	Shape similarity of corresponding realizations of random fields I and II ($d_x = d_y = 10m$). Cross-correlation coefficient $\rho_{I,II}(0) = 0.65$	42
4.6	Illustration of cross-correlation for 2-dimensional random fields I and II	42
4.7	Standard gaussian random field I before translation ($d_x = d_y = 10m$)	42
5.1	Effective length scales	47
5.2	Tensile tests on AR-glass rovings with varied length, raw data	48
5.3	Tensile tests on AR-glass rovings with varied length, corrected data by subtracting the deformation of the epoxy clamping	48
5.4	Elementary characteristics of filaments and their ordering in the yarn	48

5.5	Superposition of the filament response with varying filament strength, stiffness, length and activation strain.	49
5.6	Effective filament stiffness K_i and minimum strength R_i	50
5.7	a) Overloading of 2 elements in the neighborhood of failed element under LLS rule. b) Comparison of roving load-deformation diagrams without and with significant shear interaction between filaments. c) Stiffness activation through shear for delayed activation.	51
5.8	Yarn penetrated by the epoxy resin	52
5.9	The influence of linearly distributed addition of 2 mm to the nominal length a) . . . f)	53
5.10	The influence of randomness of diameters between the filaments	53
5.11	Comparison of three constant densities of delayed activation of filaments	55
5.12	Distribution of relative extra length for changing nominal length	55
5.13	Wave patterns with corresponding activation profiles ($i = 0 \dots (n - 1)$)	56
5.14	Activation density function reflecting the tensile tests	57
5.15	Waves in the tested yarn	57
5.16	Delayed activation densities and load deflection curves (experiment and simulation). Left: zoom into the beginning of L- ε diagrams. Right: whole L- ε diagrams.	58
5.17	Size effect observed in experiment and reverse size effect induced by delayed activation	58
5.18	Correspondence between the statistical size effect $\omega(l)$, influence of delayed activation $\delta(l)$ and measured size effect $\epsilon(l)$	59
6.1	Weibull scaling	63
6.2	Top: Gradual change of the filament strength distribution from Weibull to asymptotically Gaussian for bundles with growing number of filaments n_f (in the circle). Exact results of Daniels's recursion (6.13) for small n_f is compared to numerical results by Monte Carlo simulation using the SFR algorithm Bottom: Samples of the whole L-D diagrams obtained by the SFR algorithm for selected numbers of filaments n_f in the yarn. Yarns are sketched and the mean value of strength \pm standard deviation is marked by a circle with errorbars.	67
6.3	Comparison of simulated data, Daniels's and Smith's normal approximation for a yarn with $n_f = 1600$ filaments with independent identically distributed random strength in linear plot and normal probability paper.	69
6.4	Top: Mean size effect curves (MSEC) for increasing number of filaments n_f in a bundle for filament strength described by Weibull random process. Curves nearly overlap for n_f higher than 160. Bottom: Effective Weibull modulus m computed using Eq. (6.4) for different yarn lengths and numbers of filaments n_f	70
6.5	3D representation of bundle efficiency depending on the number of filaments and yarn length for the case of random strength described by random processes. The combined size effect of both n_f and l is displayed as a surface plot with coordinates $x = n_f$ (converge to constant value by Daniels), $y = l$ (logarithmic coordinate, function $f(l)$) and z = mean strength.	71
6.6	Comparison of the three random fields with different correlation lengths and load deflection diagrams of 16 filament yarn with fields applied to f^t and E	73
6.7	Top: Strength reduction function $r_E(l)$ due to random E -modulus in addition to random strength. Bottom: Size effect curves due to the scatter in strength and scatter in both stiffness and strength	74
6.8	Comparison of numerical simulations with experiments (red). Left: Simulations without delayed activation, randomized stiffness and strength. Diagram computed with DA plotted with dashed line. Right: Simulations with included delayed activation, randomized stiffness and strength. Diagrams computed with mean values plotted with dashed line.	76
6.9	Size effect curves obtained numerically for the randomized f^t , ε_0 , f_t together with E and all three parameters simultaneously.	77
7.1	Inelastic strain, boundary layer of cracking l_f	83
7.2	Calculated shapes of fracture process zone and load-deflection diagrams (based on data of Sabnis and Mirza (1979)) a) small beam (span 0.0381 m), b) large beam (span 4.0 m).	85

8.1	Failure probability density and cumulative distribution function for three different elemental distributions: Gaussian, Weibull and rectangular	90
8.2	Failure probability density and cumulative distribution function for three different elemental distributions: Gaussian, Weibull and rectangular	91
9.1	Failure probability density and cumulative distribution function for three different elemental distributions: Gaussian, Weibull and rectangular	97
9.2	a) Dependence of random strength on size N for elemental distributions; b) a sketch of “1D” structure failing at failure of a weakest link, the elements share a common strength distribution (IID); c) a sketch of “2D” structure (we assume that the structure fails at first failure of a weakest element; d) Comparison of the three elemental distributions used for a) with unit mean and standard deviation of 0.1	98
9.3	a) Statically determinate structure that behaves as a chain; b) Stability postulate of extreme values (chain and sub-chains)	98
9.4	a) Koide’s beams of bending span 200, 400 and 600 mm, series C ; b) Deterministic cracks for the corresponding beam sizes	102
9.5	Macroelements and examples of random crack initiation for the first size; left: random tensile strength only, right: random and correlated tensile strength and fracture energy . .	103
9.6	a) Comparison of means of Koide’s data and ATENA deterministic and statistical simulations; b) Random load deflection diagrams for one size of Koide’s beams (note the curvatures indicating appreciable stress redistributions before peak)	104
9.7	Simple 1-D Weibull model (chain) in the bottom layer of 4PB beam. Left: Random variables – macroelements. Right: a statistical “chain” model driving the strength of a whole structure	105
9.8	Illustration of stress redistribution captured by parallel chains – more sophisticated statistical model for small sizes (the bundle of chains model)	105
10.1	Best fit of extended deterministic formula. a) for a wide range of Malpasset dam sizes; b) example of two erroneous fits with simplified deterministic formula to (1) whole range of data, (2) data without the smallest size.	110
10.2	Parametric study of the proposed law. a) influence of Weibull modulus (scatter); b) interplay of the scaling lengths	112
10.3	Illustration of superimposition steps. a) Steps 1-4 resulting in deterministic formulae fit; b) Step 5 - determination of parameter L_0 ; c) Final formula and strength prediction for the real size D_t	113
10.4	Malpasset dam. Left top and bottom: Photos of the dam before and after failure. Figures from internet source http://www.aude.pref.gouv.fr/ddrm/risque-barr/bar2.html ; Right: Sketch of a dam failure redrawn from Levy and Salvadori (1992) . Note that cracks must have been much more localized	116
10.5	Deterministic NLFEM calculation for different virtual sizes of the dam: a) nominal strength vs. normalized displacement; b) Crack patterns	117
10.6	Comparison of three stochastic alternatives and deterministic results. Left: Mean value \pm standard deviation as predicted by stochastic simulations and comparison with the prediction by the new law (not fitted!). Right: comparison of the whole distribution predicted by the model and stochastic simulations (64 simulations). Curves are not fitted (m known)	120
A.1	Main program tree	126
A.2	Probability distribution window – PDF	127
A.3	Combo box for selection of PDF	128
A.4	User-defined distribution (Raw data)	128
A.5	Distribution support calculation	128
A.6	Window Statistical Correlation	129
A.7	The structure of external program unit in C++	130
A.8	The structure of external program unit in FORTRAN	130
A.9	Imposing of statistical correlation, see figure 3.6	131

A.10	Information about the achieved accuracy	131
A.11	Window “Check samples” – sampled marginal variable	132
A.12	Window “Check samples” – sampled pair of variables (correlation check)	132
A.13	Input of DLL function window	133
A.14	Basic statistical assessment – histogram and statistical characteristics	133
A.15	Response R , action of loading E , safety margin $Z = R - E$	134
A.16	Window Sensitivity Analysis – positive sensitivity (parallel coordinates)	135
A.17	Window Sensitivity Analysis – negative sensitivity (parallel coordinates)	135
A.18	Window Sensitivity Analysis – positive sensitivity (cartesian coordinates)	136
A.19	Window Sensitivity Analysis – negative sensitivity (cartesian coordinates)	136
A.20	“What-if-study” using sensitivity analysis window	137
A.21	Curve fitting and estimators of failure probability p_f	137
A.22	ATENA run-time interactive graphical window	138
A.23	Hierarchical structure of ATENA	138

Chapter 1

Introduction

1.1 Aims and general concept of the thesis

The intent of this chapter is to provide an overview of the problems tackled by the thesis and to enable easy orientation throughout all parts and chapters. This dissertation is designed such that each part can be read independently of others even though the sequence of chapters reflects gradual progress to complex size effect studies by combining stochastic approaches with fracture mechanics. The thesis may be considered a collection of author's selected papers on the topic. The whole focus looks towards complex description and understanding of size effect phenomena. The main attention is devoted to concrete as a main representative of quasibrittle material (such as rock, tough ceramics, snow and ice, etc.) and one of the most important building material in civil engineering.

The title of the thesis "Stochastic fracture mechanics and size effect" suggests the attempt to combine both, the advanced tools of fracture (nonlinear) mechanics and stochastic approaches in order to model the complex behavior of real material/structures considering material randomness or variability.

Efficient methods for numerical analysis of (reinforced) concrete structures have been the objective of much research during the last few decades, and the main difficulty has been how to best capture *material nonlinearity*. The aim is to model the complete response of a structure including the crack propagation in the pre-peak, peak and post-peak states. A form of fracture mechanics that can be applied to such kind of fracture analysis has been developed during the last three decades. Recently, commercial finite element programs, using the crack band approach, have become available for this purpose. These tools, however, remain at the deterministic level. On the other hand, the design practice in industry provides motivation mainly for efficient implementation of existing simple material models, solution strategies, discretization and interpretation of results. These topics will naturally remain as the priorities for commercial software developers. But exceptions are nowadays appearing – the interdisciplinary field of stochastic fracture mechanics is now finally infringed on by some advanced software developers, e.g. those of ATENA (Cervenka and Pukl, 2003) or DIANA (Waarts, 2001).

The properties of many physical systems and/or the input to these systems exhibit complex *random fluctuations* that cannot be captured and characterized completely by deterministic models. Probabilistic models are needed to quantify the uncertainties of these properties, to develop realistic representations of output and failure state of these system and to obtain rational and safe designs. Usually the softwares for nonlinear analysis of reinforced concrete structures taking into account recent theoretical achievements of fracture mechanics. However the software is purely deterministic, it means that all geometrical, material and load parameters of a computational model had to be fixed to deterministic values. It does not reflect the fact that generally material, geometrical and load parameters of nonlinear fracture mechanics models are rather uncertain (random) and modeling of these uncertainties of computational model in a probabilistic way is therefore highly desirable.

The achievements of material science and modeling of concrete would be less important if they do not contribute to everyday design practice and *structural reliability*. The more complicated a computational model of a structure is the more difficult is the application of reliability analysis of almost any level. Linear elastic analysis enables simple reliability calculations – the last consistent reliability approach in the design was the allowed stress method. Recent development introduced the significant inconsistency:

Eurocode 2 (1991) design standard demands a non-linear analysis using first mean values and second design values of material parameters. No real guarantee and information on safety can be obtained using partial safety concept as accepted in present design codes. The approach generally fails if the internal forces entering safety margin (failure criteria) are not proportional to the load level, as is in case of complex non-linear problems, see e.g. Vořechovský (2000a,b, 2001c); Kala et al. (2001); Vořechovský and Kala (2001).

The more complex (statically indeterminate) the structure is the less satisfying is the inconsistent approach of partial safety factors. This is quite well-known problem and there is only one straightforward solution: Implementation of safety factors to the results of statistical nonlinear analysis (failure load, stresses, deflections, etc.), not to input parameters. The general trend is toward a consistent reliability assessment as recommended by Eurocode 1 (1993). This is in agreement with effort of some research teams, e.g. (Enevoldsen, 2001) pointed out *economical consequences* of probabilistic-based assessment in bridge engineering. We aspire to contribute to solution of the aforementioned practical problems in the thesis.

This document reflects the effort to combine both tools of *nonlinear fracture mechanics* and *stochastic simulation methods* (small-sample) in order to capture the complexity of real structural behavior (Vořechovský et al., 2002b). In the thesis we provide the theoretical basis and description of numerical methods and approaches used in probabilistic module of (FREET), whose computational core is programmed by the author. The software is fully integrated into nonlinear finite element software package. Theoretical background of relevant reliability techniques is provided together with information on their role in reliability engineering.

The salient feature of quasi-brittle materials is a complex *size effect* on structural strength. Size effect phenomenon manifests itself in form of a strong dependence of the nominal strength σ_N (nominal stress at the failure load) on the characteristic dimension D (size) of the geometrically similar structures, see Fig. 1.1. Since the uncertainties and spatial variability is inherently present in nature, the nominal strength has a certain variability. The size effect is also characterized/accompanied by the change of the nominal strength variability for different structure sizes. Size effect phenomenon has a great impact on safe design and assessment of structures. The size effect is not present in current strength theories (either plasticity or elasticity). The problem is that real large structures usually fracture under smaller failure load than laboratory size specimens, see Fig. 1.1.

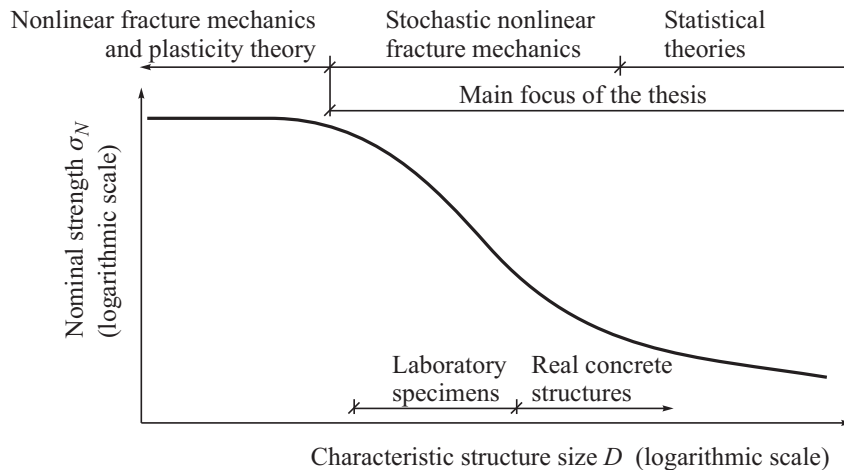


Figure 1.1: Illustration of size effect on nominal strength and the range of structural sizes of interest in the thesis

The history of description of size effect can be seen as a history of two fundamentally different approaches — deterministic and statistical explanations. The first explanation was definitely statistical — it dates back to the pioneering work of (Weibull, 1939a) and many others, mainly mathematicians. Phenomenon that larger specimens will usually fracture under relatively smaller applied load was that time associated with the statistical theory of extreme values. Then most researchers focused on the energetic basis of size effect and the main achievements were purely deterministic. Let us mention e.g.

the book of Bažant and Planas (1998) as an extensive source of information. Researchers used different theories, from early works e.g. Shinozuka (1972); Mihashi and Izumi (1977); Mazars (1982) considered uncertainties involved in concrete fracture. Some authors attempt to explain size effect by theories of fractals (Carpinteri et al., 1994, 1995). Recently, there are attempts to combine last decade's achievements of both fracture mechanics and reliability engineering e.g. Carmeliet (1994); Carmeliet and Hens (1994); Gutiérrez and de Borst (1999); Bažant and Novák (2000b) and others. This thesis is focused mainly on the range of sizes where both phenomena, statistical and deterministic plays a significant role, see the transitional zone in figure 1.1. This transition represents the range with the most difficult structural scaling theory.

Arguments mentioned above represent basis for the need to combine efficient reliability techniques with present knowledge in the field of nonlinear fracture mechanics. Remarkable development of computer hardware makes the numerical simulation of Monte Carlo type of complex nonlinear responses possible. The reasons for complex reliability treatment of nonlinear fracture mechanics problems can be summarized as follows: (i) *Modeling of uncertainties* (material, load and environments) in classical statistical sense as random variables or random processes (fields). The possibility to use statistical information from real measurements; (ii) *Inconsistency of design* to achieve safety using partial safety factors — fundamental problem; (iii) *Size effect phenomena*.

1.2 Thesis structure

The aims of the first **chapter 2** of **PART I** are: (i) to briefly review methods for efficient structural reliability assessment and (ii) to demonstrate the feasibility of the approach for analysis of nonlinear fracture mechanics computational models. The emphasize is given to the techniques which are developed for an analysis of computationally intensive problems which is typical for a nonlinear FEM analysis. The chapter shows the possibility of “randomization” of computationally intensive problems in the sense of the Monte Carlo type simulation.

Chapter 3 is focused on small-sample simulation method called Latin Hypercube Sampling (LHS). In particular the chapter is focused on the problem of efficient imposition of statistical correlation within framework of Monte Carlo type simulation (preferably LHS). Techniques presently available are discussed first. The new efficient technique of imposing the statistical correlation when using LHS is suggested. The technique is robust, efficient and very fast. The method has several advantages in comparison with former techniques.

Stochastic finite element method (SFEM) had facilitated the use of random fields in computational mechanics. Many material and other parameters are uncertain in nature and/or exhibit random spatial variability. Efficient simulation of random fields for problems of stochastic continuum mechanics is in the focus of both researchers and engineers. Achievements in stochastic finite element approaches increased the need for accurate representation and simulation of random fields to model spatially distributed uncertain parameters. To achieve this goal, the transformation of the original random variables into a set of uncorrelated random variables can be performed through an eigenvalue orthogonalization procedure. It is demonstrated that a few of these uncorrelated variables with largest eigenvalues are sufficient for the accurate representation of the random field. The error induced by such truncation will be an object of study in this chapter as well.

Chapter 4 discusses some features of combination of orthogonal transformation of covariance matrix with LHS. An attention is devoted to error assessment of simulated samples of stochastic fields. A proposed error assessment procedure has been performed for six alternatives of sampling schemes. The alternative with best performance, i.e. the convergence to target values of statistics with low variability is identified and recommended. Diminishing spurious correlation does not influence the capturing of these statistics but does influence significantly realization of autocorrelation function of random field. It has been shown that a spurious correlation influences significantly the scatter of autocorrelation function of simulated random fields. We show that a clear indication of this scatter is the fulfillment of norms used as objective functions in algorithm proposed in the preceding chapter.

PART II of the thesis is focused on *textile reinforced concrete*, a new composite material for special purposes. The tensile failure of fiber-reinforced composites is generally dominated by failure of the fiber bundle. The matrix material, whether polymer, ceramic or metal, serves mainly to transfer the load among the fibers through the elasticity, or yielding, debonding with sliding friction between the fiber and matrix. The matrix can carry some load in a metal or polymer matrix composite but, after matrix cracking, carries almost zero load in ceramic matrix composites. The two factors controlling fiber failure are (i) the statistical fiber strength and (ii) the stress distribution along the fiber direction. The stress along a fiber depends on the applied stress, but also on precisely how stress is transferred from a broken fiber to the surrounding intact fibers and matrix environment. This stress transfer is governed by the elastic properties of the constituents and by the fiber/matrix interface, and is difficult to obtain in the presence of more than one broken fiber. There are two load sharing rules. One is “global load sharing”, i.e. loads dropped due to fiber break(s) are shared equally among intact fibers. The presented work is focused particularly on fiber bundles under global (equal) load sharing. The available statistical models of strength of bundles are reviewed.

The thesis presents a newly developed micromechanical (**chapter 5**) model which is combined with advances stochastic techniques (random variables and random processes capturing the spatial variability of uncertain parameters). These models are given to context with classical approach (Weibull, 1939a) and we proved that there must exist (as opposite to Weibull integral) statistical length scale. It is explained why the nonlocal Weibull integral (Bažant and Xi, 1991; Bažant and Novák, 2000b,c) is not general enough solution for the presented problems. We propose new formulas which are designed based on asymptotic matching for approximation and prediction of the yarn strength under various conditions and for the whole range of yarn lengths. These formulas are compared to available statistical theories of strength of bundles. The detailed analysis of all substantial effect in the context of tensile test of yarn enabled design of practical procedure of testing and evaluation of yarn strength (**chapter 6**).

It is shown how to decompose, analyze and compose partial phenomena present in the yarn tensile test which is a stepping stone for coming analysis of the composite material with even more complex behavior: textile reinforce concrete.

PART III begins with presentation of state of the art in deterministic and statistical size effects on modulus of rupture of concrete structures (**chapter 7**).

Selected principles of behavior of multi-filament yarns can be applied in the context of plain concrete: the micromechanical model of concrete can be constructed as a lattice with tensile elements. Therefore some results from PART II apply to concrete and the **chapter 8** shows how to do that.

The aim is to have a full stochastic description of complex concrete behavior enabling not only deterministic analysis, but also statistical and mainly reliability analyzes and prediction. This is important from safety and economical reasons.

The next **chapter 9** introduces a new approach to stochastic nonlinear analyzes of large structures. Standing firmly on the *statistical theory of extreme values* the text proposes a practical tool for simulation of random scatter (spatial variability) in the context of FEM which is independent of the mesh. In some sense the approach brings similar features to famous crack *band model* in deterministic computational fracture mechanics (Bažant and Oh, 1983). Similarly to crack band model which is proved to be theoretically correct and compared to cohesive (fictitious) crack model due to Hillerborg et al. (1976) the developed *stochastic crack band model* is derived from elaborate theory of ordered statistics and extreme values (Fisher and Tippett, 1928; Gumbel, 1958; Gnedenko, 1943; Weibull, 1939a; Castillo, 1988). The range of applicability (large structures) is explained and it is shown that the model performs well in the size regions, where the combination of NLFEM and simulation of random fields is not useful. This is because in case of large structures the computational demands render the utilization of random fields inapplicable. The feasibility, correctness and predictive power of the approach is shown using numerical examples.

The problem of *structural scaling* in a broad range of sizes is studied in the final **chapter 10** of PART III. The behavior of general quasibrittle material is shown to be the complex case of behavior covering both the plastic and elastic-brittle behavior on two asymptotic extremes of sizes. The available knowledge of fracture mechanics is combined with new achievements presented in PART II and PART

III. This resulted in the *new combined size effect formula for crack initiation problems of quasibrittle failure*. The new law covers both the deterministic scaling (characteristic material length) and statistical scaling (autocorrelation length of variable strength) and their interaction over the whole range of sizes. The asymptotic limits are checked with help of deterministic plasticity of the small-size structures and stochastic-brittle behavior (Weibull type) of the large-size structures.

The numerical verification of the theoretical consistency with the assumptions is performed with the practical example of Malpasset Dam failure in French Alps. The last chapter of PART III can be seen as (theoretically) the most complex part of the whole thesis as it covers the knowledge gained from work on all other parts as well as the state of the art of the field.

The computational tools used for numerical modeling were not ready at the beginning of author's doctoral study. In particular the stochastic simulations were done with simulation software developed by the author. The combination of the computational core with a graphical user interface (GUI) developed by Dr. Rusina constitutes the new unique software FREET. The software is presented in the **Appendix A**. We have learned from our needs and from the weaknesses of other available programs and the newly developed software provides many helpful features. The uncertainty can be modeled by more than 20 statistical distributions which are implemented in uniform manner enabling the user simple and robust manipulation. The simulation of random variables is based on the new achievements described in PART I of the thesis.

The main aim of the software is to enable a probabilistic treatment of complex engineering problems coded into deterministic software where classical reliability approaches are not feasible. The software is designed in the form suitable for relatively easy probabilistic assessment of any user-defined problem. The name of the software reflects this strategy — FREET is the acronym for **F**easible **R**Eliability **E**ngineering **T**ool (Novák et al., 2002b,c,d, 2003b, 2004). This probabilistic software was recently successfully integrated with advanced non-linear fracture mechanics solution of concrete structures – the finite element program ATENA (Cervenka and Pukl, 2003). The software continues to be developed.

Part I

**SMALL-SAMPLE SIMULATION
METHODS AND APPROACHES
TO STOCHASTIC MECHANICS**

Chapter 2

Probabilistic assessment of computationally intensive problems

The aims of this chapter are: (i) to briefly review methods for efficient structural reliability assessment and (ii) to demonstrate the feasibility of the approach for analysis of nonlinear fracture mechanics computational models. The emphasis is given to the techniques which are developed for an analysis of computationally intensive problems which is typical for a nonlinear FEM analysis. The chapter shows the possibility of “randomization” of computationally intensive problems in the sense of the Monte Carlo type simulation. Latin hypercube sampling is used in order to keep the number of required simulations at an acceptable level. Random variables are randomly generated under their probability distribution functions, statistical correlation among them is imposed by the optimization technique, called the simulated annealing developed previously and described in the presented dissertation, section 3.3 (chapter 3).

2.1 Reliability theory

The aim of statistical and reliability analysis is mainly the estimation of statistical parameters of structural response and/or theoretical failure probability. Pure Monte Carlo simulation cannot be applied for time-consuming problems as it requires large number of simulations (repetitive calculation of structural response). Historically, this obstacle was partially solved by approximate techniques suggested by many authors, e.g. Grigoriu (1982/1983); Hasofer and Lind (1974); Li and Lumb (1985); Madsen et al. (1986); Schuëller (1998). Generally, the problematic feature of these techniques is the (in)accuracy. Research was then focused on development of advanced simulation techniques, which concentrates simulation into failure region (Bourgund and Bucher, 1986; Bucher, 1988; Schuëller and Stix, 1987; Schuëller et al., 1989). In spite of the fact that they usually require smaller number of simulations comparing pure Monte Carlo (thousands), an application for advanced structural analysis problem can be crucial and still almost impossible. But there are some feasible alternatives: Latin hypercube sampling McKay et al. (1979); Ayyub and Lai (1989); Novák et al. (1998) and response surface methodologies (Bucher and Bourgund, 1987).

The term stochastic or probabilistic finite element method (SFEM or PFEM) is used to refer to a finite element method which accounts for uncertainties in the geometry or material properties of a structure, as well as the applied loads. Such uncertainties are usually spatially distributed over the region of the structure and should be modelled as random fields. From many works on SFEM worked out in last three decades we can mention e.g. Vanmarcke et al. (1986); Yamazaki et al. (1988); Der Kiureghian and Ke (1988); Brenner (1991); Ghanem and Spanos (1991); Kleiber and Hien (1992). The interest in this area has grown from the perception that in some structures the response is strongly sensitive to the material properties, and that even small uncertainties in these characteristics can adversely affect the structural reliability. This is valid especially in the case of highly nonlinear problems of nonlinear fracture mechanics.

2.1.1 Fundamental concept of structural reliability

In general, structural design consists of proportioning the elements of structure such that it satisfies various criteria of safety, serviceability, and durability under the action of loads. In other words, the structure should be designed such that it has a higher strength or resistance than the effect caused by the loads. Schematic representation of failure probability evaluation is shown in Fig. 2.1 by considering two variables (one relating to the load S on the structure and the other to the resistance R of the structure). Both E and R are random in nature; their randomness is characterized by the corresponding probability density functions $f_E(e)$ and $f_R(r)$, respectively. Fig. 2.1 also identifies the deterministic (nominal) values of these parameters E_N and R_N used in conventional safety factor-based approach. The area of overlap between the two curves (the shaded region) provides basis for a qualitative measure of the probability of failure. This area of overlap depends on three factors:

- The relative positions of the two curves: As distance between the two curves increase, the probability of failure decreases. The position of the curves may be represented by the means (μ_E and μ_R) of the two variables.
- The dispersion of the two curves: If the two curves are narrow, then the area of overlap and the probability of failure are small. The dispersion may be characterized by the standard deviations (σ_E and σ_R) of the two variables.
- The shape of the two curves: The shapes are represented by the probability density functions $f_E(e)$ and $f_R(r)$.

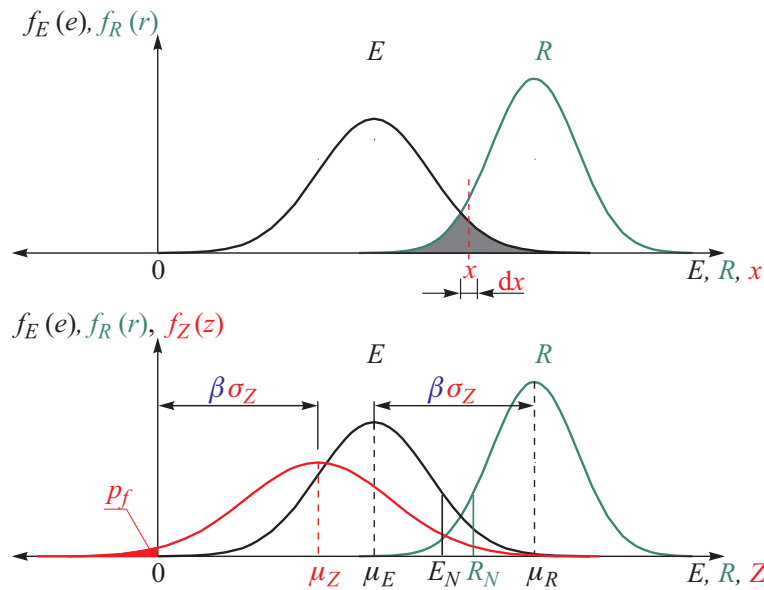


Figure 2.1: Normal distribution of safety margin as a subtraction of two normal random variables and the meaning of the safety index β

2.1.2 Response and limit state function

The classical reliability theory introduced the form of a response variable (deflection, stress, ultimate capacity, crack width etc.) or safety margin (in case that the function expresses failure condition) as the function of basic random variables $\mathbf{X} = X_1, X_2, \dots, X_{N_V}$

$$Z = g(X_1, X_2, \dots, X_{N_V}) \quad (2.1)$$

where $g(\cdot)$ represents functional relationship between elements of vector \mathbf{X} (computational model, non-linear fracture mechanics model in our case), see e.g. Freudenthal (1956b); Freudenthal et al. (1966);

Madsen et al. (1986); Schneider (1996). Elements of vector \mathbf{X} are geometrical and material parameters, load, environmental factors, etc., generally uncertainties (random variables or random fields). These quantities can be naturally also statistically correlated, see section 3.2.

In case that Z is safety margin, $g(\cdot)$ is called limit state function or performance function and can be formulated usually using comparison of a real load and failure load. The structure is considered to be safe if

$$g(\mathbf{X}) = g(X_1, X_2, \dots, X_{N_V}) \geq 0. \quad (2.2)$$

The performance of the system and its components is described considering a number of limit states. A limit state function can be explicit or implicit function of basic random variables, and it can be in a simple or rather complicated form. Usually, the convention is made that it takes negative value if a failure event occurs, so that the Eq. (2.2) holds. Therefore the failure event is defined as the space where $Z \leq 0$ and survival event is defined as the space where $Z \geq 0$. Two basic classes of failure criteria can be distinguished: structural collapse and loss of serviceability.

The primary goal of the statistical analysis is the estimation of basic statistical parameters/moments of response variable Z , e.g. mean values and variances. Also a histogram and an empirical cumulative probability distribution function are always valuable information. It can easily be done by Monte Carlo simulation, by repetitive calculations of the computational model $g(\cdot)$.

2.1.3 Reliability index

Reliability analysis methods employing reliability index or safety index take into account second moment statistics (means and variance) of the random variables. Cornell (1969) suggested to use the distance from the expectation of the limit state function to the limit state function itself as an elementary reliability measure which consider normal PDF. This yields the reliability index:

$$\beta = \frac{\mu_Z}{\sigma_Z} \quad (2.3)$$

where μ_Z and σ_Z are the mean value and the standard deviation of the safety margin Z . In this case β is actually the reciprocal value of the coefficient of variation of the variable Z . The reliability index can be interpreted geometrically as the minimum distance from the limit state function $g(\mathbf{X})$ to the origin, see fig. 2.1. Hasofer and Lind (1974) used this idea for generalized definition of the reliability index. They proposed to use the minimum distance from limit state function (usually nonlinear) to the origin in the uncorrelated normalized space as reliability measure. Such generalized reliability index is given by:

$$\beta = \min_{g(\mathbf{x})=0} \sqrt{\mathbf{u}^T \mathbf{u}} = \min_{g(\mathbf{x})=0} \left(\sqrt{\sum_{i=1}^{N_V} u_i^2} \right) \quad (2.4)$$

where β is the distance in a standard normal space \mathcal{U} and $g(\mathbf{X}) = 0$ is the limit state surface. The point \mathbf{u}^* at which β reaches the minimum is called the design point, see figs. 2.2 and 2.4.

Reliability index represents the reliability measure to express reliability. Estimation of Cornell's reliability index is rather simple, as it needs the estimation of basic statistical characteristics of safety margin. This task can be solved using Monte Carlo type simulation and will be described in section 2.5.

2.1.4 Failure probability

The main aim of reliability analysis is the estimation of reliability using probability measure called the theoretical failure probability defined as:

$$p_f = P(Z \leq 0). \quad (2.5)$$

More formally, the theoretical failure probability as a measure of unreliability is defined as:

$$p_f = \int_{D_f} f_{\mathbf{X}}(X_1, X_2, \dots, X_{N_V}) dX_1, dX_2, \dots, dX_{N_V}, \quad (2.6)$$

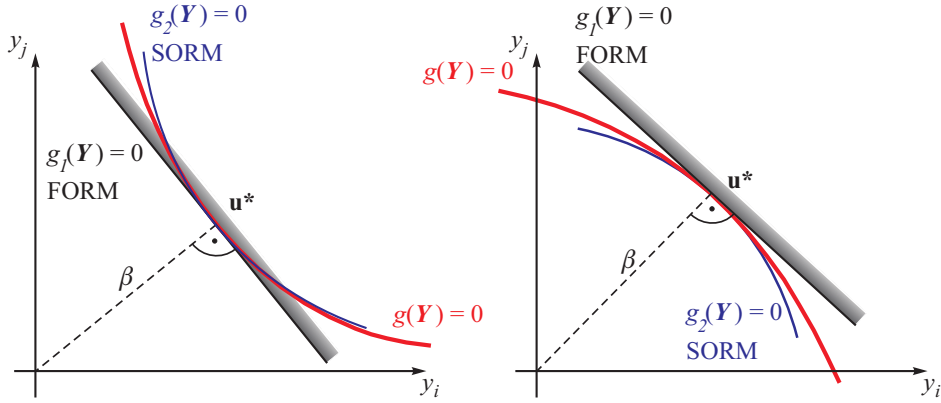


Figure 2.2: FORM and SORM methods for reliability estimation

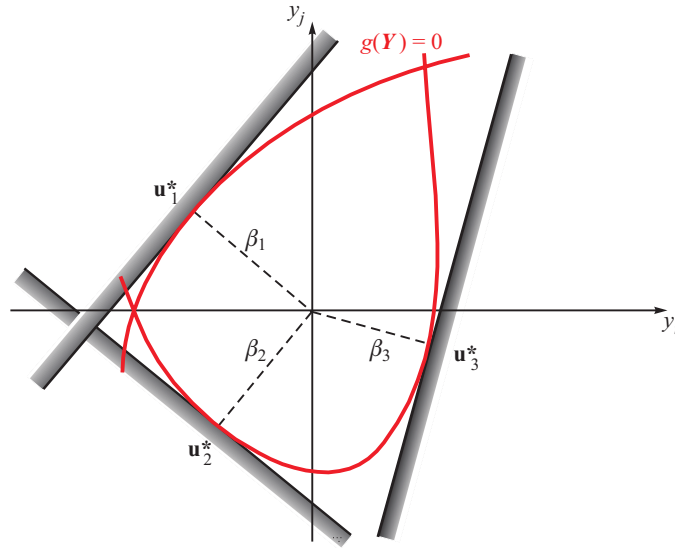


Figure 2.3: Multiple design point

where D_f represents failure region where $g(\mathbf{X}) \leq 0$ (integration should be performed over this region) and $f(X_1, X_2, \dots, X_{N_V})$ is the joint probability density function of random variables (vector \mathbf{X}).

Equality $Z = 0$ divides multidimensional space of basic random variables $\mathbf{X} = X_1, X_2, \dots, X_{N_V}$ into safe and failure region. Explicit calculation of integral (2.6) is generally impossible therefore the application of a simulation technique Monte Carlo type is the simple and in many cases feasible alternative to estimate failure probability integral (e.g. Rubenstein, 1981; Schneider, 1996; Schüller and Stix, 1987, and others).

The First Order Reliability Method (FORM) has initially been proposed by Hasofer and Lind (1974). In the FORM, a linear approximation of the limit state surface in the uncorrelated standardized Gaussian space is used to estimate the probability of failure. For this purpose it is necessary to transform the basic variables into uncorrelated standard Gaussian variables ¹ (\mathcal{U} -space):

$$Y_i = \frac{X_i - \mu_i}{\sigma_i}, \quad i = 1, \dots, N_V \quad (2.7)$$

where μ_i and σ_i are the mean value and standard deviation of the random variable X_i , respectively.

¹Such transformation can only be used if the random variables X_i are uncorrelated. Generally a Rosenblatt transformation (Liu and Der Kiureghian, 1986) or any other transformation must be used in order to obtain the vector of uncorrelated variables \mathbf{X}' . Such vector can be standardized and used for the FORM method, however, we must note that the limit state function must be transformed to the new space as well.

The reliability integral can be written in the transformed \mathcal{U} -space as:

$$p_f = \int_{g(\mathbf{Y}) \leq 0} f_{\mathbf{Y}}(Y_1, Y_2, \dots, Y_{N_V}) dY_1, dY_2, \dots, dY_{N_V}, \quad (2.8)$$

The distance from the design point of the transformed limit state function to the origin is called reliability index β .

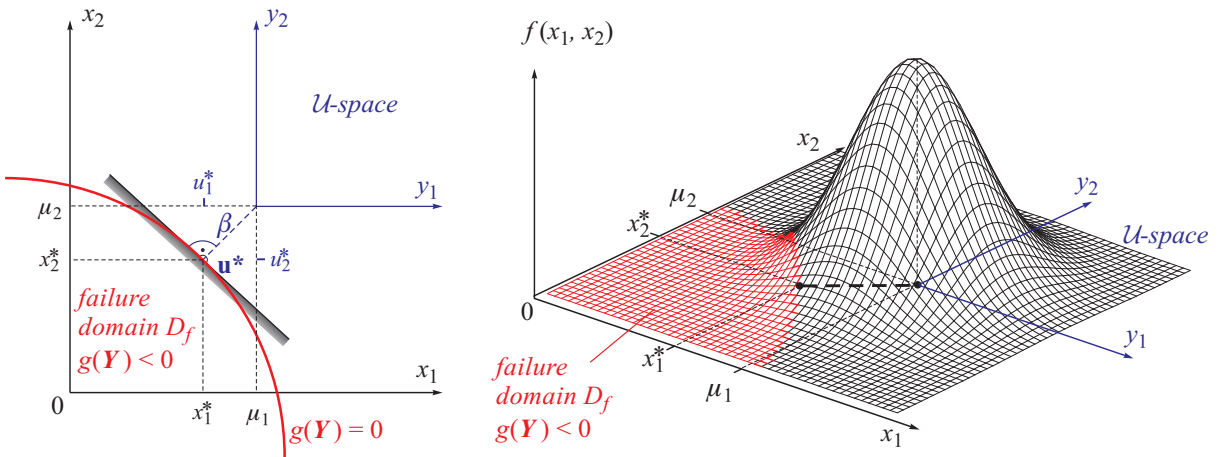


Figure 2.4: Geometrical interpretation of failure probability p_f (Eqs. 2.6 and 2.8) in case of two-variate joint probability density $f_{\mathbf{X}}(x_1, x_2)$

Note that design point is the point on the limit state surface with the minimum distance to the origin in standard normal space is considered to be important. It is also the point of maximum likelihood if the basic variables are normally distributed. This point can be obtained by solving the optimization problem expressed in Eq. 2.4. The maximum β is known as the reliability index. It can be shown that the probability of failure is approximately given by:

$$p_f = 1 - \Phi(\beta) = \Phi(-\beta), \quad (2.9)$$

where Φ denotes the standardized Gaussian distribution function. In case of linear limit state function and normally distributed basic variables no transformations are necessary and equation (1.7) yields just the exact failure probability.

In spite of the fact that the calculation of failure probability using reliability index (according to Cornell (1969) or Hasofer and Lind (1974)) does not belong to the category of very accurate reliability techniques (e.g. Bourgund and Bucher, 1986), it represents a feasible alternative in many practical cases.

2.2 Stochastic analysis software

A large number of efficient stochastic analysis methods have been developed during last years. In spite of many theoretical achievements the acceptability and a routine application in industry is still rare. Present reliability software developers should bridge the demands on the usage of effective reliability methods and easy and transparent use by an inexperienced user. We however, made an attempt to fill this gap and deliver such software (see appendix A, FREET).

Three main categories of stochastic analysis can be distinguished:

- Approaches focused on the calculation of statistical moments of response quantities, like estimation of means, variances etc. Uncertainties input into a response function. This group is usually named *statistical analysis*.
- Approaches aiming at the calculation of estimation of theoretical probability of failure. Uncertainties input into a limit state function. This group is usually named *reliability analysis*.

- Approaches aiming at the quantification of sensitivity of output (response) on variations of input variables. There are several different sensitivity measures available; each measuring a different kind of sensitivity. Uncertainties input into a response or limit state function depending on what is the output variable under investigation. This group is usually named *sensitivity analysis*.

There are many different methods developed by reliability researchers covering all the above mentioned approaches. The common feature of all the methods is the fact that they require a repetitive evaluation (simulation) of the response or limit state function. The development of reliability methods is from the historical perspective a struggle for decreasing or to avoiding an excessive number of simulation (e.g. [Schuëller, 1998](#), etc.). From this point of view of the computational demands the major groups of the methods belonging to the first category are as follows:

- Crude Monte Carlo simulation,
- Stratified sampling techniques,
- Perturbation techniques.

The methods of next category for reliability calculations can be distinguished as:

- Crude Monte Carlo simulation,
- Advanced simulation techniques, like importance sampling, adaptive sampling, directional sampling etc. ([Schuëller et al., 1989](#), e.g.),
- Approximation techniques, FORM, SORM etc. (e.g. [Hasofer and Lind, 1974](#)),
- Response surface methodologies (e.g. [Bucher and Bourgund, 1987](#)),
- Curve fitting techniques - evaluating samples of safety margin (e.g. [Grigoriu, 1983](#); [Li and Lumb, 1985](#)).

The lists above are ordered according to the computational demands (the number of simulation required) from the top downwards. There is a decreasing accuracy of the methods in the same direction. In the case of computationally intensive problems there is an overlapping domain of methods, feasible to apply. These techniques are implemented in many different alternatives in reliability software, e.g. COMREL (RCP Munich), VAP (ETH Zurich), *SLang* (Weimar University), M-STAR (UTAM Prague), CRYSTALL BALL (Decisionerring. Inc.), PROBAN (DNV software), COSSAN (Innsbruck University).

The intent of the chapter is to describe a practical tools to assess response statistics and reliability. Relevant techniques and the probabilistic software developed for easy handling of practical reliability problems are briefly described, the chapter should be considered to have just an informative value.

2.3 LHS: the small-sample stochastic technique

A special type of numerical probabilistic simulation called Latin hypercube sampling (LHS) makes it possible to use only a small number of Monte Carlo simulations. This technique, originally proposed by [McKay et al. \(1979\)](#), appeared to be useful reliability technique until present days. LHS is a special type of Monte Carlo numerical simulation, which uses the stratification of the theoretical probability distribution function of input random variables. The LHS is very efficient for the estimation of first two or three statistical moments of structural response. It requires a relatively small number of simulations - repetitive calculations of the structural response resulting from adopted computational model (tens or hundreds). The utilization of LHS strategy in reliability analysis can be rather extensive. It is not restricted just for the estimation of statistical parameters of structural response ([Novák et al., 1998](#)).

There are generally two stages of LHS, see chapter 3:

1. Samples for each variable are strategically chosen to represent the variables distribution function;
2. Samples are reordered to match required statistical correlation among variables.

The cumulative probability distribution functions (CDF) for all random variables are divided into N equivalent intervals (N is a number of simulations); one representant of each interval is then used in simulation process once. This means that the range of the probability distribution function (X_i) of each random variable is divided into N_{Sim} intervals of equal probability $1/N_{Sim}$, see fig. 3.1. Based on this precondition a table of random permutations can be used conveniently, each row of such a table belongs to the specific simulation and the column corresponds to one of the input random variables. Such a table of random permutations is presented in table 3.1 (page 21).

The second step is reordering LHS samples in such a way that they might match the prescribed statistical correlation as much as possible. It can be done by using different techniques, a robust technique based on the stochastic method of optimization called simulated annealing has been proposed recently by Vořechovský and Novák (2002); Vořechovský et al. (2002a); Vořechovský and Novák (2003b). The detailed theoretical description can be found in the referred papers or in the sections 3.2 and 3.3.

The main reasons for selection of LHS can be summarized as follows:

- EFFICIENCY - good accuracy in statistical characteristics of structural response using small number of samples.
- SIMPLICITY - the technique is suitable for implementation into complex commercial software as it requires minor modifications of program core.
- TRANSPARENCY - as it represents an alternative of Monte Carlo simulation, the method is transparent and understandable also for people who are not experts in reliability engineering; generally the Monte Carlo type approach is close to engineering thinking.

The Latin hypercube sampling (LHS) simulation technique belongs to the category of advanced simulation method (McKay et al., 1979; Novák and Kijawatworawet, 1990). It is a special type of the Monte Carlo numerical simulation which uses the stratification of the theoretical probability distribution function of input random variables. The following topics in which LHS can be applied are outlined as follows (for more details see eg. Novák et al. (1998)):

- estimation of statistical parameters of a structural response,
- estimation of the theoretical failure probability,
- sensitivity analysis,
- response approximation,
- preliminary “rough” optimization,
- reliability-based optimization.

2.4 LHS: sensitivity analysis (nonparametric rank-order)

An important task in the structural reliability analysis is to determine the significance of random variables - how they influence a response function of a specific problem. There are many different approaches of sensitivity analysis; a summary of present methods is given in (Novák et al., 1993). The sensitivity analysis can answer the question “which variables are the most important?”. In this way the dominating and non-dominating random variables can be distinguished using certain sensitivity measures.

On the base of LHS there are two kinds of sensitivity analysis: Sensitivity *in terms of coefficient of variation* and sensitivity *in terms of nonparametric rank-order correlation coefficient*.

The first approach is based on the comparison of partial coefficient of variation of the structural response variable with variation coefficient of basic random variables. The second approach utilizes the nonparametric rank-order statistical correlation between basic random variables and the structural response variable: a straightforward and simple approach. Only the later approach is considered in this text due to its advantages. LHS simulation can be efficiently used to obtain such kind of information.

The relative effect of each basic variable e.g. on the structural response can be measured using the partial correlation coefficient between each basic input variable and the response variable (Iman and Conover, 1980). The method is based on the assumption that the random variable which influences the response variable most considerably (either in a positive or negative sense) will have a higher absolute

value of the correlation coefficient between sampled input and resulting output than other variables. In case of a very weak influence the correlation coefficient will be quite close to zero. Using the Latin hypercube sampling this kind of sensitivity analysis is obtained as an additional result, and no significant additional computational effort is necessary. An advantage of this approach is the fact that the sensitivity measure for all random variables can be obtained directly within one simulation analysis. The rank-order statistical correlation can be expressed by the Spearman correlation coefficient or Kendall's tau.

Since the model for structural response is generally non-linear, a non-parametric rank-order correlation is utilized. The key concept of non-parametric correlation reads: Instead of the actual numerical values we consider the values of its rank among all other values in the sample, that is $1, 2, \dots, N_{Sim}$. Then the resulting list of numbers will be drawn from a perfectly known probability distribution function - the integers are uniformly distributed. In case of Latin Hypercube Sampling the representative values of random variables cannot be identical, therefore there is no necessity to consider mid-ranking. The non-parametric correlation is more robust than the linear correlation, more resistant to defects in data and also distribution independent. Therefore it is particularly suitable for the sensitivity analysis based on Latin Hypercube sampling.

As a measure of non-parametric correlation we use the statistic called Kendall's tau. It uses only the relative ordering of ranks: higher in rank, lower in rank, or the same in rank. Since it uses a weak property of data, Kendall's tau can be considered a very robust strategy.

As mentioned above Kendall's tau is the function of ranks q_{ji} (the rank of a representative value of the random variable X_i in an ordered sample of N_{Sim} simulated values used in the j -th simulation which is equivalent to the integers in the table of random permutations in the LHS method) and p_j (the rank in ordered sample of the response variable obtained by the j -th run of the simulation process):

$$\tau_i = \tau(q_{ji}, p_j), \quad j = 1, 2, \dots, N_{Sim} \quad (2.10)$$

In this way the correlation coefficient $\tau_i \in \langle -1, 1 \rangle$ can easily be obtained for an arbitrary random variable and we can compare them. The greater absolute value of τ_i for a variable X_i , the greater influence has this variable on the structural response. An advantage of this approach is the fact that a sensitivity measure for all random variables can be obtained directly within one simulation analysis.

The rank-order statistical correlation is expressed by the Spearman correlation coefficient (compare to Eq. 3.6, p. 22)

$$S = 1 - \frac{6 \sum_{i=1}^{N_{Sim}} d_i^2}{N_{Sim} (N_{Sim} - 1) (N_{Sim} + 1)} \quad (2.11)$$

where d_i is the difference of the order of the components in sequenced statistical files (ordered sample), or by Kendall's tau (similar results):

$$\tau_i = \frac{c - d}{\sqrt{c + d + extra - p_j} \cdot \sqrt{c + d + extra - q_{ji}}} \quad (2.12)$$

For a detailed description of calculation, see Novák et al. (1993), here we present only a symbolic formulae.

This nonparametric sensitivity can illustratively be shown by parallel coordinate representation (Wegman, 1990), which can clearly demonstrate the positive or negative influence of a basic random variable Novák et al. (1998). Pairs of orders (basic input variable vs. response variable) are plotted in parallel co-ordinates. This is shown in Fig. 2.5.

Here it should be noted that other measures of sensitivity exists, e.g. *sensitivity in terms of coefficients of variation* or *parametric stochastic sensitivity*. Methods are well mapped in work of Novák et al. (1993).

2.5 LHS: reliability estimation based on curve fitting

As it was already mentioned in the introduction, the number of simulations is a crucial point to calculate the reliability. Therefore approximation technique of FORM/SORM type are till often utilized (starting

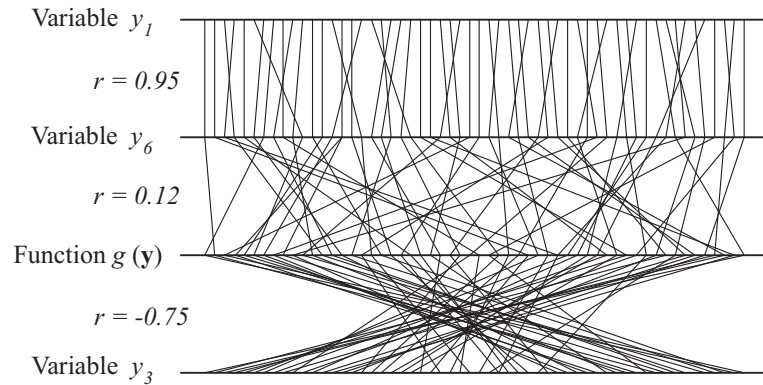


Figure 2.5: Parallel co-ordinates representations.

by fundamental paper by [Hasofer and Lind \(1974\)](#)). In the case of an extremely small number of simulations there are the following feasible alternatives only: the calculation of reliability index from the estimation of the statistical characteristics of the safety margin (reliability index of [Cornell, 1969](#)) and the curve fitting procedure. The first technique represents a simplification, and it is well known that it gives an exact result only for the normal distribution of the safety margin.

The curve fitting approach is based on the selection of the most suitable probability distribution of the safety margin. This selection is based on suitable statistical tests. When the mathematical model of probability distribution is selected, the failure probability is calculated as a percentile. There are limitations of such approach, see e.g. paper by [Novák and Kijawatworawet \(1990\)](#).

In case the response is the so-called safety margin (a limit state function is defined), statistical characteristics of safety margin can be obtained via LHS, ([Novák and Kijawatworawet, 1990](#); [Li and Lumb, 1985](#)). Then, there is a possibility to select suitable PDF for response. The selection is done by common well-known goodness-of-fit statistical tests (e.g. Kolmogorov-Smirnov test, Chi-square test), or based on the theory of comparison tests of PDFs. Once the most suitable is selected, the theoretical failure probability can be estimated as the value of CDF function at the zero point:

$$P_f = \Phi_{selected}(0) \quad (2.13)$$

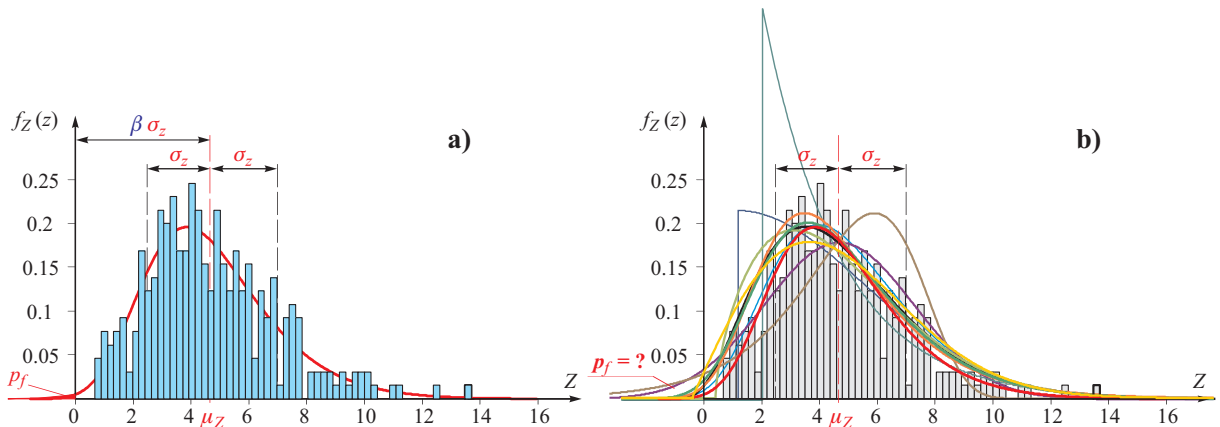


Figure 2.6: a) Best CDF obtained as a fit to computed histogram of results; b) Examples of fits (using estimated statistical moments for analytical PDF) and the uncertainty in estimation in the failure probability p_f

This curve fitting approach is not, of course, restricted only for LHS usage. The accuracy of calculations via (2.13) is rather limited for the following reasons:

- Limiting accuracy of approximate numerical algorithm for $\Phi_{selected}$,

- distribution support is around the mean value of safety margin, not in tails (as LHS is suitable for statistical calculations), therefore the selection of model distribution can be erroneous
- highly nonlinear limit state function can result in a PDF of safety margin of not one peak, then a curve fitting approach cannot work properly.

The disadvantages and limitations of the approach were analyzed in detail by Novák and Kijawat-worawet (1990). For one peak shape safety margin the approach works quite well approximately until the order of magnitude of failure probability 10^{-6} .

Another (relatively new) approach is based on *bootstrap methods* (see e.g. Kubanová and Linda, 2002); re-sampling in order to decrease variance of estimation of response moments (based on tens of bins) is done. This technique is under comprehensive study and algorithmization now, main focus is devoted to the statistical significance of re-sampled data.

In spite of the above mentioned difficulties these indirect approaches represent straightforward simple tool for failure probability estimation especially for cases when large number of simulations cannot be performed and response surface methodologies fail as well.

Chapter 3

Random variables: sampling and statistical correlation

Published in papers: Vořechovský and Novák (2002); Vořechovský et al. (2002a); Vořechovský and Novák (2003b); Vořechovský (2002c,d)

3.1 Introduction

The aim of statistical and reliability analysis of any computational problem which can be numerically simulated is mainly the estimation of statistical parameters of response variable and/or theoretical failure probability. Pure Monte Carlo simulation cannot be applied for time-consuming problems, as it requires large number of simulations (repetitive calculation of response). Small number of simulations can be used for acceptable accuracy of statistical characteristics of response using stratified sampling technique Latin Hypercube Sampling (LHS) (McKay et al., 1979; Iman and Conover, 1980; Ayyub and Lai, 1989).

Briefly, it is a special type of Monte Carlo numerical simulation which uses the stratification of the theoretical probability distribution functions of input random variables. It requires relatively small number of simulations (from tens to hundreds) – repetitive calculations of a response function resulting from a computational model analyzed. LHS strategy has been used by many authors in different fields of engineering and with both a simple and a very complicated computational model, list of applications relevant to civil engineering is provided e.g. by Novák et al. (1998). LHS is suitable for statistical and sensitivity calculations. However, there is a possibility to use it for probabilistic assessment within the framework of curve fitting, see section 2.5.

The classical reliability theory introduced the basic concept formally using the response variable $Z = g(\mathbf{Y})$, where g (computational model) represents functional relationship between elements of vector \mathbf{Y} . Elements of vector \mathbf{Y} are generally uncertainties (random variables). These quantities can naturally be also statistically correlated.

This part of dissertation is focused on the problem of efficient imposition of statistical correlation within framework of Monte Carlo type simulation (preferably LHS). Techniques presently available are discussed first. Although text in following chapters will deal with LHS, methods described in this work can be generalized to any Monte Carlo type method. So in the following LHS will be treated as a representative of Monte Carlo type simulation.

3.2 LHS: Sampling and statistical correlation

Latin hypercube sampling is a form of simultaneous stratification on all N_V variables of the unit cube $[0; 1]^{N_V}$. There are several versions of LHS. In the centered version (called lattice sampling by Patterson (1954)):

$$v_{i,j} = \frac{\pi_j(i) - 0.5}{N_{Sim}}, \quad i = 1, \dots, N_V, \quad j = 1, \dots, N_{Sim} \quad (3.1)$$

where π_j are independent uniform random permutations of 1 through N_{Sim} . Note that if $N_V = 1$ (one-dimensional integration) it represents the midpoint rule using integration points given by the formula (3.1). In the unbiased version, due to McKay et al. (1979), we can view the midpoint rule as a one-dimensional quasi-Monte Carlo sampling scheme, so the following stratified sampling method reads (in high dimension N_V):

$$v_{i,j} = \frac{\pi_j(i) - U_j^i}{N_{Sim}}, \quad i = 1, \dots, N_V, \quad j = 1, \dots, N_{Sim} \quad (3.2)$$

where U_j^i are independent identically and uniformly distributed random variables within the interval $(0, 1)$, independent of the permutations π_j .

The centered version in Eq. (3.1) was originally due to Patterson (1954) in the setting of agricultural experiments, whereas the version in Eq. (3.2) was motivated by computer experiments.

The name ‘‘Latin hypercube’’ stems from a relationship between Latin hypercubes and Latin squares. A Latin square is an N_{Sim} by N_{Sim} array of cells. Each cell has one of N_{Sim} different symbols (usually letters) written in it. Every row of the array has each of the N_{Sim} symbols exactly once. So does every column. Suppose the symbols are A , B , and so forth. Then the cells occupied by the letter A constitute a Latin hypercube sample of N_{Sim} points in the $N_V = 2$ dimensional coordinates of the array. There is a rich combinatorial theory underlying the construction of Latin squares. That theory does not play a role in the construction or analysis of Latin hypercubes, but it does become relevant in the study of randomized orthogonal arrays.

A Latin hypercube sample tends to be more uniformly distributed through the unit cube than an independent and identically distributed random variables (IID sample). A histogram of X_1^i through $X_{N_{Sim}}^i$ with N_{Sim} equal width cells would be perfectly flat for each $i = 1, \dots, N_V$ while the corresponding histograms for IID samples would typically be uneven. Perhaps the worst case Latin hypercube sample has all N_{Sim} points arranged on the diagonal in the N_V dimensional cube. The probability of such a sample is $(N_{Sim})^{1-N_V}$ as discussed later by Eq. (3.11).

Stratification with proportional allocation never increases variance compared to IID sampling, and can reduce it. Therefore it is natural to expect that N_V separate kinds of proportional stratification applied simultaneously as in LHS should might reduce variance too in which lies its effectiveness.

In the context of numerical simulation methods for structural reliability theory, LHS is based on Monte Carlo type of simulations of vector \mathbf{Y} under prescribed probability distributions. Realizations are simulated in a special way: the range of probability distribution function $f_i(Y_i)$ of each random variable Y_i is divided into N_{Sim} equidistant (equiprobable) intervals, where N_{Sim} is number of simulations planned. The identical probability $1/N_{Sim}$ for layers on distribution function is usually used. The representants of the equiprobable intervals are selected randomly, realizations are then obtained by inverse transformation of distribution function (point given by Eq. 3.2). The selection of midpoints as representants of each layer (Eq. 3.1) is the most often used strategy:

$$y_{i,j} = F_i^{-1}(v_{i,j}) = F_i^{-1}\left(\frac{j - 0.5}{N_{Sim}}\right), \quad i = 1, \dots, N_V, \quad j = 1, \dots, N_{Sim} \quad (3.3)$$

where $y_{i,j}$ is the j -th sample of i -th random variable Y_i , F_i^{-1} is the inverse of cumulative distribution function of this random variable and N_{Sim} is the number of simulations, i.e. number of samples for each random variable. It could be challenged to this simple methodology. One can criticize reduction of samples selection to the midpoints in intervals (we call it interval *median*). Such objection deals mainly with the tails of PDF, which mostly influences variance, skewness and kurtosis of sample set. This elementary simple approach was already overcome by sampling of *mean* values related to the intervals, (e.g. Keramat and Kielbasa, 1997; Huntington and Lyrantzis, 1998):

$$y_{i,j} = \frac{\int_{z_{i,j-1}}^{z_{i,j}} y \cdot f_i(y) dy}{\int_{z_{i,j-1}}^{z_{i,j}} f_i(y) dy} = N_{Sim} \int_{z_{i,j-1}}^{z_{i,j}} y \cdot f_i(y) dy \quad (3.4)$$

where f_i is the probability density function of variable X_i and the integration limits are:

$$z_{i,j} = F_i^{-1}\left(\frac{j}{N_{Sim}}\right), \quad j = 1, \dots, N_{Sim} \quad (3.5)$$

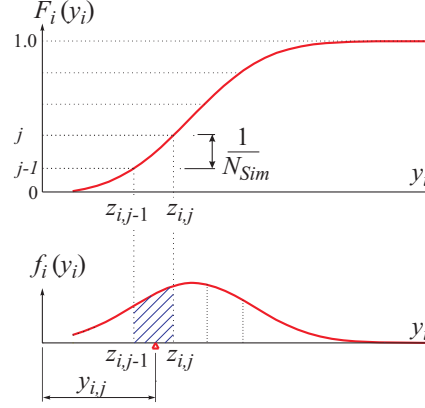


Figure 3.1: Samples as the probabilistic means of intervals

Samples then represent one-dimensional marginal PDF better in terms of distance of point estimators from the exact statistics. In particular, the mean value is achieved exactly (analytical expression preserves the mean) and estimated variance of data is much closer to the original one. For some PDFs (including Gaussian, Exponential, Laplace, Rayleigh, Logistic, Pareto, or others) the integral (3.4) can be solved analytically. In case of no or difficult solution of primitive it is necessary to use an additional effort: numerical solution of the integral. However, such increase of computational effort is worthwhile indeed. Samples selected by both described ways are almost identical close excluding those in the tails of PDFs. Therefore more difficult method could be used there only considering the fact that tail samples mostly influence estimated variance of sample set.

Generally in both cases, regularity of sampling (the range of distribution function is stratified) ensures good sampling and consequently good estimation of statistical parameters of response using small number of simulations. Sampling scheme is represented by table 3.1, where simulation numbers are in columns and rows are related to random variables, N_V is number of input variables.

Table 3.1: Sampling scheme for N_{Sim} deterministic calculations of $g(\mathbf{Y})$

sim:	1	2	...	N_{Sim}
var ₁	$y_{1,1}$	$y_{1,2}$...	$y_{1,N_{Sim}}$
var ₂	$y_{2,1}$	$y_{2,2}$
...
var _{N_V}	$y_{N_V,1}$	$y_{N_V,N_{Sim}}$

Table 3.2: Target correlation matrix for the sampling plan in table 3.1

sim:	var ₁	var ₂	...	var _{N_V}
var ₁	1	$K_{1,2}$...	$K_{1,N_{Sim}}$
var ₂	$K_{2,1}$	1
...	1	...
var _{N_V}	$K_{N_V,1}$	1

Having the samples of each marginal random variable ready, we may proceed to the second step of LHS: statistical correlation imposition. There are generally two problems related to LHS concerning statistical correlation: First, during sampling an undesired correlation can be introduced between random variables (rows in table 3.1). For example instead a correlation coefficient zero for uncorrelated random variables undesired correlation, e.g. 0.6 can be generated by random (the probability of such correlation is one over the number of all possible orderings given by Eq. (3.11)). It can happen especially in case of very small number of simulations (tens), where the number of interval combination is rather limited. Second problem we face is: how to introduce prescribed statistical correlation between random variables defined by the target correlation matrix (table 3.2). Samples in each row of table 3.1 should be rearranged in such a way to fulfill these two requirements: to diminish undesired random correlation and to introduce prescribed correlation given by table 3.2.

The efficiency of LHS technique was showed first time in work of McKay et al. (1979), but only for uncorrelated random variables. A first technique for generation of correlated random variables has been proposed by Iman and Conover (1982). One approach has been to find Latin hypercube samples in which the input variables have small correlations. Iman and Conover (1982) perturbed Latin hypercube samples in a way that reduces off diagonal correlation – they diminished an undesired random correlation. The technique is based on iterative updating of sampling matrix, Cholesky decomposition of covariance/correlation of matrix \mathbf{Y} has to be applied. In their method, as a measure of the statistical correlation, the Spearman correlation coefficient is used:

$$S_{ij} = 1 - \frac{6 \sum_{k=1}^{N_{Sim}} (R_{k,i} - R_{k,j})^2}{N_{Sim} (N_{Sim} - 1) (N_{Sim} + 1)} \quad (3.6)$$

where \mathbf{R} is the $(N_V \cdot N_{Sim})$ matrix containing a permutation of the rank numbers in each row and the coefficients $S_{i,j}$ represents the Spearman's correlation coefficients between the variables i and j . The estimated correlation matrix \mathbf{S} is symmetric, positive definite (unless some rows have an identical ordering). Therefore the Cholesky decomposition of the matrix \mathbf{S} may be performed:

$$\mathbf{S} = \mathbf{Q}^T \cdot \mathbf{Q} \quad (3.7)$$

and the new ordering matrix \mathbf{R}_B can be generated as follows:

$$\mathbf{R}_B^T = \mathbf{R}^T \cdot \mathbf{Q}^{-1} \quad (3.8)$$

The rank numbers in each row of the ordering matrix \mathbf{R} are then arranged to have the same ordering as the numbers in each row of \mathbf{R}_B . The technique can be applied iteratively and it can result in a very low correlation coefficient if generating uncorrelated random variables.

Since we are using the Cholesky decomposition of the covariance matrix \mathbf{S} of \mathbf{Y} , this matrix has to be positive definite. This constitutes a severe restriction: the number of simulations has to be larger than number of random variables ($N_{Sim} > N_V$). In relation to this restriction the usage of technique described later (Simulated Annealing) has a great consequence: there is no restriction concerning number of simulations N_{Sim} . Number of simulations can be extremely low as the covariance matrix of \mathbf{Y} does not have to be positive definite, $N_{Sim} \ll N_V$. Of course, there is a penalty for this advantage: spurious correlation can be diminished only until certain limit as well as imposition of desired statistical correlation structure. But very low number of simulations can still be used.

The problem of positive definiteness occurs here only in connection with correlation estimated by Spearman correlation coefficient. Current techniques uses this estimator of correlation due to utilization of Iman and Conover's method. For the future purpose of generation of random fields (chapter 4) random variables in matrix \mathbf{Y} are Gaussian and generally there is no reason to use (robust) Spearman's coefficient instead of classical linear Pearson's estimator of statistical correlation (product-moment correlation coefficient):

$$S_{ij} = \frac{\text{cov}(Y_i Y_j)}{\sqrt{D[Y_i] D[Y_j]}} = \frac{C_{i,j}}{C_{i,i} C_{j,j}} \quad (3.9)$$

where $C_{i,j}$ is the point estimation of covariance between variables i and j . The computational formula reads:

$$S_{ij} = \frac{\sum_{k=1}^{N_{Sim}} (y_{i,k} - \bar{y}_i) (y_{j,k} - \bar{y}_j)}{\sqrt{\sum_{k=1}^{N_{Sim}} (y_{i,k} - \bar{y}_i)^2 \sum_{k=1}^{N_{Sim}} (y_{j,k} - \bar{y}_j)^2}}, \quad \bar{y}_i = \frac{1}{N_{Sim}} \sum_{k=1}^{N_{Sim}} y_{i,k} \quad (3.10)$$

The above described iterative technique due to Iman and Conover (1982) later published by Florian (1992) under the name "Updated Latin Hypercube Sampling" (ULHS) can result in a very low correlation coefficient if generating uncorrelated random variables and the Latin hypercube samples look like random scatter in bivariate plot (top figs. 3.2 and 3.3), though they are quite regular in each univariate plot (Fig. A.11, p. 132). However, Huntington and Lyrintzis (1998) have found that the approach tends to converge

to an ordering which still gives significant correlation errors between some variables. Moreover, the scheme has more difficulties when simulating correlated variables: the correlation procedure can be performed only once, there is no way to iterate it and to improve the result. These obstacles stimulated the work of [Huntington and Lyrintzis \(1998\)](#) who proposed the so called a single-switch-optimized sample ordering scheme. The approach is based on iterative switching of the pair of samples of table 3.1 which gives the greatest reduction in error. The authors showed that their technique clearly performs well enough, but it may still converge to a non-optimum ordering. A different method is needed for simulation of both uncorrelated and correlated random variables. Such methods should be efficient enough: reliable, robust and fast, see chapter 3.3.

Note that the best possible result is obtained if all possible combinations of ranks for each row (variable) itself in table 3.1 are treated. It would be necessary to try extremely large number of rank combinations (and compute estimations of correlation matrices)

$$(N_{Sim})^{N_V-1} \quad (3.11)$$

It is clear that this rough approach is hardly applicable in spite of the fast development of computer hardware.

The number given by (3.11) represents *all equiprobable possible correlation matrices* (orderings of samples in table 3.1) in case when ordering is left random as proposed by [Iman and Conover \(1980\)](#). Here we clearly see that the only “randomness” in LHS as described above is driven by the relative ordering of samples (being sampled according to the deterministic sampling strategy, Eqs. 3.3 or 3.4).

Note that in the computational core of software FREET (see appendix A, p. 125) developed by author this “brute force” approach of testing of all possible ordering is implemented for testing purposes. However, the experience shows that in real applications it is practically not possible to test all sample orderings.

Comments on random vector’s sampling

In fact the task in multivariate LHS is to generate samples of random vector \mathbf{Y} with N_V univariate marginal components. However, practically the information available is restricted to (i) PDF of all random variables (marginals) and (ii) a correlation matrix. This does not provide us with the joint PDF of the whole random vector. If we had such information the correct procedure would be as follows: space of all admissible \mathbf{Y} -vector values should be divided into N_{Sim} equiprobable disjoint regions (of dimension N_V and probability $1/N_{Sim}$). Each region would be represented by one sample. Sampling than cover equally all possible values and the correlation structure is kept automatically. Unfortunately the explicit form of the (simultaneous) joint probability density function with any admissible correlation structure is restricted only to N -dimensional Gaussian random vector and several other particular potentialities. Majority of existing models for random vectors however, are restricted to the bivariate case and/or can only describe the small correlation between variables. Two models based on the earlier works of Nataf and Morgenstern are recommended by [Liu and Der Kiureghian \(1986\)](#). The two models are the Rosenblatt transformation due to [Segal \(1938\)](#) and [Rosenblatt \(1952\)](#) suggested by ([Hohenbichler and Rackwitz, 1981](#)) and Nataf transformation ([Nataf, 1962](#)). The former transformation requires work with a sequence of conditional distributions and is a one-to-one provided each conditional CDF is a strictly increasing function of its arguments. Transformation is convenient only if the conditional distributions are easily obtainable. Another drawback is that the transformation is dependent on the ordering of basic random variables (sequence of conditional CDF). The Nataf transformation is more flexible and allows wider range of correlation coefficients however, it employs iterative solutions of integrals on infinite domains which may become numerically unstable. Due to the limitations of both the models, this section shows approaches to find a solution of the problem by changing ranks of the samples instead of their values, while the marginal probability density functions remain intact. Note that in practise of civil engineer the information about joint PDF of a random vector is not available and the most often case is that when specification of marginal distributions or correlation structure (measured, found in literature) is more or less just rough estimate. Therefore we leave such concept and the idea of this work is to find a tool which is robust, independent of marginal distributions, sufficiently general in scope and fast.

The foreshadowed obstacles are possibly the reason why all authors cited in the preceding sections worked with sampling of marginal in one-dimensional space and combined these samples with the risk

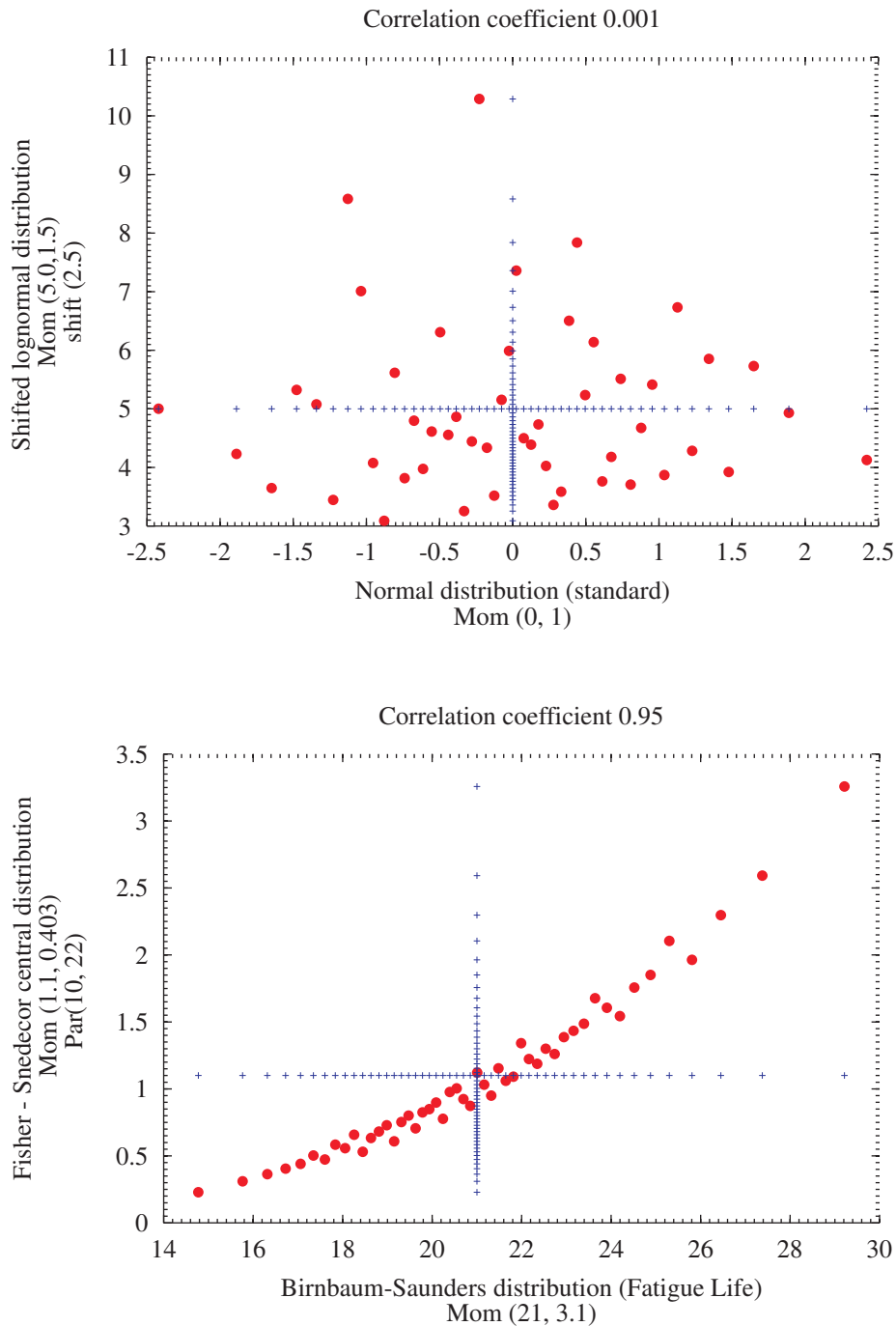


Figure 3.2: Top: Example of statistically independent samples representing two-dimensional PDF; Bottom: Example of strong positive statistical dependence between samples from random vector

that no meaningful joint PDF of random vectors are obtained. All approaches discussed above and further presume the imposition of the target correlation structure only by matrix (table 3.1) manipulations. The task can be understood as the sample simulation of the multivariate distribution model consistent with the prescribed marginals and covariances. So we leave the concept of samples selection out of N_V -dimensional PDF.

We are able to immediately visually check the correctness of sampling using the histograms of each random variable (see Fig. A.11, p. 132 for the dialogs implemented in the software FREET) and the pairs of random variables for the sake of checking the correlation, see figures 3.2, 3.3 and Fig. A.12 (p.

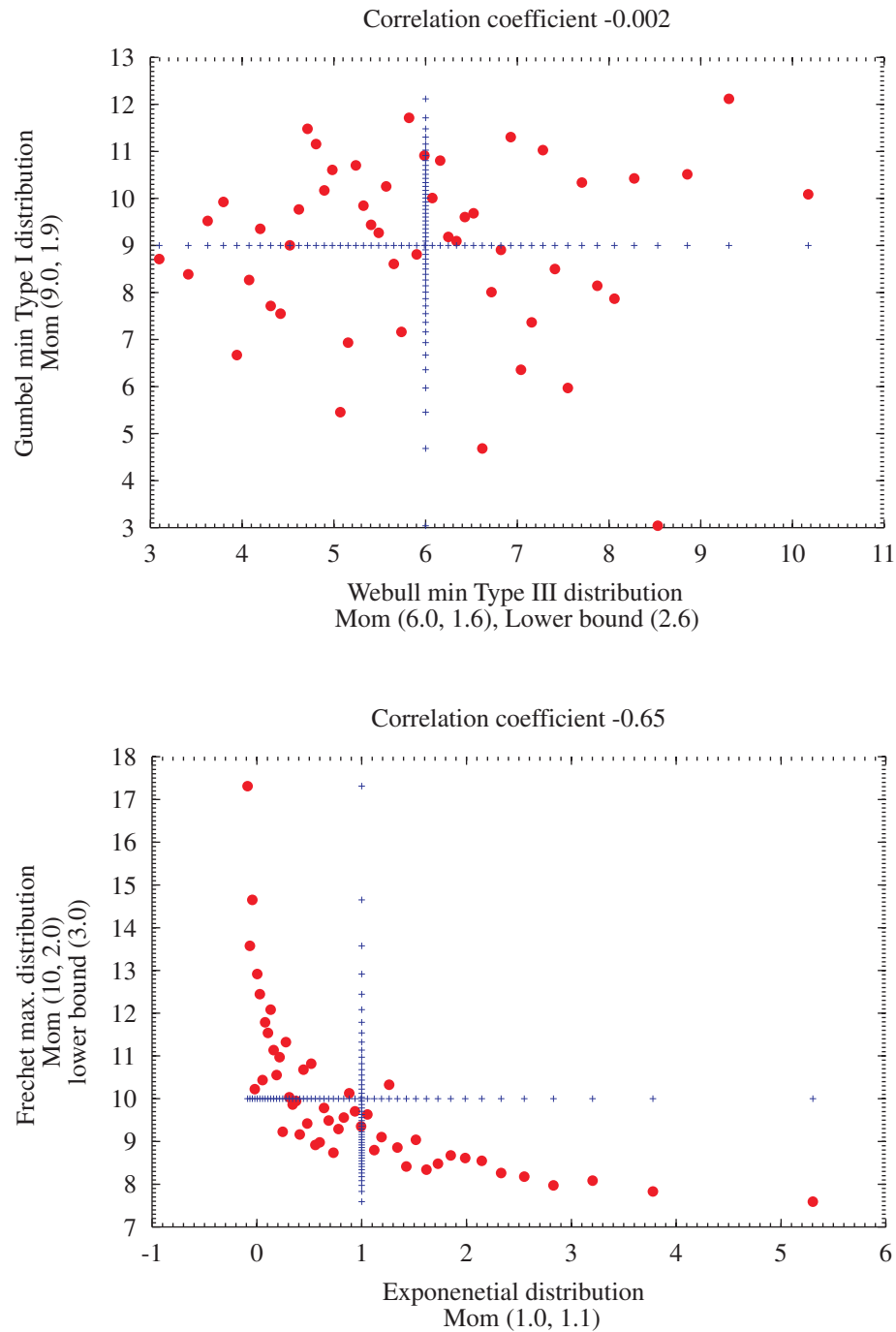


Figure 3.3: Top: Another example of statistically independent samples;
 Bottom: Example of negative statistical dependence between samples representing random vector

132) for the dialog implemented in FREET software (appendix A).

Of course, the correctness of the following technique (based on rank manipulations) should be confirmed using goodness-of-fit tests: it should be tested whether the samples simulated by the approach can represent some joint PDF of random vector. These test should be performed for cases when the joint PDF can be explicitly constructed and is known.

3.3 Stochastic optimization method Simulated Annealing

The imposition of prescribed correlation matrix into sampling scheme can be understood as an optimization problem: The difference between the prescribed \mathbf{K} and estimated (generated) \mathbf{S} correlation matrices should be as small as possible. A suitable measure of the distance between \mathbf{K} and \mathbf{S} matrices can be introduced; a possible norm is the maximal difference of correlation coefficients between matrices:

$$E_{max} = \max_{1 \leq i < j \leq N_V} |S_{i,j} - K_{i,j}| \quad (3.12)$$

or a norm E which takes into account deviations of all correlation coefficients can be more suitable:

$$E_{overall} = \sqrt{\sum_{i=1}^{N_V-1} \sum_{j=i+1}^{N_V} (S_{i,j} - K_{i,j})^2} \quad (3.13)$$

This norm can further be normalized with respect to the number of considered correlation coefficients (entries of lower triangle in the table 3.2):

$$\hat{E}_{overall} = \frac{E_{overall}}{\sum_{1 \leq i < j \leq N_V} 1} = \frac{2E_{overall}}{N_V(N_V - 1)} \quad (3.14)$$

which represents an error per entry and is therefore suitable for comparison when examples of different number of variables involved N_V is to be performed.

The norm E has to be minimized, from the point of view of definition of optimization problem, the *objective function* is E and the *design variables* are related to *ordering* in sampling scheme (table 3.1).

It is well known that deterministic optimization techniques and simple stochastic optimization approaches can very often fail to find the global minimum (Laarhoven and Aarts, 1987; Otten and Ginneken, 1989). They are generally strongly dependent on starting point (in our case the initial configuration of sampling scheme). Such techniques fail and finish with some local minimum such that there is no chance to escape from it – and to find the global minimum (Fig. 3.4). The ball in the illustrative figure is jumping from one minimum to another minimum in case that this energy landscape has a high energy (for understanding let us imagine shaking of landscape). If the energy is low, the ball will remain in one of the minima - local or global one. It is obvious, that the best procedure to find the global minimum is to start with high energy (temperature) and then step by step decrease this temperature to almost zero (*freezing* or *cooling schedule*). During such process the lowest position of the ball has to be monitored: at the end it corresponds to global minimum (or at least to a “very good” local one). It can be intuitively predicted that in our problem we are definitely facing the problem with multiple local minima. Therefore we need to use the stochastic optimization method which works with nonzero probability of escaping from local minima. The simplest form is the two-membered evolution strategy which works in two steps: **mutation** and **selection**.

Step 1 (mutation): In the r -th generation a new arrangement of random permutations matrix used in LHS is obtained using random changes of ranks, one change is applied for one random variable. Generation should be performed randomly. The objective function (norm E) can be then calculated using newly obtained correlation matrix (it is called “offspring norm” and the norm E calculated using former arrangement is called “parent norm”).

Step 2 (selection): The selection chooses the best norm between the “parent” and “offspring” to survive: For the new generation (permutation table arrangement) the best individual (table arrangement) has to give a value of objective function (norm E) smaller than before.

Such approach has been intensively tested using numerous examples. It was observed that the method in most cases could not capture the global minimum. It failed in a local minimum and there was no chance to escape from it, as only the improvement of the norm E resulted in acceptance of “offspring”. More efficient technique had to be applied. The step “Selection” can be improved by Simulated Annealing approach, a technique which is very robust concerning the starting point (initial arrangement of random permutations table). The Simulated Annealing is optimization algorithm based on randomization techniques and incorporates aspects of iterative improvement algorithms. The method represents the analogy with annealing of crystals. The difference compared to simple approach described above is that there

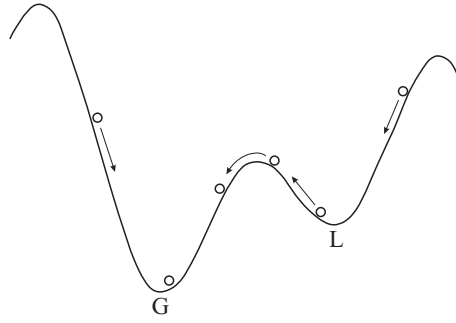


Figure 3.4: Energy landscape - problem of local and global minimum

is a chance to accept offspring leading to a worse norm E and such chance is based on the Boltzmann probability distribution:

$$P_r(\Delta E) \approx e^{\left(\frac{-\Delta E}{k_b \cdot T}\right)} \quad (3.15)$$

where ΔE is the difference between the norms E before and after random change (parent and offspring norm). This probability distribution expresses the concept when a system in thermal equilibrium at temperature T has its energy probabilistically distributed among all different energy states ΔE . Boltzmann constant k_b relates temperature and energy of the system. Even at low temperatures, there is a chance (although very small) of a system being locally in a high energy state. Therefore, there is a corresponding possibility for the system to move from a local energy minimum in favor of finding a better minimum. In other words, there is some probability to escape from local minimum. There are two possible branches to proceed in the step 2 (selection):

1. New arrangement (offspring) results in decrease of the norm E . Naturally “offspring” is accepted for the new generation.
2. New arrangement does not decrease the norm E . Such “offspring” is accepted with the probability given by (3.15). This probability changes as the temperature T changes.

As a result there is much higher probability that the global minimum is found in comparison with deterministic methods and simple evolution strategies.

Constant k_b relates E and T ; however, it can be considered to be equal to one in our case because both quantities share the same units of correlation measure. In classical application of Simulated Annealing approach for optimization there is one problem: how to set the initial temperature T ? Usually it should be considered heuristically. Fortunately, our problem is constrained in the sense that all possible elements of correlation matrix are always within the interval $\langle -1; 1 \rangle$. Based on this fact the maxima of the norms (3.12) and/or (3.13) can be estimated using prescribed and hypothetically “most remote” matrices \mathbf{K} from \mathbf{S} (filled with unit correlation coefficients, plus or minus). This approach represents a significant advantage: The heuristic estimation of initial temperature is neglected, the initial setting of parameters can be performed without the guess of the user and the “trial and error” procedure.

The initial temperature has to be decreased step by step, e.g. using reduction factor f_T after constant number of iterations (e.g. thousands) applied at temperature T_i :

$$T_{i+1} = T_i \cdot f_T \quad (3.16)$$

The simple case is to use e.g. $f_T = 0.95$. Note that more sophisticated cooling schedules are known in Simulated Annealing theory (Laarhoven and Aarts, 1987; Otten and Ginneken, 1989).

Figure 3.5 shows the general implementation of Simulated Annealing in C language. The three parameters of the method are emphasized by color and are printed in bold. All parameters can be set by user in the FREET software (see appendix A) however, they can be set automatically as described above.

```

T = T_start; //set the initial teperature
initial_arrangement(); //generate parent
E_parent = compute_E(); //compute parent norm
do{
  for(int i=0 ; i<LOOPS ; i++){
    set_change(); //generate offspring
    E_offspr = compute_E(); //compute offspring norm

    if ( E_best > E_offspr){ //seek for the best generation
      E_best = E_offspr;
      save_best_arrangement();
    }

    if ( E_parent > E_offspr){ //accept improved generation
      E_parent = E_offspr;
    }else{ //simulated annealing to decide
      dE = E_offspr - E_parent; //norm difference
      u = rand(0,1); //random number
      if(u > exp(-dE/T) ) back_change(); //not accepted
      else E_parent = E_offspr; // accepted
    }
  }
  T = T*0.95; //cooling
}while(T > T_min);

//here we accept the best arrangement from the whole process

```

Figure 3.5: Sketch of Simulated Annealing algorithm implementation in C

3.4 Numerical examples

3.4.1 Correlated properties of concrete

In order to illustrate the efficiency of the developed technique, consider an example of correlation matrix, which corresponds to properties of a concrete. They are described by 7 random variables, prescribed correlation matrix is presented in lower triangle. Upper triangle shows estimated statistical correlation after application of Simulated Annealing (SA), for two different number of LHS-simulations (8, 64). Final values of norms are included: first line corresponds to norm (3.12) second line (bold) means overall norm (3.13).

$$\mathbf{K}_8 = \begin{pmatrix} 1 & -0.017 & 0.700 & 0.863 & -0.026 & 0.487 & 0.875 \\ 0 & 1 & 0.020 & 0.067 & -0.039 & 0.104 & -0.017 \\ 0.7 & 0 & 1 & 0.729 & -0.016 & 0.823 & 0.700 \\ 0.9 & 0.1 & 0.8 & 1 & 0.024 & 0.543 & 0.863 \\ 0 & 0 & 0 & 0 & 1 & 0.031 & -0.026 \\ 0.5 & 0.1 & 0.9 & 0.6 & 0 & 1 & 0.487 \\ 0.9 & 0 & 0.6 & 0.9 & 0 & 0.5 & 1 \end{pmatrix}, \quad \mathbf{E}_8 = \begin{pmatrix} 0.0996 \\ \mathbf{0.186} \end{pmatrix}$$

$$\mathbf{K}_{64} = \begin{pmatrix} 1 & -0.001 & 0.697 & 0.902 & 0.000 & 0.502 & 0.898 \\ 0 & 1 & 0.0041 & 0.099 & 0.000 & 0.099 & 0.001 \\ 0.7 & 0 & 1 & 0.793 & 0.000 & 0.895 & 0.605 \\ 0.9 & 0.1 & 0.8 & 1 & 0.000 & 0.604 & 0.894 \\ 0 & 0 & 0 & 0 & 1 & 0.000 & 0.000 \\ 0.5 & 0.1 & 0.9 & 0.6 & 0 & 1 & 0.497 \\ 0.9 & 0 & 0.6 & 0.9 & 0 & 0.5 & 1 \end{pmatrix}, \quad \mathbf{E}_{64} = \begin{pmatrix} 0.0073 \\ \mathbf{0.014} \end{pmatrix}$$

It can be seen that as the number of simulations increases, the estimated correlation matrix is closer to the target one. Using standard PC (400MHz CPU) the computer time needed to run the SA algorithm

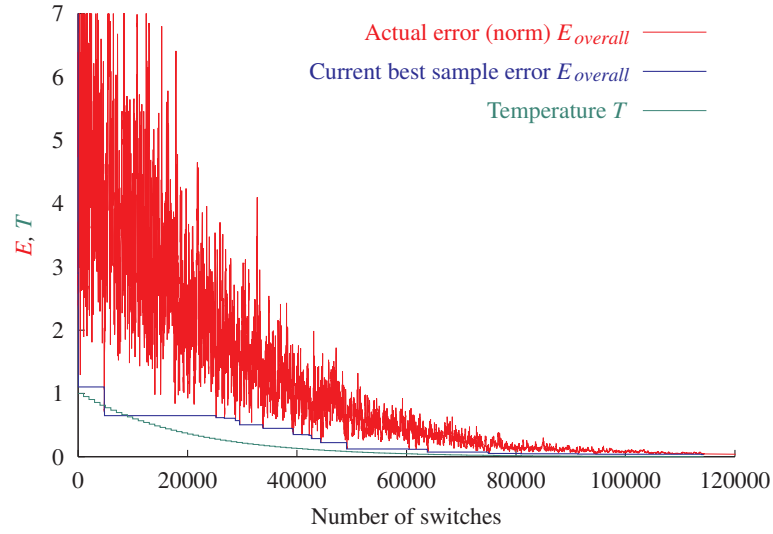


Figure 3.6: The norm E (error) vs. number of random changes; see Fig. A.9 for the image as implemented in FREET software

took about two seconds. Figure 3.6 shows the decrease of norm E during SA-process. Such figure is typical and should be monitored. An identical figure is displayed in the software FREET, see Fig. A.9 (p. 131).

3.4.2 Non-positive definite prescribed correlation matrix?

In real applications of LHS technique in engineering, statistical correlation represents very often a weak part of a priori assumptions. Because of this poor knowledge the prescribed correlation matrix \mathbf{K} on input can be non-positive definite. The user can face difficulties to update correlation coefficients in order to make the matrix positive definite, see Fig. A.6, p. 129. The example presented here demonstrates that when a non-positive definite matrix is on input, Simulated Annealing can work with it and of course, the resulting correlation matrix is positive definite. It is as close as possible to originally prescribed matrix but the dominant constraint (positive definiteness) is satisfied automatically.

Let us consider a really very unrealistic simple case of statistical correlation for three random variables A, B and C according to the matrix \mathbf{K} (columns and rows correspond to the ranks of variables A, B, C):

$$\mathbf{K} = \begin{pmatrix} 1 & 0.9 & 0.9 \\ & 1 & -0.9 \\ \text{symm.} & & 1 \end{pmatrix} \quad \rightarrow_{\text{optim.}} \quad \mathbf{S}_{(1)} = \begin{pmatrix} 1 & 0.499 & 0.499 \\ & 1 & -0.499 \\ & & 1 \end{pmatrix}, \quad \mathbf{E}_{(1)} = \begin{pmatrix} 0.401 \\ \mathbf{0.695} \end{pmatrix}$$

The correlation matrix is obviously not positive definite. Strong positive statistical correlation is required between the pairs of variables (A, B) and (A, C), but strong negative correlation between variables (B, C). It is clear that only compromise solution can be done. The method resulted in such compromise solution without any problem, $\mathbf{S}_{(1)}$ (number of simulations N_{Sim} was high enough to avoid limitation in number of rank combinations). This feature of the method can be accepted and interpreted as an advantage of the method. In practical reliability problems with non-positive definiteness exist (lack of knowledge). It represents the serious limitation for usage of some other methods (Cholesky decomposition of prescribed correlation matrix).

In real applications it can be a greater confidence to one correlation coefficient (good data) and a smaller confidence to another one (just estimation). Solution to such problems is weighted computation of both norms (3.12) and (3.13) – *Weighted Simulated Annealing Optimization Method*. For example the norm (3.13) can be modified in this way:

$$E_{\text{overall},w} = \sqrt{\sum_{i=1}^{N_V-1} \sum_{j=i+1}^{N_V} w_{i,j} \cdot (S_{i,j} - K_{i,j})^2} \quad (3.17)$$

where $w_{i,j}$ is weight of a particular correlation coefficient $K_{i,j}$.

In the spirit of thoughts leading to norm given by equation (3.14), we can standardize the result by total number of weights such that we reach comparability to case with different number of variables involved or different values of the weights:

$$\hat{E}_{overall,w} = \frac{E_{overall,w}}{\sum_{1 \leq i < j \leq N_v} \sqrt{w_{i,j}}} \quad (3.18)$$

This norm is the most universal and proved itself to be a good objective function for optimization algorithm described above. Note that this norm shrinks to the simple formula (3.13) in case of no weighting (unit weights are used).

Several examples of choices and resulting correlation matrices (with both norms) follow. Resulting matrices $\mathbf{S}_{(2)}$ and $\mathbf{S}_{(3)}$ demonstrate similarity of resulting errors (equivalent weights – symmetry) while $\mathbf{S}_{(4)}$ and $\mathbf{S}_{(5)}$ illustrate significance of proportions between weights. Matrix \mathbf{K} is targeted again. The weights $w_{i,j}$ are given in lower triangle. Weights of accentuated members and resulting values $S_{i,j}$ are underlined.

Table 3.3: Numerical study of weighted simulated annealing optimization with non-positive definite matrix \mathbf{K}

Norm name: Equation:		E_{max} (3.12)	$E_{overall}$ (3.13)	$E_{overall,w}$ (3.17, targeted)	$\hat{E}_{overall,w}$ (3.18)
$\mathbf{S}_{(2)}$	$= \begin{pmatrix} \mathbf{1} & 0.311 & 0.311 \\ 1 & \mathbf{1} & \underline{-0.806} \\ 1 & \underline{10} & \mathbf{1} \end{pmatrix}$	0.589	0.838	0.884	0.171
$\mathbf{S}_{(3)}$	$= \begin{pmatrix} \mathbf{1} & 0.311 & \underline{0.806} \\ 1 & \mathbf{1} & -0.311 \\ \underline{10} & 1 & \mathbf{1} \end{pmatrix}$	0.589	0.838	0.884	0.171
$\mathbf{S}_{(4)}$	$= \begin{pmatrix} \mathbf{1} & 0.355 & 0.355 \\ 1 & \mathbf{1} & \underline{-0.747} \\ 1 & \underline{5} & \mathbf{1} \end{pmatrix}$	0.545	0.786	0.843	0.199
$\mathbf{S}_{(5)}$	$= \begin{pmatrix} \mathbf{1} & 0.236 & 0.236 \\ 1 & \mathbf{1} & \underline{-0.888} \\ 1 & \underline{100} & \mathbf{1} \end{pmatrix}$	0.664	0.939	0.947	0.079

3.5 Concluding remarks

The increased efficiency of LHS can be achieved by the proper selection of samples representing the layered probability content of random variables. The solution to this lead to explicit formulas in many cases. Unfortunately in some cases an additional integration must be done numerically since the integral may not be solvable in closed form. However, the extra effort of doing the numerical integration is justified by the statistical accuracy gained.

The new efficient technique of imposing the statistical correlation when using LHS is suggested. The technique is robust, efficient and very fast. The method has several advantages in comparison with former techniques:

- The technique uses only changes of ranks in sampling matrix. Number of simulations does not increase CPU time in practical cases, but for increasing number of random variables more SA simulations is needed to achieve a good accuracy. The technique is robust, Simulated Annealing can be terminated if the error (norm) is acceptable (users decision).

- The problem of imposing statistical correlation is constrained precisely, therefore the initial temperature for annealing can be estimated.
- The technique can work also with non-positive definitive matrices defined unconsciously by user as input data.

The methods are implemented by author in C++ programming language in forms in dynamically linked libraries (DLL) and constitutes the computation core of the multipurpose software package FREET based on LHS for statistical, sensitivity and reliability analysis of computational problems, see appendix [A](#).

Chapter 4

Simulation of random fields and error assessment

Published in papers: [Vořechovský and Novák \(2003a\)](#); [Novák and Vořechovský \(2004\)](#)

4.1 Introduction

Stochastic finite element method (SFEM) had facilitated the use of random fields in computational mechanics. Many material and other parameters are uncertain in nature and/or exhibit random spatial variability. Efficient simulation of random fields for problems of stochastic continuum mechanics is in the focus of both researchers and engineers. Achievements in stochastic finite element approaches increased the need for accurate representation and simulation of random fields to model spatially distributed uncertain parameters.

The spatial variability of mechanical and geometrical properties of a system and intensity of load can be conveniently represented by means of random fields. Because of the discrete nature of the finite element formulation, the random field must also be discretized into random variables. This process is commonly known as random field discretization. Various methods have been developed for the representation and simulation of random fields utilized within the framework of SFEM (e.g. [Vanmarcke et al., 1986](#); [Yamazaki et al., 1988](#); [Schuëller et al., 1990](#); [Liu et al., 1995](#), and many others). Most available algorithms for random fields simulation are based on spectral representation theorem, random field is represented approximately by a finite number of waves with random amplitude and/or phase and/or frequency, (e.g. [Spanos and Ghanem, 1989](#); [Ghanem and Spanos, 1991](#)). Nowadays many types of random fields representation exist, such as *spectral representation methods*, *time- and frequency-domain hybrid simulation methods*, *covariance decomposition methods*.

In following we will deal with random fields simulation based on *orthogonal transformation of covariance matrix* in connection with different types of Monte Carlo simulation. Methodology is closely related to *Karhunen-Loève expansion* ([Loève, 1977](#)). These methods produce stationary and ergodic Gaussian processes, transformations into another distributions (translations) will be mentioned in section 4.3. We will focus on error assessment of simulated fields and utilization of LHS methodology thoroughly discussed in the preceding chapter.

The computational effort in reliability problem is proportional to the number of random variables, therefore it is desirable to use small number of random variables to represent a random field. Simulation of the random field by a few random variables is especially suitable for problems where theoretical failure probability should be calculated. It enables an efficient use of advanced simulation techniques based on *importance sampling* ([Brenner, 1991](#); [Vořechovský, 2000a](#)). To achieve this goal, the transformation of the original random variables into a set of uncorrelated random variables can be performed through an eigenvalue orthogonalization procedure ([Schuëller et al., 1990](#); [Liu et al., 1995](#)). It is demonstrated that a few of these uncorrelated variables with largest eigenvalues are sufficient for the accurate representation of the random field. The error induced by such truncation will be an object of study in this chapter as well.

4.2 Orthogonal transformation of covariance matrix

Suppose that a spatial variability of random parameter is described by the Gaussian random field $a(\mathbf{x})$, $\mathbf{x} = (x, y, z)$ is the vector coordinate which determines the position on the structure. Numerical analysis requires a discrete representation of random field. A continuous field $a(\mathbf{x})$ is described by discrete values $a(\mathbf{x}_i) = a(x_i, y_i, z_i)$, where $i = 1, \dots, N$ denotes the discretization point.

As the randomness of the spatial variability in *3-dimensional* nature is generally not isotropic, the autocorrelation function of the spatial homogeneous random field is supposed to be a function of the distances between two points $|\Delta x|$, $|\Delta y|$ and $|\Delta z|$. The following commonly used exponential form of an autocorrelation function is considered:

$$R_{aa}(\Delta x, \Delta y, \Delta z) = \sigma^2 \cdot \exp \left[- \left(\frac{|\Delta x|}{d_x} \right)^{pow} - \left(\frac{|\Delta y|}{d_y} \right)^{pow} - \left(\frac{|\Delta z|}{d_z} \right)^{pow} \right] \quad (4.1)$$

in which d_x , d_y and d_z are positive parameters called *correlation lengths* and σ is the standard deviation of the random field. With increasing d a stronger statistical correlation of a parameter in space is imposed and opposite. Of course, an isotropic autocorrelation function has all correlation lengths identical. The power pow is usually two which leads to well known *bell-shaped* autocorrelation function. In case of isotropic fields the autocorrelation would depend only on the Euclidian norm.

When the finite element method is used, the structure is divided into an appropriate number of finite elements of small sizes. The size of each finite element must be small enough from the material property variability (correlation length), as well as from the stress/strain gradient point of view. It must be small enough so that the values of random field can be considered approximately constant within each element (or vicinity of an integration point). Note that generally the discretization mesh of random field mesh and finite element mesh may be different. Consider the fluctuating components of the homogenous random field, which is assumed to model the material property variation around its expected value. Then the N values, $a_i = a(\mathbf{x}_i)$, are random with zero mean and autocorrelated. \mathbf{x}_i is the location of the centroid of element i or integration point (depending on the discretization of random field). Their correlation characteristics can be specified in term of the covariance matrix C_{aa} , whose ij -component is given by:

$$c_{ij} = Cov[a_i a_j] = R_{aa}(\Delta x_{i,j}, \Delta y_{i,j}, \Delta z_{i,j}) \quad (4.2)$$

The random variables can be transformed to the uncorrelated normal form by solution of an eigenvalue problem (e.g. Schuëller et al., 1990; Liu et al., 1995). In order to reduce the computational effort, an eigenvalue orthogonalization procedure can be employed:

$$\mathbf{C}_{\mathbf{X}\mathbf{X}} = \mathbf{\Phi} \mathbf{\Lambda} \mathbf{\Phi}^T \quad (4.3)$$

where $\mathbf{C}_{\mathbf{X}\mathbf{X}}$ is the covariance matrix (for unit variance, $\sigma^2 = 1$). The matrix $\mathbf{\Phi}$ represents the orthogonal transformation matrix (eigenvectors). The covariance matrix in the uncorrelated space \mathbf{Y} is diagonal matrix $\mathbf{\Lambda}$:

$$\mathbf{C}_{\mathbf{Y}\mathbf{Y}} = \mathbf{\Lambda} \quad (4.4)$$

where the elements of diagonal are the eigenvalues ($\lambda_1, \lambda_2, \dots, \lambda_N$) of covariance matrix $\mathbf{C}_{\mathbf{X}\mathbf{X}}$.

Usually, not all eigenvalues have to be calculated and considered for next step (simulation) as the fluctuations can be described almost completely by a few random variables. This can be done by arranging the eigenvalues in descending order, calculating the sum of the eigenvalues up to the i -th eigenvalue and dividing it by trace of $\mathbf{\Lambda}$. The reduction of number of random variables in fact depends on relationships between total dimensions and discretization of the structure (model) and given correlation lengths. If the random properties of closely adjacent elements are correlated, the original (full) set of random variables can be represented by a smaller number of uncorrelated random variables. Example of description of the randomness by the most important random variables is given in Fig. 4.2. And in addition to, reduction could be a corollary of a truncation error in solution of eigenvalues of $\mathbf{C}_{\mathbf{X}\mathbf{X}}$. In cases when correlation lengths are comparable to total dimensions of heavily discretized model the solution of eigenvalues of assembled covariance matrix results in a few dominant eigenvalues and many small eigenvalues. The latter eigenvalues (variabilities of assigned random variables) does not to be included. For example if

the smallest found eigenvalue is $1 \cdot 10^{-15}$, then corresponding random variable have standard deviation $\sqrt{1 \cdot 10^{-15}} = 3.16 \cdot 10^{-8}$.

Let the chosen number of important dominating random variables by eigenvalue analysis be N_V . Now, the eigenvector matrix Φ denotes the reduced eigenvector matrix containing only the respective eigenvectors to the N_V most important eigenvalues. Then the vector of uncorrelated Gaussian random variables $\mathbf{Y}^T = [Y_1, Y_2, \dots, Y_{N_V}]$ can be simulated by a traditional way (Monte Carlo simulation). The random variables of vector \mathbf{Y} have mean zero and standard deviation $\sqrt{\lambda_1}, \sqrt{\lambda_2}, \dots, \sqrt{\lambda_{N_V}}$. The transformation back into correlated space yields the random vector \mathbf{X} by the relation:

$$\mathbf{X} = \Phi \mathbf{Y} \quad (4.5)$$

As already mentioned, the procedure enables significant reduction of uncorrelated random variables for representation of random field especially for higher values of correlation length. These random variables can be simply generated by plain MCS, representation of random field is formed via formula (4.5).

Note that such reduction depends on:

1. *Correlation length of random field*: Only if correlation length is large (with respect to dimension of structure and discretization) the reduction is progressive. In limiting case when correlation length approaches infinity, the result is that random field can be represented by one random variable only (random field is equivalent to random variable). Opposite, if correlation length approaches zero, no reduction is possible and all random variables have to be involved for proper representation of random field.

2. *The criterion selected for reduction*: Naturally used criterion is based on control of variability captured by reduced set of random variables. Eigenvalue matrix of covariance matrix of \mathbf{Y} contains variances of random variables. They are equivalent to eigenvalues, only the largest eigenvalues are dominating and should be used. The question ‘‘how many?’’ can be answered by calculating the ratio of contribution of eigenvalues to the overall variability of field. Note that the selection is a compromise solution: Less variables is used less variability is captured. The reduction results generally to simulation of random field which have variance smaller than required. A certain underestimation of this statistics will always occur.

There are two major computational burdens associated with the method:

1. *Solution of eigenvalue problem*. This may be seen as a serious drawback of the technique for large SFEM system. But such initial computational effort is rewarded later at the step of Monte Carlo simulation resulting in efficient and transparent technique.
2. *Simulation of uncorrelated random variables*. Answers to this problem can be found in chapter 3 where a new stable, reliable and efficient generator of correlated random variables is presented.

The main advantage of this approach is that advanced simulation techniques based on the concept of importance sampling can be used for reliability calculations because these techniques can usually work efficiently under the set of limited number of random variables. The possibility of determination of theoretical failure probability with a good numerical accuracy is then guaranteed.

4.3 Latin Hypercube Sampling utilization

Majority of papers on LHS is focused on the level of random variables and LHS is rarely employed for random fields simulation in SFEM. The aim of this chapter is to repeat the possibility of improvement of the method based on orthogonal transformation of covariance matrix for random field simulation, suggested e.g. by Novák et al. (2000) and to show some new improvements to the method. The approach is based on utilization of stratified sampling technique LHS for simulation of dominating uncorrelated random variables which are gained through eigenvalue analysis of covariance matrix. The result of this combination is that only a few random variables and quite small number of simulations is necessary for accurate representation of a random field. A comparison with classical Monte Carlo simulation (MCS) reveals the superior efficiency and accuracy of the method. A parametric studies focused on the quality of simulated random fields (target statistical parameters and simulated statistical characteristics of random field) are presented later. An emphasize is given to the region of very small numbers of simulations

(tens, hundreds). This is particularly important for SFEM analysis of complex computationally intensive problems (e.g. nonlinear FEM modeling) leading to a considerable need of CPU-time. The quality of the representation of the structural response is closely related to the quality of the random fields.

Small number of simulations can be used for acceptable accuracy using some stratified sampling, one often used alternative is LHS technique. This technique belongs to the category of advanced simulation methods (McKay et al., 1979; Iman and Conover, 1980; Iman and Shortencarier, 1984). The idea of LHS is discussed in chapter (3). Utilization of LHS method for simulation of Gaussian uncorrelated variables as described in previous section (reduced space of variables) is the simple idea of improvement of random field simulation using orthogonal transformation of covariance matrix. The keypoint is that matrix \mathbf{Y} of random variables from the uncorrelated space is assembled with utilization of stratified sampling LHS. It is expected that the superiority of this stratified technique comparing MCS will continue also for accurate representation of random field, thus leading to a decrease of number of simulations needed. This should be proved at least numerically. The methodology for an assessment of error of simulations is described in section 4.4, numerical examples inclusive.

Transformation to non-gaussian processes

Simulation of the discretized random field has to take care of considerable correlations and non-Gaussian distributions. This means that a transformation from standard Gaussian space (in which random numbers are generated) to correlated non-Gaussian space has to be carried out. This requires application of the Rosenblatt-transformation. A prerequisite of this transformation is the knowledge of the joint probability density function of all random variables. Usually, this knowledge is limited to marginal distributions and correlations. In this case, the Nataf (1962) model for the joint density is widely used. For application of this model the correlation matrix in standard Gaussian space must be adjusted according to the distribution type. It should be noted that in some situations this may lead to a non-positive definite correlation matrix, which renders the model inapplicable.

Direct transformation method to values of Gaussian random field \mathbf{X} would be applied in discretization points

$$\tilde{X}_{i,j} = F^{-1} [\Phi_N (X_{i,j})] \quad (4.6)$$

where Φ_N is normal CDF and F^{-1} represents inverse of desired CDF.

4.4 Error assessment of random field simulation

When any method for random field simulation is used it is required that the statistical characteristics of the field generated be as close as possible to the target parameters. Generally, the mean values, variances, correlation and spectral characteristics (we will use the common term “statistics”) cannot be generated with absolute accuracy. Basic information about random field is captured by its second moment characteristics, i.e. the mean function μ and the covariance function C_{aa} :

$$\mu(\mathbf{x}) = E[a(\mathbf{x})] \quad (4.7)$$

$$C_{aa}(\mathbf{x}_1, \mathbf{x}_2) = E\{[a(\mathbf{x}_1) - \mu(\mathbf{x}_1)] \cdot [a(\mathbf{x}_2) - \mu(\mathbf{x}_2)]\} \quad (4.8)$$

Some samples of random fields for a parameter are simulated from the population parameters. A certain statistic of the particular simulation may be very close to or quite far away from the value of corresponding target parameter. When the seed of the pseudo-random number generator is changed other random fields are generated and other values of all sample statistics are naturally obtained. Therefore, each of these statistics can be considered as a *random variable* with some mean value and variance. The simulation technique is considered as best one which gives an estimated mean value of the statistics very close to the target mean value and also closest to zero variance of the statistics. In our case of zero mean value and unit variance of random field (basic target statistical parameters) we expect to get estimated mean around zero and variance around one.

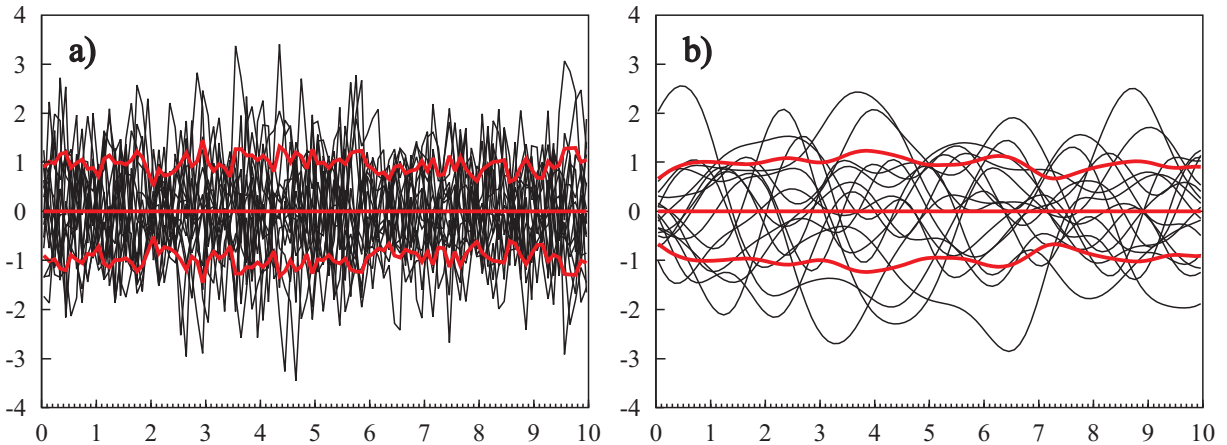


Figure 4.1: Random field realizations for correlation length a) $d = 0.1$ m; and b) $d = 1$ m. Means and \pm standard deviations are plotted.

The assessment can be done by performing more runs of the same simulation process with a different random setting of the seed of pseudo random number generator. Thus samples are artificially generated from the population in this way.

The procedure itemized above is repeated N_{run} times each time with different initial random setting of the seed. Naturally statistics obtained in each run are different, e.g. different mean \bar{a}_s and variance σ_{a_s} . As measures of the accuracy of simulation, the mean values and variances are calculated from N_{run} statistics obtained.

Here should be tackled some extremely important aspects of random fields simulation for stochastic finite element analysis (SFEM): Spurious correlation reduction, a restriction resulting from Cholesky decomposition of covariance matrix, orthogonal transformation of covariance matrix (called sometimes *spectral decomposition*) and the utilization of Latin hypercube sampling (LHS) for random fields simulation. All these aspects are important for computational efficiency, robustness and accuracy in SFEM. A superiority of correlation control LHS was already showed by many researchers, e.g. [Schuëller et al. \(1990\)](#); [Brenner \(1991\)](#); [Liu et al. \(1995\)](#); [Novák et al. \(2000\)](#); [Bucher and Ebert \(2000\)](#) and others. A practical consequence is using small number of simulations of random field to achieve satisfactory accuracy. In spite of these achievements some arising questions remained not answered and remarks should be done.

4.4.1 Reduction of spurious correlation

Sampling scheme of Monte Carlo type methods (such as stratified sampling LHS) can be represented by Table 3.1, where input variables are columns in matrix \mathbf{Y} . Orthogonal transformation of covariance matrix (correlation control, section 4.2) leads to significant improvement – a reduction of number of random variables to represent random field (truncation $N_V \ll N$). These aspects are illustrated in Fig. 4.2 where the sum of eigenvalues divided by trace (portion of normalized variability expressed in percentage) is plotted vs. number of random variables used for representation. The figure is constructed for 1D homogenous stationary normalized Gaussian random field with exponential autocorrelation function, structure size 10 m, two correlation lengths $d = 0.1$ m and $d = 1$ m, $N = 128$. It can be seen that in order to capture the variability of random field, smaller number of random variables r is needed in case of larger correlation length. For example, in order to simulate 95 % of variability we need only $N_V = 10$ in case $d = 1$ m, but for $d = 0.1$ m $N_V = 89$.

What are the consequences of spurious correlation to autocorrelation function variability of simulated random fields? The study has been done for correlation length 1 m and for two numbers of simulations – an error assessment based on samples simulations from population is described later. From all 128 random variables only 52 has been used after orthogonalization procedure to represent random field (the smallest eigenvalue taken into account was $1 \cdot 10^{-15}$, which represents a random variable with negligible standard deviation). The results are shown in Fig. 4.3, mean values and the scatterband represented

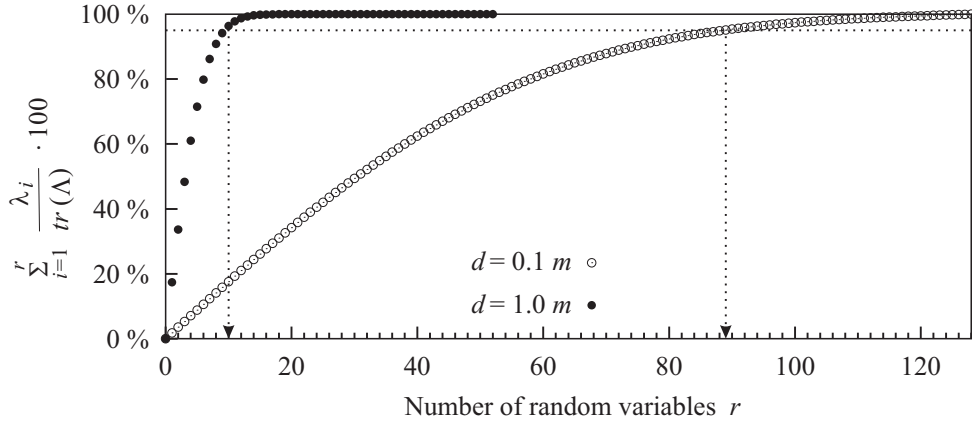


Figure 4.2: Reduction of number of random variables based on normalized variability.

by mean \pm standard deviation of autocorrelation function is plotted. Figure 4.3a) shows the result for $N_{Sim} = 32$, spurious correlation is not diminished (LHS-mean-SC). It is obvious that capturing of target autocorrelation function is weak and the scatterband is large. The explanation is clear, using only $N_{Sim} = 32$ leads to large both norms (3.12) and (3.13), see page 26. Only a slight improvement can be seen if spurious correlation is diminished (LHS-mean-SCD), Fig. 4.3b). When N_{Sim} increases to 64, capturing of autocorrelation function is better, Fig. 4.3c), d). Note that now the alternative with diminished spurious correlation by SA resulted in excellent function capturing with very small variability, see figure 4.3d). This fact corresponds with both norms which are in case d) very small. It can be seen that the spurious correlation at the level of simulation of independent random variables influences negatively the autocorrelation function. These illustrative figures also clearly indicate that norms used as objective functions in Simulated Annealing algorithm (section 3.3) can be interpreted as a qualitative prediction of resulting quality of autocorrelation structure.

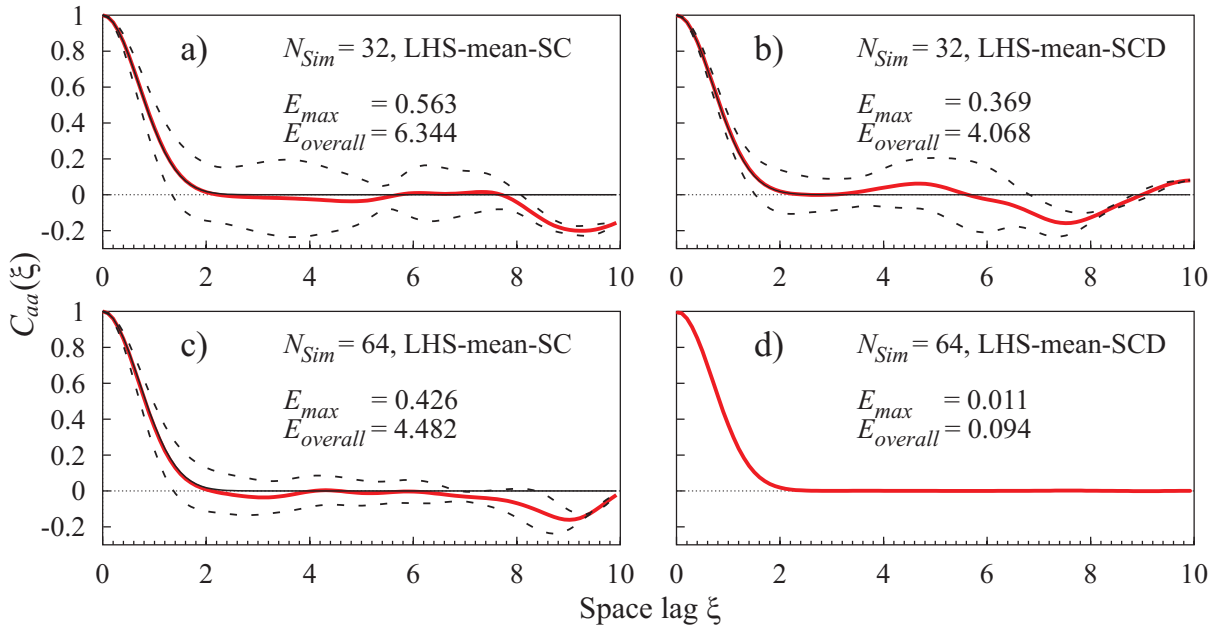


Figure 4.3: Scatterband of autocorrelation function $C_{aa}(\xi)$ for $N_{Sim} = 32$: a) LHS-mean-SC; b) LHS-mean-SCD; and $N_{Sim} = 64$: c) LHS-mean-SC; d) LHS-mean-SCD

4.4.2 Classification of sampling schemes

Next comment should be given to present state of art of LHS procedures. LHS is utilized by authors for simulation of statistically uncorrelated random variables with Gaussian distribution. The classical approach is to use centroids of layers on distribution function to obtain realizations (see mapping represented by formula (6) of the discussed paper). [Huntington and Lyrintzis \(1998\)](#) showed that this approach gives samples with a mean close to desired one, but sample variances can be significantly different. They proposed a new sampling scheme (also used by [Keramat and Kielbasa \(1997\)](#) (section 3.2). All possibilities of sampling method can be summarized as follows:

- crude Monte Carlo simulation (MCS);
- Latin hypercube sampling under original scheme, [McKay et al. \(1979\)](#), (LHS-median);
- Latin hypercube sampling under improved scheme, [Huntington and Lyrintzis \(1998\)](#) (LHS-mean).

These schemes can be applied in two alternatives:

- No attention is paid to spurious correlation (SC);
- Spurious correlation diminished (SCD)

There are three different method to diminish spurious correlation available nowadays: Method based on Cholesky decomposition of covariance matrix, ([Iman and Conover, 1982](#)); Single-switch optimization scheme, ([Huntington and Lyrintzis, 1998](#)); Method based on simulated annealing due to [Vořechovský and Novák \(2002\)](#) which will be used in the following.

There are 6 combinations, cases with SC and SCD, which are sampled by MC, LHS-half and LHS-mean. What is the best alternative? Naturally, the quality of sampling schemes can be intuitively predicted even without numerical experiment, e.g. combination (MCS) and (SC) should definitely belong to worst case and combination of (LHS-mean) and (SCD) should be the most efficient. Note, that in case of random field simulation using the orthogonal transformation of covariance matrix, the quality of sampling is influenced by criterion for a reduction of number of random variables. A proper error assessment based on numerical experiment is the most objective method for qualitative assessment of sampling schemes listed above.

The quality of generated random field is a primary task and should be tested first. The approach for error assessment can be elaborated in a similar way to as the general error assessment procedure due to ([Novák et al., 1995, 2000](#)).

When any method for random field simulation is used, it is required that the statistical characteristics of the field generated should be as close as possible to the target statistical parameters. Generally, the mean values, standard deviations, correlation and spectral characteristics (we will use the common term “statistics”) cannot be generated with absolute accuracy. In our case the accuracy will be influenced by:

- Number of random variables N_V used for representation of random field (reduction of original space via orthogonal transformation of covariance matrix);
- Correlation length d ;
- Sampling technique of uncorrelated Gaussian random variables (MCS or LHS) in connection with fulfilment of correlation structure;
- Number of discretization points N ;
- Number of simulations used N_{Sim} .

Some samples of random fields for a parameter are simulated from the population parameters. A certain statistics of the particular simulation may be very close to or quite far away from the value of corresponding target parameter. When the seed of the pseudo-random number generator is changed, other random fields are generated and other values of all sample statistics are naturally obtained. Therefore, each of these statistics can be considered as a random variable with some mean value and variance. The simulation technique is considered as best one which gives an estimated mean value of the statistics very close to the target mean value and also closest to zero variance of the statistics. In our case of zero mean value and unit variance of random field (basic target statistical parameters) we expect to get estimated mean around zero and variance around one.

The assessment can be done by performing more runs of the same simulation process with a different random setting of the seed of pseudo random number generator. Thus samples are artificially generated from the population in this way. Procedure can be described as follows (for one particular run):

- N_{Sim} simulations of random field are performed with initial random seed setting and prescribed parameters;
- Statistics are evaluated from N_{Sim} generated realizations of the random field over all N discretization points (capturing also the ergodicity as the basic property of random field) *mean* \bar{a}_s and *standard deviation* σ_{a_s} are evaluated.
- Correlation and spectral characteristics can be examined too (autocorrelation function or power spectral density).

The procedure itemized above is repeated N_{run} times, each time with different initial random setting of the seed. Naturally, statistics obtained in each run are different, e.g. different *mean* \bar{a}_s and *standard deviation* σ_{a_s} . As measures of the accuracy of simulation, the mean values and standard deviation are calculated from N_{run} statistics obtained. Symbolically, we assign the following symbols:

- $\text{Mean}(\bar{a}_s)$, $\text{Mean}(\sigma_{a_s})$ for mean values of *mean* \bar{a}_s and *standard deviation* σ_{a_s} .
- $\text{Std}(\bar{a}_s)$, $\text{Std}(\sigma_{a_s})$ for standard deviations of *mean* \bar{a}_s and *standard deviation* σ_{a_s} .

If the simulation is successful, then $\text{Mean}(\bar{a}_s) \rightarrow 0$, $\text{Mean}(\sigma_{a_s}) \rightarrow 1$ and standard deviations $\text{Std}(\cdot) \rightarrow 0$ (hypothetical limits for $N_{Sim} \rightarrow \infty$).

Let us consider 1D structure of length 10 m (e.g. beam), the structure is divided into 128 discretization points associated with finite elements ($N = 128$). For univariate Gaussian random field with zero mean two values of correlation length are considered in order to show the influence of this parameter, $d = 0.1$ m and $d = 1$ m. Random field realizations are illustratively shown in Fig. 4.1 for 16 simulations only. The region of small number of simulations ($N_{Sim} = 8, 16, 32, 64, 128, 256, 512$) has been selected in parametric study – implicitly it was supposed that the superiority of LHS should appear for small number simulations (tens, hundreds). Number of runs $N_{run} = 30$ was selected for estimation of statistics. So the random fields had to be simulated $N_{run} \times N_{Sim}$ times for a statistics of interest.

The following alternatives have been selected for the error assessment: MCS-SC, MCS-SCD, LHS-half-SC, LHS-half-SCD, LHS-mean-SC and LHS-mean-SCD. The results are plotted in Fig. 4.4.

Mean value: An ability to simulate *mean value* of random field is excellent in all alternatives of LHS (figures a) and b)), even for very low number of simulations. This ability is rather poor in case of MCS, mean value of *mean* fluctuates and standard deviation of *mean* is high in comparison to LHS (around the order 10^{-18} for LHS alternatives, which is just a noise due to numerical inaccuracy).

Standard deviation: The ability to simulate *standard deviation* of random field is documented in figures c) and d). Again, capturing of this statistics is “random” in case of MCS, standard deviation of *standard deviation* is high in comparison to LHS. LHS-half underestimates mean value of *standard deviation* (figure c)) for low number of simulations. The capability of improved sampling scheme LHS-mean is much better and convergence to target statistic (unit standard deviation) is faster. This is a general feature of LHS tested at the level of random variables.

An important fact is documented: There is no significant difference between alternatives SC and SCD in case of MCS, LHS-half and LHS-mean sampling schemes. Both LHS methodologies generally prescribes *mean value* in section (discretization point) of a field, but variability (*standard deviation*) in section is better for LHS-mean sampling.

Diminishing spurious correlation has small influence on these basic statistics of random field (in our study statistics of random fields are “smeared” lengthwise, but an impact of spurious correlation could remain in sections of random field realizations). In most cases differences are negligible and points coincide in presented figures. As was shown above, a spurious correlation influences negatively the autocorrelation structure of random field. Note, that if we construct statistics presented in Fig. 4.4 for different correlation length of the field, similar trends will be obtained.

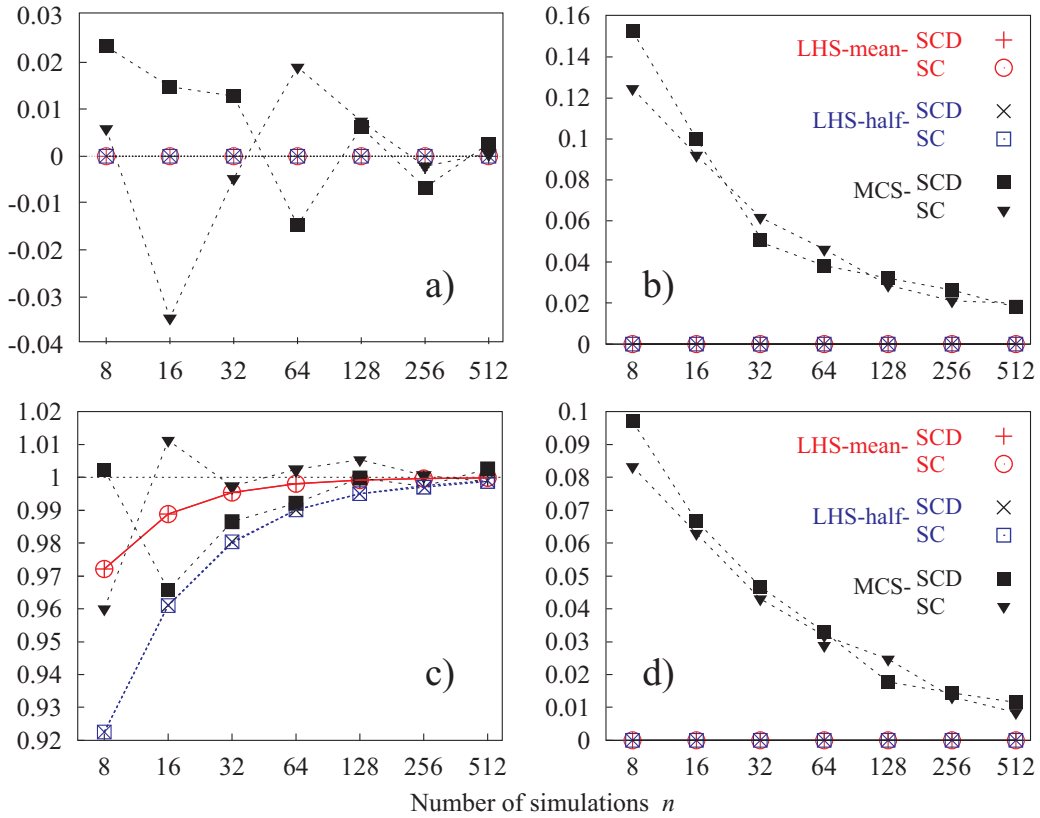


Figure 4.4: Statistics of *mean* and *standard deviation* ($d = 1$ m): a) mean of *mean*; b) standard deviation of *mean*; c) mean of *standard deviation*; d) standard deviation of *standard deviation*

4.5 Conclusions

It has been shown that a spurious correlation influences significantly the scatter of autocorrelation function of simulated random fields. A decrease of scatter-band is influenced by the possibility to diminish the spurious correlation. The method for diminishing spurious correlation based on stochastic optimization method SA appeared to be robust and efficient for random field simulation. This possibility is limited in case of very small number of simulations (with respect to number of random variables representing random field). A clear indication of this limitation is the fulfillment of norms used as objective functions in SA to diminish spurious correlation.

The quality of simulated random fields should be assessed by usage of both basic statistics (mean value and standard deviations) applied for simulated mean and standard deviation is more suitable and recommended. An error assessment has been performed for six alternatives of sampling schemes. The best performance, i.e. the convergence to target values of statistics with low variability has been achieved in case of LHS approach with improvement (LHS-mean). Diminishing spurious correlation does not influence the capturing of these statistics but does influence significantly realization of autocorrelation function of random field.

The superior efficiency of LHS and correlation control is confirmed. But attempt has been done to show better the role of correlation control – diminishing spurious correlation in random field simulation and importance of sampling schemes for simulation of uncorrelated random variables.

Generally the quality of both estimated autocorrelation and cross-correlation depends on the quality of imposition of correlation among random variables. Cross-correlation is estimated using N_{Sim} realizations in N discretization points. Therefore one can obtain N point estimations of cross-correlation coefficient for each pair of random fields **I** and **II** $\rho_{I,II}(0)$. Of course, it should be estimated also cross-correlation with coordinate (time) separation vector $\mathbf{d}_{A,B}$, i.e. cross-correlation of two different discretization points A, B for each pair of random fields $\rho_{I,II}(\mathbf{d}_{A,B})$. Meaning of these terms is illustrated in figures 4.5

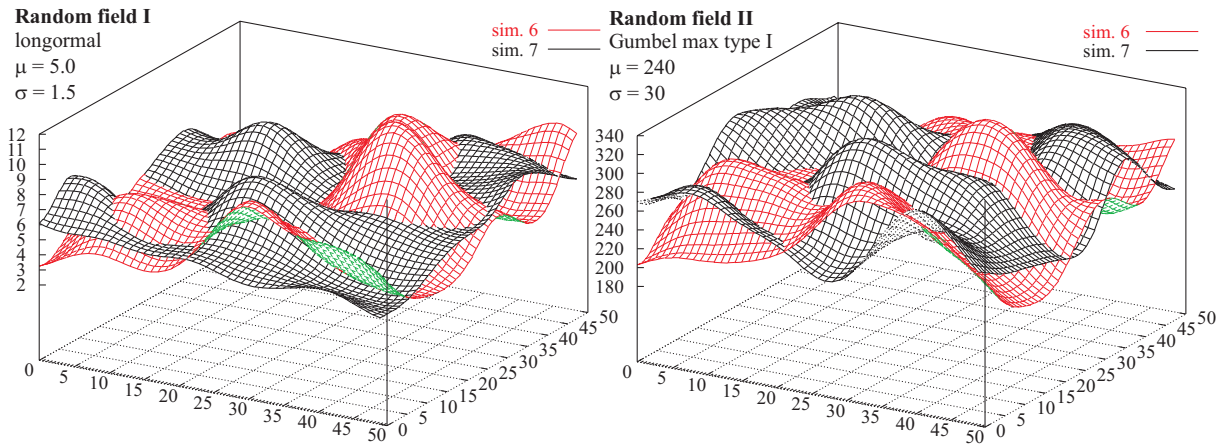


Figure 4.5: Shape similarity of corresponding realizations of random fields **I** and **II** ($d_x = d_y = 10m$). Cross-correlation coefficient $\rho_{I,II}(0) = 0.65$

and 4.6. Both random fields **I** and **II** were obtained from standard Gaussian random field using simple memoryless translation by Eq. (4.6), chapter 4.3. Corresponding realizations of random field **I** before translation are given in figure 4.7.

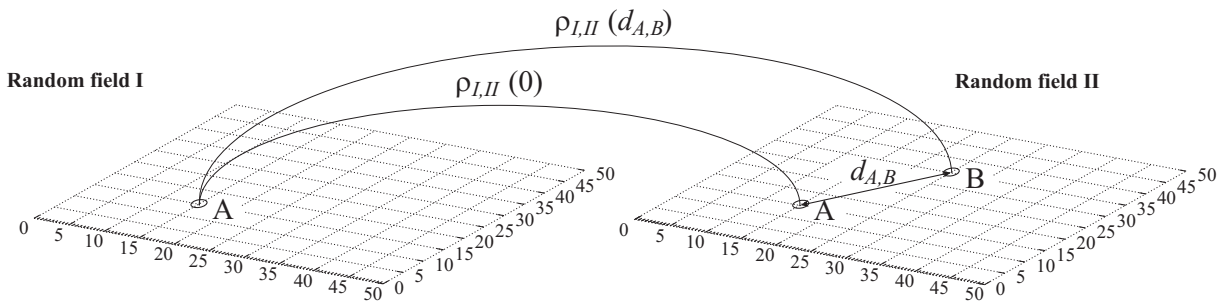


Figure 4.6: Illustration of cross-correlation for 2-dimensional random fields **I** and **II**

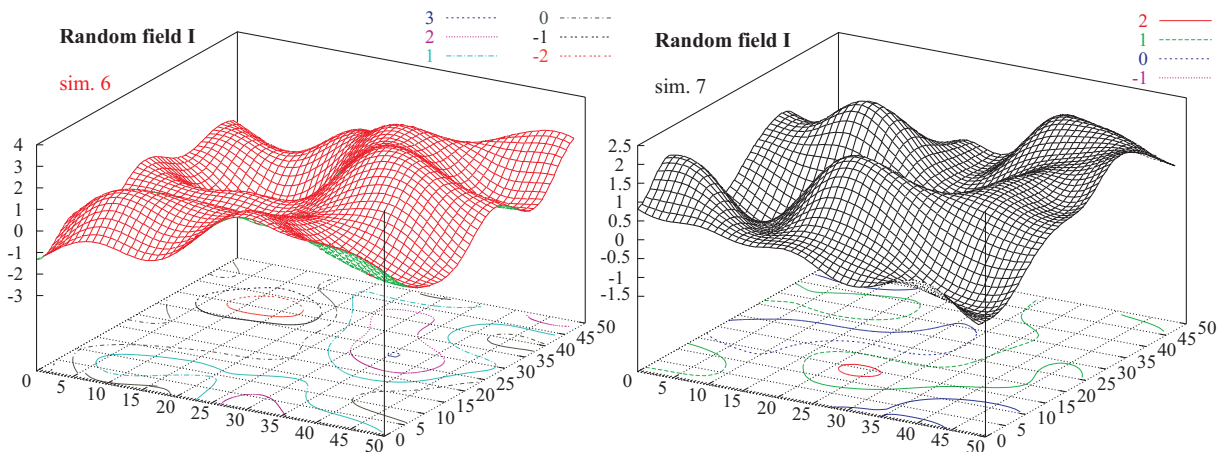


Figure 4.7: Standard gaussian random field **I** before translation ($d_x = d_y = 10m$)

Part II

**STOCHASTIC MODELING OF
MULTI-FILAMENT YARNS FOR
TEXTILE REINFORCED
CONCRETE**

Chapter 5

Micromechanical model and random properties within the yarn cross section

Published in paper: [Chudoba, Vořechovský, and Konrad \(2004\)](#)

The chapter presents numerical study of sources of randomness/disorder in the multi-filament yarn as they occur in the tensile test. For the analysis, we formulate an efficient deterministic model based on the superposition of the filament response. The considered distributions of the material properties include both the variations of properties from filament to filament and the variations of strength and stiffness over the length of each filament. In the chapter, we introduce the developed modeling technique and study the influence of filament-related distributions of material properties with respect to the size effect. In the following chapter 6 or in the paper by [Vořechovský and Chudoba \(2004a\)](#), the length-related distributions are considered. Both papers provide the basis for correct interpretation of the data obtained from the tensile test on multi-filament yarn with varied specimen length.

5.1 Introduction

The composite material combining the cementitious matrix with textile reinforcement has become a subject of an intensive research in the last decade ([Curbach and Hegger, 2001](#)). The forming flexibility of the textile structures and the ductility of the produced composites opens up new possibilities especially in two application areas of civil engineering:

- production of efficient light-weight structural elements ([Hegger, 2002](#)) and
- strengthening and retrofitting of existing buildings ([Curbach, 2002](#)).

The heterogeneous nature of both the reinforcement and the matrix introduces sources of randomness at several scales of the material structure. For the robust modeling of the overall material behavior it is inevitable to identify and analyze the sources of randomness both experimentally and numerically. In particular, it is very important to capture the disorder in the material structure and the random distribution of defects and material properties. These sources of randomness introduce the length (volume) dependent behavior that is generally referred to as statistical size effect ([Bažant, 2002a](#)).

The primary motivation for the present study was to determine the statistical distributions of filament properties in order to analyze their performance in the crack bridges and in the heterogeneous bond layer of cementitious composites. The need for a sound description of the length-dependent behavior of reinforcing yarns is documented in Fig. 5.1 with the classification of the effective length scales of the tensile test, of the crack bridge (sleeve filaments) and of the structure (core filaments).

The direct experimental determination of the statistical distributions using an expensive filament tensile test turned out to be very difficult to construct in a reproducible manner. The only way to obtain the filament data was to derive them indirectly from the tensile tests on the bundles by applying

a numerical model. The tests have been performed with varied yarn length in order to quantify the statistical size effect inherent to the bundle as an additional effect to be reproduced in the modeling.

The key concept in capturing the statistical size effect of a single filament is the weakest link model, mathematically first formulated by Fisher and Tippett (1928) and Weibull (1939a), later also by Epstein (1948). This concept has been applied in the formulation of the fiber bundle models (FBM) originally introduced by Daniels (1945) and Coleman (1958). The FBM's are constructed as a parallel set of fibers, each of which has a Weibull distribution of strength (e.g. Phoenix, 1978a; Harlow and Phoenix, 1978b,a; Smith and Phoenix, 1981). Fibers break if the load acting on them exceeds their local strength (threshold value). Upon the fiber failure, there are two possible rules for the stress redistribution: (1) equal load sharing (ELS) with equal redistribution of the load among all the intact fibers (filaments) remaining in the set, and (2) some type of local load sharing (LLS) where the force released by the broken fiber is transferred to its nearest neighbors. In spite of their simplicity, these models capture the most important aspect of material damage and provide a deeper understanding of the fracture process.

The FBM's provided a basis for successful micro-mechanical models considering localization (Byeerlein and Phoenix, 1997), the effect of the matrix between the filaments (Phoenix et al., 1997) and the nonlinear behavior (Krajcinovic and Silva, 1982) extensions of FBM's have been introduced taking into account the possible multiple cracking of the filaments by replacing the brittle filament failure with a continuous damage parameter (Kun et al., 2000).

When considering other sources of randomness than strength, the FBM's must be replaced by a deterministic micromechanical model combined with full Monte-Carlo simulation technique. This approach has been used in analyzing the influence of the distribution of the bundle strength for different fiber arrangements on the stress concentration around the broken fibers (Ibnabdeljalil and Curtin, 1997). The prohibitive computational costs have been reduced by simplified micromechanical models like break-influence superposition based on the shear-lag model (Beyerlein and Phoenix, 1996) or the lattice Green's function technique adopted to composite failure (Zhou and Curtin, 1995).

Another source of randomness in form of the interaction patterns randomly distributed over the yarn has been studied by Hidalgo et al. (2002). The disordered structure of filaments has been captured by continuous redistribution law ranging from the LLS to ELS rules and randomizing the interaction diameter in a Monte-Carlo simulation.

In the case of the AR-glass or carbon yarns, the FBM's do not cover all the effects observed in the experiment. The difficulty is, that besides the randomly distributed strength, the tensile test setup necessarily introduces additional sources of randomness that may essentially influence the response of the specimen. In particular, it is inevitable to include the influence of delayed activation and varying filament length. Furthermore, for some types of rovings (e.g. AR-glass) there are also differences between cross sectional area of individual filaments in the yarn sample.

By including these effects in the numerical model together with the influence of the stochastic distribution of material properties over the length we are able to capture/reproduce the whole loading and failure process during the test, size effect inclusive. As a result, we obtain more information about the filament properties and their interactions in the bundle. The filament bundle model capturing all the interacting effects occurring in the tensile experiment with varied specimen length provides the stepping stone for robust modeling of the failure process in the bond layer with cementitious matrix.

In the present chapter we first describe the effects occurring during the tensile experiment of the yarn with the special focus on the yarn types used in the Textile Reinforced Concrete (TRC), see Sec. 5.2. After that, we describe the deterministic model covering the effects identified in the tensile experiment (Sec. 5.3) and study their qualitative influence on the load-displacement diagram (Sec. 5.4). The influence of delayed activation is then studied on selected wave patterns in detail (Sec. 5.5) and discussed in connection with the performed experiments in the Sec. 5.6.

In the following chapter 6 we study the influence of random distribution of strength and stiffness along filaments. In the same paper, the resulting size effect (roving strength dependence on the length) is studied with and without the effect of delayed activation using the numerical model.

5.2 Effects included in the tensile test

Before constructing the numerical model we review the general behavior of a multi-filament yarn in the tensile test. Fig. 5.2 shows the load-displacement curves obtained from the tensile test on AR-glass

rovings with lengths varied in the range from 10 to 500 mm. The velocity of loading has been set to 1% strain in a minute.

The response curves allow us to identify the following four effects:

- A Gradual increase of the stiffness up to the maximum stiffness of the bundle. This phenomenon is amplified for short samples.
- B Reduction of the maximum stiffness with the decreasing length of the sample.
- C High scatter of the stiffness and maximum force for short samples and reduced scatter for long samples.
- D Brittle failure of short samples as opposed to the ductile failure of long samples.
- E Maximum deformation ε_{max} [%] differs significantly for different lengths although identical material was used.

In order to model the yarn behavior in various loading conditions, these complex effects must be explained and quantified in terms of simpler or even elementary effects that may be appointed either to the (1) material constituents, i. e. the individual filaments, or to the (2) filament ensemble or (3) to the experimental setup.

In the first case, linear elastic brittle behavior of the AR-glass is assumed. Its characteristics (strength $f^t(x)$, material stiffness $E(x)$ and area $A(x)$) may exhibit variations along the filament: as shown in the Fig. 5.4. If there are flaws in the glass microstructure, there may also be locally concentrated reductions of strength. Finally, the interaction between filaments is realized either by the bonding or friction between filament surfaces.

Second, the cross sectional area varies from filament to filament within the ensemble: $A_i(x) \neq A_j(x)$, where i, j are filament labels. Further, the disorder distribution in the bundle leads to two effects essentially influencing the overall behavior depending on the wave pattern geometry: (1) in case of loose independent waves it results in delayed filament activation and unequal stress distribution in filaments at a given control load and (2) in case of wave geometry inducing pressure between filaments, e.g. spiral form, it leads to higher interaction between filaments through friction and damage localization in clusters.

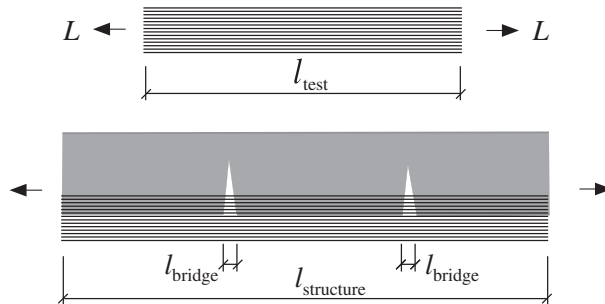


Figure 5.1: Effective length scales

Third, the most crucial part in the construction of the tensile experiment is the clamping of the yarn ends. In general, an ideal clamping is impossible and some kind of response distortion is always present. Therefore, it is important to construct the clamping in a way that allows us to factor out its influence from the measured response. In the applied experimental setup developed at the Institute for Textile Technology of the Aachen University, the yarn ends are fixed in epoxy resin (Gries and Royé, 2003). Without going into details of this setup we summarize the sources of distortion of the measured response that must be considered: First, the length of the individual filaments l_i varies due to the uneven surface of the epoxy resin (see Fig. 5.4). This effect is present both for bundles with a flat cross sections as well as with a circular cross section. Second, for short samples the deformation of the epoxy resin cannot be neglected since it significantly distorts the measured deformation. Third, in the post-peak region, the epoxy resin gets unloaded and contracts with an uncontrolled velocity that may induce dynamic loading effects especially for short filaments.

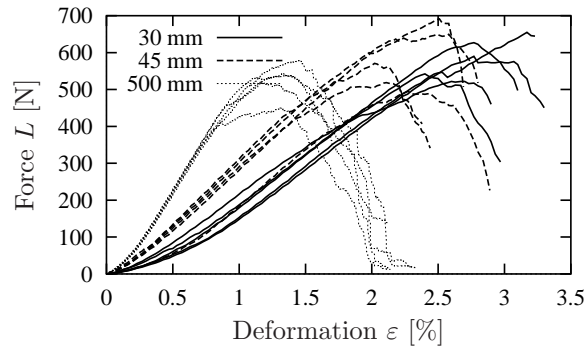


Figure 5.2: Tensile tests on AR-glass rovings with varied length, raw data

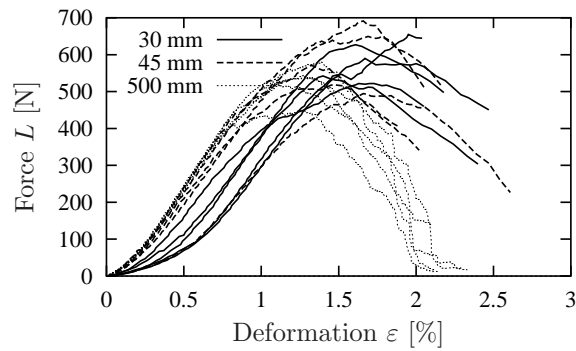


Figure 5.3: Tensile tests on AR-glass rovings with varied length, corrected data by subtracting the deformation of the epoxy clamping

Since the forces transmitted by short and long yarns are comparable and the deformable epoxy-made clamping is kept identical, the resulting diagram is distorted mainly for short samples. Corrected diagrams (deformation of epoxy resin subtracted) are presented in Fig. 5.3. These manifest very brittle failure after the peak load instead of expected long post-peak zone due to the scatter in stiffness.

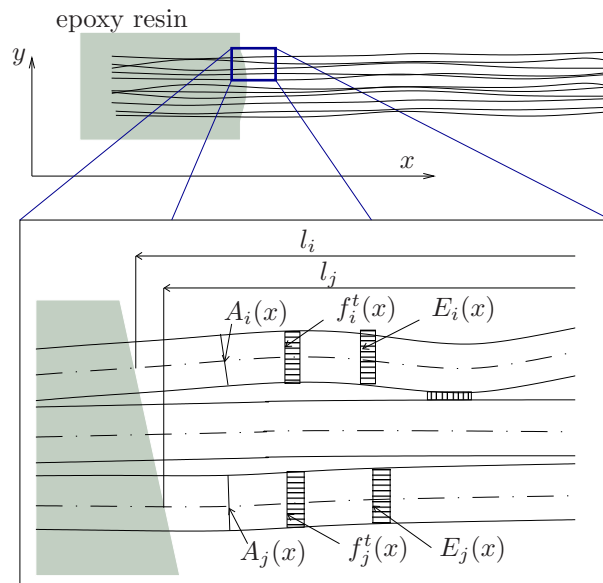


Figure 5.4: Elementary characteristics of filaments and their ordering in the yarn

5.3 Deterministic model

The full coverage of the specified elementary effects would be possible using the finite element model including the specified sources of randomness. However, by realizing that we are dealing with bundles consisting of up to 3000 filaments with relatively dense discretization (e.g. for short autocorrelation structure of the material properties) we have to conclude that the computational complexity of the deterministic model makes the statistical evaluation by means of the Monte Carlo computation impracticable due to the prohibitive computational cost. In particular, with n_f number of filaments and with n_n nodes and $n_e = n_n - 1$ finite elements in each filament the order of structural stiffness matrix becomes $n_f n_n$.

In case that shear interaction is modeled in adjacent nodes, the stiffness/structural matrix is a band diagonal matrix with the number of nonzero elements equal to circa $n_n n_f (2n_f + 1)$. In a realistic case of $n_f = 1600$ and $n_n = 100$ the number of nonzero elements is $160000 \cdot 1601 = 256.16 \cdot 10^6$. For double precision numbers, this corresponds to memory size of 2 GB and is obviously unaffordable for stochastic non-linear computation even using today's high performance computers.

In case that no interaction between filaments is taken into account the structural matrix is tridiagonal so that, using the symmetry, the number of nonzero entries is $2n_f n_n$. This corresponds to a moderate size of the system matrix of 2.6 MB. However, using the finite element discretization with Newton-Raphson scheme to trace the load displacement diagram for this problem would be just like using a sledge hammer to crack a nut. As we show next, the explicit computation of the load-displacement curves of filament bundles in tension is possible by superposition of the filament response (SFR) during the tensile loading. The model is applicable to the material with a negligible friction, like AR-glass, and allows us to drastically reduce the computational costs to such extent, that the statistical analysis of the nonlinear response becomes feasible.

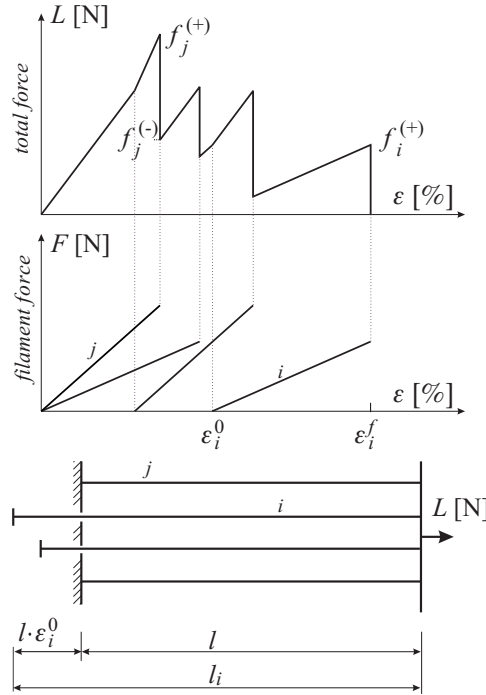


Figure 5.5: Superposition of the filament response with varying filament strength, stiffness, length and activation strain.

The yarn idealization reflecting the filament geometry and structure schematically exemplified in the Fig. 5.4 is shown in the Fig. 5.5. The bundle with the nominal length l is represented by an ordered set \mathcal{F} of parallel filaments. For each filament $i \in \mathcal{F}$, the following material properties are defined:

- l_i filament length
- \bar{A}_i average cross sectional area
- ε_i^0 activation strain

The properties of the i -th filament may fluctuate over its length. Their discrete values are represented by an ordered set of material points \mathcal{M}_i . The number of material points m is equal for all filaments. The material properties of the filament i are represented as a set of value triples in equidistant points

$$\mathcal{M}_i := \{ [E_{i,j}, A_{i,j}, f_{i,j}^t] \mid j = 1 \dots m \}, \quad (5.1)$$

where $E_{i,j}$ is the Young modulus, $A_{i,j}$ the cross sectional area and $f_{i,j}^t$ the strength in the i -th filament and j -th material point.

The maximum force in each material point is computed as

$$R_{i,j} = f_{i,j}^t A_{i,j}. \quad (5.2)$$

Applying the fact that the filament strength equals to the strength of the weakest member/element we define the maximum force transmitted by the i -th filament as

$$R_i = \min_{j \in \mathcal{M}_i} (R_{i,j}). \quad (5.3)$$

Using the equidistant sampling of the material points the overall stiffness of the i -th filament may be computed by static condensation (Fig. 5.6):

$$\frac{1}{K_i} = \sum_{j \in \mathcal{M}_i} \frac{1}{K_{i,j}} = l_i \sum_{j \in \mathcal{M}_i} \frac{1}{E_{i,j} A_{i,j}}. \quad (5.4)$$

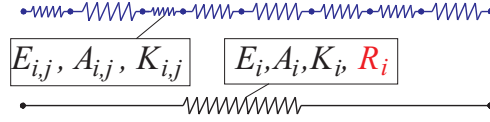


Figure 5.6: Effective filament stiffness K_i and minimum strength R_i

With the evaluated resistance and stiffness at hand we can determine the nominal strain at the filament failure

$$\varepsilon_i^f = \frac{R_i}{l K_i} + \varepsilon_i^0, \quad (5.5)$$

so that the strains at the breaking of all filaments can be enumerated in an ordered set

$$\mathcal{E} := \{ \varepsilon_i^f \in R \mid \varepsilon_i^f \leq \varepsilon_{i+1}^f, \forall i \in \mathcal{F} \}. \quad (5.6)$$

The subset of unbroken filaments at breaking of the i -th filament is defined as follows

$$\mathcal{Z}_i := \{ k \mid \varepsilon_k^f \geq \varepsilon_i^f, \forall k \in \mathcal{F} \}. \quad (5.7)$$

The total force transmitted by the roving at the breaking strain ε_i^f of the i -th filament is computed as the sum of forces transmitted by the unbroken filaments

$$F_i^{(+)} = \sum_{j \in \mathcal{Z}_i} K_j (\varepsilon_j^f - \varepsilon_j^0). \quad (5.8)$$

The force after the rupture of the i -th filament is obtained by subtracting its contribution from $F_i^{(+)}$

$$F_i^{(-)} = F_i^{(+)} - K_i (\varepsilon_i^f - \varepsilon_i^0). \quad (5.9)$$

By evaluating the Eqs. (5.8) and (5.9) for each ε_i^f from the ordered set \mathcal{E} we may directly calculate the levels of loads at all filament breaks. Thus, the load-displacement curve can be constructed as a set of force-displacement triples ordered according to the set \mathcal{E}

$$\mathcal{R} := \left\{ \left[\varepsilon_i^f, F_i^{(+)}, F_i^{(-)} \right] \mid \varepsilon_i^f \in \mathcal{E} \right\}. \quad (5.10)$$

Here, every deformation ε_i^F has two associated forces: before ($F_i^{(+)}$) and after ($F_i^{(-)}$) the filament break. For further numerical studies we can now define the maximum tensile force at the nominal length l as

$$R(l) = \max_{i \in \mathcal{F}} f_i^{(+)}. \quad (5.11)$$

As already stated, this computation neglects any kind of interaction between filaments and corresponds to the ELS. Therefore, the model is only applicable if the influence of shear is small. The Fig. 5.7 shows the localization of failure for a bundle after the rupture of a filament, a phenomenon that cannot be captured by the present model. Localization of failure into narrow zones due to shearing asserts mainly for long yarns providing sufficient length to build up forces comparable with the filament strength. Obviously, the increasing shearing capacity leads to more homogeneous force distribution within the bundle, and consequently to a more brittle failure as shown in the Fig. 5.7b. In case of delayed activation, the increased shear transmission leads to faster activation of yarn stiffness due to the interaction of filaments between the waves (See Fig. 5.7c).

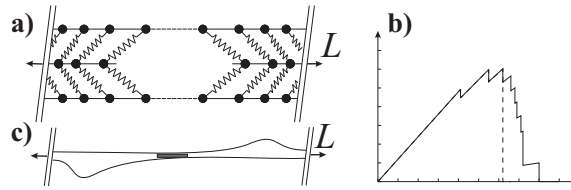


Figure 5.7: a) Overloading of 2 elements in the neighborhood of failed element under LLS rule. b) Comparison of roving load-deformation diagrams without and with significant shear interaction between filaments. c) Stiffness activation through shear for delayed activation.

Still, there is a range of yarns that exhibit very small influence of shear as can be observed on the random distribution of breaks along the yarn length during the tensile test. The evaluation of the tensile response in terms of the set \mathcal{R} defined in Eq. 5.10 is absolutely inexpensive in comparison with the full finite element computation and, therefore, very suitable for the statistical analysis including random variables and random fields.

5.4 Parametric studies

The formulated SFR model allows us to get a deeper insight into the behavior of the idealized bundle by analyzing the qualitative influence of the included effects in detail. In the examples below we study the influence of randomness of each single parameter simultaneously. The study is limited to the material parameters varying only across the filaments $i \in \mathcal{F}$ in the bundle.

The filament material is AR-glass with the following expected values of the (generally random) tensile strength, modulus of elasticity and filament diameter:

$$\begin{aligned} E[f^t] &= 1.49 \text{ GPa}, \\ E[E] &= 70 \text{ GPa}, \\ E[D] &= 26 \text{ } \mu\text{m} \end{aligned} \quad (5.12)$$

The analysis of the random properties over filament length (\mathcal{M}_i) is provided in the following chapter 6.

We illustrate the behavior of the yarn using a load-deformation diagram. For the sake of simplicity we use 16 filaments only, while the real number of filaments in the studied yarn is approximately 100-times higher. In order to have the resulting forces in the figures comparable to the real values, the forces are given in cN. Diagrams of the deterministic yarns with parameters on mean values are always plotted by dashed line for comparison.

5.4.1 Different filament lengths

As mentioned previously, in the applied experimental setup the yarn ends were fixed by using epoxy resin enfolding all the filament in the cross section. The cut through the clamping in the Fig. 5.8 shows that

the yarn cross section has been homogeneously penetrated by the resin to enable gradual transmission of the force into the individual filaments.

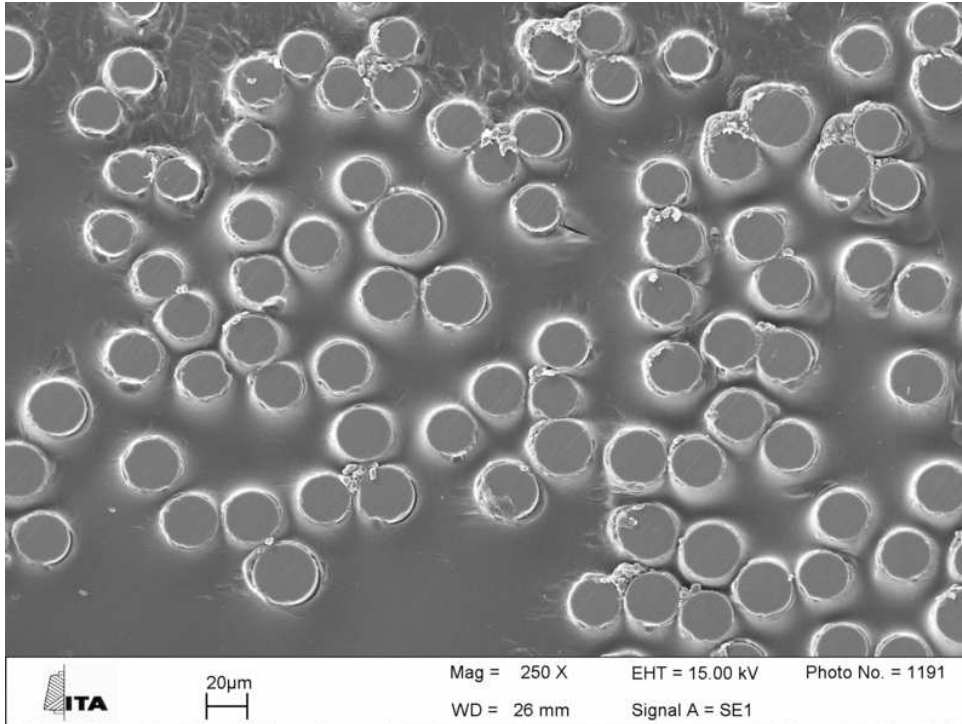


Figure 5.8: Yarn penetrated by the epoxy resin

The difficulty with this kind of fixing is that the resin penetrates also in the x direction (see Fig. 5.4) with the consequence that the individual filaments have different lengths. For this reason, it is important to study the sensitivity of the response with respect to the scatter in the filament length. The load-deformation diagrams for the yarn 100, 50, 10, 5, 1 and 0.5 mm long with a variation range 2 mm of the individual filaments and constant E, f^t, A are shown in the Fig. 5.9. Here, the distribution was assumed linear between the minimum and maximum filament length. The minimum filament length $\min_{i \in \mathcal{F}}(l_i)$ is set equal to the nominal length l and the maximum length $\max_{i \in \mathcal{F}}(l_i)$ is set to $l + 2\text{mm}$, roughly corresponding to 1mm unevenness of the epoxy resin surface at both clamped ends.

Obviously, the scatter in the filament length leads to the scatter in the stiffness (see filament diagrams in Fig. 5.9). As a result, the maximum strength cannot be reached simultaneously in all filaments which causes reduction of the maximum tensile force transmitted by the yarn. This is especially true for short specimen (Fig. 5.9c and 5.9d) with relatively ductile failure. The examples in Fig. 5.9 e) and f) represent an unrealistic case where the nominal length is shorter than the maximum additional length of 2 mm. With an increasing length, the relative differences in length become smaller and the strength of the bundle approaches the nominal strength of the bundle (Fig. 5.9a and 5.9b).

As a result, we may conclude that the variations in the filament lengths act as an opposite effect with respect to the statistical size effect and may even drown the size effect for short specimen lengths. Second, this effect introduces ductile failure of short specimen which contrasts with the response measured in the test (see Fig. 5.3).

5.4.2 Differences in filament diameters

The cross sectional area of the filaments in the bundle exhibits relatively high scatter. In the particular case depicted in the Fig. 5.8 the diameter takes values between 23 and 29 μm .

Let us assume constant E, f^t, l as in the previous example (see Eq. 5.12) and the variation of the filament diameter within the cross section given as $E[D] = 26 \mu\text{m}$ and $COV(D) = 10\%$ (standard deviation is 2.6 μm). The cross sectional area of the filament i over its length is assumed $A_{i,j} = \text{const}, \forall j \in$

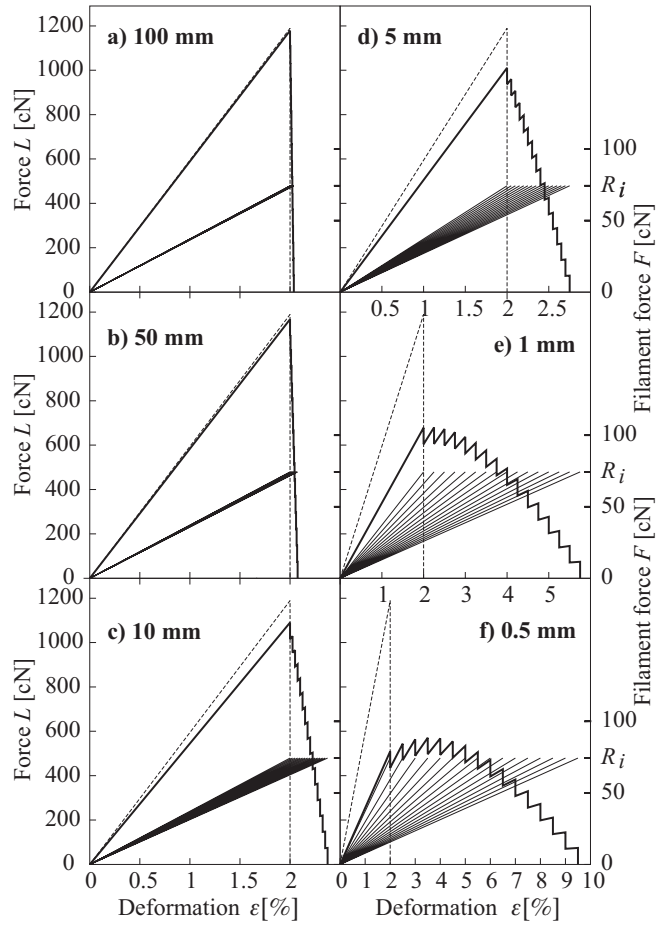


Figure 5.9: The influence of linearly distributed addition of 2 mm to the nominal length a)... f)

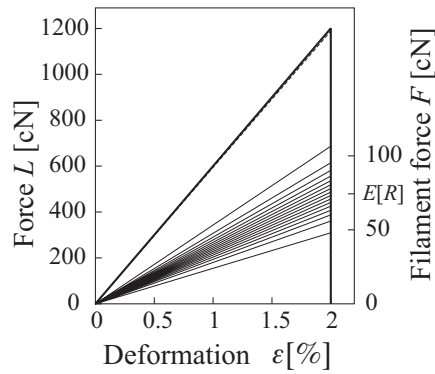


Figure 5.10: The influence of randomness of diameters between the filaments

\mathcal{M}_i we conclude that this kind of scatter does not influence the maximum deformation: all the filaments fail simultaneously at the displacement

$$u_i^f = \frac{R_i}{K_i} = \frac{f^t A_i l}{EA_i} = u^f = \varepsilon^f l. \quad (5.13)$$

The maximum strength of a yarn equals to that of a perfect one only if the cross sectional area of the filament i ($A_{i,j}$) is symmetrically distributed around the nominal (mean) value $E[A]$. The total stiffness

of the yarn with random D_i is calculated as

$$\begin{aligned} K &= \sum_{i \in \mathcal{F}} K_i = \frac{E}{l} \sum_{i \in \mathcal{F}} A_i(\theta) \\ &= \frac{E}{l} \frac{\pi}{4} \sum_{i \in \mathcal{F}} D_i^2(\theta), \end{aligned} \tag{5.14}$$

where θ stands for the random nature. If we assume that the diameter $D(\theta)$ is a Gaussian random variable with statistical moments specified above, the distribution of cross-sectional areas A_i of the filaments in the bundle is not symmetrical around the mean (associated with gamma distribution). Nevertheless, it can be seen in Fig. 5.10 that the stiffness of the yarn with 16 normally distributed D_i 's is only slightly higher than the stiffness of the perfect yarn. It is because the mean value of the sum of squares is almost equal to the average filament area: $1/n \sum_{j=1 \dots n} D_j^2(\theta) \approx \bar{A}$.

We may conclude that the ‘‘symmetric around mean’’ scatter of the filament cross sectional area does not significantly change the response with respect to the response of the deterministic computation with mean area. However, it should be noted, that this conclusion does not hold when considering also the scatter of $A_{i,j}$ along the filament length \mathcal{M}_i .

5.4.3 Delayed activation of filaments

The waviness of filaments leads to their delayed activation during the loading process. In order to study its qualitative influence on the response we have defined a constant activation density function (see Fig. 5.11) distributed over the activation range $0 \leq \varepsilon^0 \leq \varepsilon_n^0$, where $\varepsilon_n^0 \in \mathcal{E}$ is the activation strain of the last filament. Depending on the relation between strain at the first filament rupture $\varepsilon_1^f = R_1/K_1$ and activation strain of the last filament ε_n^0 we may distinguish three qualitatively different load displacement diagrams:

- a) For $\varepsilon_1^f = \varepsilon_n^0/2$ the constant maximum force is reached in the range $\varepsilon_1^f \leq \varepsilon \leq \varepsilon_n^0$ due to the equal activation and failure rates. The maximum achieved stiffness is the half of the stiffness of a perfect yarn without delayed activation.
- b) For $\varepsilon_1^f = \varepsilon_n^0$ the loading deformation range and failure deformation range are equal and the stiffness activated at the maximum force is the equal to the total stiffness of a perfect bundle without delayed activation.
- c) For $\varepsilon_1^f = 2\varepsilon_n^0$ the maximum bundle stiffness is activated over a longer deformation range leading to higher maximum force and to shorter failure deformation range.

By realizing that the activation strain is computed as a relative extra length of the filament i with respect to the nominal length $\varepsilon_i^0 = (l_i - l)/l$ we may expect wider activation range for short specimen (Fig. 5.11a) and narrow activation range for long specimen (Fig. 5.11b). As can be seen in the figure, the maximum force is lower for short samples than for long samples. Thus, we may conclude that waviness drowns the statistical size effect and must be included in the interpretation of the measured data in order to assess the length dependent strength of the bundle accurately.

5.5 Correspondence between the delayed activation and waviness

In order to provide the correct interpretation of the experimental data we need to explain the qualitative correspondence between the waviness and the delayed activation. As shown in the Fig. 5.12, the activation density function changes with the length of the sample. During the production of the yarn and during the preparation of the experimental setup several waviness patterns may be included in the yarn structure. It is helpful to classify the fundamental waviness patterns according to their influence on the delayed activation with respect to the changing nominal specimen length l (Fig. 5.12). We may distinguish the

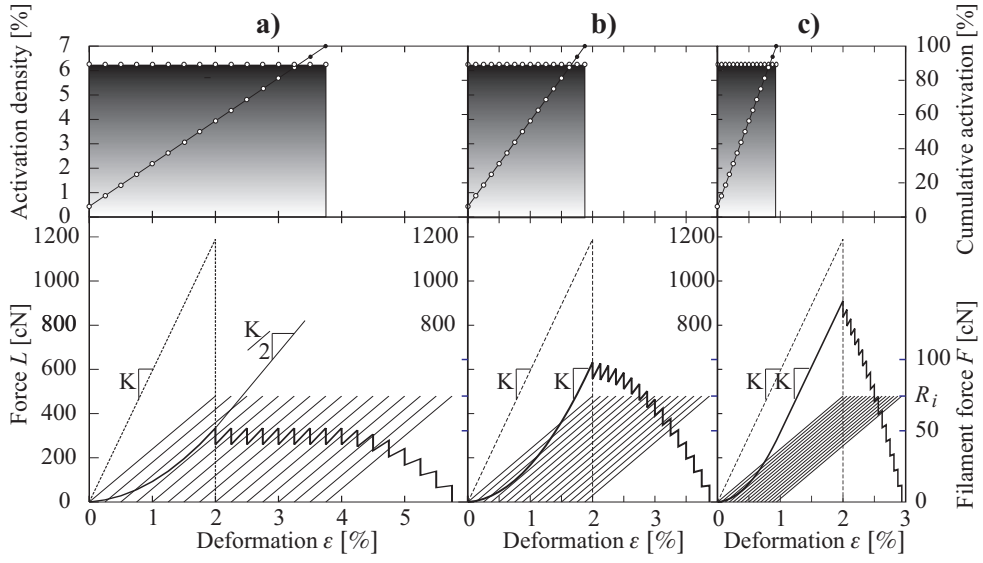


Figure 5.11: Comparison of three constant densities of delayed activation of filaments

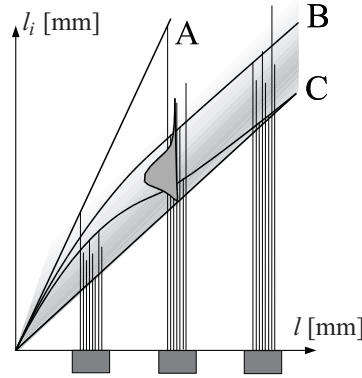


Figure 5.12: Distribution of relative extra length for changing nominal length

following three limiting cases: (A) unbounded scale up of the delayed activation, (B) the stabilization in the finite limit shape and (C) the disappearance of delayed activation with $l \rightarrow \infty$.

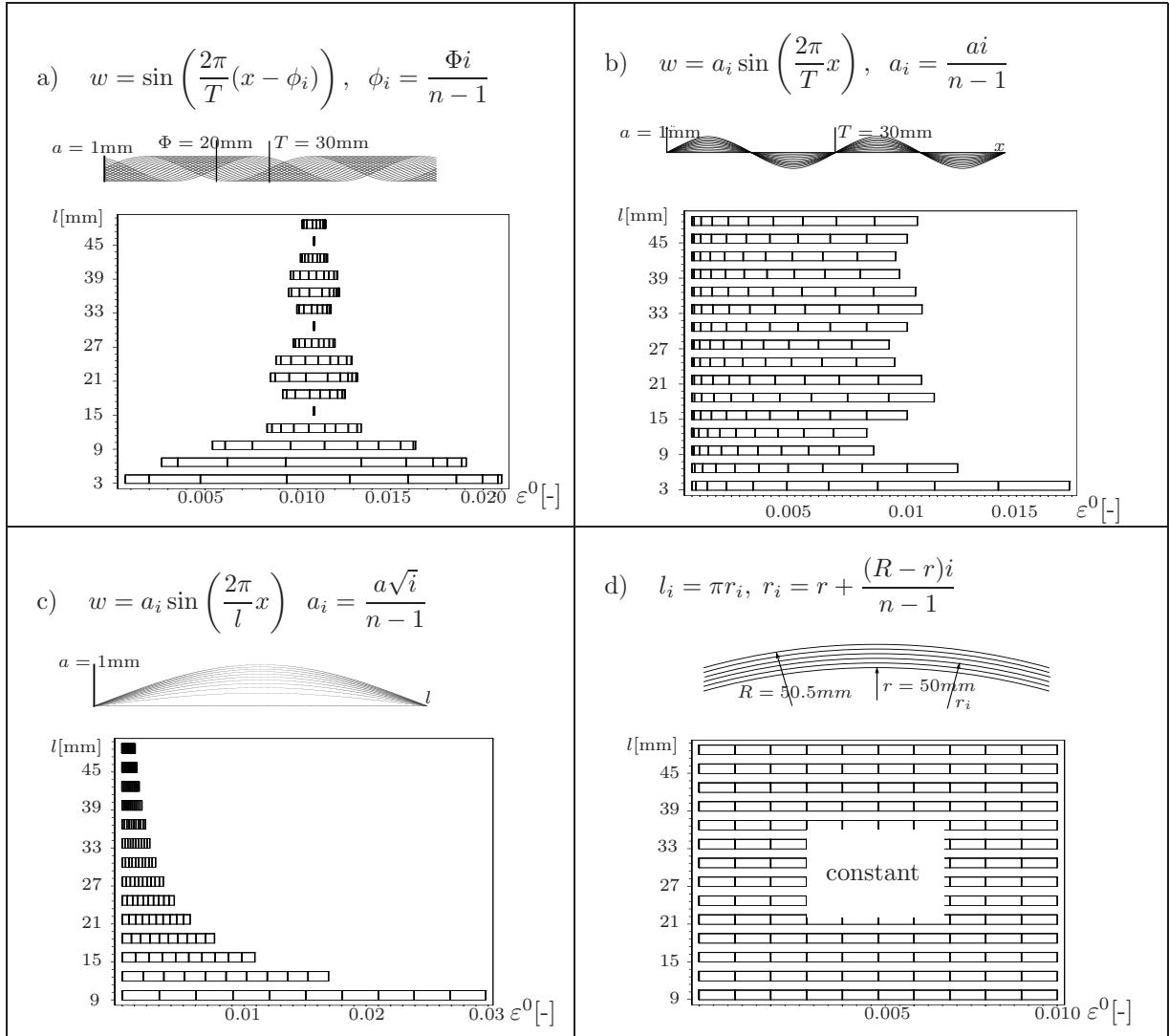
In order to answer the question which case comes in question for a particular type of yarn we evaluate the delayed activation for selected types of waviness shown the Fig. 5.13. The study includes patterns (a) and (b) that are introduced during the production process, (c) arising during the test preparation, and (d) appearing during the packaging.

Let the filament geometry within the bundle be defined by the wave function $w(x, a)$, where $a \in (0, 1)$ is the parameter fixing the filament position within the bundle. The relative extra length of a single filament is computed as

$$l_i = \int_0^l \sqrt{1 + w(x, a)'^2} dx. \quad (5.15)$$

and the activation strain is obtained as the normalized extra length of the filament: $\varepsilon_i^0 = (l_i - l)/l$. The activation density can then be constructed as a histogram of $\varepsilon_i^0, i \in \mathcal{F}$. The Fig. 5.13 shows four selected types of $w(x, a)$ with the obtained ε_i^0 histograms for varied nominal length. The histograms are plotted as bars divided in 10 segments, each representing 10% fractions of filaments in the whole yarn. The shorter the histogram segment, the narrower the activation range of the corresponding 10% fraction of filaments in the yarn.

In the first pattern (a) we have defined a periodic waviness with a uniform wave shift in the x

Figure 5.13: Wave patterns with corresponding activation profiles ($i = 0 \dots (n-1)$)

direction. The corresponding histograms oscillate around the limit activation strain. Uniform activation can be assumed from the length 100mm. This kind of waviness pattern leads to the stabilized delayed activation for sufficiently long specimens (case B in Fig. 5.12).

In the second pattern (b) we show waviness pattern with a uniform distribution of amplitudes within regular periodic waves. The corresponding histograms show that most of the filaments get activated in the beginning of the loading. For large l the differences in filament lengths become negligible and the influence of delayed activation disappears (case C)

The third pattern (c) shows a single wave that is scaled with the nominal length l . There is a higher fraction of filaments with larger amplitudes. In particular, we have chosen a linear distribution of filaments along the amplitude. The activation diagrams show constant activation density functions that get reduced to simultaneous activation for large l (case C).

The last pattern (d) shows the length distribution resulting from the coiling of the yarns onto the bobbins. Obviously, this length distribution leads to the constant delayed activation density that does not change with the length l . The length differences scale up linearly with the nominal length (case A in Fig. 5.12).

The performed study allows us to assess the plausibility of the applied delayed activation density with respect to its change with the specimen length. In particular, it allows us to identify the type of waviness included in the yarn from the load/deformation diagrams and compare them with the explicitly

observable waviness.

5.6 Identification of the parameter distributions

The distribution of the activation density can be estimated directly from the experimental curves by fitting the gradual increase of the stiffness up to its maximum value. In case that $\varepsilon_1^f \leq \varepsilon_n^0$ we can directly identify ε_n^0 as a point at which the maximum stiffness is achieved. The densities obtained by fitting are shown in the left four diagrams of the Fig. 5.16 and re-plotted as a sequence of histograms in the Fig. 5.14 in order to make them comparable with the densities resulting from the wave patterns studied in the Sec. 5.5. The comparison shows that the tested yarn possesses the combination of the waviness patterns of type (a), (b) and (c), while the pattern (d) is apparently negligible.

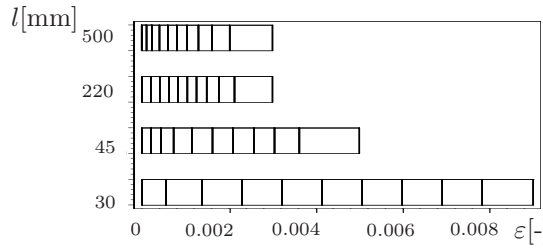


Figure 5.14: Activation density function reflecting the tensile tests

The pattern (a) and (b) may be observed visually in the picture of the tested yarn (Fig. 5.15). The wave pattern (c) develops during the specimen preparation and becomes dominating for short specimens.



Figure 5.15: Waves in the tested yarn

In particular, the influence of the periodic patterns (a) and (b) disappears for specimen lengths relatively short with respect to the wave period $T/2$. Then, the pattern (c) starts to play dominating role and the profile of the delayed activation approaches a constant function. Unfortunately, reliable experimental results for short lengths of 10 mm could not be produced during the work on this paper. The reason is that the deformation of the epoxy resin clamping becomes significant for the interpretation of the results. This effect can be seen in the Fig. 5.2 on the reduced slope (stiffness) of the load-deformation curve measured for the short specimen.

The load-deformation curves calculated for the considered lengths using the obtained activation densities are plotted in the right four diagrams of the Fig. 5.16. The resulting maximum forces are plotted for each length in the upper curve of the Fig. 5.17 together with the experimentally obtained results plotted in the lower curve. As already indicated in the Sec. 5.4.3 the delayed activation results in the strength reduction for shorter specimens. This contrasts with the statistical size effect bringing about strength reduction for longer specimens.

Obviously, the measured response must be interpreted as a combination of both effects. In order to perform the decomposition of the measured size effect $R^\epsilon(l)$ into the statistical size effect $R^\omega(l)$ and the effect of delayed activation $R^\delta(l)$ we introduce the corresponding size effect functions in the normalized form:

$$\epsilon(l) = R^\epsilon(l)/R^{\text{ideal}}, \quad \omega(l) = R^\omega(l)/R^{\text{ideal}}, \quad \delta(l) = R^\delta(l)/R^{\text{ideal}}, \quad (5.16)$$

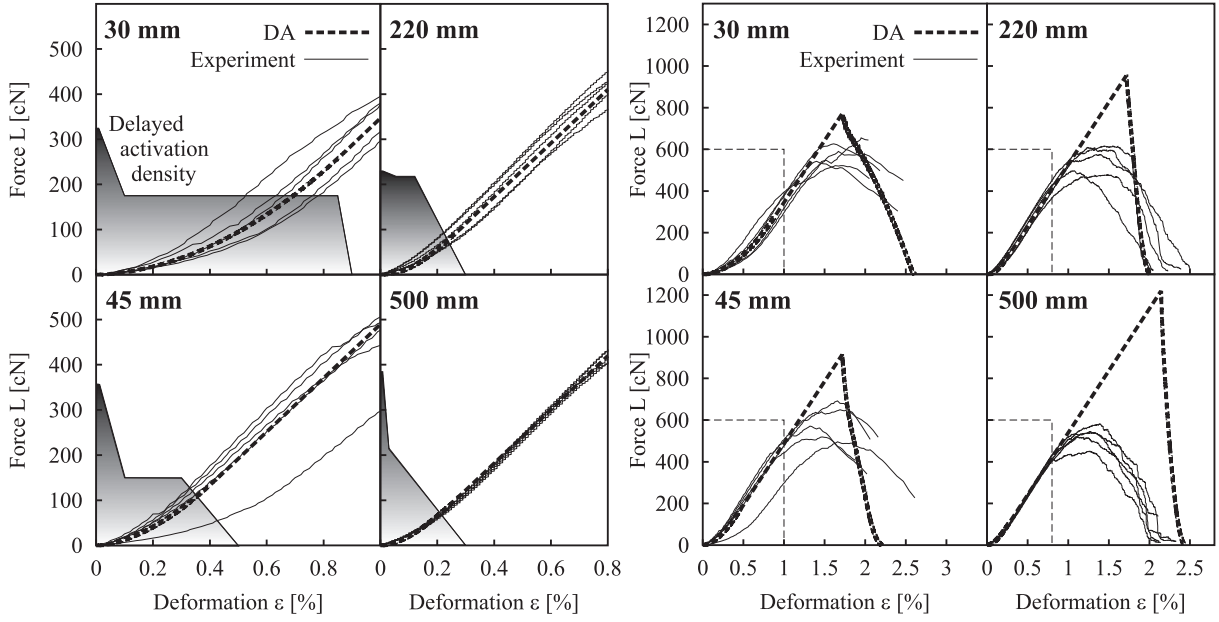


Figure 5.16: Delayed activation densities and load deflection curves (experiment and simulation). Left: zoom into the beginning of L - ε diagrams. Right: whole L - ε diagrams.

where R^{ideal} stands for the maximum total force of a perfect bundle. Then, the limiting cases of the statistical size effect $\omega(l)$ and of the delayed activation effect $\delta(l)$ are:

$$\begin{aligned} \lim_{l \rightarrow 0} \omega(l) &= 1, & \lim_{l \rightarrow \infty} \omega(l) &= 0 \\ \lim_{l \rightarrow 0} \delta(l) &= \max_{i \in \mathcal{F}} R_i / R^{\text{ideal}}, & \lim_{l \rightarrow \infty} \delta(l) &= 1 \end{aligned} \quad (5.17)$$

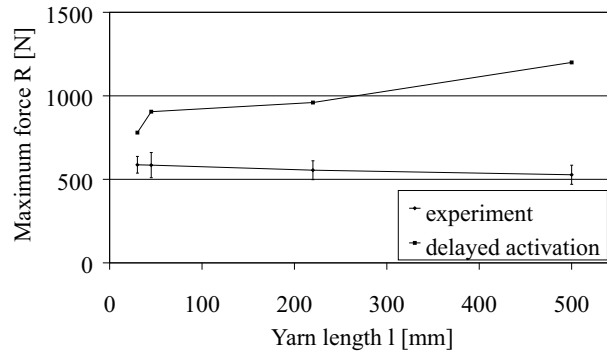


Figure 5.17: Size effect observed in experiment and reverse size effect induced by delayed activation

While the limits of $\omega(l)$ are obvious from the weakest link model, the limits of $\delta(l)$ deserve more detailed discussion. In the extreme case of an infinitely long specimen we would obtain immediate activation of all filaments and achieve the maximum achievable strength R^{ideal} with $\delta(\infty) = 1$. In the other extreme of an infinitely small specimen we can only draw a conditional theoretical conclusion: Realizing that the wave patterns considered in the Fig. 5.13 lead either to a finite activation range in cases (a), (b), (d) or even to an infinite activation range in case (c) we can state that there exists a sufficiently small specimen length $\Lambda \geq 0$ so that for $l \leq \Lambda$ each filament fails before the next one gets activated. As a result, the maximum total force is given as the maximum filament strength occurring in the bundle:

$$R(l) = \max_{i \in \mathcal{F}} R_i \quad \text{for } l \leq \Lambda \quad (5.18)$$

In other words, the bundle does not reach the state of a parallel load transmission, but acts as a zip fastener being opened. Of course, this picture is only illustrative since the model does not reflect the two and three-dimensional aspects of the material structure when l gets comparable with the filament diameter.

With the constructed limits, the normalized measured size effect may be expressed in a multiplicative form

$$\epsilon(l) = \omega(l) \delta(l) \quad (5.19)$$

with the qualitative plot shown in the Fig. 5.18. Again, this relation is only illustrative and neglects other length-dependent effects discussed in this paper or even their interactions. Nevertheless, an important message is that at least in the case of multi-filament yarn, the size effect must be considered in a complex sense: including both the sources of randomness affecting the filament strength and those affecting the stiffness evolution of the bundle in a length-dependent manner.

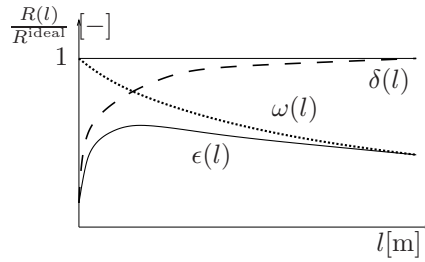


Figure 5.18: Correspondence between the statistical size effect $\omega(l)$, influence of delayed activation $\delta(l)$ and measured size effect $\epsilon(l)$

5.7 Conclusions

The available fiber bundle models could not be used for modeling the response measured in the yarn tensile test, because they impose practically unachievable assumptions of regular force transmission in the clamping at the ends and do not capture the disorder in the structure of filaments in the bundle. For this reason, we have developed a deterministic simplified computational model in order to include additional sources of randomness affecting the evolution of the stiffness during the loading.

We have shown that the stiffness evolution in the early stages of loading influences the maximum tensile force in the bundle. The model serves as a basis for a complex stochastic analysis of the complex size effects including all mentioned effects employing the random field simulation technique. The modeling technique and the evaluation of the complex size effect is described in detail in the following chapter 6.

Even without the full stochastic analysis, we may provide two important general results now:

- In qualitative terms, the numerical studies have shown, that the experimentally observed size effect is underestimated for shorter samples. As a consequence, an extrapolation of the size effect curve using the standard fiber bundle models from short-length experiments to long lengths would lead to an overestimation of their strength.
- The traditional FBM's cannot be used in order to derive the filament properties directly from the experimental data. The correct procedure is shown in the following chapter 6 or in the paper by [Vořechovský and Chudoba \(2004a\)](#).

As a final remark, we note that the phenomena of delayed activation may be present in any material structure. The only question is at which length scale of material structure it appears. In case of multi-filament yarns the length scale of delayed activation overlaps with the length scale of other sources of randomness (varying strength and stiffness) so that it must be included in the evaluation of the true size effect.

Chapter 6

Random properties over the length and size effect

Published in paper: [Vořechovský and Chudoba \(2004a\)](#)

The present study addresses the influence of variations in material properties along the multi-filament yarn on the overall response in the tensile test. In previous chapter we have described the applied model and studied the influence of scatter in material characteristics varying in the cross section with no variations along the filaments. In particular, we analyzed the influence of varying cross sectional area, filament length and delayed activation. Inclusion of these effects allowed us a better interpretation of the experimental data, especially with respect to the gradual stiffness activation, post-peak behavior and size effect. In the present paper, the length-related distributions of stiffness and strength are included by applying the Monte Carlo type simulation of random fields. Such an approach allows us (1) to demonstrate the strong need for including length scale to random fluctuation of strength along the filaments and (2) to combine several sources of randomness in a single analysis so that their significance can be evaluated from the tensile test response.

6.1 Introduction

The present work has arisen from the need to evaluate the variations of material properties in a AR-glass multi-filament yarn used in the production of textile-reinforced concrete. The heterogeneous nature of both the reinforcement and the matrix calls for thorough study of several sources of randomness that must be accounted for simultaneously.

In the preceding chapter ([Chudoba et al., 2004](#)) we have analyzed the influence of variations in the filament characteristics on the total response of a multi-filament bundle in the tensile test. The study included variations in three parameters influencing the stiffness and stress evolution of a bundle during the loading in different ways: filament diameter, filament length and delayed activation of individual filaments. In spite of the differences in the form of the calculated response curve, the variations in the three studied parameters have a common effect: the maximum tensile force gets reduced with a decreasing yarn length, i.e. in an opposite direction of length dependency compared to the statistical size effect in the classical sense (e.g. [Weibull, 1939a](#); [Bažant and Xi, 1991](#); [Bažant and Planas, 1998](#); [Bažant and Novák, 2000b](#)).

The main result of the previous study was a detailed description of the influence of waviness especially for short yarns on the maximum tensile force as an assumption for the correct interpretation of the tensile test response. It has been shown that the gradual increase of stiffness in the beginning of loading may be used to calibrate the activation density function and to evaluate its impact on the maximum tensile force. In order to establish the correspondence between the delayed activation and the wave patterns in the yarn (waviness) we have derived the activation density function for four idealized types of wave patterns. This study helped us to describe the kind of waviness occurring in the studied AR-glass yarn.

An algorithm used for the stochastic analysis is based on the superposition of the filament response (SFR) and provides an efficient tool for numerical tracing of the failure process in a material structure

consisting of linear-elastic brittle components. Similar algorithm has been used to visualize damage patterns in the anti-plane analysis of a two-phase composite [Alzebdeh et al. \(1998\)](#). The evaluation of the tensile response based on the SFR procedure is inexpensive in comparison with the full finite element computation and, therefore, very suitable for stochastic analyzes employing simulation of random fields. Furthermore, in the case of the studied AR-glass yarns, the friction between filaments has been neglected. This simplification has been justified by the post-peak amount of friction observed in the tensile experiment and allowed us to use the global load sharing rule for stress redistribution upon a filament failure ([Phoenix, 1978a](#)).

Up to this point, our study of variations in the filament parameters has been conducted on a one-at-a-time basis, the random nature of the distribution could be disregarded. In the present study, we focus on the effect of the spatial distribution of the material characteristics including their autocorrelation structure, in particular the strength f^t and E -modulus. In this case, we consider the randomness of their distribution stationary random processes. In particular we use a Monte Carlo type simulation method (Latin Hypercube Sampling) combined with orthogonal transformation of covariance matrix for representation of random fluctuation of filament properties. For the repeated evaluation of the randomized response we use the SFR algorithm ([Chudoba et al., 2004](#)).

By including both cross sectional and length-related variations in the modeling framework we are able to capture the whole loading and failure process during the test, including the size effect. An independent representation of the mentioned sources of randomness in the model allows us to focus the analysis on the separate effects in the test one after the other. Following the devised calibration procedure, the influence of the considered sources of randomness on the overall response can be traced back in a systematic way.

In this chapter, we first present the applied method of capturing the size effect due to the strength fluctuations along a single filament and relate the results to the local (classical) Weibull and non-local Weibull strength-based models in [Sec. 6.2](#). After that in [Sec. 6.3](#) we analyze the size effect due to the variations of the strength along the parallel system of filaments using both the stochastic numerical simulations and the analytical and numerical models due to [Daniels \(1945\)](#). The effect of the randomized stiffness along the bundle is added in [Sec. 6.4](#). Finally, in [Sec. 6.5](#) the stochastic model is applied to the performed tests on AR-glass rovings with the demonstration of the systematic calibration procedure for identifying the material parameters and their statistical characteristics.

6.2 Random strength along the filament

In the randomization of the material properties of the simulated yarn we distinguish the variability over the filaments $i \in \mathcal{F}$ in the yarn sections and the variability of stiffness and strength parameters over the material points of each filament \mathcal{M}_i . In the latter case of the spatial randomization (along the filament) it is necessary to account for distance-dependent autocorrelation of properties at two sampling points. Further, in case of strength randomization it is particularly necessary to correctly reflect the tails of the distribution in order to capture its minima.

In order to address these issues we analyze the correspondence between the two possible approaches to spatial randomization of the strength:

- The filament is considered as a chain of independent random parts/sub-chains with a given length and, therefore, can be simulated by independent identically distributed random variables. This kind of spatial randomness is built in the derivation of the Weibull integral ([6.1](#)) for the failure probability P_f .
- The other possible approach is to include autocorrelation along the filament and represent randomness of material parameters by one-dimensional random field (random process). This can be supported by the argument that there must exist some distance in which the fluctuation of parameters is correlated. This distance is independent of filament length and is a constant.

Due to the direct link between the strength randomization using the independent identical distributions (IID) and the Weibull distribution of P_f with a known asymptotic behavior we will use it to verify the ability of the stochastic model to cover the tails of the strength distribution.

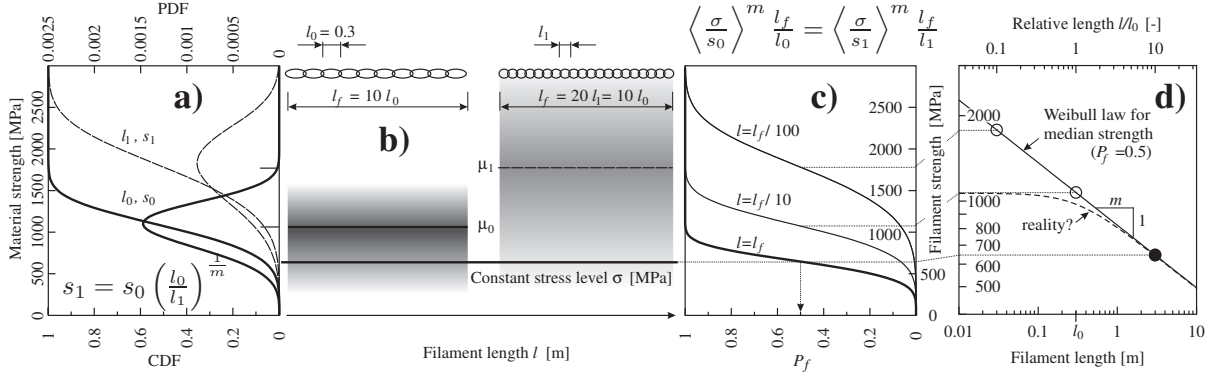


Figure 6.1: Weibull scaling

6.2.1 Spatial strength randomization using IID

Since we are dealing with strength of a fiber, we are interested particularly in the minima of strength realization over the filament length. It is well known from the theory of extreme values of IID that there are three and only three possible asymptotic (nondegenerate) limit distributions for minima (Fisher and Tippett, 1928) satisfying the condition $F_n(x) = [1 - (1 - F(x))^n]$. In order to avoid degeneration we look for the linear transformations with constants a_n and b_n (depending on n_f) such that the limit distributions $L(x) = \lim_{n \rightarrow \infty} L_n(a_n x + b_n) = \lim_{n \rightarrow \infty} 1 - [1 - L_n(a_n x + b_n)]^n$. Since we are using the Weibull elemental distribution the extreme values (minima) belong to the domain of attraction of Weibull distribution, and the sequences of constants a_n and b_n are known, see (e.g. Gnedenko, 1943; Gumbel, 1958; Castillo, 1988).

Using the weakest-link model together with the Weibull-type function for concentration of defects, the probability of failure P_f at a given level of stress σ is expressed as the so-called Weibull integral (Weibull, 1939a):

$$P_f(\sigma) = 1 - \exp \left[- \int_l \left\langle \frac{\sigma}{s_0} \right\rangle^m \frac{dl}{l_0} \right] \quad (6.1)$$

where the Malacuya brackets stand for positive part $\langle \bullet \rangle = \max(\bullet, 0)$. For a given Weibull modulus (shape parameter) m we have a length l_0 with the corresponding scale parameter of random strength distribution s_0 . In the case of a single filament, the stress σ is a positive constant so that we can rewrite the Eq. (6.1) as $-\ln(1 - P_f) = l/l_0 (\sigma/s_0)^m$. The strength level for a chosen level of P_f can now be expressed as a function of the filament length l :

$$\sigma(l) = s_0 [-\ln(1 - P_f)]^{1/m} \left(\frac{l_0}{l} \right)^{1/m}. \quad (6.2)$$

This size effect equation is a power law represented as a straight line in the double-log plot of l vs. σ with the slope $-1/m$ and passing through s_0 at l_0 (see Fig. 6.1d). The analytical determination of the mean strength requires an integration over all possible lengths l and leads to an expression employing the Gamma function Γ :

$$\bar{\sigma}(l) = s_0 \Gamma(1 + 1/m) \left(\frac{l_0}{l} \right)^{1/m} \quad (6.3)$$

The corresponding coefficient of variation (COV) of filament strength distribution is a constant independent of the filament length given by the Weibull modulus m :

$$\text{COV} = \sqrt{\frac{\Gamma(1 + 2/m)}{\Gamma^2(1 + 1/m)}} - 1. \quad (6.4)$$

Now, in order to establish the correspondence with the strength randomization by IID we visualize the important property of the Weibull distribution (Eq. 6.1): the scale parameter of the Weibull distribution

can be adjusted by for any length l_1 to deliver the same P_f as for the original reference length l_0 :

$$\frac{s_1}{s_0} = \left(\frac{l_0}{l_1} \right)^{1/m} \quad (6.5)$$

The length l_0 is sometimes referred to as “representative” but its choice is arbitrary so that we call it “reference length” throughout the text.

The two chains displayed in Fig. 6.1b have the same length l_f and different reference lengths l_0 and l_1 with corresponding scale parameters s_0 and s_1 complying with Eq. (6.5). Probability density function is denoted by PDF and cumulative density denoted by CDF. The diagram in Fig. 6.1a shows the scaled strength distributions corresponding to l_0 and l_1 . For a given stress level both distributions yield the same value of P_f as shown in Fig. 6.1c.

As a consequence the size effect $\sigma(l)$ obtained from Eq. (6.2) is identical for both reference lengths l_0, l_1 and the scale parameters s_0, s_1 , respectively. This can be seen on the example of the median size effect ($P_f = 0.5$) displayed in double-logarithmic plot in the Fig. 6.1d. This demonstrates the inherent feature of the Weibull distribution in the context of the weakest-link model already revealed in the Eq. (6.5): it is arbitrarily scalable with respect to the reference length l_0 .

This feature must be kept in mind when assessing the applicability of the independent identically distributed random variable simulations. Regarding the chain segments in Fig. 6.1b as sampling points $j \in \mathcal{M}$ of an IID random variable simulation we may reproduce the size effect with the slope $-1/m$ from Fig. 6.1b numerically in the following way:

1. assign each segment $j \in \langle 1, n_m = l/l_0 \rangle$ random strength level f_j^t following the distribution in the Fig. 6.1a,
2. determine the filament strength by finding the minimum segment strength $\min_{j \in \mathcal{M}}(f_j^t)$,
3. repeat (1) and (2) in n_{sim} number of simulations and evaluate the mean filament strength,
4. perform the step (3) for all the filament lengths l of interest.

Realizing that the reference length of one segment l_1 is arbitrarily scalable, we may perform this randomization with arbitrary segment length, including very small $l_1 \rightarrow 0$ with the scaling parameter $s_1 \rightarrow \infty$ and still obtain the same size effect. However, such a randomization has nothing to do with the real spatial distribution of strength along the fiber. Obviously, the strength scale must remain bounded for short segments. Otherwise, it would be theoretically possible to measure an arbitrarily high strength with very short specimens.

This discrepancy calls for the introduction of a length scale at which the assumption of IID at the neighboring sampling points must be abandoned. The anticipated shape of the size effect law reflecting the real spatial distribution of strength for short reference lengths is plotted in the Fig. 6.1d as a dashed line.

6.2.2 Spatial strength randomization using stationary random process

The length scale gets conveniently introduced in the form of an autocorrelation structure of the strength random field. From here on any applied random field will be stationary homogeneous and ergodic with autocorrelation function:

$$R_{aa}(\Delta d) = \exp \left[- \left(\frac{|\Delta d|}{l_\rho} \right)^p \right] \quad (6.6)$$

where l_ρ is positive parameter called *correlation length* of the random field. With decreasing distance d a stronger statistical correlation of a parameter in space is imposed. By setting the power $p = 2$ we construct the so called *squared exponential autocorrelation function* or *bell-shaped* or *Gaussian* autocorrelation function.

Advanced simulation techniques for the simulation of underlying random variables (Latin Hypercube Sampling) are coupled with an efficient implementation of orthogonal transformation of covariance matrix (see e.g. Novák et al., 2000; Olsson and Sandberg, 2002; Vořechovský and Novák, 2003a) needed for discrete representation of random fields (vectors). Latin Hypercube Sampling method is usually used

for cheap estimation of first statistical moments of response by means of simulations. This Monte Carlo type method has been tested to converge to correct results for extremes of random variables and the required number of simulations needed to capture the statistics of extremes accurately has been found, too (Vořechovský, 2004a).

A method by Vořechovský (2004b) with the possibility of cross-correlated random fields has been applied to obtain material parameters reflecting the input probability distributions. For accurate generation of uncorrelated Gaussian random variables needed for the expansion of a field the optimization technique Simulated annealing has been used (Vořechovský and Novák, 2002). A comparison of efficiency of different random variable simulation techniques needed for expansion of stochastic fields with a detailed error assessment has recently been published by Vořechovský and Novák (2003a).

The algorithm for the evaluation of the filament strength remains the same as described in the previous section, except for the randomization of the strength using the LHS technique in order to capture its extremes properly. Examples of the simulated random strength field realizations are shown later in the paper in the Fig. 6.6 for three filament lengths.

Since the most important value of the random strength process is its global minimum throughout the filament/process length, we used very dense discretization of the field. In particular 15 discretization points were used within the autocorrelation length. Clearly, this imposes a limit for modeling of filaments, let alone yarns, because such dense grids cannot be handled by today's computers in spite of their fast development. Fortunately, such detailed modeling of minima of long process is not necessary if we know its asymptotic properties (as will be shown later).

The calculated mean size effect curve (mean minima vs. length) qualitatively follows the dashed line shown in Fig. 6.1d. While the right asymptote converges to the size effect obtained from the IID randomization, the left asymptote becomes constant at the level of the basic (elemental) strength distribution. This means that for very long filaments ($l \gg l_\rho$), the influence of autocorrelation between neighboring points becomes negligible and the extremes of the field become identical to extremes of IID. On the other hand, for very short filaments ($l \ll l_\rho$) the spatial fluctuations in strength become insignificant, the random strength field is replaced by one random variable.

The transition zone between the two asymptotes is of special interest. It is an occasional practice (e.g. Bažant et al., 2004c) to avoid the more expensive random field simulations by defining the mean size effect as a bilinear curve consisting of the two described asymptotes with an intersection at $[l_\rho, \mu_0]$, see chapter 10. In such an approach the Weibull distributed IID randomization (with COV given by the Weibull modulus in Eq. (6.4)) is performed with the chain segments of the length l_0 . Random elements larger than l_0 (considered a known material parameter) are assigned with random mean strength scaled according to Eq. (6.5). However, elements smaller than l_0 are assigned with the mean μ_0 being equal to the mean strength of the filament of zero length and also being the mean corresponding to the length l_0 . In other words, the Weibull power law gets limited by a constant level of mean strength for elements smaller than l_0 . Then, the mean strength of a filament with the length $l = l_0$ lies exactly on the intersection of the two introduced asymptotes, see Fig. 6.1d. While this approach gives a good approximation of the field extremes (minima) for long filaments (large structures), it obviously leads to an overestimation of the mean strength for lengths $l \approx l_\rho$ (see Fig. 6.4). The reason is that the spatial correlation is too high and strongly influences the random strength field.

In order to introduce the statistical length scale in the Weibull power law for the mean size effect, we modify the Eq. (6.2) by introducing the length-dependent function $f(l)$ as a replacement of $(l_0/l)^{(1/m)}$ in the following form

$$\sigma(l) = s_0 [-\ln(1 - P_f)]^{1/m} f(l) \quad (6.7)$$

Here we preserve the approximation of the minima by Weibull distribution ($P_f = 1 - \exp[-\sigma/(s_0 f(l))]^m$). The coefficient of variation of Weibull distribution depends on m (similarly to the Weibull IID case) and is length-independent. Therefore, it is again given by the Eq. (6.4).

The means size effect can be analogically to Eq. (6.3) as:

$$\bar{\sigma}(l) = s_0 \Gamma(1 + 1/m) f(l) \quad (6.8)$$

The calculated mean of minima of one Weibull random process (single filament) covering the whole range of lengths is plotted in the upper curve of Fig. 6.4. The three introduced zones of the statistical size effect are denoted: single random variable ($l/l_\rho \rightarrow 0$), autocorrelated random field ($l/l_\rho \approx 1$) and the set of independent identically distributed random variables ($l/l_\rho \rightarrow \infty$).

We suggest to approximate the numerically obtained size effect by Eq. (6.7) with $f(l)$ expressed by one of the following formulas:

$$f(l) = \left(\frac{l}{l_\rho} + \frac{l_\rho}{l_\rho + l} \right)^{-1/m} \quad (6.9)$$

or

$$f(l) = \left(\frac{l_\rho}{l_\rho + l} \right)^{1/m} \quad (6.10)$$

This approach is done intuitively by asymptotic matching (left and right asymptotes are advocated above by the reasoning; and for the transitional sizes we use a smooth “interpolation”). The numerically obtained mean of minima lies in between these two approximations.

It should be mentioned, that another commonly applied way of introducing the length scale into the framework of the Weibull integral of P_f is to introduce the dependence between the sampling points of a strength randomization using IID indirectly by averaging the instantaneous stresses in the neighborhood of a material point (called non-local Weibull integral), see e.g. (Bažant and Xi, 1991; Bažant and Novák, 2000b). However, in our case of a uni-axial stress state and elastic-brittle filaments, the stress level is constant along the filament so that no averaging can be performed. In our opinion, this reveals an inconsistency in combining the stress averaging and the Weibull form of the P_f in order to introduce some kind of spatial correlation. The problem is that the key concept in deriving the Weibull integral of P_f is the independency of the failure probability $P_{f,1}$ of a subelement on its neighbors (survival probabilities are multiplied), see Weibull (1939a). This approach misuses the length scale introduced in phenomenological terms to mimic autocorrelation in the process zone, see section 7.3.1 p. 85. However, it does not necessarily reflect the statistical length scale associated with material randomness.

The nonlocal averaging is nowadays widely used as a limiter of spurious strain localization (e.g. Bažant and Planas, 1998). It proved itself to be a strong tool for regularization of ill-posed problems. But the statistical non-locality introduced by averaging of stresses entering Weibull integral (Bažant and Xi, 1991; Bažant and Novák, 2000b) aims at introducing the spatial correlation (dependence) of neighbor stresses. However, the approach (see section 7.3.1) may become inconsistent with the derivation of integral, which is local by definition. Moreover, it brings the length scale driven by deterministic nature (deterministic characteristic length) which generally may differ from the statistical length caused by material randomness. The argument is that statistical description of material should not depend on structural geometry or loading conditions.

6.3 Random strength along filaments within the bundle

Having demonstrated the correspondence between the stochastic simulation and the classical Weibull theory we proceed in a similar way in the validation of the stochastic model for the bundle of n_f parallel filaments. Again, we shall first focus on the randomization of strength using both the random process and the independent identically distributed random variables simulations, in order to allow for the comparison with the classical model of n_f parallel fibers formulated by Daniels (1945). The comparison will be performed by means of the size effect both for the numerical (sec. 6.3.1) and for the asymptotic analytical (sec. 6.3.2) forms of the Daniels’s model for the distribution of bundle strength Q_n^* .

In the stochastic simulations, we shall exploit the efficiency of the explicit response tracing algorithm based on the superposition of the filament response (SFR) described in the previous chapter or by Chudoba, Vořechovský, and Konrad (2004).

6.3.1 Comparison with Daniels’s numerical recursion

Daniels (1945) considered a system of n_f independent parallel fibers stretched between two clamps with equal load sharing. Filaments $i \in \mathcal{F}$ share the identical distribution function of strength $F_X(x) = F_i(x) = P_i(f^t \leq x/A)$. Besides the distribution, the filaments have also equal cross sectional area. The maximum tensile force of a filament given as $R(\theta) = Af^t(\theta)$ (θ stands for random nature) gets randomized for the individual filaments: $R_{(i)}$ and ordered ($R_{(i)} \leq R_{(i+1)}$) so that the marginal probability distribution

function of $R_{(k)}$ can be obtained in terms of $f_X(x)$ and $F_X(x)$ as (see e.g. [Gumbel, 1958](#)):

$$f_i(x_i) = i \binom{n_f}{i} [F_X(x_i)]^{i-1} [1 - F_X(x_i)]^{n_f-i} f_X(x_i) \quad (6.11)$$

The maximum tensile force of the bundle is given by:

$$Q_n^* = \max_{1 \leq i \leq n_f} \left(R_{(i)} \cdot \frac{n_f - i + 1}{n_f} \right) \quad (6.12)$$

Here, the yarn load is measured in terms of load per filament, i.e. $1/n_f$ times the total load on the system. The distribution of Q_n^* was investigated by [Daniels \(1945\)](#) under the assumption that filament strengths are independent and identically distributed random variables with known common distribution function. [Daniels \(1945\)](#) showed the distribution function of the maximum tensile force of the bundle with (IID) filaments to be:

$$G_n(x) = P(Q_n^* \leq x) = \sum_{i=1}^{n_f} (-1)^{i+1} \binom{n_f}{i} [F_X(x)]^i G_{n-i} \left(\frac{n_f x}{n_f - i} \right) \quad (6.13)$$

where $G_0(x) \equiv 1$ and $G_1(x) = F_X(x)$. The distribution functions $G_n(x)$ obtained from this recursive formula for $n_f = 1, 2, 4, 8, 16$ filaments are shown as dotted curves in the top diagram of the Fig. 6.2 for forces higher than 700 N for better legibility.

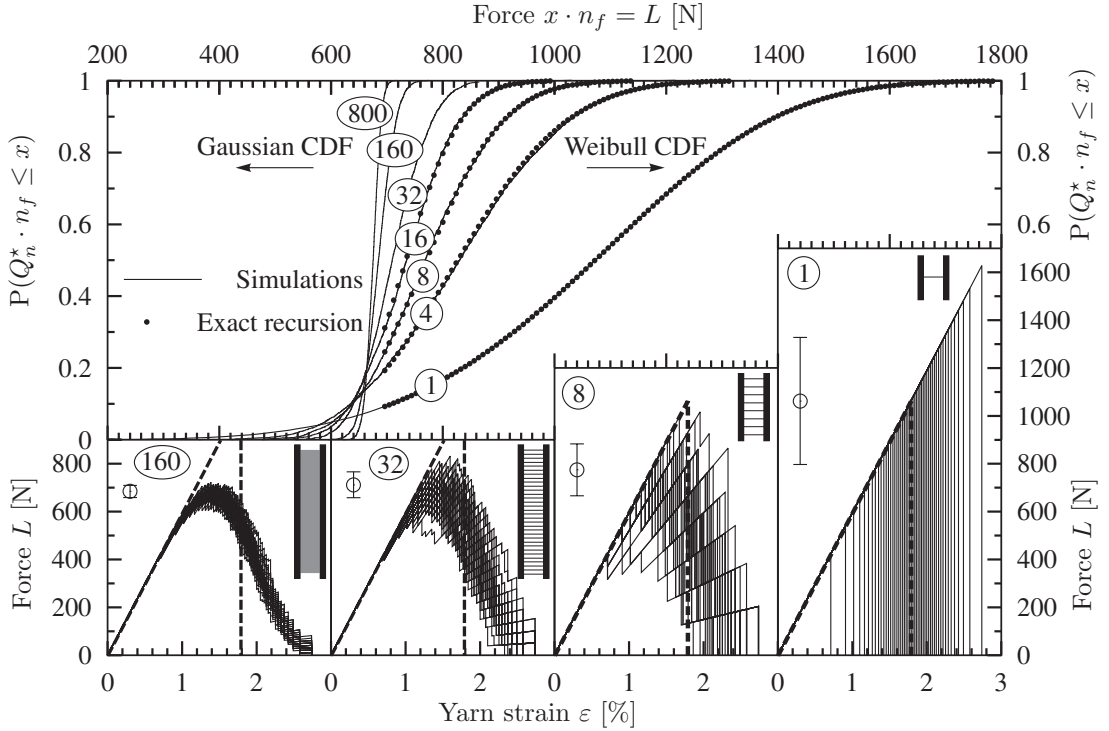


Figure 6.2: Top: Gradual change of the filament strength distribution from Weibull to asymptotically Gaussian for bundles with growing number of filaments n_f (in the circle). Exact results of Daniels's recursion (6.13) for small n_f is compared to numerical results by Monte Carlo simulation using the SFR algorithm Bottom: Samples of the whole L-D diagrams obtained by the SFR algorithm for selected numbers of filaments n_f in the yarn. Yarns are sketched and the mean value of strength \pm standard deviation is marked by a circle with errorbars.

In the same Figure we show the results of the stochastic simulation using the IID randomization of the filament strength for the bundles with up to 800 filaments. As plotting positions of the simulations we use $i/(n_{\text{sim}} + 1)$ (for reasons see [Gumbel \(1958, sec. 1.2.6\)](#)). It can be seen that the agreement between

the simulation and the recursive Daniels's formula is perfect. Nevertheless, the determination of failure probabilities at the low level of stress using Monte-Carlo method requires large number of simulations. On the other hand, the recursive formula does not require any additional computational effort for small probabilities. However, as n_f becomes larger than 32 the recursion becomes very demanding and then the only way to estimate the probability distribution is the use stochastic simulation. In addition, the stochastic simulation combined with the SFR algorithm delivers not only the strength distribution but is also able to trace the whole loading process as shown in the three diagrams at the bottom of the Fig. 6.2.

6.3.2 Comparison with Daniels's and Smith's asymptotic result

For the verification of the asymptotic convergence of stochastic simulation with independent identically distributed random filament strength we shall exploit the fact that for $n_f \rightarrow \infty$ the distribution function $G_n(x)$ converges to normal distribution (Daniels, 1945). In particular, Daniels obtained positive constants μ^* and σ^* such that $\sqrt{n_f}(Q_n^* - \mu^*)/\sigma^*$ tends to a normal random variable with zero mean and unit standard deviation. In other words, for large n_f the distribution function of the yarn strength, $G_n(x)$ can be approximated as

$$G_n(x) = P(Q_n^* \leq x) \approx \Phi\left(\frac{x - \mu^*}{\sigma^*} \sqrt{n_f}\right) \quad (6.14)$$

where $\Phi(\cdot)$ stands for standard normal cumulative density. The parameters of distribution (the mean value and variance) are: $\mu^* = E[Q_n^*] = x_0 [1 - F(x_0)]$, $\sigma^{*2}/n_f = D[Q_n^*] = x_0^2 F(x_0) [1 - F(x_0)]$. The result is valid under the conditions that a number x_0 maximizing the function $\mu(y) = y[1 - F(y)]$ is unique and positive and $\lim_{y \rightarrow \infty} \mu(y) = 0$, so $\mu^* = \mu(x_0) = \sup[\mu(y)]$, $y \geq 0$.

In the case of Weibull strength distribution of each filament $F_X(x) = 1 - \exp(-(x/s)^m)$ (zero threshold), where s is the scale parameter and m the Weibull modulus; the parameters can be easily obtained as:

$$\begin{aligned} x_0 &= s \cdot m^{-1/m} \\ \mu^* &= s \cdot m^{-1/m} \cdot e^{-1/m} \\ \sigma^* &= s \cdot m^{-1/m} \cdot \sqrt{e^{-1/m} [1 - e^{-1/m}]} \end{aligned} \quad (6.15)$$

In this case the result of asymptotic normality of strength Q_n^* is valid in the central region of the distribution. Clearly, if the strength of filaments is Weibull (limited from left by a zero threshold) the tail of Q_n^* cannot become Gaussian (Q_n^* must have a Weibull tail). However, the distance from the mean value (central part) to the tail measured in the number of standard deviations gets so large with high n_f that the tail gets practically unimportant.

Taking a closer look at the asymptote one can observe slowness of convergence (as $n_f^{-1/6}$). It should be pointed out that $G_n(x)$ is quite straight on normal probability papers even for small n_f so in that respect the approximation is good. Also the variance of numerically obtained $G_n(x)$ is very close to that predicted by Daniels's result. However, the error in mean value (shift) disappears extremely slowly with growing n_f . The reason is that for small number of filaments n_f the maximum Q_n^* can be reached at wide range of y , not just x_0 . As $n \rightarrow \infty$ the action point y shrinks from the wide range to x_0 only.

Smith (1982) found a way to eliminate the gap between the real $G_n(x)$ and Daniels's normal approximation by adjusting μ^* to μ^{**} using the actual (finite) number of filaments n_f in the following way

$$\mu^{**} = \mu^{**}(n_f) = \mu^* + n_f^{-2/3} b^* \lambda \quad (6.16)$$

For full derivation see Smith (1982). In case of Weibull $F(x)$ the parameter $b^* = s \cdot m^{-(1/m+1/3)} e^{-1/(3m)}$. Best results are obtained for the coefficient $\lambda = 0.996$. The error of approximation is then at most $O(n^{-1/3} (\log n_f)^2)$ which is an excellent improvement, mainly for small numbers of filaments in the yarn. For $n_f \rightarrow \infty$ the Smith's prediction μ^{**} converges to Daniels's μ^* .

The strength randomization of 1600 filaments by IID is displayed both in the linear plot and normal probability paper in the Fig. 6.3 and its best fit by a Gaussian distribution is compared to Daniels's and Smith's analytical results respectively. In our case the Weibull modulus is $m \doteq 4.54$, value typical for glass or polymer fibers ($COV_{ft} = 0.25$). The scale parameter $s = 0.727$ N corresponds to the maximum force of one filament and results in the mean filament strength μ_0 for reference length l_0 . For the example

of a yarn with $n_f = 1600$ filaments the mean value of normal approximation of maximal bundle force predicted by Daniels is $(n_f \cdot \mu^*) = 668.7\text{N}$ and Smith's refined value is $(n_f \cdot \mu_{1600}^{**}) = 672.1\text{N}$. Our numerical simulation by Monte Carlo gives estimation of the mean $\mu = 672.7\text{N}$ so the Smith's refinement is an excellent performer. The standard deviation of the yarn strength is numerically estimated to be equal to 9.674N and Daniels's formula multiplied by n_f gives the value of 8.297N . For the sake of comparison of results, plots of Daniels's approximation, Smith's refinement and the Monte Carlo simulations on a probability paper are plotted in Fig. 6.3. The analytical formula due to Daniels (1945) results in mean

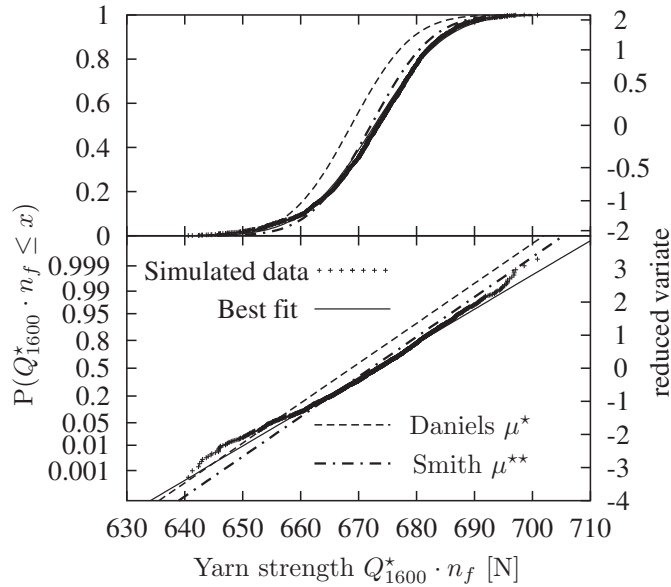


Figure 6.3: Comparison of simulated data, Daniels's and Smith's normal approximation for a yarn with $n_f = 1600$ filaments with independent identically distributed random strength in linear plot and normal probability paper.

strength shifted far from the exact one for small bundles.

6.3.3 Size effect of bundles for increasing number of filaments n_f

In the stochastic simulations, we used the response tracing algorithm based on the superposition of the filament response (SFR) described in the previous paper by Chudoba et al. (2004) together with simulation of random process needed for spatial randomization of strength. From here on we will use the abbreviation MSEC for mean size effect curve (a curve in the bi-logarithmic plot of size vs. mean strength). In Fig. 6.4 we have plotted the MSEC for various number of filaments in the randomized bundle. The right scale in the Fig. (6.4) shows the efficiency of the bundle depending on the number of filaments n_f and the yarn length l . It looks like the parallel curves are only shifted downwards with increasing number of filaments. The intersection of the horizontal asymptote with the inclined IID asymptote seems to happen always at the autocorrelation length of l_ρ , so the autocorrelation length propagates to bundles unchanged causing curvature of MSEC compared to classical Weibull IID case (straight line). This is an important property because it indicates that the size effect can be expressed as a product of the length effect with the effect of increasing number of filaments.

Indeed, with regard to the Daniels's assumption of common strength distribution of independent filaments that applies for any length we may express the Weibull bundle strength per filament in dependence on l and n_f using the Eq. (6.16) as

$$\mu_I^{**}(n_f, l) = \mu^{**}(n_f) f(l). \quad (6.17)$$

In other words both effects can be evaluated independently using either analytical formulation or stochastic SFR simulation. Subsequently, they can be composed using Eq. (6.17) into a combined size effect surface. An example of such a surface constructed with $f(l)$ of the form (6.10) and with bundle efficiency

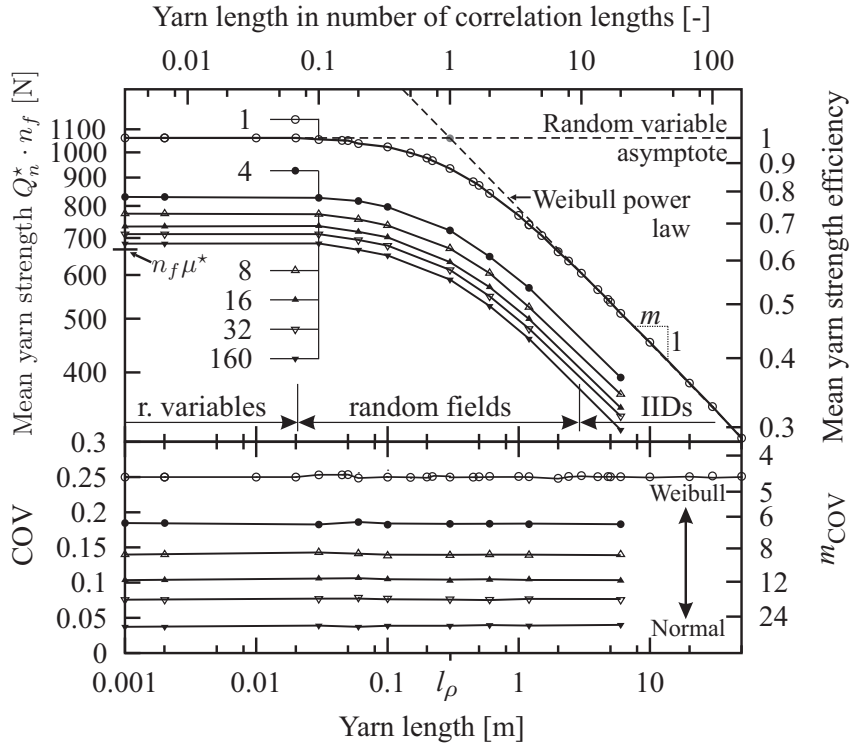


Figure 6.4: Top: Mean size effect curves (MSEC) for increasing number of filaments n_f in a bundle for filament strength described by Weibull random process. Curves nearly overlap for n_f higher than 160. Bottom: Effective Weibull modulus m computed using Eq. (6.4) for different yarn lengths and numbers of filaments n_f .

$\mu^{**}(n_f)$ calculated numerically for a short bundle with the SFR algorithm is plotted in Fig. 6.5. Obviously, with $n_f \rightarrow \infty$ the surface (6.17) reduces to the curve $\mu^*f(l)$. This demonstrates that the mean strength is asymptotically independent of the number of filaments n_f .

Regarding the strength variability of the yarn we note that COV of strength depends on Weibull modulus m irrespective the length. The Fig. (6.4) presents effective values of the Weibull modulus m_{COV} computed for different number of filaments from COV by solving the formula (6.4). Of course, only for the case of a single-filament-bundle the value m_{COV} really represents a shape parameter of Weibull strength distribution. On the other hand, COV decreases for growing n_f with the rate $1/\sqrt{n_f}$. To summarize, while the weakest-link model (series coupling & extending in length) leads to the decrease of mean and constant COV, the yarn (parallel coupling & increasing n_f) results in asymptotically constant mean and fast decay of COV.

The last question is the distribution of the strength. In case of a single filament, the PDF of Q_1^* remains Weibull. With increasing n_f the probability distribution of Q_n^* gradually changes to Gaussian (Daniels, 1945), see Fig. 6.5.

6.4 Random stiffness along the bundle

6.4.1 Asymptotic behavior with random stiffness

The results obtained for bundles with random filament strength are not sufficient to describe the size effect of real bundles, where also the stiffness filament stiffness is variable. The original Daniels's results (both, the numerical recursion and asymptotic normality of strength) are derived under the assumption of equal (deterministic) stiffness.

The asymptotic normality of the distribution of the fiber bundle strength has been demonstrated under less strict assumptions than those used by Daniels (see Hohenbichler, 1983, for a review). It has

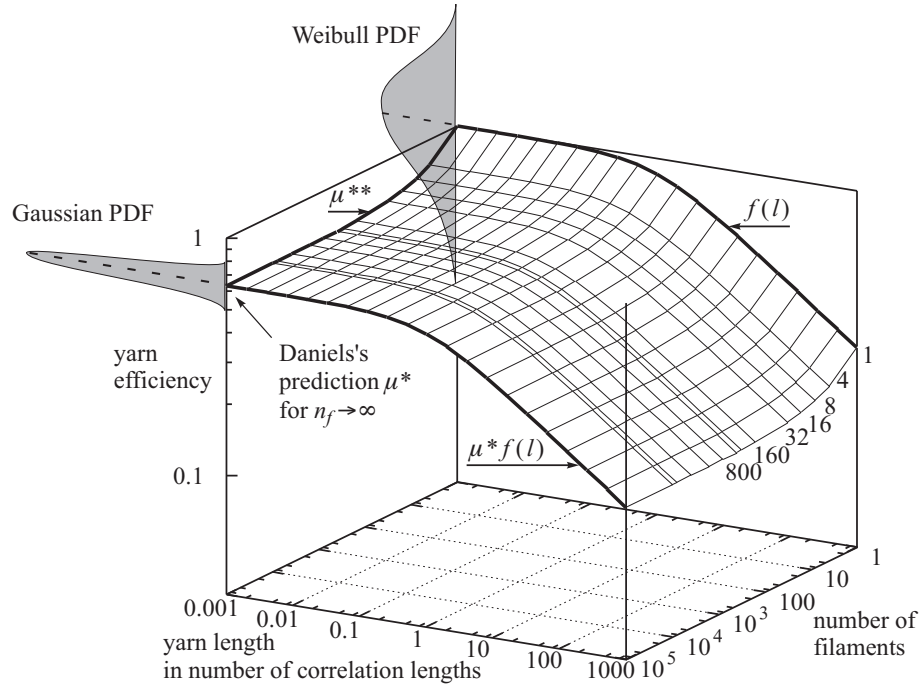


Figure 6.5: 3D representation of bundle efficiency depending on the number of filaments and yarn length for the case of random strength described by random processes. The combined size effect of both n_f and l is displayed as a surface plot with coordinates $x = n_f$ (converge to constant value by Daniels), $y = l$ (logarithmic coordinate, function $f(l)$) and $z = \text{mean strength}$.

been shown that the asymptotic normality is also valid under certain weak dependencies between filament strengths and for independent filaments but with general force-displacement relations.

Even though the asymptotic distribution is known for many cases, this result is not always a good approximation for small to medium-size yarns. This is because the convergence to the asymptotic distribution is very slow. Based on the procedure of [Hohenbichler and Rackwitz \(1983\)](#) the exact distribution can be determined from the system reliability results. The authors used transformation of two pairs of input random variables (filament strength f^t and a corresponding peak strain) into standardized space of uncorrelated normal variables and solved the reliability using First Order Reliability Method (FORM).

When the stiffness is random together with random strength (but linear stress-strain law until sudden failure is kept) the total force $L(\varepsilon)$ as a function of deformation is:

$$L(\varepsilon) = \sum F_i(\varepsilon)$$

where the summation is over all unbroken filaments from the set $i \in \mathcal{F}$. Strength of the yarn is

$$Q_n^* = \max_{\varepsilon} L(\varepsilon) = \max_{\varepsilon} \sum F_i(\varepsilon) \quad (6.18)$$

The distribution function of Q_n^* is

$$G_n(x) = P\left(\max_{\varepsilon} \sum F_i(\varepsilon) \leq x\right) = P\left(\bigcap_{\varepsilon} \left[\sum F_i(\varepsilon) - x \leq 0\right]\right) \quad (6.19)$$

and from the reliability bound of parallel systems we can write the inequality

$$G_n(x) \leq \min_{\varepsilon} \left[P\left(\sum F_i(\varepsilon) - x \leq 0\right) \right] \quad (6.20)$$

The maximum value of $F(\varepsilon)$ occurs in peak points of the filaments so the intersection in the formula is therefore over n_f events.

Let the ordered deformations of fiber failures be a set of random variables: $\varepsilon_{(1)}^f \leq \varepsilon_{(2)}^f \leq \dots \leq \varepsilon_{(n_f)}^f$. The total yarn force at $\varepsilon = \varepsilon_{(k)}^f$ is

$$L(\varepsilon_{(k)}^f) = \sum_{i=k}^n F_i(\varepsilon_{(k)}^f) = \sum_{i=k}^n \varepsilon_{(k)}^f \frac{R_{(i)}}{\varepsilon_{(i)}^f} \quad (6.21)$$

Let us consider $F_{(i)}$ the strength of filament with maximal strain $\varepsilon_{(i)}$. The yarn strength is then

$$Q_n^* = \max_{1 \leq k \leq n} L(\varepsilon_{(k)}^f) = \max_{1 \leq k \leq n} \sum_{i=k}^n \varepsilon_{(k)}^f \frac{R_{(i)}}{\varepsilon_{(i)}^f} \quad (6.22)$$

(which simplifies to formula (6.12) for equal stiffness). The distribution function of Q_n^* is

$$G_n(x) = \mathbb{P} \left[\bigcap_{k=1}^n \left\{ \sum_{i=k}^n \varepsilon_{(k)}^f \frac{R_{(i)}}{\varepsilon_{(i)}^f} - x \leq 0 \right\} \right] \quad (6.23)$$

Unfortunately, in our case we have also the activation deformation of each filament a random variable distributed according to the ‘‘activation density’’. (ε_i^0 activation strain) and we will seek the distribution numerically.

In our model we have the set of n_f triples - basic random variables $(R_1, \varepsilon_1^0, \varepsilon_1^f)$, $(R_2, \varepsilon_2^0, \varepsilon_2^f)$, \dots , $(R_n, \varepsilon_n^0, \varepsilon_n^f)$. The random variables R_i , ε_i^0 and ε_i^f within each triple may be dependent. In the expression for $G_n(x)$ the basic random variables have been ordered as $(R_{(1)}, \varepsilon_{(1)}^0, \varepsilon_{(1)}^f)$, \dots , $(R_{(n)}, \varepsilon_{(n)}^0, \varepsilon_{(n)}^f)$ and these triples are no longer independent. We may perform the Rosenblatt transformation to make them independent.

6.4.2 Comparison between the effect of random strength and stiffness

The numerical study using the randomized E -modulus has been performed with n_f variate uncorrelated fields. In order to demonstrate the differences with respect to the strength-induced size effect, the strength randomization is included as well. The parameters of applied normal distributions of randomized E -modulus and f^t are summarized by Eq. (6.27) and Eq. (6.28). The spatial randomization has been performed with common squared-exponential autocorrelation function (6.6) both for E -modulus and for strength f^t .

Similarly to the Part I the yarn performance is illustrated qualitatively using the load-strain diagram on a yarn with 16 filaments only. The real number of filaments in the yarn is approximately 100-times higher. In order to have the resulting forces in the figures comparable to the real values, the forces are given in cN. Of course, the true maximum force of 1600 filament bundle cannot be obtained by scaling up the results from the small bundle. Nevertheless, the small bundle can be effectively used to study the effects of random stiffness, strength and their interactions with varying length. The simulation of real yarns is postponed to the Sec. 6.5.2.

In particular, two 16-variate processes for the two random parameters E and f^t were simulated as the 16-variate Gaussian random process discretized using vectors with the m number of material points $j \in \mathcal{M}_i$ for each filament i , $i = 1, \dots, 16$. The simulated random process for three ratios between the nominal length and the autocorrelation length l/l_ρ is shown in the first row of the Fig. 6.6. The left scale in the first row shows values of the *tensile strength* f^t while the right hand scale presents values of the *Young's modulus*. The $n_{\text{sim}} = 50$ realizations of the random field is plotted representing the properties of the first filament in a bundle of 16 (filaments). Due to the identical autocorrelation structure the realizations of E and f^t are qualitatively similar. For the purpose of this study, 50 bundle realizations (simulations) have been performed, which might not be sufficient for real simulation of statistics, especially when higher statistical moments of the response (or even reliability) are targeted. We must keep in mind that n_{sim} must be significantly increased to ensure that the samples represent high-dimensional space of independent Gaussian random variables needed for expansion of the fields in case of long specimens ($l/l_\rho \rightarrow \infty$). Besides the calculated response load-strain curves for random strength f^t and E -modulus,

the Fig. 6.6 also shows the mean value and standard deviation of the resulting maximum tensile force together with the sketch of corresponding PDF.

The results obtained with the randomized strength are shown in the second row of the Fig. 6.6 and demonstrate once again the reduction of maximum tensile force with an increasing nominal length l . Except of the reduction of the maximum load we observe the reduced scatter in the response for long samples which is a classical feature of the statistical size effect.

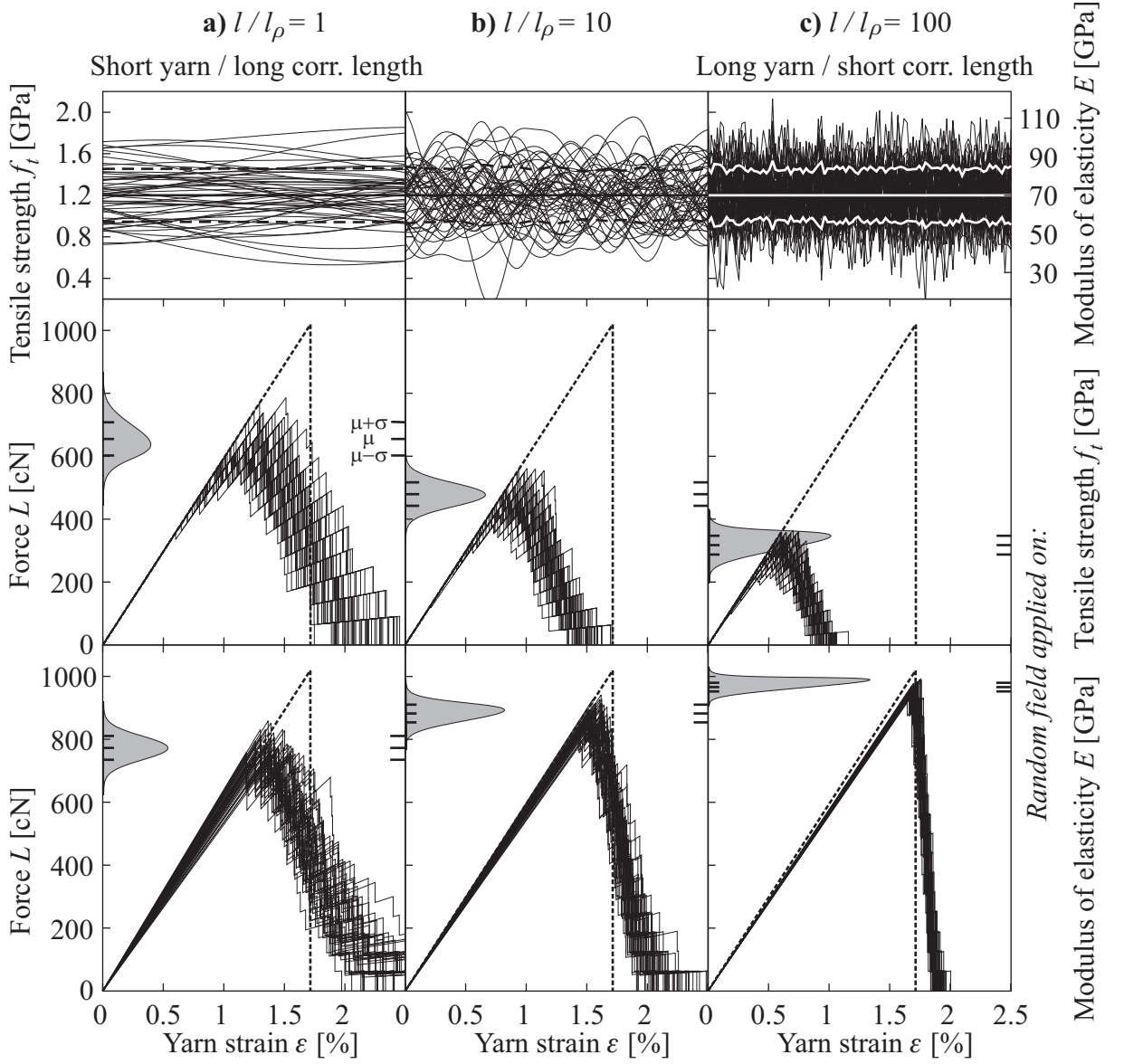


Figure 6.6: Comparison of the three random fields with different correlation lengths and load deflection diagrams of 16 filament yarn with fields applied to f^t and E .

All three chosen ratios between the process length and its autocorrelation length fall into the transition zone ($l/l_\rho \in \langle 1, 100 \rangle$) between the random variable case and the IID case for each filament.

The effect of the fluctuating E -modulus described by 16-variate vector random field (16 uncorrelated random processes) is shown in the third row of the Fig. 6.6. The response curves reveal a scatter in stiffness that gets amplified for short yarns (or shorter correlation lengths) and that vanishes for long yarns. The explanation for this is obvious: realizing that the stiffness of the i -th filament with n_m number

of discretization points gets computed as

$$K_{(i)} = \left(\sum_{j=1}^m K_{(i),j}^{-1} \right)^{-1} = \frac{\prod_{j=1}^m K_{(i),j}}{\sum_{s=1}^m \prod_{j=1; j \neq s}^m K_{(i),j}} \quad (6.24)$$

and the stiffness of the bundle with n_f filaments is obtained as

$$K = \sum_{i=1}^n K_{(i)} = \left[\sum_{i=1}^n \frac{\prod_{j=1}^m K_{(i),j}}{\sum_{s=1}^m \prod_{j=1; j \neq s}^m K_{(i),j}} \right] \quad (6.25)$$

we notice that the fluctuations get smeared for long filaments ($l/l_\rho \rightarrow \infty$) and overall stiffness converges to the value $K_\infty = n_f \mu_E A/l$.

Regarding the ultimate strength, the short yarns fail at lower forces, because of the irregular stress distribution across the yarn during the loading. Filaments with lower effective stiffness accomplish only a reduced contribution to the overall force transmission at the peak load and reach their maximum force only later in the post-peak region. This effect gets amplified for specimens of the length $l \ll l_\rho$ with constant stiffness along the filament. Then, the random field can be reduced to random variable assigning constant stiffness to each filament in the bundle. This case furnishes the lower bound on strength reduction due to the scatter in stiffness. The qualitative form of the size effect curve with (i) both E -modulus and f^t random is compared to (ii) case with random f^t in Fig. 6.7 bottom.

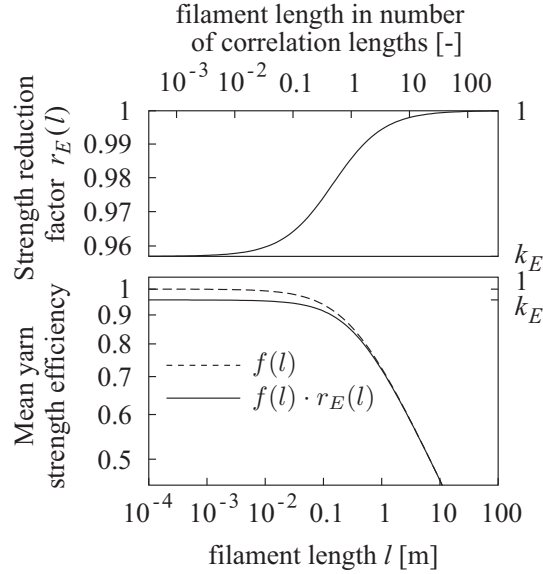


Figure 6.7: Top: Strength reduction function $r_E(l)$ due to random E -modulus in addition to random strength. Bottom: Size effect curves due to the scatter in strength and scatter in both stiffness and strength

The relative amount of strength reduction $r_E(l)$ due to the random stiffness for varying specimen length may be approximately expressed using the function:

$$r_E(l) = k_E \left(1 + \frac{l_\rho}{\frac{1}{l} + L_p} \right), \quad L_p = l_\rho \frac{k_E}{1 - k_E} \quad (6.26)$$

where k_E is the ratio between short yarn ($l \ll l_\rho$) strength with (i) both E and f^t random and (ii) random f^t . This suggested function has horizontal asymptotes and defines smooth transition between k_E for short yarns and 1 for long yarns, see Fig. 6.7 top.

6.5 Application to the experiment

Putting the results from the preceding and from the present chapter together allows us to account for all the considered sources of disorder in the yarn and in the distortions of the test setup within a single computational model. With the stochastic simulation framework at hand we now proceed with the simulation of the tensile test on yarns and filaments with varied length in order to quantify the significance of the included sources of randomness in a real material.

6.5.1 Testing of single filament

The most natural way of identifying the distributions of the filament strength and stiffness is to test single filaments with varied length. These experiments have been performed by carefully extracting single filaments from the AR-glass 2400 tex yarns on the testing machine (Fafegraph ME).

However, the tensile test on AR-glass filament has turned out infeasible as far as the measured strength was concerned. The problem was that the measured maximum forces were obviously distorted due to the damage of the glass in the clamps as documented by the big portion of the specimens that broke in the vicinity of the clamps. As a result, lower strength has been measured than actually available.

Nevertheless, some information could be extracted from the test results since the positions of break (either free length, or clamp) have been recorded for all specimens. Surprisingly enough, no size effect could be observed on the filaments that broke in the free length with the lengths $l = 0.01, 0.018, 0.030, 0.055, 0.10$ m. The explanation for this has been delivered later by the simulations of the bundle tests. As documented further, all the tested lengths fall into the range $l < l_p$ (see Fig. 6.9) with negligible fluctuations of strength and, consequently, without significant size effect.

Fortunately, the measurement of stiffness provided reliable data, especially thanks to the careful documentation of the association between the specimens and the measured response and also of the original positioning of specimens along the filament. Due to the large differences between the filament diameters in the bundle but low fluctuations over its length, it turned out to be very important to quantify the stiffness separately for each group of specimens stemming from the same filament. We appointed the scatter in stiffness solely to the E -modulus. The cross sectional area has been considered constant and has been set to the mean value of diameter determined from the micrographs of the yarn cross section (see Fig. 5.8, page 52).

$$\begin{array}{|l} \mu_E = 70 \text{ GPa}, \sigma_E = 10.5 \text{ GPa}, (\text{COV}_E = 15\%) \\ \text{filament diameter (circular cross section)} = 26 \mu\text{m} \end{array} \quad (6.27)$$

Clearly, a good testing of isolated filaments is desirable for its statistical characterization, but the design of a reliable testing set up is by no means trivial. Except of the mentioned distortions, also problems with capturing the influence of coating and of the pre-selection of “better” (stronger) specimens during their extraction from the bundle would have to be addressed.

6.5.2 Tensile test on a bundle

Because of the difficulties with determining f^t using the tensile test on filament, we had to identify the sought distributions with the help of the stochastic simulation of the tests on bundles. Before starting with the calibration procedure we summarize the types of influence of the investigated sources of randomness on the load-deformation response for increasing specimen length.

The Table 6.1 shows the tendencies in the measured load-deformation curve for increasing nominal length l for a finite level of scatter in the material parameters. For example, the first row indicates that the observed gradual increase of stiffness in the beginning of loading is affected only by the relative differences in the filament lengths and that it diminishes for longer specimens. As a consequence, this effect can be considered in an isolated way and the distribution of $\varepsilon_{(i)}^0$ can be calibrated separately from the other parameters as has been done in the preceding chapter or paper due to Chudoba, Vořechovský, and Konrad (2004).

Using the distributions of $\varepsilon_{(i)}^0$ obtained for the studied lengths in Part I the gradual growth of stiffness can be reproduced as shown there in the Fig. 16. For the sake of simplicity, ε_0 has not been randomized. Instead of this, the inverse cumulative activation density function has been used to deterministically

	$\sigma(l_{(i)})$	$\sigma(A_{(i)})$	$\sigma(\varepsilon_{(i)}^0)$	$\sigma(f_{(i),j}^t)$	$\sigma(E_{(i),j})$
$A(l)$: delayed activation	(.)	(.)	(-)	(.)	(.)
$B(l)$: max. tensile force	(+)	(.)	(+)	(-)	(+)
$C(l)$: scatter in tensile force	(.)	(.)	(-)	(-)	(-)
$D(l)$: stiffness	(+)	(.)	(+)	(.)	(.)
$E(l)$: scatter in stiffness	(-)	(.)	(-)	(.)	(-)
$F(l)$: post-peak range	(-)	(.)	(-)	(-)	(-)

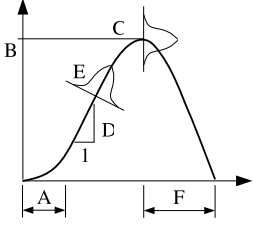


Table 6.1: Influence of randomness in material parameters on the measured load-deformation diagrams with increasing length

assign the appropriate fraction of activation strain to the corresponding fraction of filaments. In this way, only the mean load-deformation curve gets reproduced but not the variations in different specimens. In other words, there is no scatter in the observed delayed activation denoted as A in Table 6.1. This little methodological transgression can be accepted in the light of the overall simulation concept and does not reduce the generality of the present modeling strategy.

As demonstrated in previous chapter, the effect of random $l_{(i)}$ and $A_{(i)}$ can be neglected so that we may focus on the calibration of the last two parameters listed in Fig. 6.1 – $E_{(i),j}$ and $f_{(i)}^t$. The results of the simulation are shown in Fig. 6.8 without and with the delayed activation. Both filament tensile strength f^t and stiffness in form of Young’s modulus E were represented by Weibull distributed random process with the autocorrelation structure given in Eq. 6.6. These two properties were assumed mutually independent and independency was assumed also among filaments. The following values were found to best fit the experiments:

$$\mu_{f^t} = 1.25 \text{ GPa}, \quad \sigma_{f^t} = 0.3125 \text{ GPa}, \quad (\text{COV}_{f^t} = 25\%) \quad (6.28)$$

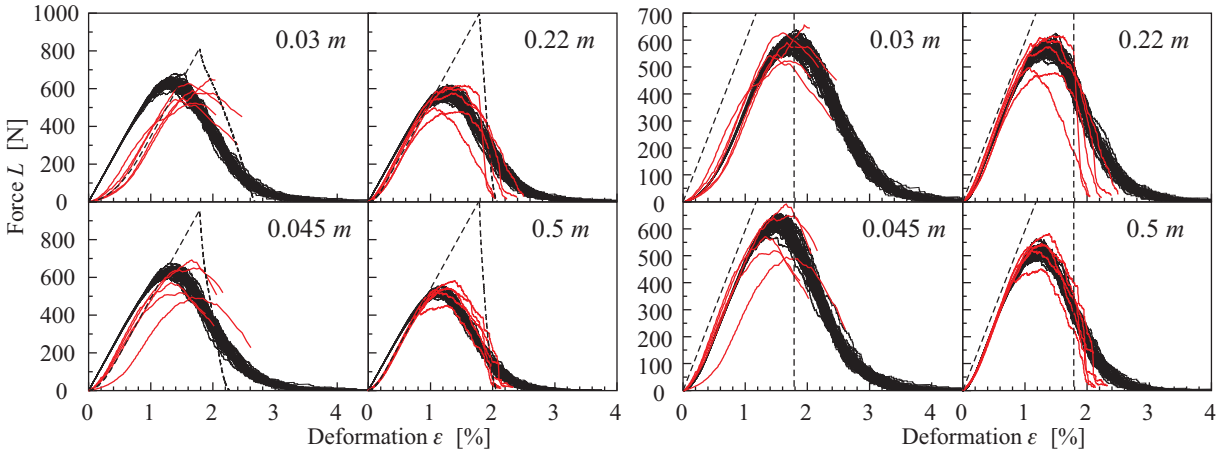


Figure 6.8: Comparison of numerical simulations with experiments (red). Left: Simulations without delayed activation, randomized stiffness and strength. Diagram computed with DA plotted with dashed line. Right: Simulations with included delayed activation, randomized stiffness and strength. Diagrams computed with mean values plotted with dashed line.

The correspondence between the size effect curves obtained in previous sections and the complex size effect observed in the tensile test is shown in Fig. 6.9. The experimental curve has been reproduced by the stochastic model including the influence of all three random properties simultaneously: E , f^t and ε_0 . In order to show the influence of randomness of each parameter separately, the size effect curves have been plotted for isolated randomizations of (ε_0) , (f^t) and (f^t, E)

In addition to the size effect curves obtained from the random process simulations Fig. 6.9 also shows the size effect obtained with the Daniels’s and Smith’s models calculated with $n_f = 1600$. Assuming that

6.5.3 Systematic identification of the distribution parameters

Based on the experience with fitting the performed tests we are able to suggest a systematic approach for deriving the statistical characteristics of the multi-filament yarn. The previously described procedure represents the most difficult case including the delayed activation and may be simplified for other types of yarns for which this effect is less pronounced (e.g. polypropylene yarns).

The crucial problem in planning the experimental sequence for constructing the size effect curve is the estimation of the autocorrelation length l_ρ . A possible strategy to estimate the right asymptote of the size effect law is to perform replicated tests on at least two selected lengths $l \gg l_\rho$ and to determine the slope ($1/m_{\text{slope}}$) of the line connecting the obtained mean strength values in double logarithmic plot.

The determination of the left asymptote requires the test of short bundles $l \ll l_\rho$ usually exhibiting a high amount of experimental distortions (irregular load transmission from the clamps to the filaments). Due to these difficulties it is more effective to test single filaments extracted from the bundle. The statistical data analysis allows us to determine the Weibull modulus m_{scatter} from Eq. (6.4). We recommend to test the filaments for at least two lengths in order to ensure that the condition $l \ll l_\rho$ applies for both, i.e. that the estimate of l_ρ is realistic and the mean strength of both lengths is equal. Of course, the modulus m_{scatter} obtained for each length must be equal.

Now, the condition $m_{\text{slope}} = m_{\text{scatter}}$ may be used to verify that the two bundle lengths used to determine the right asymptote slope fulfill the condition $l \gg l_\rho$. If $m_{\text{slope}} > m_{\text{scatter}}$, the autocorrelation length l_ρ has probably been underestimated and the chosen specimen lengths are in range $l \approx l_\rho$. In such a case, longer specimens must be tested.

The mean strength measured on filaments may be easily transferred to the mean bundle strength with n_f filaments by using the Daniels's or Smith's formulas (6.15), (6.16).

Besides of determining the mean strength, the tests on single filaments can further be exploited to determine the randomness of the E -modulus. In order to determine the reduction of strength k_E introduced in Eq. (6.26) random variable simulation with the experimentally obtained distribution parameters together with the SFR algorithm may be employed.

Finally, the sought autocorrelation length can be determined as an intersection of the two independently determined asymptotes. With the known l_ρ at hand we may express the resulting approximation of the MSEC as a product of Eqns. (6.17) with (6.26)

$$\mu_{II}^{**}(n_f, l, E) = \mu^{**}(n_f) \cdot f(l) \cdot r_E(l). \quad (6.30)$$

If the strength of single filaments cannot be measured reliably (as in the case of the used glass filaments) and there is no chance to judge about the autocorrelation length, we have to fit the formula (6.30) to the data by applying the stochastic simulation of the bundle and find all the parameters of the MSEC by fitting as shown in the previous section.

6.6 Conclusions

In the two companion chapters we have identified and studied five different sources of disorder in the bundle tensile test: delayed activation of filaments, variable cross sectional area of filaments, differences in filament lengths, variability of E -modulus and of tensile strength along the filaments.

Based on the efficient micromechanical model of the fiber bundle developed in Part I we have performed stochastic simulation with randomized stiffness and strength along the filaments in the bundle. The stochastic modeling framework has been used to derive size effect laws for each of the considered sources of randomness separately. Based on the lessons learned from the numerical analysis we have suggested approximation formulas describing the size effect laws due to the random strength or stiffness along the bundle. The obtained results have been verified with the help of the available analytical and numerical fiber bundle models by Smith and Daniels.

The available fiber bundle models could not be used for modeling the response measured in the yarn tensile test, because they impose piritically unachievable assumptions of regular force transmission in the clamping and do not capture the disorder in the structure of filaments in the bundle. For this reason, we have developed a deterministic simplified computational model in order to include additional sources of randomness affecting the evolution of the stiffness during the loading.

The detailed knowledge of the length-dependent performance of the yarn allowed us to quantify the parameters of the statistical distribution of the filament and bundle properties as a means of disorder in the material structure. An extensive testing program has been worked out so that the results of the simulation could be compared with the test results of the tensile test on bundles and on filaments with varied length.

The performed stochastic simulations with the available experimental data revealed the existence of statistical length scale that could be captured by introducing autocorrelation of random material properties. This represents the departure from the classical Weibull-based models that are lacking any kind of length-scale.

The introduced model delivers a quasi-ductile response of the bundle from the ensemble of interacting linear-elastic brittle components with irregular properties. In this respect the present approach falls into the category of lattice models used to model quasi-brittle behavior of concrete. It should be noted, that due to the possibility to trace the failure process in a detailed way both in the experiment and in the simulation, the modeling of multi-filament yarns provides a unique opportunity to study the local effects in quasi-brittle materials. To possibility to generalize the results for other quasi-brittle materials is worth further intensive studies.

The obtained statistical material characteristics turned out to be of crucial importance for robust modeling of crack bridges occurring in the cementitious textile composites. The “well designed” microstructure of the yarn and of the bond layer in the crack bridge may significantly increase the overall deformation capacity (ductility) of structural elements. The lessons learned from the present study can be applied in a more targeted development of new yarn and textile structures with an improved performance of crack bridges.

As a final remark, we note that the phenomena of delayed activation may be present in any material structure. The only question is at which length scale of material structure it appears. In case of multi-filament yarns the length scale of delayed activation overlaps with the length scale of other sources of randomness (varying strength and stiffness) so that it must be included in the evaluation of the true size effect. Generally effects similar to (or caused by) delayed activation or large variability of stiffness may distorts experimental data. For example in case size effect test of dog-bone specimens made of concrete and loaded in tension ([Van Vliet and Van Mier, 1998, 2000](#)) the unusual shape of mean size effect curve can certainly be satisfactorily explained by the structural disorder in testing the small scale sample.

Part III

**STOCHASTIC MODELING OF
QUASIBRITTLE MATERIALS**

Chapter 7

Size effect on modulus of rupture of concrete structures: state of the art

The chapter introduces the problem of modulus of rupture of concrete structures. The state of the art is reviewed as the starting point for author's investigations presented in the following chapters of this part of thesis.

7.1 Introduction

The modulus of rupture, which characterizes the bending strength (or the apparent tensile strength) of unreinforced beams, is known to depend on the beam size. The structure size effect on the modulus of rupture of plain concrete beams as well as other quasibrittle materials (such as rocks, composites, ceramics or ice) has classically been explained purely statistically – the randomness of the intrinsic material strength (see e.g. Bažant and Planas, 1998, for a review), as suggested already by Mariotte (1686) and mathematically described in a final form by the theory of Weibull (1939a,b).

However, as revealed by the finite element calculations of Hillerborg et al. (1976) and thoroughly demonstrated by Petersson (1981), the statistical explanation ignores the stress redistributions caused by cracking prior to the maximum load and the mean observed size effect can be described deterministically by the cohesive (or fictitious) crack model. A simple analytical formula based on this redistribution was derived by Bažant et al. (1995) and was shown to match all the important test data reasonably well. The same formula was proposed earlier on an empirical basis by (Rokugo et al., 1995) (cf. Bažant 1996). It was also shown that this formula can be derived from fracture mechanics if the non-negligible size of the fracture process zone near the tensile face of beam is taken into account (Bažant, 1997), Fig. 7.1.

The size effect on the modulus of rupture is of a different kind than the size effect on failures that occur after a long stable crack growth that is typical for reinforced concrete structures. Until the mid 1980's, that size effect was also generally believed to be statistical but it is now widely accepted that its cause is primarily deterministic – the energy release due to crack growth (Bažant, 1984). The basic explanation to the deterministic part of size effect on the modulus of rupture is to be found in the theory

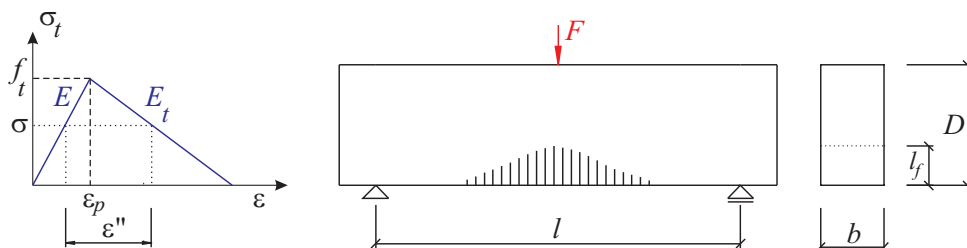


Figure 7.1: Inelastic strain, boundary layer of cracking l_f

of quasibrittle fracture, describing materials of heterogeneous microstructure in which the formation of distinct fractures is preceded by distributed cracking.

The maximum load of plain concrete beams occurs before a continuous crack initiates. But it occurs only after a *boundary layer of distributed cracking* of a certain critical thickness develops at the tensile face of beam. For beams of different sizes made of the same concrete, the thickness of this layer appears to be about the same, probably dictated mainly by the maximum aggregate size. Formation of this boundary layer, representing a fracture process zone (FPZ), is the principal reason why the direct tensile strength f'_t differs from the modulus of rupture, f_r , which is defined (for an unreinforced beam of a rectangular cross section) as:

$$f_r = \frac{6 M_u}{bD^2} \quad (7.1)$$

where M_u = ultimate bending moment, D = characteristic size of the structure, chosen to coincide with the beam depth (often denoted as h), and b = beam width (see figure 7.1).

The randomness of the heterogeneous microstructure of concrete and of its strength must nevertheless have at least some influence, as demonstrated by nonlocal finite element simulations with random spatially correlated strength (e.g. Breysse, 1990; Breysse and Fokwa, 1992; Breysse et al., 1994; Breysse and Renaudin, 1996; Frantziskonis, 1998). For quasibrittle structures failing after large stable crack growth, this question was studied by Bažant and Xi (1991) and Bažant and Planas (1998). They presented a generalization of Weibull-type theory in which the material failure probability depends not only on the local continuum stress but also on the average strain of a characteristic volume of the material.

The key point in Bažant and Xi's analysis Bažant and Xi (1991), which allows handling of the crack tip singularity, is the introduction of the *nonlocal continuum concept* for determining the failure probability of a material element. If the Weibull probability integral is applied to the redistributed stress field, the dominant contribution comes from the fracture process zone at the crack tip. The contribution from the rest of the structure is nearly vanishing, which is explained by the fact that the fracture cannot occur outside the process zone.

In the case of the modulus of rupture (different type of strength dependency on the size), the Weibull-type size effect can dominate only in unreinforced beams that are far deeper than the boundary layer of distributed cracking and thus fail right at crack initiation, as suggested by Petersson (1981). The beam depth D , however, would have to exceed about a few meters (for a standard concrete mix), which is hardly a realistic case. Besides, good practice requires designing structures so as not to fail at crack initiation.

A recent studies of Bažant and Novák (2000b,c) resulted in a statistical structural analysis model that takes into account the post-peak strain softening of the material and calculates the failure probability from the redistributed stress field using the nonlocal Weibull approach of Bažant and Xi (1991), representing an extension of deterministic nonlocal damage theory (Pijaudier-Cabot, 1987; Bažant and Planas, 1998). They demonstrated a good agreement with the existing test results on the modulus of rupture of concrete.

7.2 Nonlinear fracture mechanics and deterministic size effect of concrete structures

Deterministic size effect represents a transition from ductile behavior of relatively small specimens to brittle behavior of large structures. In the numerical investigations, the ductile behavior can be covered by plasticity, while the brittle behavior corresponds to the *linear elastic fracture mechanics* (LEFM). For the transition nonlinear fracture mechanics (NLFEM) with softening based on fracture energy (Bažant and Planas, 1998) can be effectively used. NLFEM is suitable for analysis of quasi-brittle materials with certain toughness like concrete. The plastic and the elastic-brittle behavior can be treated as limit situations. Due to the energetic basis deterministic size effect can be obtained efficiently by NLFEM. The nonlinear analysis of the concrete beams presented here has been performed by computer program ATENA. Suitability of this program for simulation of size effect behavior of concrete structures was reported by Pukl et al. (1992) and by Cervenka and Pukl (1994). The constitutive model used in ATENA reflects all the essential features of concrete behavior, namely cracking in tension. It is based on nonlinear damage and failure functions in plane stress state (Cervenka, 2000). A smeared crack approach simulates discrete cracks occurring in real concrete structures by *strain localization* in a continuous

displacement field. Concrete fracture is covered by nonlinear fracture mechanics based on fracture energy (Margoldová et al., 1998). Objectivity of the finite element solution is assured by crack band approach – the descending branch of the stress-strain relationship is adjusted according to the finite element size and mesh orientation (Bažant and Oh, 1983). The transition from ductile (small beam) to brittle (large beam) behavior is documented in fig. 7.2. The shape of the fracture process zone obtained in ATENA simulations for very small (a) and very large (b) beams using data of Sabnis and Mirza (1979) is shown. Corresponding load-deflection diagrams are included (Vořechovský, 2000a).

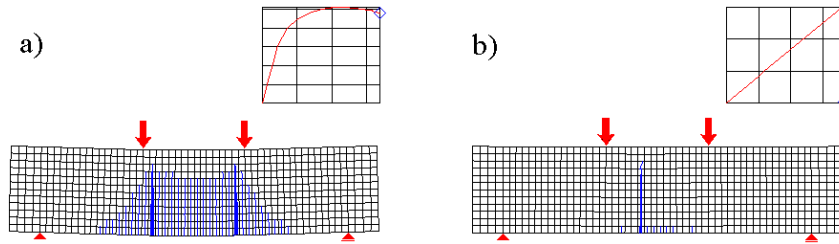


Figure 7.2: Calculated shapes of fracture process zone and load-deflection diagrams (based on data of Sabnis and Mirza (1979)) a) small beam (span 0.0381 m), b) large beam (span 4.0 m).

7.3 Stochastic nonlinear fracture mechanics and complex size effect

The difference between the deterministic (energetic) and statistical size effect was discussed. It is a clear demonstration that without random fields modeling the trend cannot be captured using any sophisticated nonlinear fracture mechanics analysis. Some preliminary statistical numerical experiments in order to show cumulative probability distribution functions of modulus of rupture f_r were already performed by Novák, Vořechovský, Pukl, and Červenka (2001).

Two basic approaches should be applied and compared for size effect prediction: *Extreme value theory* and *random field theory* eventually simplified into the *random variable level*. Relationships between the characteristic length (driving the deterministic size effect) and the autocorrelation length of random/variable material properties should be clarified. It was shown by Carmeliet (1994) that generally both *characteristic length* and *correlation length* are needed: first to avoid *strain localization*, second to introduce *spatial randomness*. The question remains what is the relationship of these two fundamental parameters related to the material (de Borst and Carmeliet, 1996; Gutiérrez and de Borst, 2002). As will be shown in the part III and explained in section 6.2 an appropriate stochastic alternative for strength representation should be chosen for calculation depending on both correlation length l_ρ and total dimension of a structure l (Vořechovský, 2002b).

It is expected that correlation length modifies size effect curve in the way that higher correlation length (stronger spatial correlation) of strength along the structure causes smaller decrease of nominal strength. As mentioned before, a theory for size effect explanation should be general enough to capture the complex phenomenon for both, reasonable sizes of beams and very large sizes (asymptotics). For very large sizes the solution would bring just above mentioned *extreme value theory*. The problematic transition from small and reasonable sizes to very large sizes is tackled in the following chapter.

7.3.1 Statistical size effect and Nonlocal Weibull theory

The history of description of phenomenon called size effect can be seen as history of two fundamentally different approaches, deterministic and statistical explanations. First explanation was statistical, it dates back to the pioneering works of Weibull (1939a); Tippett (1925); Fisher and Tippett (1928) and many others, mainly mathematicians. Phenomenon that larger specimens will usually fracture under smaller applied load was that time purely associated with the statistical theory of extreme values and size of defects.

Then most of researchers focused on energetic basis of size effect and all achievements were purely deterministic, leading to a “mean size effect curve” (MSEC). Let us mention e.g. the book of [Bažant and Planas \(1998\)](#) as an extensive source of information. Failure in quasi-brittle materials is associated with strain localization, as a consequence nonlinear finite element method exhibit a severe mesh sensitivity. This fact verified e.g. by [Pijaudier-Cabot \(1987\)](#) brought nonlocal formulations of damage, which provides proper regularization techniques to avoid *strain localization*. *Local* and *nonlocal* formulations appeared to be decisive to capture *deterministic* size effect (section 7.2).

But because of heterogeneity of quasi-brittle materials like concrete, the randomness must play some role and the use of statistical description and stochastic approaches seems to be essential. That is why recent research concentrated to this point. Weibull weakest link theory for stochastic damage model was utilized by [Mazars \(1982\)](#) and [Mazars et al. \(1991\)](#). Probabilistic formulation of damage based on probabilistic law of fracture in Weibull form was presented by [Breysse \(1990\)](#). These models do not provide full statistical information on nominal strength, which represent the important restriction.

According to the weakest-link model ([Tippett, 1925](#); [Fisher and Tippett, 1928](#)) underlying the classical Weibull theory, the theoretical failure probability of a structure with a continuously variable uniaxial stress $\sigma(\mathbf{x})$ is ([Bažant and Planas, 1998](#)):

$$p_f = 1 - \exp \left\{ - \int_V \left\langle \frac{\sigma(\mathbf{x}) - \sigma_u}{\sigma_0} \right\rangle^m \frac{dV(\mathbf{x})}{V_r} \right\} \quad (7.2)$$

Here V = volume of structure; σ_0 , σ_u and m are the parameters of Weibull probability distribution of the strength of the material (scale parameter, strength threshold and shape parameter), V_r is the representative volume of the material, and \mathbf{x} is the coordinate vector of material point. $\langle \rangle$ denotes the positive part of the argument (used because only positive tensile stresses contribute to failure probability).

The integral in (7.2) diverges (for realistic m values) if the singular stress field of a sharp crack or notch is substituted. This means that the classical Weibull theory cannot be applied to failure (stability loss) that occurs only after large stable crack growth. To overcome this problem, a nonlocal continuum approach has been introduced ([Bažant and Xi, 1991](#); [Bažant and Planas, 1998](#)). In this approach, the stress at a point depends not only on the strain at that point but also on the strain field within a certain neighborhood of that point. In the simplest version, it depends on the weighted spatial average of the strain in that neighborhood, representing the representative volume of the material. In the case of materials with strain-softening, the nonlocal concept is necessary to regularize the boundary value problem. Within the framework of Weibull integral, such kind of averaging introduces, in a statistical sense, a spatial correlation (this is also demonstrated by the numerical results of [Breysse and Fokwa \(1992\)](#)).

The fact that very different strength thresholds (with very different m -values) can usually give equally good representations of test data lead to assume a zero threshold $\sigma_u = 0$. Then, if the stresses are at the same time replaced by the nonlocal stresses as proposed by [Bažant and Xi \(1991\)](#) and ([Bažant and Novák, 2000b,c](#)), the multi-dimensional generalization of Eq. (7.2) may be written as:

$$p_f = 1 - \exp \left\{ - \int_V \sum_{i=1}^n \left\langle \frac{\bar{\sigma}_i(\mathbf{x})}{\sigma_0} \right\rangle^m \frac{dV(\mathbf{x})}{V_r} \right\} \quad (7.3)$$

where n is the number of dimensions, σ_i are the principal stresses ($i = 1, \dots, n$), and an overbar denotes nonlocal averaging. The failure probability now depends not on the local stresses $\sigma_i(\mathbf{x})$ but on the nonlocal stresses $\bar{\sigma}_i(\mathbf{x})$ which are the results of some form of spatial averaging.

One suitable form of averaging type is the spatial averaging of the inelastic strain, representing the difference of the current strain and the elastic strain corresponding to the same stress (Fig. 7.1):

$$\bar{\epsilon}''(x, y) = \frac{1}{\bar{\alpha}(x, y)} \int_0^L \int_{-h/2}^{h/2} \alpha(x' - x, y' - y) \epsilon''[\sigma(x', y')] dx' dy' \quad (7.4)$$

Integral is written for 2D case – concrete beam of depth D . Then nonlocal stresses are:

$$\bar{\sigma}(x, y) = E [\epsilon(x, y) + \bar{\epsilon}''(x, y)] \quad (7.5)$$

The spatial averaging integral is approximated by a finite sum over all the points of the structure. Different choices of the weight function $\alpha(x, y)$ for spatial averaging are possible, but the results are

not too sensitive to the choice made. For instance, one may simply choose a uniform weight function that is non-zero only over a certain representative volume such as a circle (or for convenience a square). However, according to the computational experience, a better convergence is achieved by using a smooth, bell-shaped weight function, which also appears more realistic. One suitable form of such a weight function, which is adopted here, is the modified bivariate normal (Gaussian) probability distribution function suggested by [Bažant et al. \(1984\)](#):

$$\alpha(x, y) = e^{-2\sqrt{x^2+y^2}/l} \quad (7.6)$$

Here l is the characteristic length of the nonlocal continuum (or material length), which characterizes the size of the representative volume V_r . It represents the diameter of a cylinder of height 1 that has the same volume as the weight function. This condition requires that $V_r = \pi l/8$. For concrete, the characteristic length can be approximately taken as $l = 3d_a$, which is the band width used for the crack band model (d_a = maximum aggregate size).

For $l \rightarrow 0$, the material becomes local and Eq. (7.3) becomes the classical Weibull probability integral. So the classical Weibull theory is a special case of the present theory. For beams so large that the characteristic length is negligible compared to the depth of the cross section, the classical Weibull size effect on the modulus of rupture must be approached (as observed by [Petersson \(1981\)](#)).

Compared to the stochastic finite element approaches (see, e.g., the review by [Breysse et al. \(1994\)](#) or the ‘numerical concrete’ model ([Roelfstra et al., 1985](#)), an important feature which brings about great simplification is that the nonlocal structural analysis with strain softening, or the structural analysis with a cohesive crack, can be carried out deterministically, i.e. independently of the probability analysis. However, iterations of the deterministic solution are required if the failure probability of the structure is specified. But the number of these iterations is very small compared to the classical approaches of reliability engineering (where calculations of failure probability usually require thousands of repetitive deterministic solutions using advanced Monte Carlo type simulation techniques). [Bažant and Novák \(2000b,c\)](#) showed efficiency of this theory for prediction of size efficient on modulus of rupture.

Chapter 8

Connections of fiber bundles models and size effect of concrete structures

Published in paper: Bažant, Pang, Vořechovský, Novák, and Pukl (2004b)

This chapter analyzes various modeling alternatives for the statistical size effect in quasibrittle structures. The role of reliability techniques, encompassing the classical reliability theory at random variables level, the theory of extreme values in Weibull form, and the stochastic finite element method with random strength field, is examined with a view toward capturing both the deterministic and statistical size effects. The theoretical development describing deterministic and statistical size effects is documented using the crack initiation problem. Theoretical predictions are compared with the existing test data in the following chapter.

8.1 General size effect theory

8.1.1 Energetic size effect

There are two basic types of energetic size effect which are distinguishable (Bažant, 1997, 2001; Bažant and Chen, 1997; Bažant, 2002b). Structures of positive geometry having no notches or preexisting cracks are classified as Type 1 size effect (Bažant et al., 1995, 1996; Bažant, 1998a, 2001). For positive structure geometries, the maximum load occur as soon as the fracture process zone (FPZ) gets fully developed. Positive geometry is one of the requirements for the applicability of Weibull-type weakest link model. Type 2 size effect (Bažant, 1984, 2002b; Bažant and Kazemi, 1990) occurs also for positive geometry structures but with notches, as in fracture specimens, or with large stress-free (fatigued) cracks that have grown in a stable manner prior to the maximum load. The mean nominal strength for this type of size effect is not significantly affected by material randomness (Bažant and Xi, 1991; Bažant, 2002b), but the variance of course is. There exists also a Type 3 size effect (Bažant, 2001, 2002b), occurring in structures with initially negative geometry. However, this type is so similar to Type 2 that it is barely distinguishable experimentally.

8.1.2 Probabilistic size effect

Traditionally, the probabilistic size effect has been explained by Weibull-type statistical weakest link model (Fisher and Tippett, 1928; Weibull, 1939b,a, 1949, 1951, 1956; Epstein, 1948; Freudenthal and Gumbel, 1953; Freudenthal, 1956a, 1968; Gumbel, 1958; Saibel, 1969). Its basic hypothesis is that the structure fails as soon as the material strength is exhausted at one point of the structure. This is true for quasibrittle materials only if the size of the structure is much larger than the FPZ. For quasibrittle failures of smaller sizes, there are other avenues of research which could explain the stress redistribution before failure. Fiber bundle model due to Daniels (1945) is one of the earliest generalizations of the extreme value statistics of the weakest link model, in which a hypothesis of load-sharing among fibers is invoked. This avenue of approach has been thoroughly investigated by S. Leigh Phoenix and co-workers (Harlow

and Phoenix, 1978a,b; Smith and Phoenix, 1981; Smith, 1982; Phoenix and Smith, 1983; McCartney and Smith, 1983; Phoenix, 1978b; Phoenix et al., 1997; Phoenix and Beyerlein, 2000; Mahesh et al., 2002). The other, more recent, avenue of approach attempts to amalgamate the statistical and deterministic theories by means of a nonlocal generalization of Weibull theory (Bažant and Xi, 1991; Bažant and Novák, 2000b,c, 2001; Bažant, 2002a). This allows stochastic numerical simulations of the mean as well as variance of the deterministic-statistical size effect in structures of arbitrary geometry. In particular, this approach automatically captures the dependence of stress redistribution and energy release rate on the structure size D .

8.2 Asymptotics of size effect

8.2.1 Small-size asymptotes

The small-size mean asymptotic properties should agree with the theoretical small-size asymptotic properties of the underlying continuum model, which can be the cohesive crack model, the crack band model, or the nonlocal damage model. Each of these models implies that the value of the nominal strength σ_N for $D \rightarrow 0$ should be finite and should be approached linearly in D (Bažant, 2002b), as shown in Fig. 8.1. Agreement with these small-size asymptotic properties can be achieved by modeling the failure

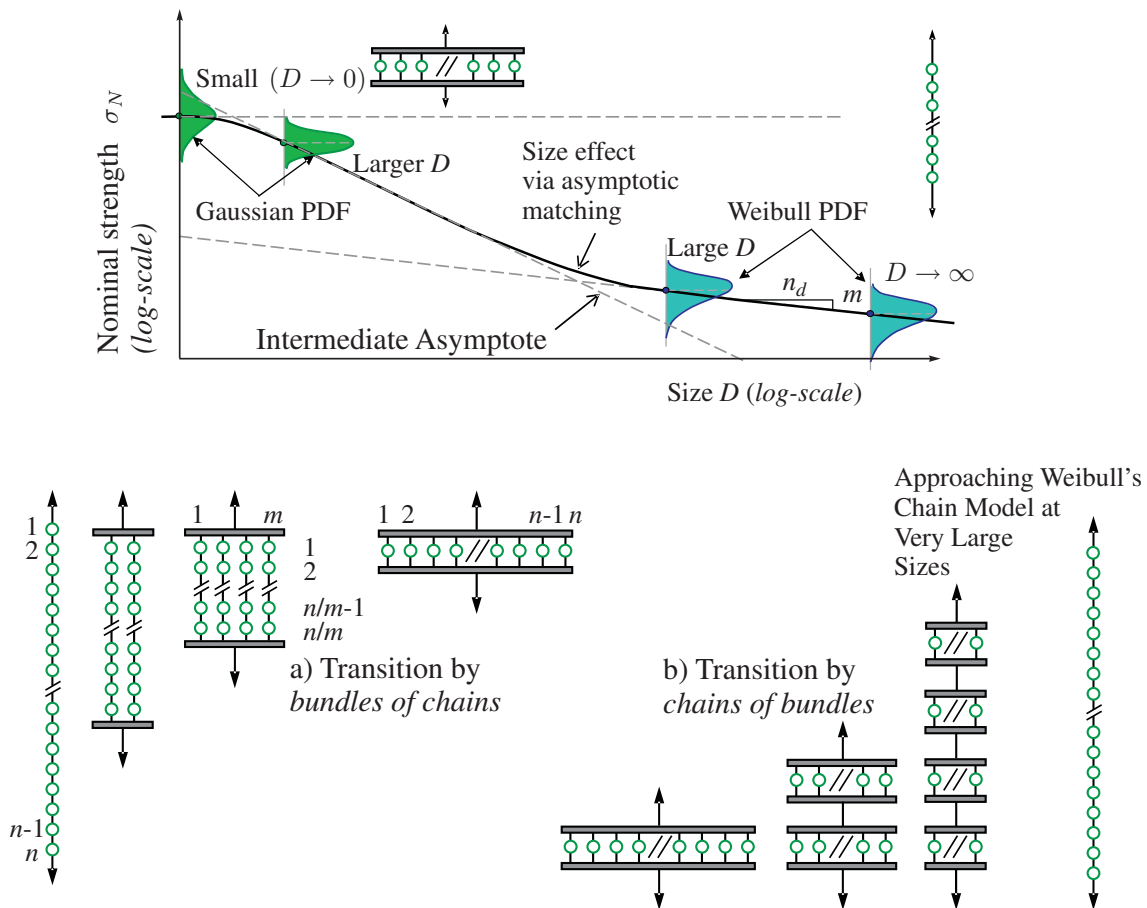


Figure 8.1: Failure probability density and cumulative distribution function for three different elemental distributions: Gaussian, Weibull and rectangular

mechanism for the small-size limit with a fiber bundle. For a vanishing size, the failure tends to follow the theory of plasticity, and it is well known (e.g. Jirásek and Bažant, 2002) that in plasticity the failure proceeds according to a single-degree-of-freedom mechanism, i.e., is simultaneous, non-propagating. It

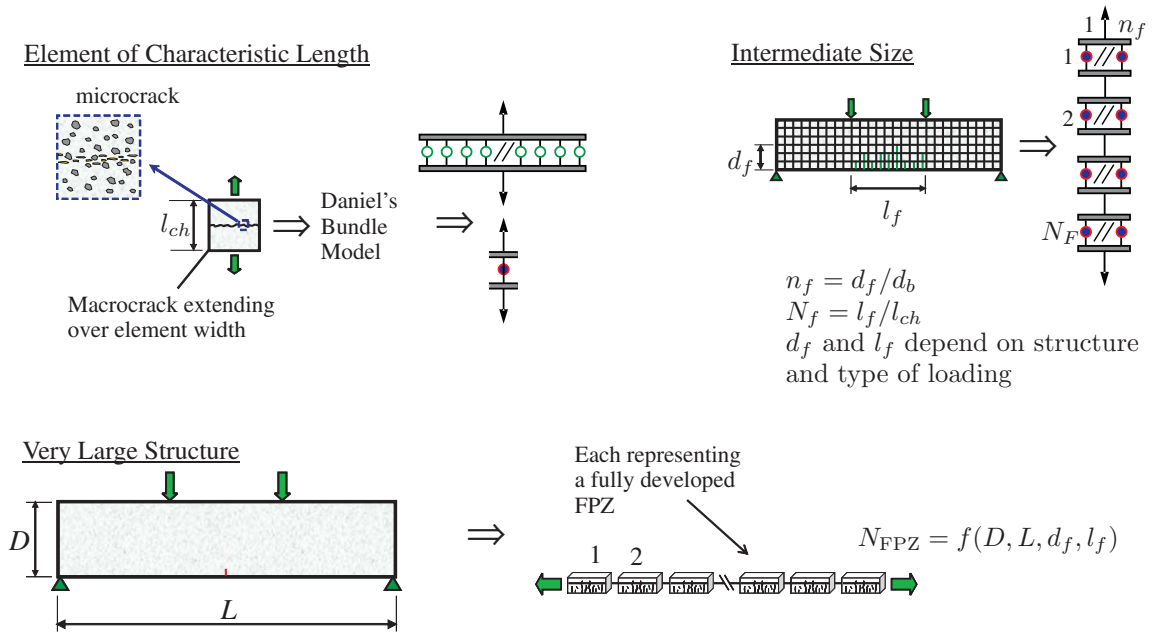


Figure 8.2: Failure probability density and cumulative distribution function for three different elemental distributions: Gaussian, Weibull and rectangular

follows that the failure probability distribution for $D \rightarrow 0$ ought to obey Daniel’s (1945) ‘fiber bundle’, model rather than the Weibull-type weakest link model for a chain.

For $D \rightarrow 0$, a body with a cohesive crack (or crack band) approaches the case of an elastic body containing a perfectly plastic cohesive crack. The fits of the energetic size effect to extensive experimental data on the modulus of rupture (or flexural strength) of unreinforced concrete beams (Bažant and Novák, 2000a,c,b) and of fiber-polymer composite laminates (Bažant, 2003), which reveal that the small-size asymptote is closely approached only for extrapolation to specimen sizes much smaller than a representative volume of the concrete, considered here to be about three aggregates in size. This volume fractures simultaneously, which is why its statistics should be adequately described by the fiber bundle model, in which the breakages of fibers correspond to the breaks of microscopic bonds along the failure surface. By formulating and solving a recursive relation for the failure probability distribution, Daniels (1945) showed that the failure probability $G_n(x)$ follows the standard normal distribution given by Eq. (6.14), where the mean μ^* and variance σ^{*2}/n can be expressed implicitly as follows using the probability distribution of failure of the fibers $F(x)$ (see page 68), which are assumed to be identical and statistically independent (IID).

8.2.2 Large-size asymptotes

On the other extreme, the failure for a very large structure of positive geometry occurs as soon as the FPZ becomes fully developed. Structures of positive geometry are those in which the stress intensity factor, or the energy release rate, increases if the crack extends at constant load. The failure of such a structure could be modeled with a single chain of elements, each representing a FPZ and the failure probability of such a structure follows the weakest link model (Eq. 9.1; compare to Eq. 6.11). The equations feature $P_1(\sigma)$, the cumulative probability distribution of the element, which represents the FPZ in this case. $P_N(\sigma)$ is the cumulative distribution function of the chain.

Although there are no substantial amount of experimental data that test on very large structures to verify the correctness of the weakest link model, numerical simulation on such large scale such as dams (to be presented in another paper) and the theoretical argument that very large positive definite structures fail at crack initiation, provides strong argument for the weakest link model.

(Fisher and Tippett, 1928) has proved that there exist three and only three asymptotic forms of the extreme value distribution:

- Fisher-Tippett-Gumbel distribution
- Fréchet distribution
- Weibull distribution

In this document, we focus on generic Weibull distribution with zero threshold for each FPZ; the cumulative probability distribution can be expressed as follows:

$$P_1(\sigma) = 1 - e^{-(\sigma/s_0)^m} \quad (8.1)$$

where m and s_0 are the Weibull shape and scale parameters respectively (m = Weibull modulus). The asymptotic probability distribution for the weakest link model will remain Weibull at varying D but the mean and standard deviation will shift as follows (compare to Eq. 9.8):

$$\mu_N = \mu_1 (N)^{-1/m} = s_0 (N)^{-1/m} \Gamma(1 + 1/m) \quad (8.2)$$

According to the expressions in Eqs. (8.2, 9.8) & (9.9), it is clear that the coefficient of variation of σ_N depends only on the shape parameter and can be expressed as follows given by Eq. 6.4.

Note that the coefficient of variation of σ_N is independent of the structure size D . This implies that, if the size effect is purely statistical, the Weibull modulus, m , which is completely determined by the experimentally observed scatter of the results of tests of identical specimens of one size, must be the same as the m identified from the size effect tests. This is a check on the validity of the statistical theory which has been omitted in many studies. For small and intermediate size structures, the Weibull statistical theory does not apply and this is most easily recognized by the fact that moduli m obtained according to Eq. 6.4 from tests at very different sizes do not match each other. For more discussion on this topic (in the context of composites and fiber structures) see sec. 6.5.3, p. 78.

8.3 Transition between small and large size asymptotes

8.3.1 Chain of bundles model

For intermediate size structures, the size of FPZ is large as compared to the size of the structure. Stress redistribution and energy release are significant for these structures, which suggests that the deterministic effect should not be neglected. The size effect curve could be determined by numerous simulations of intermediate size structures using a nonlinear stochastic finite element program. This is reviewed later in the paper. Now an alternative approach with a transition based on the chain of bundles model (Figs. 8.1, 8.2) proposed by Freudenthal (1963) and later by Bažant (2004) will be studied.

Visible macro-cracks are assumed to appear at a minimum crack spacing equal to characteristic length which is approximately three maximum aggregate sizes. For hypothetical specimens smaller than this characteristic length, the failure should follow the fiber bundle model in which each fiber in the bundle of the lowest hierarchy represents a micro-bond. The failure probability distribution of the fiber bundle (Fig. 8.1) consisting of a large number of fibers can be described well by Daniels's approximation in Eq. (6.14). For typical test specimen sizes (larger than the aforementioned characteristic length), the failure mechanism is modeled with a hybrid of series and parallel coupling as shown in (Figs. 8.1, 8.2). The statistical effect of the stress redistribution causing energy release can be modeled by the parallel coupling of elements, each of a characteristic volume. The number of characteristic volumes in a normal structure would be small and the probability distribution could not be approximated accurately by Eq. (6.14). The failure probability could be computed exactly by a recursive formula (Daniels, 1945; Smith and Phoenix, 1981; Smith, 1982) expressed by Eq. (6.13), where n is the number of elements of characteristic volumes in a bundle and $F(x)$ is the probability distribution of each element.

On the other hand, the possibility of cracks appearing along the span of a flexed beam or along the length a tensioned bar can be accounted for by coupling the bundles in a chain-like manner. In this way, the deterministic and statistical size effect can be fused in a single approximate model which also provides an asymptotically correct transition from small to large size asymptotes. In one extreme, in which the specimens are very small, the chain-of-bundles model would collapse into a bundle of micro-bonds. In the other extreme for large structures, the size of the bundles is fixed since the FPZ has been fully developed

while the number of bundles in the chain scales according to the size of the structure and the model behaves as a weakest link.

The chain of bundles model offers flexibility in the choice of the generic probability distribution for the micro-bonds, resulting in different size effect curves. Existing literature on limited tensile test data suggested different probability distributions, namely Weibull, Normal and Log-normal distribution and the chain of bundles model can be used to gain insight into the probability distribution for the generic probability distribution by using the computed size effect curve with different probability distribution to match to experimental data.

8.3.2 Nonlinear stochastic finite element method

A simple but primitive approach to stochastic finite element analysis is to subdivide a structure into elements of the size of the characteristic volume. Such an approach is feasible for small structures but would be hardly possible to implement in very large structures. As proposed by [Novák, Bažant, and Vořechovský \(2003a\)](#), this difficulty could be overcome by using stochastic macro-elements where each macro-element has stochastic properties that are scaled according to Fisher & Tippett's (1928) fundamental stability postulate of extreme value distributions (see section 9.3, p. 100).

The advantage is that the number of macro-elements can be kept fixed but while their size is increased in proportion to structure size D . This allows efficient stochastic computations for very large structures. The treatment of the macro-element and the selection of the extreme value for each macro-element is described in detail in [Novák, Bažant, and Vořechovský \(2003a\)](#). The scaling of the mean strength and variance of the macro-element are given by Eqs. (9.8,8.2) and (9.9). The scaling formula is applicable only if the probability distribution of each micro-element of characteristic length could be described by Weibull distribution of Weibull modulus m and scale parameter s_0 . An additional condition of validity is that the structure must reach the peak load at crack initiation. The macro-element approach is checked against [Koide et al. \(1998, 2000\)](#) tests of plain concrete beams under four-point bending with different bending spans (200, 400 and 600mm) but identical cross sections (100 by 100mm) (which eliminates the energetic part of size effect). Nonlinear fracture mechanics software ATENA ([Cervenka and Pukl, 2003](#)) is integrated with probabilistic software FREET (see Appendix A or papers by [Novák et al. \(2002d, 2004\)](#)) to perform statistical simulation of Koide's beam. The detailed description of the numerical example can be found in the following chapter 9 (sec. 9.4, p. 101).

8.4 Concluding remarks

The chapter shows how the statistical size effect at fracture initiation can be captured by a stochastic finite element code based on extreme value statistics, simulation of the random field of material properties, and chain of bundles transition. The computer simulations of the statistical size effect in 1D based on stability postulate of extreme value distributions match the test data. However, the correct behavior cannot be achieved for other tests using a 1D treatment. A proper way of treating the stress redistribution is by the proposed macro-elements in 2D (or 3D), the scaling which is based on the fiber bundle model capturing partial load-sharing and ductility in the finite element system, see next chapter.

Chapter 9

Computational modeling of statistical size effect: extreme value approach

Published in papers: [Novák, Bažant, and Vořechovský \(2003a\)](#); [Vořechovský \(2003\)](#); [Vořechovský and Novák \(2004\)](#); [Bažant, Novák, Vořechovský, and Pang \(2004a\)](#); [Bažant, Pang, Vořechovský, Novák, and Pukl \(2004b\)](#)

The chapter begins by discussing some fundamental features of the statistics of extremes important for the computational modeling of the statistical size effect, whose asymptotic behavior is not correctly reproduced by the existing stochastic finite element methods. The chapter proposes a new approach to finite element estimation of loads of very small probability. A simple strategy for capturing of statistical size effect using stochastic finite element methods in the sense of extreme value statistics is suggested. Such probabilistic treatment of complex fracture mechanics problems using the combination of feasible type of Monte Carlo simulation and nonlinear fracture mechanics computational modeling are presented using numerical example of crack initiation problem - size effect due to bending span of four-point bending tests.

9.1 Introduction

Large concrete structures usually fracture under a lower nominal stress than geometrically similar small structures (the nominal stress being defined as the load divided by the characteristic cross section area). This phenomenon, called the size effect, has in general two physical sources – deterministic and statistical. The deterministic source consists of the stress redistribution and the associated energy release described by nonlinear fracture mechanics (in finite element setting, the crack band model or cohesive crack model). The deterministic size effect represents a transition from ductile failure with no size effect, asymptotically approached for very small structures, to brittle failure with the strongest possible size effect, asymptotically approached for very large structures ([Bažant and Planas, 1998](#)).

The classical explanation of size effect used to be purely statistical – simply the fact that the minimum random local strength of the material encountered in a structure decreases with an increasing volume of the structure. This idea was qualitatively proposed already in the middle of the 17th century by [Mariotte \(1686\)](#). Although what became known as the Weibull distribution was in mathematics discovered already in 1928 by [Fisher and Tippett \(1928\)](#) (in connection with Tippett's studies of the length effect on the strength of long fibers, see [Tippett \(1925\)](#)), the need for this extreme value distribution in describing fatigue fracture of metals and the size effect in structural engineering was first developed, independently of Fisher & Tippett's cardinal contribution, by [Weibull \(1939a,b\)](#). His pioneering work was subsequently refined by many other researchers, mainly mathematicians; e.g. [Epstein \(1948\)](#) and [Saibel \(1969\)](#).

The classical (but erroneous) view that any observed size effect should be described by extreme value statistics prevailed in structural engineering until about 1990. However, beginning with the studies at Northwestern University initiated in the mid 1970s, it gradually emerged that there exists a purely

deterministic size effect, caused by energy release associated with stress redistribution prior to failure, and that this energetic size effect usually dominates in the so-called quasibrittle structures (i.e., structures in which fracture propagation is preceded by a relatively large fracture process zone which, in contrast to brittle-ductile fracture of metals, exhibits almost no plastic deformations but undergoes progressive softening due to microcracking). Beginning with the 1990s, many studies focused on the deterministic size effect; see the reviews in Bažant (1986); Bažant and Chen (1997); Bažant and Planas (1998); Bažant (1999a,b).

The recent development of nonlocal Weibull theory by Bažant and Novák (2000b,c) in connection with statistical studies of the modulus of rupture (or flexural strength) of plain concrete beams showed that, for large quasibrittle structures failing at crack initiation, the deterministic energetic size effect needs to be combined with the Weibull probabilistic size effect. In this connection, some fundamental questions arose regarding the applicability of various statistical approaches to the statistical size effect. As shown by Bažant and Novák (2000b) and Bažant (2002a), the existing stochastic finite element method (SFEM) does not have the correct large size asymptotic behavior and fails to capture the statistical size effect on nominal strength.

Arguments mentioned above are basis for the need to combine efficient reliability techniques with present knowledge in the field of nonlinear fracture mechanics. There are stronger calls for complex reliability treatment of nonlinear fracture mechanics problems.

The decisive parameter in SFEM is the correlation length which governs spatial correlation over the structure. The correlation length modifies the size effect curve in the region where this parameter is smaller than the element size. There is a clear relationship – the larger the correlation length, the stronger is the spatial correlation of strength along the structure and, consequently, the weaker is the decrease (due to local strength randomness) of the nominal strength with increasing structure size. Computational problems, however, develop in trying to simulate the extreme value asymptotic size effect using the random field approach. Approximately, the requirement is that the ratio of the correlation length to the element size should not drop below one. This poses a major obstacle to using SFEM for describing the size effect, especially for large structure sizes.

Some advances in this problem were achieved by several authors, e.g. Gutiérrez and de Borst (2002) who, however, confined their studies to the size range of real structures. The ratio of the correlation length to the element size implies, unfortunately, a severe limitation. To actually compute the extreme value asymptote using the random field approach, the number of discretization points (e.g. nodes in a finite element mesh) would have to increase proportionally to the structure size, which is in practice impossible since an extremely large structure size would have to be considered to approach the asymptotic behavior closely. To make computations feasible, it is necessary to devise a way to increase the element size in proportion to the structure size, keeping the number of elements constant. Therefore, the aims of this chapter are:

1. To introduce the problem by summarizing the vital features of the statistics of extremes established by mathematical statisticians in a form meaningful to engineers, putting emphasis on the philosophy of derivation of the probability distribution of extreme values in a set of independent stochastic variables having an arbitrary elemental probability distribution.
2. To draw the consequence for capturing the statistical size effect with the help of SFEM.
3. To propose a method for computer simulation of the statistical size effect based directly on the basic concept of extreme value statistics in combination with nonlinear fracture mechanics, and verify it by an example (size effect of four-point bending strength due to bending span).

9.2 Weakest link concept and theory of extreme values

The weakest link concept for the strength of a chain-like structure with N elements (Fig. 9.2b) is equivalent to the distribution of the smallest values in samples of size N . If one element, the weakest element, fails, the whole structure fails, i.e., the failure is governed solely by the element of the smallest strength. To clarify the problem, it will be useful to recall some basic formulae of the statistical theory of extremely small values. The strength distribution of an element of a chain-like (or statically determinate) structure, see Fig. 9.3a), i.e., the distribution of the failure probability of an element as a function of the

applied stress σ , may be characterized by continuous probability density function $p_1(\sigma)$ with the associated cumulative distribution function $P_1(\sigma)$ (in statistical literature called the elemental, underlying, basic or primary distribution). Then the cumulative distribution of the failure probability of a structure of N elements (or the distribution of the smallest strength value in samples of size N) is given by

$$P_N(\sigma) = \int_{-\infty}^{\sigma} p_1(\sigma) d\sigma = 1 - (1 - P_1(\sigma))^N \tag{9.1}$$

and the failure probability density is (compare to Eq. 6.11, p. 67, part II)

$$p_N(\sigma) = np_1(\sigma)(1 - P_1(\sigma))^{(N-1)} \tag{9.2}$$

These basic equations provide an overall representation of the failure distribution $p_N(\sigma)$ (or $P_N(\sigma)$) corresponding to a given elemental distribution $p_1(\sigma)$. Different elemental distributions can give different failure distributions $P_N(\sigma)$, however, it is remarkable that the asymptotic forms $P_N(\sigma)$ can be only three. Before discussing this fact, let us illustrate the influence of the type of elemental distribution on the failure distribution graphically.

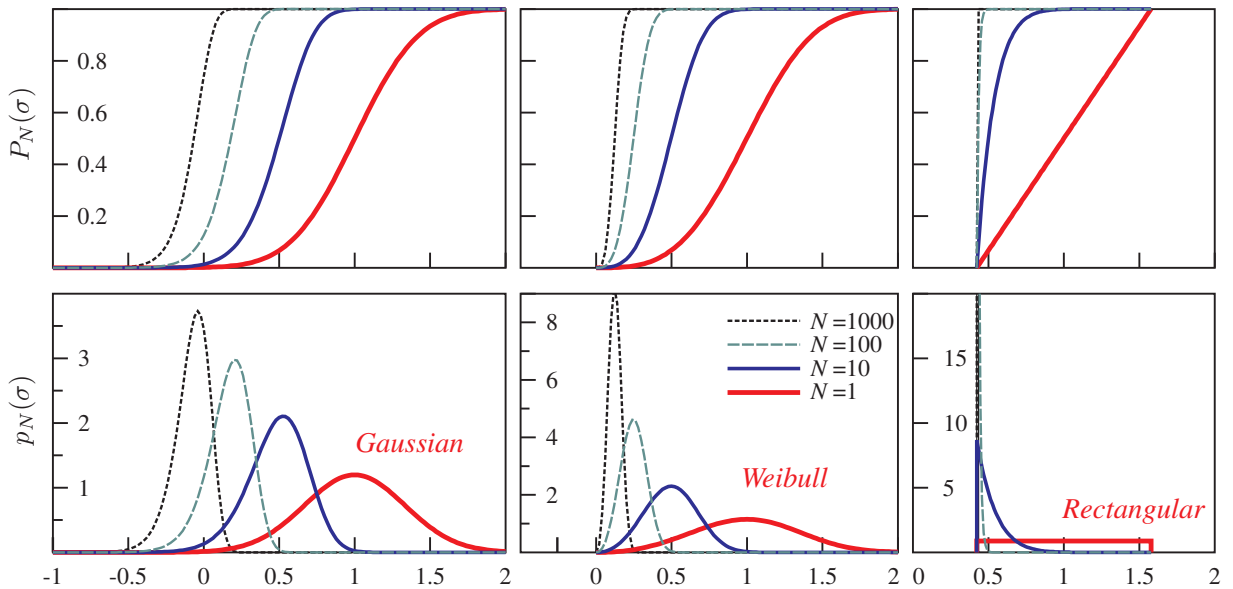


Figure 9.1: Failure probability density and cumulative distribution function for three different elemental distributions: Gaussian, Weibull and rectangular

Figure 9.1 shows the plots of the failure probability density functions $p_N(\sigma)$ and the cumulative distribution functions $P_N(\sigma)$ calculated for $N = 1, 10, 100$ and 1000 according to eqs. (9.1–9.2) for the various elemental distributions, in particular the (a) normal, (b) Weibull and (c) rectangular distributions (the last one is included merely for comparison purposes). All three elemental distributions are chosen to have a common unit mean value, and standard deviation of $1/3$. A general trend may be noticed: Both the mean value and the variance decrease with an increasing sample size (i.e., number N of elements). Cases (a) and (b) are very similar in these overall plots, having a bell-shaped form. But, as discussed later, for large N , the differences are becoming very significant especially for very small probabilities normally required in design (the domain of attraction of minima Weibull distribution is Weibull but the minima of Gaussian converge to Gumbel extreme value distribution allowing negative strength values). When the elemental distribution is rectangular (case c), the extreme value is seen to converge very quickly to the threshold of the rectangular distribution. This distribution exhibits no size effect, which makes it unacceptable (aside from physical reasons) for strength modeling. But the elemental normal and lognormal distributions give also a physically unacceptable distribution of structural strength, since for small enough probability they give a negative strength value. Thus Fig. 9.1 provides a qualitative insight into the statistics of extremes.

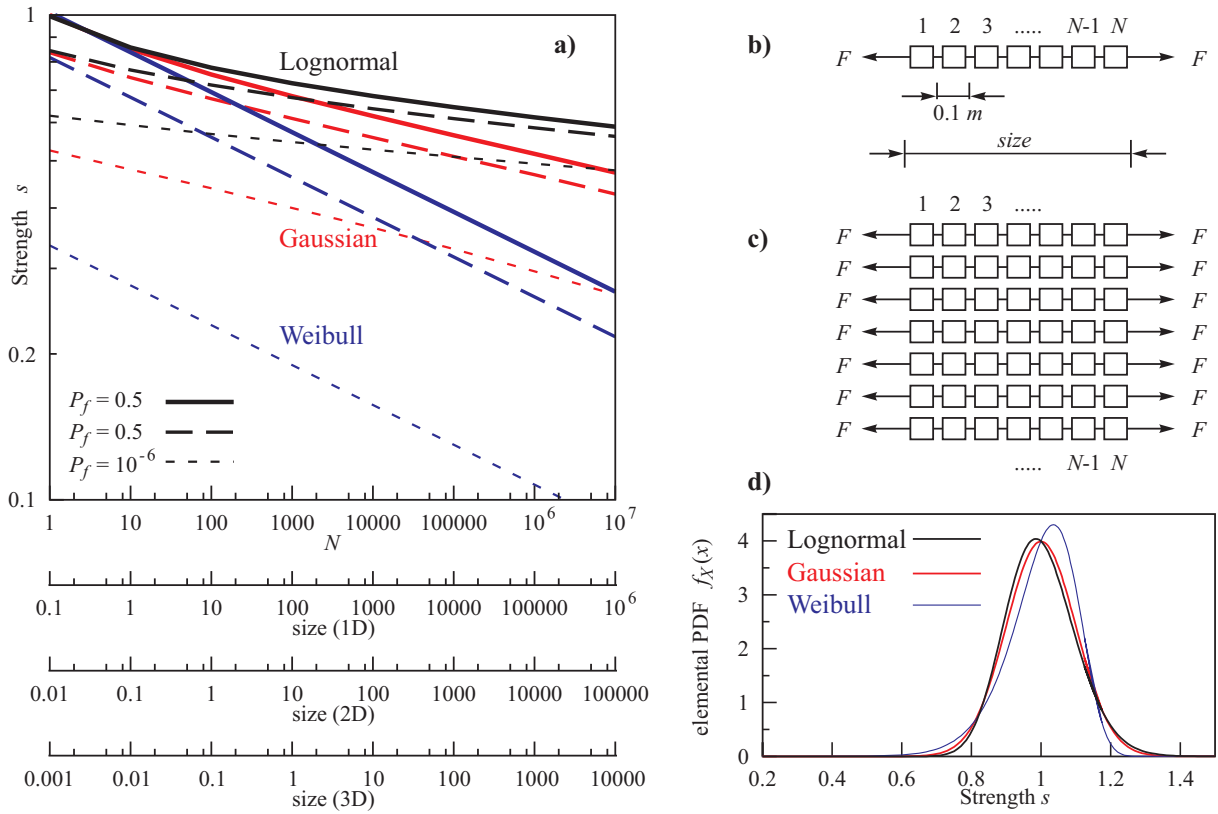


Figure 9.2: a) Dependence of random strength on size N for elemental distributions; b) a sketch of “1D” structure failing at failure of a weakest link, the elements share a common strength distribution (IID); c) a sketch of “2D” structure (we assume that the structure fails at first failure of a weakest element; d) Comparison of the three elemental distributions used for a) with unit mean and standard deviation of 0.1

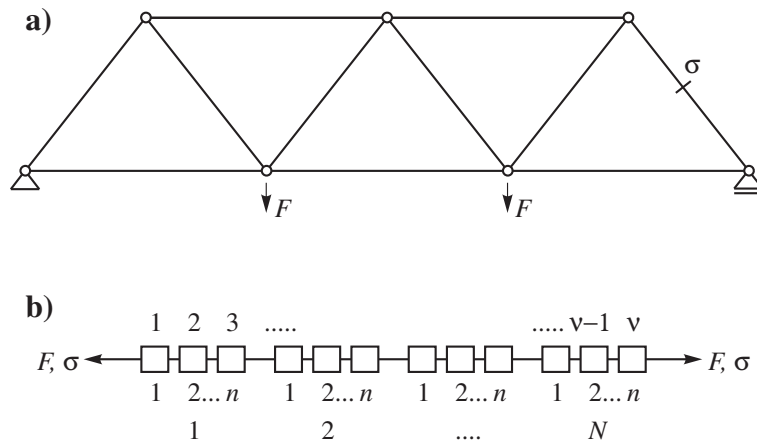


Figure 9.3: a) Statically determinate structure that behaves as a chain; b) Stability postulate of extreme values (chain and sub-chains)

Differences in structural strength for various elemental distribution are particularly pronounced for large N and small probabilities (i.e., in the tail). This phenomenon is illustrated in Fig. 9.2, in which the basic equation (9.1) is used in the inverse: For a chosen failure probability $P_N(\sigma)$, the strength σ is solved. Naturally, even for the elemental distributions, the main differences lie in their tails (case $N = 1$). But as N increases, the differences in strength get larger and larger, not only for the tails but also for

the medians. The dependence of strength on N is plotted in Fig. 9.2 for selected failure probabilities $P_N = 0.5, 0.05, 10^{-6}$. Three elemental distributions, normal, Weibull and lognormal, with common unit mean, and common standard deviation of 0.1, are considered and compared (see Fig. 9.2d), and enormous differences among them are found. For the elemental normal distribution, the fact that the size effect on the mean is stronger than on the tail is unrealistic. A more realistic, and much stronger, size effect is observed for the Weibull elemental distribution. For the elemental mean 1 and standard deviation 0.1, the statistical parameters for the Weibull (two-parametric) distribution are: $m = 12.15$ (Weibull modulus) and $s_0 = 1.043$ (scale parameter). In the double logarithmic plot of Fig. 9.2a, the Weibull size effect is, for any specified failure probability, a straight line of slope $-1/m$, see eqs. (6.1, 6.2), p. 63.

To show the differences among structures that are scaled in one-, two- and three-dimensions (1D, 2D, 3D), figure 9.2a includes three horizontal scales (a sketch of 1D structure is in Fig. 9.2b and a 2D structure in Fig. 9.2c.). For the validity of (9.1) and (9.2) in multi-dimensional situations, it is required that the whole structure fails when a single element fails (can be considered to be connected in series –weakest link principle of a chain). This is a property of a chain as well as all statically determinate structural systems, and is also a good approximation for fracture of unnotched structures of positive geometry (e.g., unreinforced concrete beams in flexure). In that case, N represents the ratio of the structure volume to the characteristic volume V_c of the micro-heterogeneous material. V_c is here understood as the volume having the size of the autocorrelation length of the random field of the local material strength, in which case the strength limits of various characteristic volumes can be considered as nearly statistically independent (uncorrelated) random variables, a basic hypothesis in the statistical theory of extremes (note that V_c is in general different (and larger) than the representative volume V_r of the material, which is the smallest volume for which the continuum concepts of stress and strength make sense, or a volume for which the mean strength is unaffected by randomness of microstructure as this volume is shifted through the material). With respect to the situation in concrete structures, V_r may be considered to be approximately 0.01 m^2 (for 2D) and 0.001 m^3 (for 3D).

The foregoing illustrations bring to light a salient point (which will be discussed in detail later) – namely, the selection of the elemental probability distribution is of fundamental importance for the statistical size effect, and must therefore be realistic. The importance of extreme value theory in stochastic mechanics has been emphasized by Bažant (2002a).

9.2.1 Limiting forms of distribution of minimum

In a population of N statistically independent IID random variables X_i ($i = 1, 2, \dots, N$), i.e. with arbitrary but independent and identical statistical distributions $\text{Prob}(X_i \leq x) = P_1(x)$, henceforth called the elemental distribution ($x = \sigma/s_0 =$ scaled stress, $X_i =$ scaled random strength), the distribution of $Y_N = \min_{i=1}^N X_i$ for very large N has the general expression:

$$P_N(y) = 1 - e^{-NP_1(y)} \quad (9.3)$$

where $P_N(y) = \text{Prob}(\min_{i=1}^N X_i \leq y)$; $P_N(y) = P_f =$ failure probability of structure, provided that the failure of one element causes the whole structure to fail. As proven by Fisher and Tippett (1928), there exist three and only three asymptotic forms (or limiting forms for $N \rightarrow \infty$) of the extreme value distribution $P_N(y)$:

- 1) Fisher-Tippett-Gumbel distribution:

$$P_N(y) = 1 - e^{-e^y} \quad (9.4)$$

- 2) Fréchet distribution:

$$P_N(y) = 1 - e^{-|y|^{-m}} \quad (9.5)$$

- 3) Weibull distribution:

$$P_N(y) = 1 - e^{-y^m} \quad (9.6)$$

(Case 1 is usually called the Gumbel distribution, but Fisher and Tippett derived it much earlier and Gumbel gave them credit for it.) Case 3 is obtained if the elemental distribution $P_1(y)$ has a power-law tail with a finite threshold (the simplest case is the rectangular probability density function, for which

$m = 1$). Case 1 is obtained if $P_1(y)$ has an infinite exponentially decaying tail, and case 2 if $P_1(y)$ has an infinite tail with an inverse power law (such as $|\sigma|^{-m}$) (see also Gnedenko, 1943; Gumbel, 1958; Bouchaud and Potters, 2000).

Fisher and Tippett (1928) based their proof on three arguments: (1) The key idea is that the extreme of a sample of $\nu = Nn$ independent identical random variables x (the strengths of the individual links of a chain) can be regarded as the extreme of the set of N extremes of the subsets of n variables, e.g., the strengths of n links of a chain (Fig. 9.3 b). (2) As both $n \rightarrow \infty$ and $N \rightarrow \infty$, the distributions of the extremes of samples of sizes n and Nn must have a similar form if an asymptotic form exists. This implies that that these distribution must be related by a linear transformation in which only the mean and the standard deviation can change; i.e., $\sigma' = a_N\sigma + b_N$ where a_N and b_N are functions of N ($N \sim$ structure size). Although an asymptotic distribution of the extremes, as a limit for $N \rightarrow \infty$, does not exist, an asymptotic *form* (or shape) of the extreme value distribution should exist, i.e., the asymptotic distribution form should be stable with regard to increasing N .

The asymptotic behavior rests on the so-called stability postulate of extreme value statistics, generally accepted beginning with Fréchet (1927). In this postulate, the extreme value of a set of $\nu = Nn$ identical independent random variables x (the strengths) is regarded as the extreme of the set of n extremes of the subsets of N variables. When both $n \rightarrow \infty$ and $N \rightarrow \infty$, it is perfectly reasonable to postulate that the distribution of the extreme of set Nn must be similar to the distribution of the extreme of each subset N (i.e., related to it by a linear transformation). In other words, the asymptotic form of the distribution must be stable. From this property it can be shown that the survival probability f_N of a structural system with a very large size N as a function of applied strength σ must asymptotically satisfy the functional equation below, (9.7).

Thus the argument of a joint probability of survival of all N segments of the chain yields for the asymptotic form of the cumulative distribution of the survival probability $F(\sigma) = 1 - P_f = 1 - P_N$ of a very long chain the recursive functional equation:

$$[F(\sigma)]^N = F(a_N\sigma + b_N) \quad (9.7)$$

which is called the stability postulate of extreme value distribution, where a_N and b_N are functions of size N . In the most important paper of extreme value statistics motivated by the strength of textile fibers, Fisher and Tippett (1928) showed that this recursive functional relation for function $F(\sigma)$ can be satisfied by three and only three distributions, and that they are given by eqs. (9.4)–(9.6). One of them had already been found by Fréchet (1927) and the other two have later become known as the Gumbel and Weibull distributions (curiously, not the Fisher and Tippett distributions). By substituting these forms into functional equation (9.7), one can check that indeed this equation is satisfied. The substitutions further give the dependence of a_N and b_N on N , which in turn characterizes the dependence of the mean and the standard deviation of each asymptotic distribution on N .

The infinite negative tails of P_N of the Fréchet distribution and the Fisher-Tippett-Gumbel distribution are not acceptable for describing the strength. Therefore, these two distributions are ruled out. So, in the case of strength, there is no other acceptable tail distribution but Weibull distribution.

9.3 Implications for finite element method

Since the failure probabilities acceptable for design are of the order of 10^{-7} , at least 1 billion material tests of identical specimens would be needed to verify the elemental statistical distribution purely experimentally. This is obviously impossible. However, a verification is made possible by scaling up the structure to a very large size, a size that would comprise 1000^3 characteristic volumes. Thus a verification of the strength distribution of such a structure is equivalent to conducting 1 billion material tests, provided that the structure is of a type for which the failure of one element causes the whole structure to fail. The strength distribution of such a structure is known, based on a mathematical argument. Therefore, one needs to consider the large size asymptotic behavior and verify that it conforms to this distribution (Bažant, 2004; Bažant and Novák, 2003).

The first two distributions have no threshold and admit negative values of the argument, and so are unsuitable for strength. Hence, the Weibull distribution is the only realistic distribution for structural strength.

Consequently, the only way to ensure the correctness of SFEM for failure analysis is to make it match the large size asymptotic behavior, in particular, the Weibull power law size effect, typical of structures failing at crack initiation. But how to overcome the obstacle of a forbiddingly large number of random variables associated with all the finite elements?

The basic idea proposed here is to exploit directly the fundamental stability postulate from which Fisher and Tippett (1928) derived the asymptotic forms of the extreme value distributions. In regard to SFEM, this postulate may be literally implemented as follows: Instead of subdividing a very large structure into the impracticably large number ν of finite elements having the fixed size of the characteristic volume, we must use a mesh with only n macroelements (finite elements) associated with n random strength variables, keeping n fixed and increasing the macroelement size with the structure size, while the subdivision N of each macroelement is defined as the ratio of its volume to the characteristic volume of the material. Then each of these n subsets of N variables is simulated statistically, and for each subset the extreme is selected to be the representative statistical property of the finite element (macroelement). These n extremes of the subsets of N variables are then used in FEM analysis of the whole structure. This procedure ensures that the extreme value statistics is correctly approached, with one crucial advantage—the number n of finite elements (macroelements) remains reasonable from the computational point of view. Although N increases with the structure size, the determination of the extreme from the subdivision of each macroelement does not add to the computational burden since it is carried out outside FEM analysis.

One basic hypothesis of the classical Weibull theory of structural strength is the statistical independence of the strengths of the individual characteristic volumes l_0^2 (in 2D) or l_0^3 (in 3D), where l_0 is the characteristic length. The strength of each of these volumes can be described by Weibull distribution with Weibull modulus m and scale parameter σ_0 (the threshold being taken as zero, as usual). Each of the aforementioned macroelements, whose characteristic size is L_0 and characteristic volume L_0^2 or L_0^3 , may be imagined of being discretized into N characteristic volumes l_0^2 or l_0^3 , i.e. $N = L_0^2/l_0^2$ or L_0^3/l_0^3 . This consideration provides, according to (9.1) or (9.2), the statistical properties of the macroelement. Since we are interested only in very small tail probabilities, we may substitute in these equations the tail approximation of the elemental (generic) Weibull distribution with a certain modulus and scale parameter. The tail approximation is the power function σ^m (times a constant), and its substitution leads for the strength of the macroelement again to Weibull distribution but with a different modulus and scale parameter, and thus with a different mean and variance, which are expressed as follows:

$$\mu = \sigma_0(N)^{-1/m}\Gamma(1 + 1/m), \quad (9.8)$$

$$\sigma^2 = \mu^2 \left(\frac{\Gamma(1 + 2/m)}{\Gamma^2(1 + 1/m)} - 1 \right) \quad (9.9)$$

9.4 Numerical example: size effect of span in four-point bending tests

9.4.1 Experiment and attempt at deterministic simulation

By this time, abundant experimental evidence on the statistical size effect on plain concrete beams has been accumulated by now in the literature. Unfortunately, test data on bending of plain concrete beams are usually within the range of reasonable sizes (dictated by experimental feasibility). Recently, Koide et al. (1998, 2000) tested 279 plain concrete beams under four-point bending, aimed at determining the influence of the beam length L on the flexural strength of beams. These excellent data permit a comparison of the cumulative probability distribution function (CPDF) of the maximum bending moment M_{max} at failure (Bažant and Novák, 2000c; Novák, Vořechovský, Pukl, and Červenka, 2001). Beams of three different bending spans, 200, 400 and 600 mm (series C of Koide et al.) are shown in figure 9.4a), along with the cracks obtained by deterministic finite element calculations, figure 9.4b) (with the code ATENA, Červenka and Pukl (2003); Vořechovský and Červenka (2002)). The cross-sections of all the beams were kept constant (0.1 m \times 0.1 m). The experimental data show that M_{max} decreases as the span increases. To explain this size effect of the span, shown in Fig. 9.6a), Koide et al. (1998, 2000) provided a Weibull theory based approach.

Unfortunately, only the compression strength of the concrete used is known, whereas the direct tensile strength and fracture energy have not been tested. The experimental data depicted in Fig. 9.6a) represent the mean values for each size. The double logarithmic plot of M_{max} versus the span forms a straight line with a slope $D^{-n/m}$, where n is the spatial dimension and m is the Weibull modulus. The problem is properly analyzed as one-dimensional, and then the overall slope of the experimental data in the figure is matched best using $m = 8$ (which is an unusually low value for concrete, indicating a relatively high scatter).

Deterministic simulation with nonlinear fracture mechanics software ATENA yields results consistent with a flat size effect curve, i.e., absence of size effect. This is not surprising. According to fracture mechanics, there is almost no deterministic size effect in flexure of unreinforced beams when the beam depth is not varied because the energy release function is almost independent of the beam span. This is useful for our focus on the statistical size effect. It allows a purely statistical analysis of the test data in figure 9.6a), reflecting the fact that, the longer the beam, the higher is the probability of encountering in it a material element of a given low strength.

In finite element simulations, the beams were loaded by force increments in order to avoid a non-symmetric bending moment distribution when the crack pattern (Fig. 9.4b) becomes nonsymmetric, due to material randomness. The load-deflection curves, including the peak and postpeak, were calculated under load control using the arc length method.

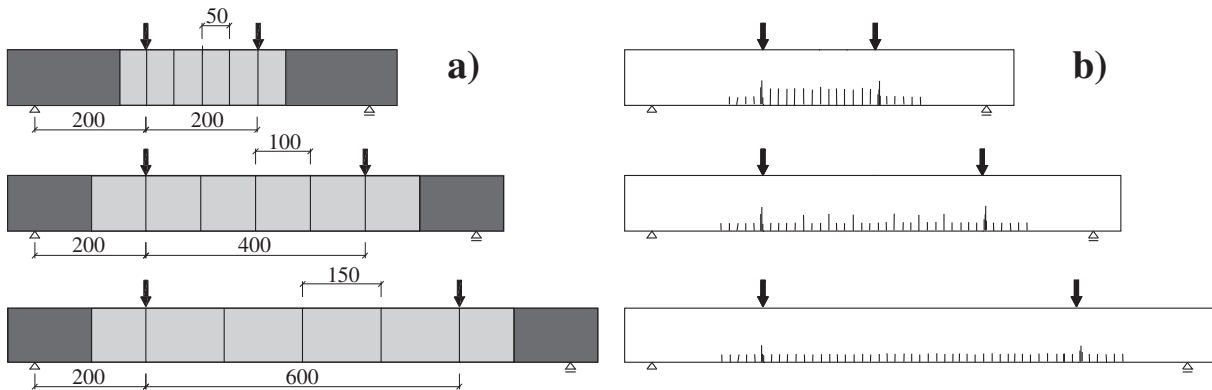


Figure 9.4: a) Koide's beams of bending span 200, 400 and 600 mm, series C ; b) Deterministic cracks for the corresponding beam sizes

9.4.2 Statistical size effect

The question stands: how to simulate the observed statistical size effect by finite elements? The probabilistic version of nonlinear fracture mechanics software ATENA (Pukl et al. 2003) was utilized to simulate the tests of Koide et al. (1998, 2000) by finite elements, in accordance with the theory of extreme values. This was made possible by integrating ATENA with the probabilistic software Novák et al. (2002d, 2004).

In this simulation, the finite element mesh is defined by using only 6 stochastic macroelements placed in the central region of test beams in which fracture initiates randomly; see Fig. 9.5. The chosen macroelements have the form of strips. The strips suffice for simulating the Weibull size effect. We imagine N elements per macroelement of width L_0 , while the finite element meshes for all the sizes are identical (except for a horizontal stretch).

The characteristic length is considered to be approximately 3-times the maximum aggregate size, i.e., about 50 mm. The Weibull modulus is taken as $m=8$, and the scale parameter is 1.0. The statistical parameters of the strength of the macroelements, imagined to consist of $N = L_0/l_0$ material elements each, are calculated from (9.8). For the three sizes (spans) considered here, $L_0 = 50, 100, 150$ mm and $N = 1, 2, 3$.

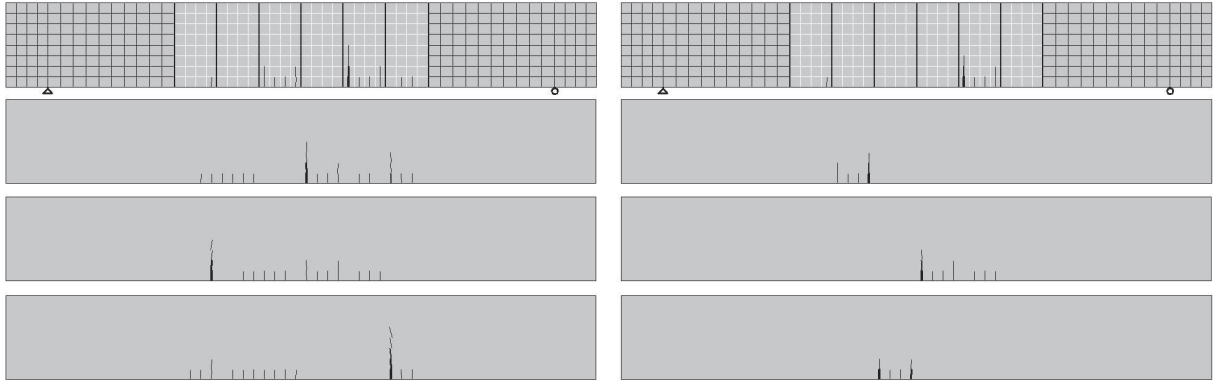


Figure 9.5: Macroelements and examples of random crack initiation for the first size; left: random tensile strength only, right: random and correlated tensile strength and fracture energy

In the present approach, a stochastic computational model with $n=6$ random tensile strength variables is defined for each beam size (span); 16 random simulations of these 6 statistically independent variables, based on the method of Latin hypercube sampling, are performed using FREET and ATENA softwares (Vořechovský and Novák, 2002, 2003b; Novák et al., 2003b, 2002d, 2004; Cervenka and Pukl, 2004; Pukl et al., 2003b), using methods described in chapters 3 and appendix A. The statistical characteristics of the ultimate force can then be evaluated. The mean values of nominal strength obtained from a statistical set of maximum forces are determined first. Figure 9.5 shows the random cracking pattern at failure, obtained for four realizations of three progressively improved alternatives of solution.

To illustrate the random failures, the corresponding random load-deflection curves are shown in figure 9.6b). The three alternatives, for which the results are presented in Fig. 9.6a), are as follows:

- **Alternative I:** The first alternative is a pure Weibull type approach in which only the random scatter of tensile strength is considered, the generic mean value of tensile strength being fixed as 3.7 MPa. For the three sizes (spans) considered here then, according to formulas (9.8) and (9.9) the means of tensile strengths are $\mu = 3.484, 3.195$ and 3.037 MPa, coefficient of variation $\text{COV} = 0.148$ (driven by the Weibull modulus m only).

The resulting size effect curve obtained by probabilistic simulation is found to have a smaller slope than the experimental data trend, in spite of the fact that an unusually low Weibull modulus ($m = 8$) is used. This can be explained easily. The Weibull theory strictly applies only when the failure occurs at crack initiation, before any (macroscopically) significant stress redistribution with energy release. However, the material, concrete, is relatively coarse, the test beams not being large enough compared to the aggregate size, and so a nonnegligible fracture process zone must form before a macroscopic crack can form and propagate, dissipating the required fracture energy G_f per unit crack surface. Therefore, the beam, analyzed by nonlinear fracture mechanics (the crack band model, approximating the cohesive crack model) does not fail when the first element fails (as required by the weakest link model imitating the failure of a chain). Rather, it fails only after a group of elements fails, and several groups of failing elements can develop before the beam fails; see Fig. 9.5. The finite element simulations are able to capture this behavior thanks to the cohesive nature of softening in a crack, reflecting the energy release requirement of fracture mechanics.

- **Alternative II:** The idea to overcome the problem and match the size effect data is to take the randomness of fracture energy G_f into account. Using the generic mean of fracture energy, $G_f = 93$ N/m, for the three spans, according to formulas (9.8) and (9.9) the means of fracture energy are $G_f = 87.6, 80.3$ and 76.3 N/m, $\text{COV} = 0.148$. The generic mean of tensile strength is again $\mu = 3.7$ MPa. But we cannot ignore the statistical correlation of G_f to tensile strength. For lack of available data, we simply assume a very strong correlation, characterized by correlation coefficient 0.9. Such a correlation tends to cause an earlier onset of (macroscopic) crack propagation, compared to Alternative I. The result is shown in Fig. 9.6a) as Alternative II. The resulting slope of the simulated size effect curve is now close to the slope of experimental data. However, the whole

curve is shifted down, i.e., all the beams are weaker than they should be. It can be seen that the strong correlation between tensile strength and fracture energy causes the macroelements with a lower tensile strength to be more brittle. The failure, therefore, localizes into these macroelements (Fig. 9.5).

- **Alternative III:** In seeking a remedy, we must realize that Koide *et al.* have not measured the tensile strength nor the fracture energy, and our foregoing estimate may have been too low. So a heuristic approach is the only option. While keeping Alternative II, we are free to shift the size effect curve up by increasing the generic mean value of tensile strength and the fracture energy value. We increase them to 4.1 MPa and 102 N/m, respectively, and this adjustment is found to furnish satisfactory results; see Fig. 9.6a). Although the size effect of Alternative III in the double logarithmic plot is not as straight as the trend of data, the differences from the data are negligible. These small differences may have been easily caused, for instance, by insufficient size of the calculated data set, or by weaker numerical stability near the peak load, making a precise detection of the peak (under load control) less accurate.

Finally, it may be emphasized that the result of Alternative III is in excellent agreement with the previous analysis of these data according to the nonlocal Weibull theory (Bažant and Novák, 2000c).

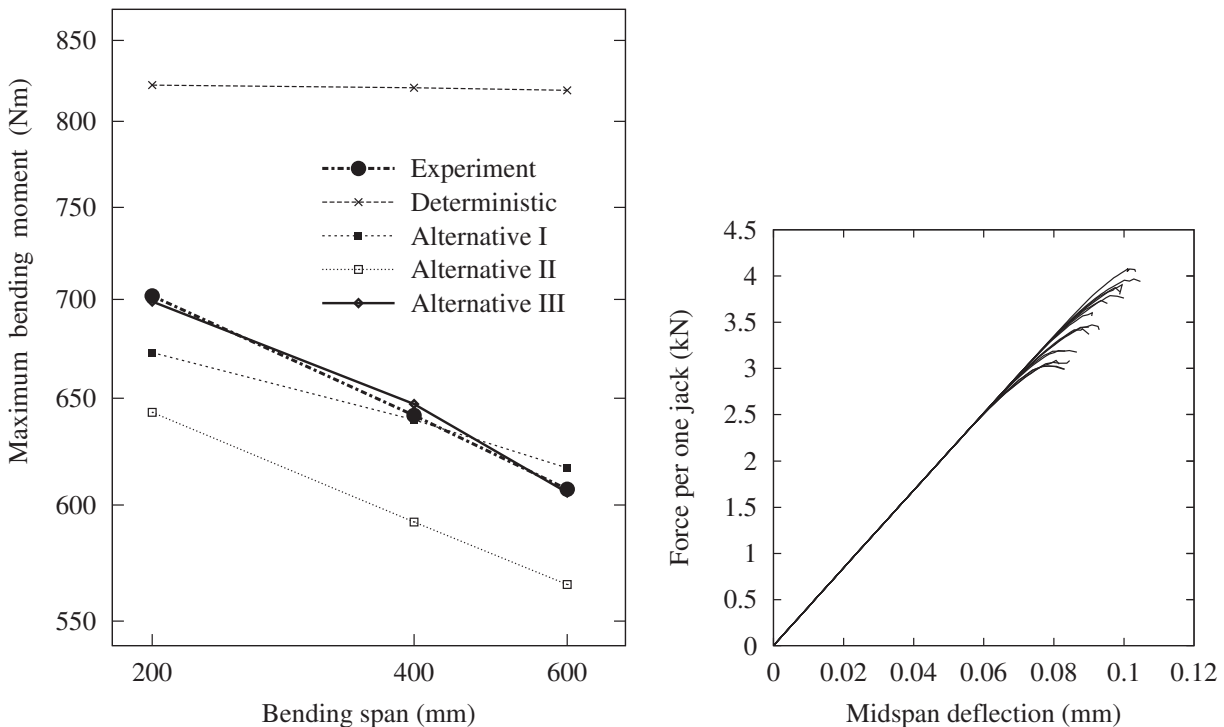


Figure 9.6: a) Comparison of means of Koide's data and ATENA deterministic and statistical simulations; b) Random load deflection diagrams for one size of Koide's beams (note the curvatures indicating appreciable stress redistributions before peak)

9.5 Conclusions

The chapter tackles a problematic feature of stochastic finite element method: How to capture the statistical size effect for structures of *very large sizes*. A simple and effective strategy for capturing the statistical size effect using stochastic finite element methods is developed. The idea is to emulate the recursive stability property from which the extreme value distribution, the Weibull distribution, is derived. Using the combination of a well feasible type of Monte Carlo simulation and of computational modeling of nonlinear fracture mechanics, a probabilistic treatment of complex fracture mechanics problems is

rendered possible. The approach may be understood as a computational trick based on extreme value theory similar to its counterpart in deterministic nonlinear analysis of fracture – crack band model.

The feasibility of the approach is documented by simulating the size effect in plain concrete beams under four-point bending, for which extensive statistical test data have recently been reported by Koide et al. (1998, 2000). The idea works well for large enough structures where the deterministic part of size effect (causing the stress redistribution) is weak.

9.6 Further discussion

The third alternative leading to a good mean size effect curve (MSEC) still does not mean that the statistical size effect is captured correctly. In order to ensure this one would have to check the whole distribution function for each size. If the real structure is brittle or if it fails right after the first crack initiation, the distribution function for each size must be Weibull and moreover, the COV (or m) must be the same, constant and equal to those used for the elemental strength distribution. Although Koide measured the strength for a relatively high number of specimens for each size (35-40) this still does not allow us to draw conclusions about the whole distribution, mainly the tail behavior. Although we approached more “brittle” behavior by high positive correlation between the strength and fracture energy, the load-deflection diagrams (Fig. 9.6b) still shows considerable strength redistribution before the peak is reached. This may cause deviation from the simple 1-dimensional Weibull statistical model illustrated in Fig. 9.7.

In case of quasibrittle materials, such as concrete, the largest beams must fail after development of relatively short cracks (in comparison with the beam depth D). But this is not the case for small beams. When the peak load is reached the crack length is not negligible and this calls for more sophisticated statistical model illustrated in Fig. 9.8.

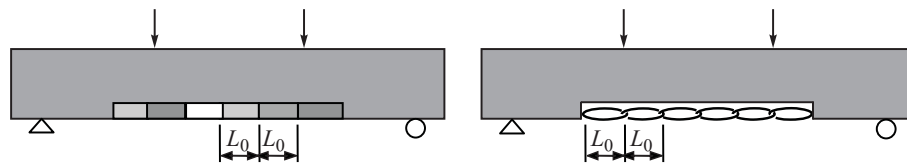


Figure 9.7: Simple 1-D Weibull model (chain) in the bottom layer of 4PB beam. Left: Random variables – macroelements. Right: a statistical “chain” model driving the strength of a whole structure

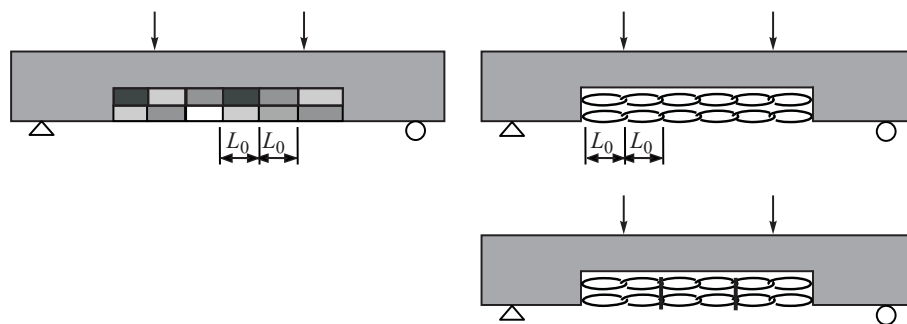


Figure 9.8: Illustration of stress redistribution captured by parallel chains – more sophisticated statistical model for small sizes (the bundle of chains model)

Since the deterministic size effect is highly suppressed by having the depth D constant, we may expect the MSEC (plot in Fig. 9.6a) inclined due to statistical size effect only (straight line in double-logarithmic plot). However, the influence of different load-sharing rules in case of the model in Fig. 9.8 may cause deviation of statistics for all sizes from the pure Weibull type scaling. This is under investigation now.

The comparison of three alternatives studied reveals the influence of the basic parameters: A decrease of modulus m or the characteristic length causes a stronger size effect, reflected in a larger slope in

the MSEC. An increase of tensile strength shifts the entire MSEC upwards. A decrease of the fracture energy, or the correlation factor between strength and fracture energy, leads to a stronger size effect (slope of MSEC) and at the same time shifts the MSEC downwards, which represents better the behavior of a chain. The third alternative of the study is able to fit the size effect curve by changing the mean tensile strength and fracture energy of the finite elements, which is admissible because Koide's tests did not include measurement of these parameters. Despite the good fit of Koide's test data, the Weibull modulus, found to be $m = 8$, is surprisingly low compared to Weibull modulus $m = 24$ obtained by fitting many data with a nonlocal generalization of Weibull theory (Bažant and Novák, 2000b,c).

The Weibull modulus found for Koide's beams could reflect the slope near the intermediate asymptote (see Fig. 8.1, p. 90), which however decreases when the deterministic size effect wears out as the size $D \rightarrow \infty$. Although Koide's results could not be extended or directly applied to very large structures, they reveal strong Weibull-type stochastic behavior when a slender structure is scaled longitudinally. Koide's beam has been simulated in ATENA with a macro-element, the parameters of which are scaled in one dimension (1D). This represents the weakest-link chain model which can be imagined to describe the bottom layer of finite elements in the beam. Despite the good match with 1D treatment, the material parameters used in these computations could not be reproduced on a different set of experiment. The deterministic size effect is not properly treated with the 1D model as this model does not fail immediately at the first crack initiation (Fig. 9.6b). The scaling of Koide's beams for the strength should better be done in two dimensions (2D) because it involves considerable stress redistribution across the beam depth.

The difficulty with the 2D treatment is that the stability postulate could not be directly applied to the macro-elements. The coupling of the macro-elements in a load-sharing manner violates the assumption of the weakest-link chain model. The probability distribution of the macro-element could be derived by other methods, e.g. a bundle model capturing the coupling effect of the macro-element, and the shift in mean and variance could be computed accordingly using the fiber bundle model. Such an approach is currently being pursued by the author.

To conclude, we may say that there are two main problems of the proposed technique: (i) stress redistribution prior failure cannot be captured by a statistical model of a chain (extreme value statistics) and (ii) spatial correlation of random properties (e.g. strength) in cases when the autocorrelation length is not negligible compared to structure size (or FPZ size) is not taken into account. The first problem can be to some extent captured by chain of bundle or bundle of chain models with various load sharing rules, see e.g. Peirce (1926); Daniels (1945); Epstein (1948); Coleman (1958); Phoenix (1978a,b); Harlow and Phoenix (1978b,a); Smith and Phoenix (1981); Smith (1982); Hohenbichler and Rackwitz (1983); Hohenbichler (1983); Madsen et al. (1986); Bogdanoff and Kozin (1987, 1989); Grigoriu (1990); Beyerlein and Phoenix (1996); Byeerlein and Phoenix (1997); Beyerlein and Phoenix (1997); Phoenix et al. (1997); Ibnabdeljalil and Curtin (1997); Marston et al. (1997); Kun et al. (2000); Mahesh et al. (2002); Vořechovský and Chudoba (2004a). The second problem of autocorrelated material properties can be effectively solved by modeling the properties with spatially fluctuating random fields. Both problems are tackled in the following chapter.

However, both problems disappear in modeling of structures that are larger than both the statistical length scale (measure of autocorrelation) and deterministic length scale (the length related to size of zone of stress redistribution). For such problems, the proposed approach is advantageously utilized in the theoretical and numerical verification of the new size effect law proposed in the following chapter.

Chapter 10

Combined deterministic-energetic and statistical size effect in quasibrittle failure

Published in papers: [Bažant, Vořechovský, and Novák \(2004c\)](#); [Vořechovský, Bažant, and Novák \(2005\)](#)

An improved generalized law for combined energetic-probabilistic size effect on the nominal strength for structures failing by crack initiation from a smooth surface is proposed. The law features two separate scaling lengths of structures governing the two different source of size effect: deterministic and statistical. The role of these two lengths in the transition from energetic to statistical size effect of Weibull type is clarified. Relations to the previously developed deterministic-energetic and energetic-statistical formulas are presented.

Theoretical achievements are then utilized for practical purposes - the paper proposes a procedure to capture both deterministic and statistical size effects on the nominal strength of quasibrittle structures failing at crack initiation. The advantage of the proposed approach is that the necessity of time consuming statistical simulation is avoided, only deterministic nonlinear fracture mechanics FEM calculation must be performed.

Results of deterministic FEM calculation should follow deterministic-energetic formula, a superimposition with the Weibull size effect, which dominates for large sizes using the energetic-statistical formula, is possible. As the procedure does not require a numerical simulation of Monte Carlo type and uses only the results obtained by deterministic computation using any commercial FEM code (which can capture satisfactorily deterministic size effect), it can be a simple practical engineering tool. The efficiency of the procedure is demonstrated on the numerical example of Malpasset dam failure reinterpretation.

10.1 Introduction

The necessity to combine achievements of both fracture mechanics and reliability engineering became appealing recently. On one side, many sophisticated efficient computational approaches of nonlinear fracture mechanics have been developed, some of them utilized even within the framework of commercial computer software developers. They are generally able to capture the deterministic size effect phenomenon. On the other side, in reliability engineering field, proper fracture mechanics models are still used quite rarely, but some exemptions already exists ([Pukl et al., 2003b](#); [Bergmeister et al., 2002](#); [Novák et al., 2002b, 2003a](#); [Pukl et al., 2003a](#); [Waarts, 2001](#)). To combine these two fields is generally difficult: Computational effort of FEM nonlinear fracture mechanics in combination with Monte Carlo based simulation techniques (generally necessary) could be enormous even for simple problems.

Importance of randomness was realized long time ago, prior to the 1990's, it was commonplace in design to assume the maximum load of such structures to be governed by the strength of the material, and sometimes the possibility of a purely statistical, classical size effect of [Weibull \(1939a\)](#) was admitted. But no attention was paid to the possibility of a deterministic size effect. More than two decades ago, however, the finite element calculations with the cohesive (or fictitious) crack model by [Hillerborg et al.](#)

(1976) revealed the necessity of a strong deterministic size effect engendered by stress redistribution within the cross section due to softening inelastic response of the material in a boundary layer of cracking near the tensile face. A detailed finite element analysis of the size effect on the modulus of rupture with the cohesive crack model was presented by Petersson (1981). He numerically demonstrated that the deterministic size effect curve terminates with a horizontal asymptote and also observed that, for very deep beams, for which the deterministic size effect asymptotically disappears, the classical Weibull-type statistical size effect must take over.

A combination of the statistical and deterministic aspects of the problem has recently been achieved by the probabilistic nonlocal continuum model developed by Bažant and Xi (1991); Bažant and Novák (2000b,c). They showed that this model satisfies the condition that the classical Weibull theory of size effect must ensue as the limit for infinite structure size. They also deduced a simple energetic-statistical size effect formula (Bažant and Novák, 2001). Their formula represents asymptotic matching between the deterministic-energetic formula, which is approached for small sizes, and the power law size effect of the classical Weibull statistical theory, which is approached for large sizes.

If a nonlinear fracture mechanics computer code is used for modeling of failure at fracture initiation, the result from the size effect point of view should be purely deterministic. It should follow the energetic size effect formula (Bažant and Novák, 2001). This was shown on modulus of rupture extensive data by Novák, Vořechovský, Pukl, and Červenka (2001). But because energetic-statistical size effect formula developed by Bažant and Novák (2001) is based on the asymptotic matching, the same procedure can be used to update deterministic FEM size effect results - to combine them with the classical Weibull statistical size effect. Superposition of these two types of size effect can be suggested and represent a logical complement of latest research on size effect at crack initiation.

Practical and simple approach to incorporate the statistical size effect into the design or the assessment of very large unreinforced concrete structures (such as arch dams, foundations and earth retaining structures, where statistical size effect plays a significant role) is important. Failure load prediction can be done without simulation of Monte Carlo type utilizing the energetic-statistical size effect formula in mean sense together with deterministic results of FEM nonlinear fracture mechanics codes.

A new law with two scaling lengths (deterministic and statistical) for combined energetic-probabilistic size effect on the nominal strength for structures failing by crack initiation from smooth surface is proposed. The role of these two lengths in the transition from energetic to statistical size effect of Weibull type is clarified. Relations to the recently developed deterministic-energetic and energetic-statistical formulas are presented. This paper clarifies the role and interplay of two material lengths deterministic and statistical.

10.2 Deterministic-energetic size effect formula

The deterministic energetic size effect formula is (Bažant and Novák, 2001):

$$\sigma_N(D) = f_r^\infty \left(1 + \frac{rD_b}{D} \right)^{1/r} \quad (10.1)$$

where the structural size is D . Parameters f_r^∞ , D_b , r are positive constants, representing the unknown empirical parameters to be determined. Parameter f_r^∞ represents solution of the elastic-brittle strength reached as a nominal strength for a large structural sizes. The exponent r (a constant) controls the curvature and the slope of the law. The exponent offers a degree of freedom while having no effect on the expansion in derivation of the law (Bažant and Planas, 1998). Parameter D_b has the meaning of the thickness of cracked layer. Variation of the parameter D_b moves the whole curve left or right - represents the deterministic scaling parameter and is in principle related to grain size. Drives the transition from elastic brittle ($D_b = 0$) to quasibrittle ($D_b > 0$) behavior.

An extension to the law can be made by considering the fact, that extremely small structures (smaller than D_b) must exhibit the plastic limit, introducing a new parameter to control this convergence, l_p (Bažant, 2002b):

$$\sigma_N(D) = f_r^\infty \left(1 + \frac{rD_b}{D + l_p} \right)^{1/r} \quad (10.2)$$

This formula represents the full size range transition from perfectly plastic behavior (when $D \rightarrow 0$; $D \ll l_p$) to elastic brittle behavior ($D \rightarrow \infty$; $D \gg D_b$) through quasibrittle behavior. Parameter l_p governs the transition to plasticity for small sizes D (crack band models or averaging in nonlocal models leads to horizontal asymptote). The case of $l_p \neq 0$ shows the plastic limit for vanishing size D and the cohesive crack and perfectly plastic material in the crack both predicts equivalent plastic behavior. For large sizes the influence of l_p decays fast and the case of $l_p \neq 0$ is therefore asymptotically equivalent to case of $l_p = 0$ for large D .

Therefore the predicted strength of an infinitely small structure should equal to what theoretical limit plastic analysis provides us with (uniform stress, full rotation capability, . . . etc). This fact should be used to calibrate the formula: the limiting strength for $D \rightarrow 0$ is given by the asymptote which is a horizontal line at the nominal strength (for $l_p \neq 0$):

$$\lim_{D \rightarrow 0} \sigma_N(D) = f_r^\infty \left(1 + \frac{rD_b}{l_p}\right)^{1/r} \quad (10.3)$$

Knowing the ratio between the maximum plastic and elastic moment - nominal strength of fully plasticized $\lim_{D \rightarrow 0} \sigma_N(D)$ and elastic solution $\lim_{D \rightarrow \infty} \sigma_N(D) = f_r^\infty$ (plastic reserve)

$$\eta_p = \frac{M_{pl}}{M_{el}} = \left(1 + \frac{rD_b}{l_p}\right)^{1/r} \quad (10.4)$$

one can solve the equation (10.2) for the parameter l_p :

$$l_p = \frac{rD_b}{\eta_p^r - 1} \quad (10.5)$$

For example in case of rectangular cross section (used for the numerical example later in the paper) the highest possible ratio η_p is 3: the cross section is stressed by tensile stresses equal to f_r^∞ and resulting force is balanced by force acting in thin compressed layer of infinite compressive strength.

In practical cases of concrete structures the transition to fully plastic behavior occurs for structure sizes far bellow the maximum aggregate size and is therefore purely theoretical. For practical purposes we may take the parameter $l_p = 0$ which leads to change of asymptotic behavior of the law for small sizes:

$$\lim_{D \rightarrow 0} \sigma_N(D) = f_r^\infty \left(\frac{rD_b}{D}\right)^{1/r} \propto D^{-1/r}$$

a straight line of the slope $-1/r$ in double log plot of characteristic size against the nominal strength.

10.3 Energetic-statistical size effect formula

The large size asymptote of the deterministic energetic size effect formulas (10.1,10.2) is horizontal, $\sigma_N/f_r^\infty = 1$, see figures 10.3 and 10.1. The same is true of all the existing formulae for the modulus of rupture, see e.g. Bažant and Planas (1998). But this is not in agreement with the results of Bažant and Novák (2000b,c) nonlocal Weibull theory as applied to modulus of rupture, in which the large-size asymptote in the logarithmic plot has the slope $-n/m$ corresponding to the power law of the classical Weibull statistical theory (Weibull, 1939a). In view of this theoretical evidence, there is a need to superimpose the energetic and statistical theories. Such superimposition is important, for example, for analyzing the size effect in vertical bending fracture of arch dams, foundation plinths or retaining walls.

A statistical generalization of (10.1) may be deduced as follows (Bažant and Novák, 2001). According to the deterministic energetic model, $\Delta^r = (f_r/f_r^0)^r - rD_b/D = 1$, which is the value of the large-size horizontal asymptote. From the statistical viewpoint, this difference, characterizing the deviation of the nominal strength from the asymptotic energetic size effect for a relatively small fracture process zone (large D), should conform to the size effect of Weibull theory, $D^{-n/m}$, where m = Weibull modulus and n = number of spatial dimensions ($n = 1, 2$ or 3 , in the present calculations 2). Therefore, instead of $\Delta = 1$,

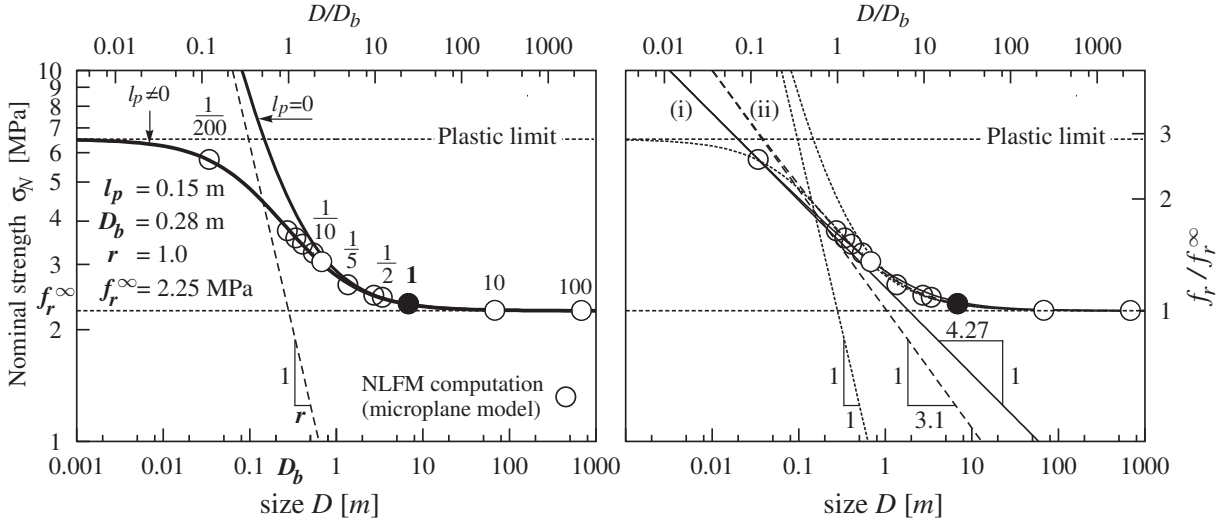


Figure 10.1: Best fit of extended deterministic formula. a) for a wide range of Malpasset dam sizes; b) example of two erroneous fits with simplified deterministic formula to (1) whole range of data, (2) data without the smallest size.

one should set $\Delta = (D/D_b)^{-n/m}$. This leads to the following Weibull-type statistical generalization of the energetic size effect formula (10.1):

$$\sigma_N(D) = f_r^\infty \left[\left(\frac{D_b}{D} \right)^{rn/m} + \frac{rD_b}{D} \right]^{1/r} \quad (10.6)$$

Because in all practical cases $rn/m < 1$ (in fact, $\ll 1$), formula (10.6) satisfies three asymptotic conditions:

1. For small sizes, $D \rightarrow 0$, it asymptotically approaches the deterministic energetic formula (10.1);

$$\lim_{D \rightarrow 0} \sigma_N(D) = f_r^\infty r^{1/r} \left(\frac{D_b}{D} \right)^{1/r} \propto D^{-1/r} \quad (10.7)$$

2. For large sizes, $D \rightarrow \infty$, it asymptotically approaches the Weibull size effect;

$$\lim_{D \rightarrow \infty} \sigma_N(D) = f_r^\infty \left(\frac{D_b}{D} \right)^{n/m} \propto D^{-n/m} \quad (10.8)$$

3. For $m \rightarrow \infty$, the limit of (10.6) is the deterministic energetic formula (10.1).

Equation (10.6) is in fact the simplest formula with these three asymptotic properties. It may be regarded as the asymptotic matching of the small-size deterministic and the large-size statistical size effects.

In case we consider the extended deterministic law (with plastic limit), the statistical generalization reads:

$$\sigma_N(D) = f_r^\infty \left[\left(\frac{D_b}{D} \right)^{rn/m} + \frac{rD_b}{D + l_p} \right]^{1/r} \quad (10.9)$$

and the asymptotic strength behavior for small structural size is not a power law (straight line with the slope $1/r$ in double-log plot).

In the recent paper by Bazant (2004) a generalized law for the mean size effect is derived together with approximate PDF for the whole range by asymptotic matching. The paper argues with the existence of intermediate asymptotics. The resulting size effect formula for any specified probability of failure reads:

$$\sigma_N = [-\ln(1 - P_f)]^{1/m} s_D \quad (10.10)$$

where

$$s_D = s_0 f_0 \left[\left(\frac{D_b}{D + \gamma l} \right)^{rn/m} + \alpha r \frac{D_b}{D + \gamma l} \right]^{1/r} \quad (10.11)$$

where the coefficient $\gamma > 0$ in denominators limit both: statistical and deterministic part from growing to infinity for small D . So it remedies the problem that all the previous statistical formulas intersect the deterministic law at the size $D = D_b$ and therefore gives higher mean nominal strength prediction for small structures compared to the deterministic case.

The statistical part of size effect and the existence of statistical length scale has been investigated in detail by [Vořechovský and Chudoba \(2004a\)](#) for particular case of glass fibers. The authors argue that having the summation in the denominator of mean statistical size effect term in formula imposes a horizontal asymptote of the mean strength (as opposed to local Weibull approach) because the randomly fluctuating strength field must be limited (since it is autocorrelated). An important outcome of their paper is the comparison of statistical size effect due to extremes of random strength field and classical (local) Weibull approach (concentration of flaws, power law). Their work shows, briefly, that the statistical part of size effect in structures with stationary strength random field has a large-size asymptote in the classical Weibull form (straight line in double-log plot n/m) while the left (small size) asymptote is horizontal. The value of the horizontal asymptote for $D \rightarrow 0$ is the mean strength of the random field, and in Weibull understanding it is mean strength measured for the reference length being equal to the autocorrelation length l_ρ . So by introduction of the random strength field we introduce the length scale (l_ρ).

Clearly, if strength is the matter, we always deal with the minimum value of a random strength field realization. When a structure is much smaller compared to l_ρ , the random strength field reduces to a random variable (material is treated as one random element) whose mean of minimum is the variable mean itself (“minimum of a variable is the variable itself so the statistics are preserved”). In case of large structure the autocorrelation length l_ρ becomes negligible and the random field minimum is represented by minimum of independent identically distributed random variables (IID).

The extreme values in IID case is well elaborated field. For Weibull distributed strength random field the IID’s are Weibull and extreme values (minima) belong to the domain of attraction of Weibull. The recursive stability postulate of extreme value distribution ([Fisher and Tippett, 1928](#); [Gnedenko, 1943](#); [Gumbel, 1958](#)) shows that the scaling of minima for arbitrary number of random variables (strengths of material points) leads to power law.

In case of minima of strength random field the remaining problem is the transition between small enough sizes (lengths) and large sizes. [Vořechovský and Chudoba \(2004a\)](#) have shown that the mean of extremes of Weibull random process can be well approximated with asymptotic matching by $\mu(\sigma_N(D)) = \mu_0 (l_\rho / (D + l_\rho))^{(1/m)}$, where μ_0 is the mean value of the process and l_ρ is the autocorrelation length.

By incorporating this result (statistical part) into the formula (10.9) we get a final law (similar to that derived by [Bažant \(2004\)](#)):

$$f_r = f_r^\infty \left[\left(\frac{L_0}{D + L_0} \right)^{rn/m} + \frac{r D_b}{D + l_p} \right]^{1/r} \quad (10.12)$$

This new formula exhibits following features:

- Small size left asymptote is correct (deterministic), parameter l_p drives to fully plastic transition for small sizes.
- Large size asymptote is Weibull (statistical, with the slope $-n/m$)
- The formula introduces two scaling lengths, deterministic (D_b) and statistical (L_0). The mean size effect is partitioned into deterministic and statistical parts. Each have its own length scale, the interplay of both embodies behavior expected and justified by previous research. D_b drives the transition from elastic-brittle to quasibrittle and L_0 drives the transitional zone from constant property to local Weibull via strength random field.

Note that the autocorrelation length l_ρ has direct connection to our statistical length L_0 . This correspondence is explained later and illustrated by formula (10.14)

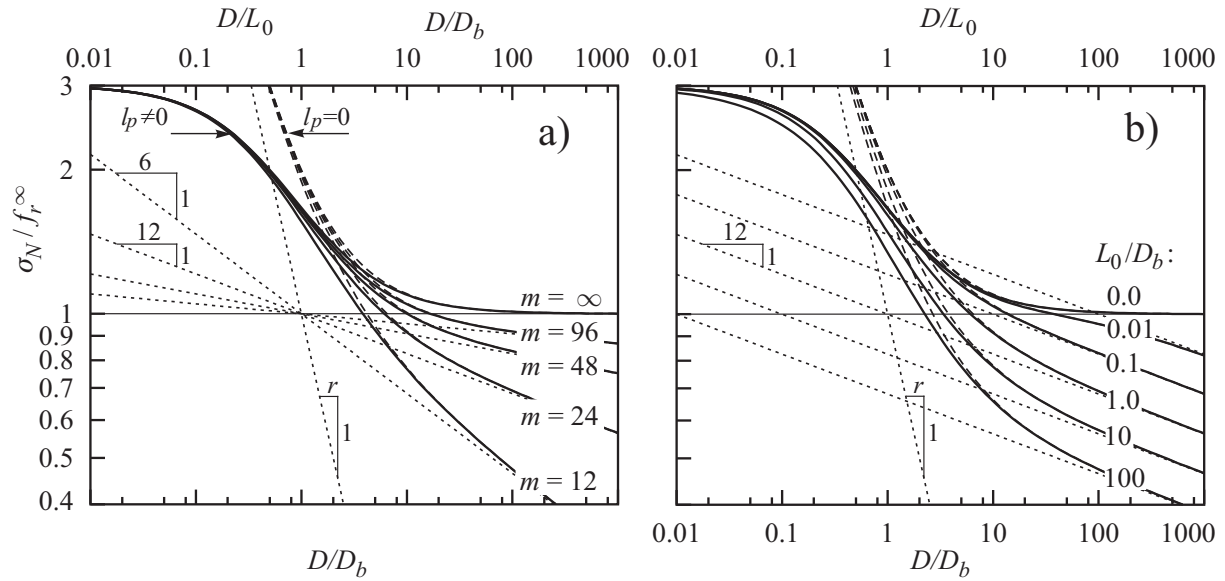


Figure 10.2: Parametric study of the proposed law. a) influence of Weibull modulus (scatter); b) interplay of the scaling lengths

Fig. 10.2 shows the behavior of formula – parametric study (10.12) for a broad range of introduced parameters. Fig. 10.2a) shows the behavior for different Weibull modulus m , note that for $m = \infty$ it degenerates to deterministic formula. The same applies if $L_0 \rightarrow \infty$. The interplay of two scaling lengths using the ratio L_0/D_b is demonstrated in Fig. 10.2b) for constant Weibull modulus m . For large structures the ratios of L_0/D_b results in parallel bundle of Weibull asymptotes. Note that the ratio η_p between plastic and elastic brittle nominal strength used here is that for rectangular cross section ($\eta_p = 3$).

The question arises what is in reality the ratio L_0/D_b ? Since both scaling lengths are in concrete probably driven mainly by grain sizes, we expect $L_0 \approx D_b$, so the simpler law with ($D_b = L_0$) should be an excellent performer in practical cases. We do not answer this question at this moment purposely, it is beyond the scope of this paper. But it is certainly a key point for next investigation. However, the arguments for splitting and generalization of a new formulae are fundamentally clear.

The statistical (or probabilistic) part must approach the Weibull asymptotic straight line for size $D \rightarrow \infty$, but different statistical formulations lead to different formula for the statistical mean size effect curve (MSEC). From the statistical point of view the deterministic alternative can be captured follows: No scatter of material properties, statistical part of size effect shrinks to 1 for all sizes and the MSEC is the only result (the law is deterministic). Such result is not possible in nature (where the scatter is inherently present) and represents a theoretical limit for the $\text{COV} \rightarrow 0$ (or Weibull modulus $m \rightarrow \infty$).

10.4 Superimposition of FEM deterministic-energetic and statistical size effects

As was already mentioned deterministic modeling with NLFEM can capture only deterministic size effect. A procedure of superimposition with statistical part should be established. Such procedure of the improvement of the failure load (nominal stress at failure, deterministic size effect prediction) obtained by a nonlinear fracture mechanics computer code can be as follows:

1. Suppose that the modeled structure has characteristic dimension D_t . The natural first step is to create FEM computational model for this real size. At this level the computational model should be tuned and calibrated as much as possible (meshing, boundary conditions, material etc.). Note that we obtain a prediction of nominal strength of the structure (using failure load corresponding to the peak load of load-deflection diagram) for size D_t , but it reflects only deterministic-energetic features

of fracture. Simply, the strength is usually overestimated at this (first) step, the overestimation is more significant as real structure is larger. Result of this step is a point in the size effect plot presented by a filled circle in Fig. 10.3 a).

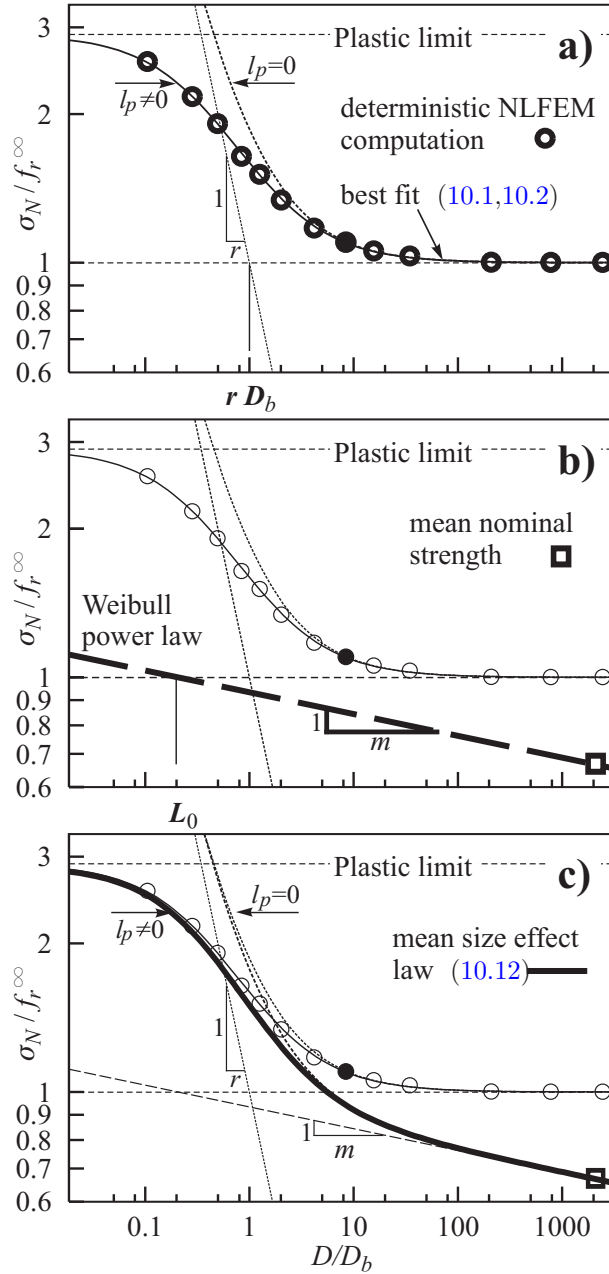


Figure 10.3: Illustration of superimposition steps. a) Steps 1-4 resulting in deterministic formulae fit; b) Step 5 - determination of parameter L_0 ; c) Final formula and strength prediction for the real size D_t

2. Scale down and up geometry of our computational model in order to obtain the set of similar structures with characteristic sizes $D_i, i = 1, \dots, N$. Consider $N = 3$ as the minimum set size, however higher number of sizes is recommended. Based on numerical experience a reasonable number is around 10 sizes and depends how the sizes cover transition phases. Therefore, sizes D_i should span over large region from very small to very large sizes. Then calculate nominal strength for each size $\sigma_{N,i}, i = 1, \dots, N$. Note that for two very large sizes nominal strengths should be almost identical as this calculation follows energetic size effect with horizontal asymptote. If not,

failure mechanism is not just only crack initiation, other phenomena (stress redistribution) plays more significant role and the procedure suggested here cannot be applied. The computational model has to be mesh-objective in order to obtain objective results (eg. crack band model, nonlocal damage continuum) for all sizes.

In order to ensure that phenomenon of stress redistribution (causing the size effect for the range of sizes) is correctly captured, well tested models are recommended for strength prediction. A special attention should be paid to the selection of constitutive law and localization limiter. The result of this step is a set of point (circles) in the size effect plot as shown in Fig. 10.3 a).

3. Next step is to obtain the optimum fit of the deterministic-energetic formula (10.1 or 10.2) using the set of N pairs $\{D_i, \sigma_{N,i}\} : i = 1, \dots, t, \dots, N$. Since the deterministic formula is generally nonlinear in fitted parameters (if $r \neq 1$ or $l_p \neq 0$) the algorithm for nonlinear regression fit is needed. The Levenberg - Marquardt optimization algorithm is the most suitable technique to determine unknown parameters of formula (10.1 or 10.2). The result of this step are values of three parameters: f_r^∞ , D_b and r . We consider the parameter l_p to be substituted based on the fact that the ratio η_p is determined using the plastic analysis of very small structure and elastic-brittle analysis of very large structure. Knowing the ratio η_p we incorporate formula (10.5) into the deterministic formula (10.2):

$$\sigma_{N, determ}(D_i) = f_r^\infty \left(1 + \frac{(\eta_p^r - 1)rD_b}{D_i(\eta_p^r - 1) + rD_b} \right)^{1/r} \quad i = 1, \dots, N \quad (10.13)$$

Two alternatives of fit can be utilized, fit of all three parameters (f_r^∞ , D_b and r) or fit of only two parameters D_b and r . The second alternative is possible and recommended as it is reasonable to prescribe for very large sizes $\sigma_N/f_r^\infty = 1$ as asymptotic limit. This limit can be estimated from nonlinear FEM analysis as the value to which the nominal strength converges with increasing size. The result of this step is illustrated by a fitted curve to the set of points in Fig. 10.3 a).

4. There are three remaining parameters which should be substituted into statistical-energetic formula (10.6): n , m and L_0 :

Parameter n is the number of spatial dimensions ($n = 1, 2$ or 3).

Parameter m represents the Weibull modulus of FPZ with Weibull distribution of random strength. Recent study (Bažant and Novák, 2000a) reveals that, for concrete and mortar, the asymptotic value of Weibull modulus $m \approx 24$ rather than 12, the value widely accepted so far. Ratio n/m therefore represents the slope of MSEC in size effect plot for $D \rightarrow \infty$. This means that for extreme sizes the nominal strength decreases, for two-dimensional (2D) similarity ($n = 2$), as the $-1/12$ power of the structure size. Note, that for different material the asymptotic value of Weibull modulus is different, eg. for laminates much higher than 24. Result of these 4 steps are shown for illustration in Fig. 10.3a).

Parameter L_0 is now only remaining parameter to be determined. As it represents statistical length scale it seems to be that we will need to utilize a statistical software incorporated into your NLFEM code. But there is much simpler alternative based on simple calculation of local Weibull integral. A choice of statistical length scale l_p is a primary task (a good judge may be probably $l_p \approx D_b$). Since the choice about a scatter of FPZ strength is made (Weibull modulus m driving the power of size effect for large sizes), one can compute large size structure having the Weibull strength of each FPZ. Once the mean strength of such large structure is known (a point in the size effect plot with coordinates $D_{stat}, \hat{\sigma}_{stat}$), one can pass a straight line of slope n/m through the point (Weibull asymptote). Graphically, the intersection of the statistical (Weibull) asymptote with deterministic strength for infinite structure size (horizontal asymptote) f_r^∞ gives the statistical scaling length on D -axis, see Fig. 10.3b). The numerical solution to L_0 is written as:

$$L_0 = D_{stat} \left(\frac{\hat{\sigma}_{stat}}{f_r^\infty} \right)^{m/n} \quad (10.14)$$

so this parameter does not need to be fitted, analytical expression can be used. Note that the large size strength (mean strength $\hat{\sigma}_{stat}$) can be computed by Weibull integral (described in detail e.g. by Bažant and Planas (1998)):

$$P_f = 1 - \exp\left(-\int_V \left\langle \frac{\sigma(\mathbf{x})}{s_0} \right\rangle^m \frac{dV(\mathbf{x})}{V_0}\right) \quad (10.15)$$

where V is the volume (area, length) of the structure depending on dimension (n), s_0 is the Weibull scaling parameter and V_0 is an elementary volume of the material for which the Weibull distribution has parameters m and s_0 . $\sigma(\mathbf{x})$ is maximum principal stress at a point of coordinate vector \mathbf{x} .

One can avoid the computation of nonlocal integral (and determination of load leading to P_f corresponding to the mean load) by means of numerical simulation of Monte Carlo type. In such case we recommend to use the stability postulate of extreme values for discretization of random blocks and their association with scaled PDF. This approach is later shown/used for the numerical example and has been described in detail by Novák et al. (2003a) and is described in the preceding chapter.

5. As all parameters of statistical-energetic formula are determined, nominal strength can be calculated for any size. Using real size of the structure D_t the prediction of corresponding nominal strength $\sigma_{N,t}$ can be done using (10.6). This prediction will be generally different (lower) from initial deterministic prediction, Fig. 10.3c). The larger structure the larger difference is.

The formula will provide us the strength prediction for the mean strength. Additionally, a scatter of strength can be determined just using the fundamental assumption of Weibull distribution.

For the distribution we know two parameters, shape parameter m is prescribed initially, and scale parameters s can be calculated easily from predicted mean and Weibull modulus.

10.5 Numerical example

Case description

In order to show the applicability of the proposed approach to a real structural problem of failure at crack initiation, a very special example of structural failure has been selected. The Malpasset Dam in French Maritime Alps, an arch dam of record-breaking slenderness built in 1954, failed catastrophically on its first complete filling in 1959 (Fig. 10.4), causing a flood which wiped out the town of Fréjus founded by the Romans (e.g. Levy and Salvadori, 1992). The arch angle was 133° and the thickness at the base $D = 6.78$ m. Catastrophic failure of Malpasset dam left 412 people died. The failure started by vertical cracks due to flexural action in the horizontal plane and was attributed to the movement of rock in the left abutment, magnified by a thin clay-filled seam. There can be no dispute that this explanation was correct. The energetic size effect was unknown in 1959 and the Weibull statistical size effect was not yet established for concrete. Bažant and Novák (2000c) already showed, the size effect must have been a significant contributing factor including statistical one. That analysis was based only on simplified judgement of parameters of deterministic-energetic and statistical-energetic formulas without any computational modeling. The case is analyzed here more precisely utilizing the new formula and superimposition procedure described above.

10.5.1 Tool of deterministic NLFEM modeling

For FEM nonlinear fracture mechanics calculations, the commercial software ATENA was used (Cervenka and Pukl, 2003). Suitability of the software for simulation of size effect behavior of concrete structures was reported by Pukl et al. (1992) and by Cervenka and Pukl (1994). ATENA includes several material models for concrete reflecting all the essential features of concrete behavior, namely cracking in tension. It is based on nonlinear damage and failure functions in plane stress state. A smeared crack approach simulates discrete cracks occurring in real concrete structures by strain localization in a continuous displacement field. Objectivity of the finite element solution is assured by crack band approach (Bažant

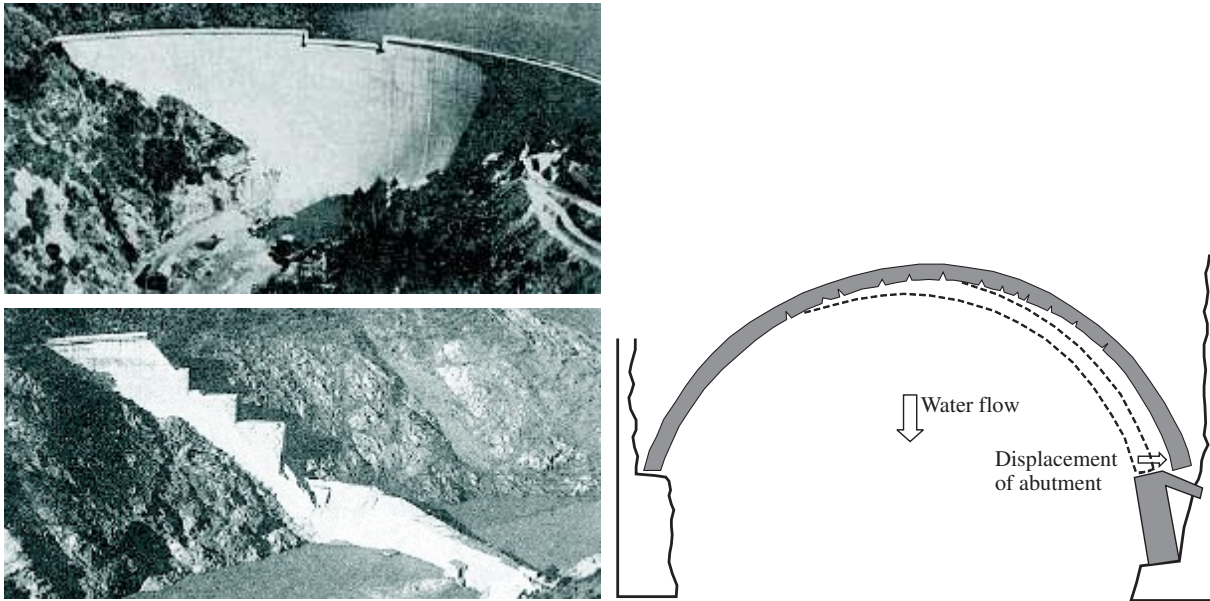


Figure 10.4: Malpasset dam. Left top and bottom: Photos of the dam before and after failure. Figures from internet source <http://www.aude.pref.gouv.fr/ddrm/risque-barr/bar2.html>; Right: Sketch of a dam failure redrawn from Levy and Salvadori (1992). Note that cracks must have been much more localized

and Oh, 1983), which is built in microplane model. Recently also microplane model for concrete in the version of M4 has been implemented into ATENA. Simplified failure modeling of Malpasset dam worked out at 2D level has been performed using ATENA.

10.5.2 Superimposition modeling

A simplified 2D plane strain computational NLFEM model is worked out, one abutment is fixed, second is subjected to movement. This is modelled by prescribed deformation in chord direction. This is a rough assumption as no proper information on direction of rock abutment movement is available. For the simplicity no loading by water is considered, the behavior of dam strip in principle should be approximately similar. We do not account for the continuous clamping of the bottom of the dam to rock. Model of the dam height 1 m is performed. Only 1 meter height of a dam at the bottom is modelled as plain strain problem. The example serves as simplified example, the reality is substituted by very rough 2D computational model.

Microplane model for concrete was selected as the most efficient material constitutive law available in ATENA. The concrete compression strength measured during construction was 32.5 MPa and the same value was used in ATENA microplane model. Based on compression strength other microplane model parameters have been generated/proposed by the software as a default. In particular, the (strength related) parameter called K_1 was set to $1.19 \cdot 10^{-4}$, other parameters were: $K_2 = 500$, $K_3 = 15$ and $K_4 = 150$. The modulus of elasticity $E = 31.3 \text{ GPa}$. We used 21 microplanes and the crack band width of 30 mm has been used. This crack band width was chosen as an estimation and it leads to relatively brittle behavior for the real size dam model (as can be judged from the size of aggregate vs. size of the dam), see Fig. 10.1. As will be shown later, the crack band width of 3 cm resulted in D_b approximately 28 cm (the layer of cracking width – perpendicular to the face of strip).

The real size has been scaled down (ratios $1/2$, $1/5$, $1/10$ and $1/200$ were basic scaling, other sizes were modelled as well) and up (ratios 10 , 100 and 1000). The reaction vs. deformation of abutment (in direction of line connecting the supports) for all sizes of the dam together with crack patterns are shown in Fig. 10.5. Nominal strength σ_N was defined as $\sigma_N = 6M_f/D^2$. The $M_f = Rd$ is the maximum bending moment at failure in the middle of the dam computed as a product of horizontal reaction R in the direction of prescribed deformation and the perpendicular distance d .

The nominal strength for real characteristic size (thickness of the strip) $D = 6.78 \text{ m}$ was computed

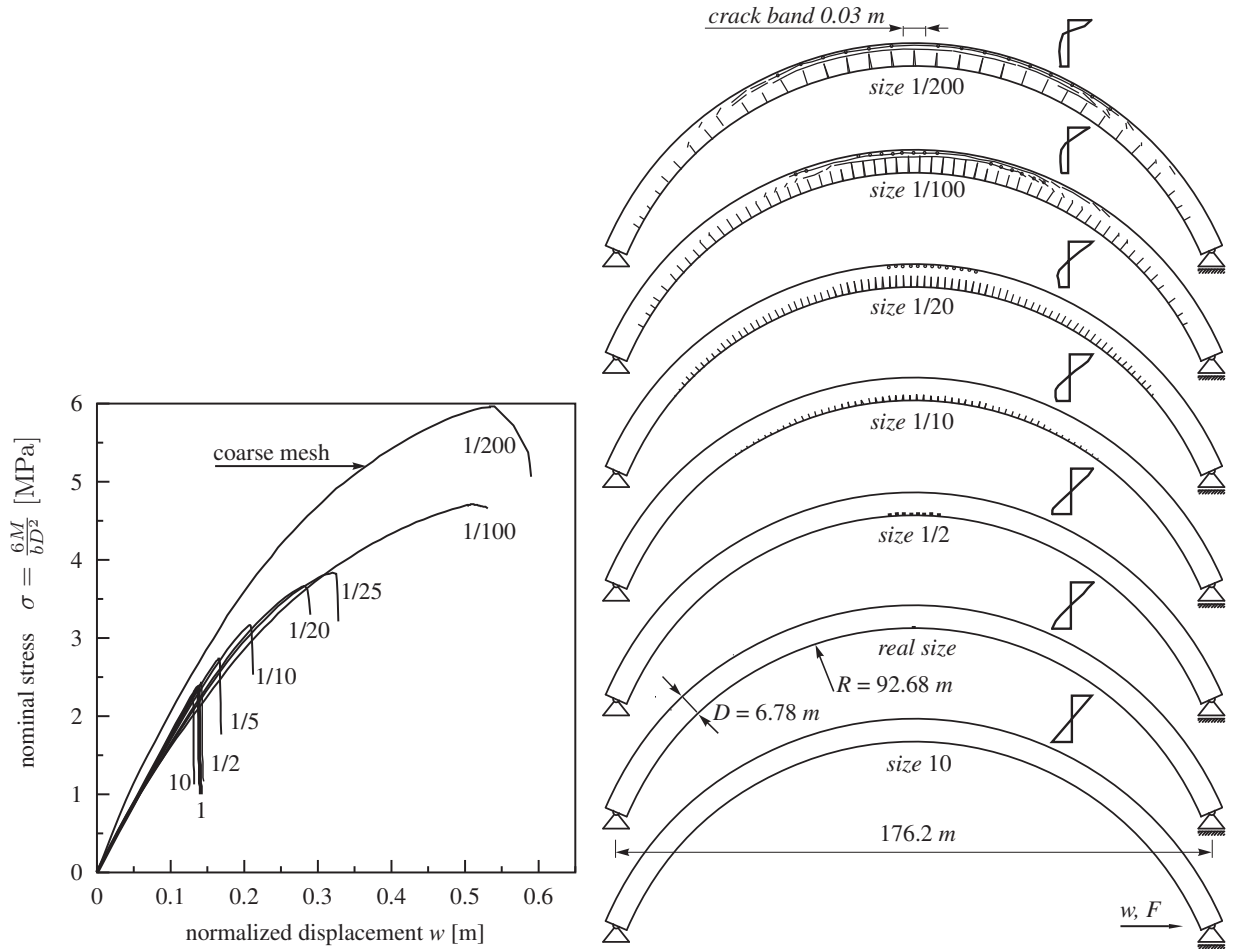


Figure 10.5: Deterministic NLFEM calculation for different virtual sizes of the dam: a) nominal strength vs. normalized displacement; b) Crack patterns

2.35 MPa and for size 10 times larger the nominal strength decreased to 2.25 MPa. When it was virtually scaled up again by ratios 10 and 100, the same value was obtained, it means that horizontal flat large size asymptote of deterministic formula was achieved and we can prescribe $f_r^\infty = 2.25$ MPa. Scaling the real size down (to the minimum thickness of 33.9 mm) nominal strength significantly increased (nearly three times: $\eta_p = 2.9 \Rightarrow l_p = 0.147$ m), Fig. 10.5a).

The range of sizes of “virtual” size effect testing was 1 : 200,000. Figure 10.5b) shows predicted deterministic crack patterns obtained by microplane model with crack band approach for various sizes of Malpasset dam. The distribution of horizontal stresses σ_x in the middle of the span as predicted by the model is also sketched. Both crack patterns and stress distribution are presented for the peak load. Compressive cracks occur during pre-peak for small sizes. Crack band remains constant throughout the range of scaled dams in order to keep objectivity of modeling. It poses a limitation of finite elements for small sizes as coarse mesh leads to too stiff models of smallest and the second smallest size because of rough mesh: crack band model localization crack elements in microplane model.

For optimum fit of deterministic formula (10.13) the stable alternative with two parameters was used. Results are: $D_b = 280$ mm and $r = 1.0$. The best fit of extended formula (10.2) is shown in Fig. 10.1. The fit is very good. However, an attention must be paid to fitting of formula parameters to computational results: if the small structure size computations are not available the fit may result in considerable higher value of r for the simplified formula ($l_p = 0$) compared to the case where a broad/proper range of results is available. The problem is that computed results (points in the graph) in practical small size range may look to have a straight left asymptote (take a look on the numerical results, points are nearly on a line). This may explain very high values of r fitted by Bažant and Novák (2000b); authors used a real

size range and a simpler formula (10.6; $l_p = 0$). We can recommend to estimate the ratio η_p and fit the limited range with the full formula. Of course, practically l_p may than be taken as zero, but the correct r remains to be determined.

Computations of the small size structure with crack band method may lead to practical problems: one must ensure the crack band be smaller than the finite element (band must be embedded) and so we have difficulties to analyze structure smaller than a certain size: the mesh is too coarse. Therefore we suggest to estimate the maximum plastic strength, compute the ratio η_p (Eq. 10.4) and use the extended law for deterministic-energetic size effect (10.2). Comparison of formulas with or without l_p and the influence on r value is given in Fig. 10.1b). The fitted r depends on the range of structural sizes with computed nominal strengths. Example of two erroneous fits of deterministic formula are shown in Fig. 10.1b).

Based on analysis we can conclude, the abutment movement that could have been tolerated in order to prevent the maximum flexural stress multiplied by safety factor from attaining the tensile strength limit must have been correspondingly smaller than that estimated at that time by the investigating committee unaware of size effect.

10.5.3 Statistical size effect and formula verification

The study has been made for three different combinations/pairs of Weibull modulus and statistical length L_0 . The strength/predictivity of the newly derived formula is documented in Fig. 10.5.3 for the three alternatives. These alternatives differ in Weibull modulus m and the ration of length scales L_0 and D_b . Let us remind that targets were to show using a simplified calculation:

- what is the reduction of design strength caused by statistical/probabilistic size effect using estimation by the statistical formula taking into account particular value of Weibull modulus m)
- to show that if the value m is known, one can say that in the range real sizes of the dam the distribution of (random) nominal strength is exactly Weibull and the characteristic strength (5% percentile) and the design strength (1% percentile) can be estimated accurately without sophisticated and time-consuming statistical simulation based on SFEM.

The alternatives in Fig. 10.5.3 shows that the superimposition procedure is feasible.

The question arises how can we check the correctness of new formula in mean sense and also the variability? Recently developed stochastic fracture mechanics tool based on ATENA software and probabilistic simulation software FREET has been utilized for this purpose. The feasibility and outcomes of stochastic fracture analysis using such combination have been recently documented on practical examples of statistical failure simulation and reliability assessment of some existing bridge structures. The software system can consider uncertainties in material model as random variables with prescribed statistical distribution and correlation structure. As the basis of superimposition here was NLFEM ATENA software, utilization of randomized version is a logical step forward to correct numerical verification.

There were two discretization meshes in this stochastic finite element computation: (i) deterministic FEM mesh; (ii) mesh of stochastic blocks (random variables).

Ad. (i) deterministic mesh must be dense enough to capture stress and strain gradients. But on the other hand the width of elements (dimension perpendicular to cracks/principal stresses) must be higher than the crack band width (we use crack band model). The number of elements has been kept for the majority of scaled dam sizes (8 elements per D , squared elements if possible, small sizes got very “long” elements due to the requirement of embedded crack band within finite element). The curved edge has been modelled by circular line.

Ad. (ii) “stochastic mesh” (mesh of random blocks – variables) must be small enough to capture prescribed spatial variability of the strength parameter K_1 . However, this would be hardly possible for large scaled dams: large models would consist of thousands of random variables. Therefore a stability postulate trick has been used leading to reduction of number of random variables. The fundamental principle of the role of stability postulate was given by Bažant (1997, 1998b), direct utilization in practical FEM simulation has been shown by Novák, Bažant, and Vořechovský (2003a) and Lehký and Novák (2002). Since the bending moment is not constant throughout the span (large dams), the discretization of random part had to be relatively dense even if we used the stability postulate of extreme values (we could not use one scaled random variable for the whole span - the stress is not constant).

The random variables (blocks) has been assigned with random strength scaled according to their actual size l (Weibull scaling): mean strength $\mu(l) = \mu(l_0)(l/l_0)^{(1/m)}$, COV= const. given by Weibull modulus m (see Eq. 6.4 p. 63 for two-parameter Weibull PDF).

$$\mu(l_0) = s(l_0)\Gamma(1 + 1/m) \quad (10.16)$$

where l_0 is the reference length at which the mean (strength) is $\mu(l_0)$ (mean of the random strength field) and the shape parameter of the Weibull distribution is $s(l_0)$. We have chosen the reference length l_0 to be the autocorrelation length l_ρ . Therefore for large sizes we actually model the (minima of) Weibull strength random field with the mean value $\mu(l_0)$ and autocorrelation length l_ρ because the minima of random process converge to minima of IID for large lengths (see Vořechovský and Chudoba (2004a) for details and numerical study).

The exception to the scaling has been made for random elements (variables) smaller than l_0 . For those the mean strength has been used ($\mu(l_0)$) supported by the argument that the real random strength field is spatially correlated (the autocorrelation) and the mean value of strength cannot exceed a certain limit (the mean value of the random field $\mu(l_0)$).

Statistical simulation could capture size effect curve in mean sense and also the scatter represented by the whole cumulative probability distributions, right part of Fig. 10.5.3. Both position (mean strength) and slope (representing variability) is captured well. Note that neither the mean size effect curve nor the distribution are the best fits!!! Some discrepancies appeared, but they can be attributed to numerical obstacles of nonlinear fracture mechanics calculation and probabilistic simulation LHS (tail sensitivity).

The following table 1 shows the strength reduction (compared to the deterministic value obtained by NLFEM simulation) due to the statistical size effect for increasing value of Weibull modulus m .

Table 10.1: Reduction of nominal strength of a real size dam. Shows the difference between NLFEM prediction and Stochastic NLFEM. First column represents reduction percentage factor (a factor by which the deterministically calculated strength must be multiplied to predict the statistical-energetic size effect strength)

Weibull modulus m	COV [*100 %]	strength reduction factor due to statistical size effect	percentage difference [%]
10	12.0%	54%	-46%
12	10.1%	60%	-40%
18	6.9%	71%	-29%
24	5.2%	77%	-23%
30	4.2%	81%	-19%
40	3.2%	85%	-15%

We predict the mean nominal strength by the formula and the whole distribution can be considered Weibull (whose parameters are known!!)

10.6 Concluding remarks

The chapter clarifies the *interplay of deterministic and statistical length scales* of quasibrittle structures and proposes/derives an analytical formula for the nominal mean strength prediction of crack initiation problems.

The paper suggest a practical procedure of superimposition of deterministic and statistical size effect at crack initiation. It requires only a few FEM analysis using scaled sizes. The prediction can be done without any special Monte Carlo simulation, which is usually used to deal with influence of uncertainties on structural strength.

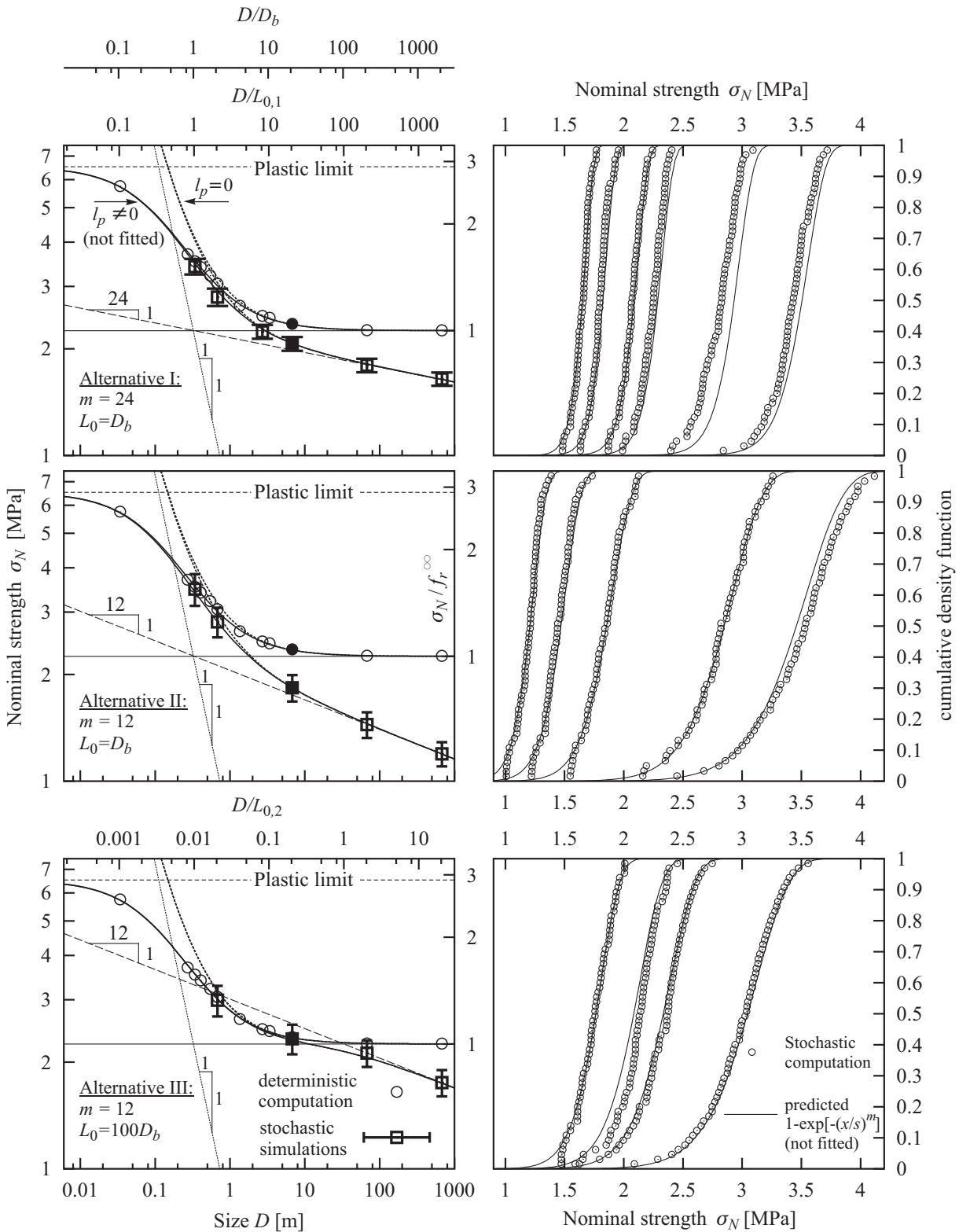


Figure 10.6: Comparison of three stochastic alternatives and deterministic results. Left: Mean value \pm standard deviation as predicted by stochastic simulations and comparison with the prediction by the new law (not fitted!). Right: comparison of the whole distribution predicted by the model and stochastic simulations (64 simulations). Curves are not fitted (m known)

Chapter 11

Overall conclusions and recommendations for future research

The conclusions, main contributions and possible future work directions in four main areas of the thesis are summarized in the following text.

Simulation of random variables and reliability techniques

The new achievement is mainly the new efficient technique of imposing the statistical correlation based on Simulated Annealing. The technique is robust, efficient and very fast and has many advantages in comparison with former techniques. The increased efficiency of small-sample simulation technique LHS can also be achieved by the proper selection of samples representing the layered probability content of random variables. The methods are implemented by author and constitutes the computation core of the multipurpose software package FREET for statistical, sensitivity and reliability analysis of computational problems (appendix A).

A future work is recommended in:

- Implementation of advanced method for probabilistic analysis, in particular response surface, FORM and Importance Sampling;
- Further research in simulation of random vectors with prescribed simultaneous probability density function or just marginals and covariances.

Development and testing of random fields simulation

The superior efficiency of LHS and correlation control is confirmed in the context of sample simulation of random fields. An attempt has been done to show better the role of correlation control – diminishing spurious correlation in random field simulation and importance of sampling schemes for simulation of uncorrelated random variables. It has been shown that a spurious correlation influences significantly the scatter of estimated autocorrelation function of simulated random fields. A clear indication of this scatter is the fulfillment of norms used as objective functions in Simulated Annealing algorithm to diminish spurious correlation at the level of underlying random variables.

The quality of simulated samples of random fields should be assessed. An error assessment procedure has been proposed and performed for six alternatives of sampling schemes. Diminishing spurious correlation does not influence the capturing of these statistics but does influence significantly a realization of autocorrelation function of a random field.

A future work is recommended in:

- Study, development and implementation of simulation of non-Gaussian stochastic fields;

- The newly developed tools of stochastic computational mechanics in the form of stochastic finite element method (SFEM) will now enable complex numerical investigations. We expect both (i) verification of newly achieved theoretical results (e.g. in the form of the proposed size effect law for quasibrittle failure at crack initiation) and (ii) numerical computations of real examples focused on the influence of nonlinearities on failure probability estimations.

Analysis of sources of randomness and size effect on strength of yarns for textile reinforced concrete

Deterministic micromechanical computational model has been developed and used for identification and study of sources of randomness affecting the evolution of the stiffness during the loading of yarns in tension. It has been shown that the stiffness evolution in the early stages of loading influences the maximum tensile force in the bundle. The model serves as a basis for a complex stochastic analysis of the complex size effects including all mentioned effects employing the random field simulation technique. Such stochastic modeling framework has been used for derivation of *new size effect laws* for each of the considered sources of randomness separately. Based on the lessons learned from the numerical analysis we have suggested approximation formulas describing the size effect laws due to the random strength or stiffness along the bundle. The obtained results have been verified with the help of the available analytical and numerical fiber bundle models by Smith and Daniels. However, the available fiber bundle models could not be used for modeling the response measured in the yarn tensile test, because they impose practically unachievable assumptions of regular force transmission in the clamping and do not capture the disorder in the structure of filaments in the bundle.

The performed stochastic simulations with the available experimental data revealed the *existence of statistical length scale* that could be captured by introducing an autocorrelation of random material properties. This represents the departure from the classical Weibull-based models that are lacking any kind of length-scale.

A future work is recommended in the following areas:

- The introduced model delivers a quasi-ductile response of the bundle from the ensemble of interacting linear-elastic brittle components with irregular properties. In this respect the present approach falls into the category of lattice models used to model quasi-brittle behavior of concrete. It should be noted, that due to the possibility to trace the failure process in a detailed way both in the experiment and in the simulation, the modeling of multi-filament yarns provides a unique opportunity to study the local effects in quasi-brittle materials. The possibility to generalize the results for other quasi-brittle materials is worth further intensive studies;
- The obtained statistical material characteristics turned out to be of crucial importance for robust modeling of crack bridges occurring in the cementitious textile composites. The “well designed” microstructure of the yarn and of the bond layer in the crack bridge may significantly increase the overall deformation capacity (ductility) of structural elements. The lessons learned from the present study will be applied in a more targeted development of new yarn and textile structures with an improved performance of crack bridges. Development of micromechanical model of bond behavior and its coupling with the developed models will be pursued next.

Combined energetic and statistical size effect of quasibrittle materials

We have presented a broader theoretical treatment of connections between fiber bundle models and size effect of concrete structures. It has been shown how the statistical size effect at fracture initiation can be captured by a stochastic finite element code based on extreme value statistics, simulation of the random field of material properties, and chain of bundles transition. The computer simulations of the statistical size effect in 1D based on *stability postulate of extreme value distributions* match the test data. However, in some cases the correct behavior cannot be achieved for other tests using a 1D treatment. A proper way of treating the stress redistribution is by the proposed macro-elements in 2D (or 3D), the scaling of which is based on the fiber bundle model capturing partial load-sharing and ductility in the finite element system.

A simple and effective strategy for capturing the statistical size effect using stochastic finite element methods is developed which overcomes the problematic feature of stochastic finite element method: How

to capture the statistical size effect for structures of *very large sizes*. The idea is to emulate the recursive stability property from which the Weibull extreme value distribution is derived. Using the combination of a well feasible type of Monte Carlo simulation and computational modeling of nonlinear fracture mechanics, a probabilistic treatment of complex fracture mechanics problems is rendered possible. The approach may be understood as a computational trick based on extreme value theory similar to its counterpart in deterministic nonlinear analysis of fracture – crack band model.

The *interplay of deterministic and statistical length scales* of quasibrittle structures has been clarified and the *analytical formula* for the nominal mean strength prediction of crack initiation problems has been derived and proposed. The law features two separate scaling lengths of structures governing two different sources of size effect: deterministic and statistical. The role of these two lengths in the transition from energetic to statistical size effect of Weibull type is explained.

A practical procedure of superimposition of the deterministic and statistical size effects at crack initiation has been suggested. It requires only a few NLFEM analysis using scaled sizes so the necessity of time consuming statistical simulation is avoided. The prediction can be done without any special Monte Carlo simulation, which is usually used to deal with the influence of uncertainties on structural strength. The efficiency of the procedure is demonstrated on the numerical example of Malpasset dam failure reinterpretation.

A future work is recommended in the following areas:

- Study of nonlocal continuum is needed for its extension to probabilistic nonlocal continuum model. Numerical studies are needed with strain and stress fields entering the Weibull integral for failure probability which were computed by an efficient material model and NLFEM code;
- The role of other fracture mechanics parameters besides the tensile strength should be clarified in the Weibull-type formulation;
- The statistical distribution of the first eigenvalue of the tangential stiffness matrix of the structure becoming non-positive (a criterion of failure, in the case of load control) should be explored in the context of several alternatives of SFEM;
- Comparisons with results obtained by discrete lattice models. Questions about the dependence and/or interaction of deterministic and statistical length scales in the context of this class of models;
- Study and development of the mean universal size effect law and the whole distribution of nominal strength covering the transition from crack initiation problems to notched specimens will be pursued next.

Appendix A

Software FREET

Based on papers: Novák, Vořechovský, Rusina, Lehký, Teplý, and Keršner (2002d); Novák, Teplý, Keršner, and Vořechovský (2004)

A.1 Introduction

The aim of this chapter is to describe a multi-purpose probabilistic software for statistical, sensitivity and reliability analyzes of engineering problems FREET (Novák, Vořechovský, Rusina, Lehký, Teplý, and Keršner, 2002d; Novák, Teplý, Keršner, and Vořechovský, 2004). The software is based on efficient reliability techniques described above (chapters 3 and 2) and the computational core is implemented by the author in C++ programming language. The GUI (graphical user interface) is being implemented by Dr. Rusina in C++. The software is designed in the form suitable for relatively easy assessment of any user-defined computational problem written in C++, FORTRAN or any other programming languages. The approach is general and can be applied for basic statistical analysis of computationally intensive problems. The basic aim of statistical analysis is to obtain the estimation of the structural response statistics (failure load, deflections, cracks, stresses, etc.). All steps will be illustrated using particular windows of the software.

The software is based on “randomization” of a particular problem in the sense of Monte Carlo simulation using small-sample Monte Carlo simulation technique LHS (McKay et al., 1979; Ayyub and Lai, 1989; Novák et al., 1998). Random variables are randomly generated under their probability distribution functions, statistical correlation among them is imposed by the optimization technique called Simulated Annealing, (Vořechovský and Novák, 2002, 2003b; Vořechovský et al., 2002a). Consequently, the analyzed problem is repeatedly solved and statistical characteristics of structural response can be obtained and assessed. The results of such statistical simulation are basically statistical characteristics of structural response (eg. ultimate capacity, stress, deflection, crack width, etc.). Additionally, sensitivity analysis can be performed based on non-parametric rank-order statistical correlation. Reliability analysis is suggested based on simplified approach - curve fitting enabling estimation of theoretical failure probability and/or reliability index. This technique appeared to be very robust.

The software is designed in the form suitable for relatively easy probabilistic assessment of any user-defined problem. The name of the software reflects this strategy – FREET is the acronym for **F**easible **R**eliability **E**ngineering **T**ool. FREET can be utilized in two versions – as “stand alone” multipurpose program for any user-defined problem (M-version) and as module integrated with ATENA (A-version). FREET is now developed in two versions: the first version FREET–M - the analyzed response or limit state function is defined completely outside as a subroutine written in C++ or FORTRAN programming languages (a particular problem may be implemented into FREET as DLL unit). This concept allows to work with complicated problems which have already been tested deterministically at the level of programming languages. In the second version FREET–A - the ATENA computational model of nonlinear fracture mechanics for concrete is fully integrated. The main aim of this text is to describe how to efficiently utilize software FREET with all details and possibilities provided by the graphic user interface.

The second aim is to demonstrate the feasibility of the approach to analyze nonlinear fracture mechanics computational models (developed particularly with the commercial FEM software package ATENA: advanced nonlinear fracture mechanics code to which the FREET software was integrated). The integration is controlled by SARA Studio software [Cervenka and Pukl \(2004\)](#). Full understanding of the concept of this integration is beyond the framework of this text. The user of A-version of FREET should get next information support from ATENA and SARA documentation.

This probabilistic software has been recently successfully integrated with an advanced nonlinear fracture mechanics solution of concrete structures - the finite element program ATENA ([Cervenka and Pukl, 2003](#); [Vořechovský and Červenka, 2002](#)). The modeling of uncertainties by random fields (chapter 4) is under development by the author ([Vořechovský and Novák, 2003a](#); [Vořechovský, 2004b](#)) using efficient simulation techniques (e.g. [Yamazaki and Shinozuka, 1990](#); [Zhang and Ellingwood, 1994, 1995](#); [Novák et al., 2000](#); [Olsson and Sandberg, 2002](#), and many others).

FREET software has been applied recently for the probabilistic analysis of problems from both the industrial and academic fields. Due to the limited space and the focus of this thesis no applications are presented except specialized *size effect studies*. We only mention that the approach has been already shown, e.g., on the modulus of rupture size effect problem ([Novák, Vořechovský, Pukl, and Červenka, 2001](#)), reliability analysis of concrete bridge ([Pukl et al., 2003b](#)).

The FREET software integrated with the ATENA software were used to capture both the statistical and deterministic size effect obtained from experiments. Probabilistic treatment of nonlinear fracture mechanics in the sense of extreme value statistics has been recently applied for two crack initiation problems which exhibits Weibull-type the statistical size effect: four point bending plane concrete beams due to bending span, ([Novák et al., 2003a](#)). This work (and many other applications) are presented in the final Part III of the dissertation.

A.2 Main program tree

Main program tree is located in the left field of the program window. It represents main features – key entries of the program guide the user when using the program. There are three basic user’s dialog parts in present version of software FREET, see Fig. A.1.

1. STOCHASTIC MODEL
 - Random Variables
 - Statistical Correlation
2. LATIN HYPERCUBE SAMPLING
 - General Data
 - Check Samples
 - Model Analysis
3. SIMULATION RESULTS ASSESSMENT
 - Histograms
 - LSF Definition
 - Sensitivity Analysis
 - Reliability

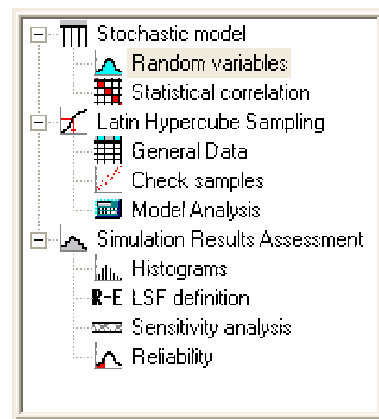


Figure A.1: Main program tree

A.3 Stochastic model

A.3.1 Random variables

The window “Random Variables”, Fig. A.2, allows the user-friendly input of basic random variables of analyzed problem. Uncertainties are modeled as random variables described by their probability

density functions (PDF). Every random variable has its name and is described by theoretical probability distribution and statistical characteristics, statistical parameters or by combination of characteristics and parameters – button “Descriptors”. The user can select from the set of 20 selected theoretical models like normal, lognormal, Weibull, rectangular, etc. The current list of distributions implemented by the author is summarized at the end of this chapter, section A.9 The model is selected from the list of distributions which will appear when clicking on “Distribution”, see Fig. A.3. Random variables should be basically described by statistical characteristics (statistical moments): Mean value, standard deviation (or coefficient of variation) and coefficient of skewness, respectively. Standard deviation or coefficient of variation is recalculated automatically with respect to mean value when entering the value. Statistical characteristics or statistical parameters or combination of characteristics and parameters are used to describe distribution. Parameters symbols are unique for each distribution and the meaning of parameters is explained fully in section A.9. In order to furnish user with others possible ways to describe random variables, the three sets of descriptors are available. The first option is a set of statistical moments (in number of degrees of freedom). The second option of through parameters of distribution. Since sometimes a mixed information is available (some of parameters and some moments), the third possibility enables to input the most usual combination of the descriptors. This is possible through the complex library of distribution functions written by the author in fully object setting and with utilization of virtual (abstract) classes. There is additional option for calculation at the level of selected PDF model based on the design of library: “Distribution support calculation” button allows cross-recalculation of moments, parameters and their combination, probabilities, percentiles, etc., see Fig. A.5.

Random variable can be described also by raw data here – select “User-defined distribution”, Fig A.4. In this case the name of input text file with statistical set arranged in columns or rows is required or data can be directly written into the edit box. The shape of probability distribution of particular random variable is shown in main graphical window, checkbox “Drawing” serves for selection of probability distribution (PDF) or cumulative probability distribution (CDF) windows.

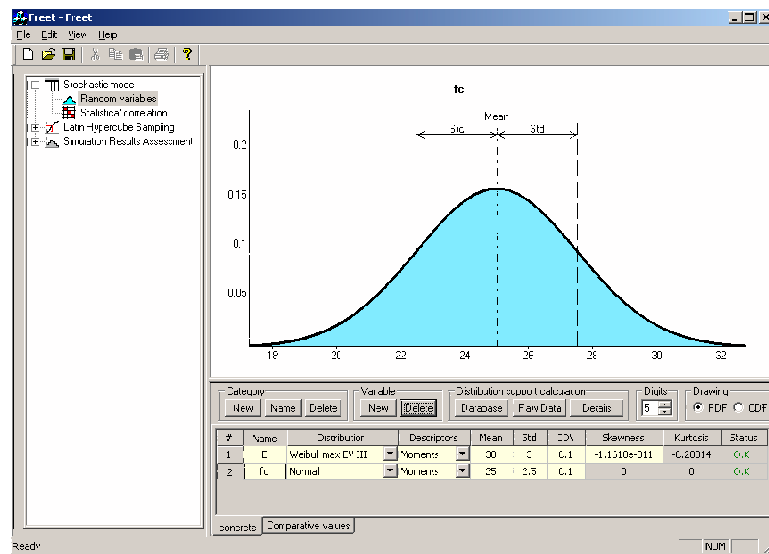


Figure A.2: Probability distribution window – PDF

Random variables can be divided into several categories (see bottom of the window). User can select a new category and within a selected category a new variable. This option is included in order to make handling of large number of random variables more transparent.

The category “Comparative values” is always included in window and can be used in the limit state function definition. But this category is not always utilized: in case we analyze only a response function or all variables of limit state function is defined using DLL function (section A.4.1). Briefly, a user-supplied dynamically linked library gives the user absolute freedom in the type of problem to be solved. User simply writes his own algorithm and link it independently of FREET program.

M-version: Basic random variables related to response/limit state function should be defined in

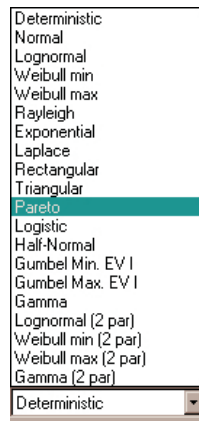


Figure A.3: Combo box for selection of PDF

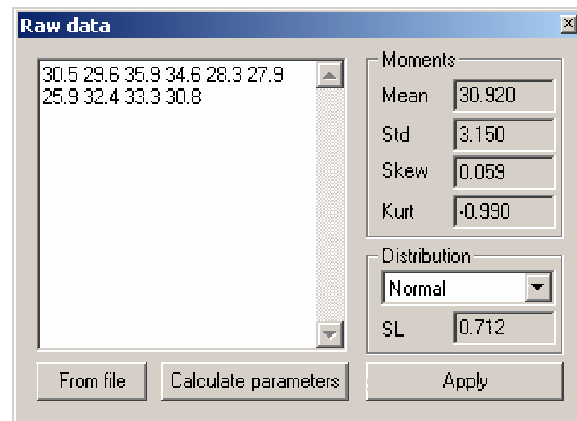


Figure A.4: User-defined distribution (Raw data)

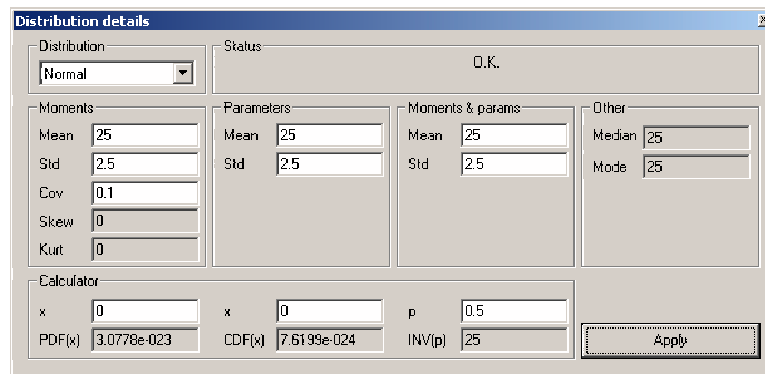


Figure A.5: Distribution support calculation

increasing order – Category 1 – Variable 1, 2, ..., etc., Category 2 – Variable 1, 2, ..., etc., Category 3 ..., etc. This order must correspond with a vector of random variables defined in special DLL unit written in C++, FORTRAN or other programming languages. The structure of a special DLL unit of M-version is described in section A.4.1.

A-version: Input parameters of ATENA deterministic computational model (decided to be randomized in ATENA) are transferred into FREET (with their name and deterministic value). Groups in FREET are equivalent to numbers of materials defined in ATENA. Additional random variables can be defined by “New variable” button to form limit state function in the category “Comparative values”. This is necessary if reliability analysis is planned – ATENA provides response function (maximum capacity corresponding to peak load, deflection or crack width) and these quantities should be “compared” (with load, maximum allowable deflection or maximum crack width) in order to form limit state function.

In order to support the input of statistical characteristics the possibility to work with user-defined database was worked out. This is fully described in the FREET program documentation (Novák et al., 2002d).

A.3.2 Statistical correlation

The window “Statistical Correlation” serves for the input of statistical correlation among random variables described by correlation matrix, see Fig. A.6 or table 3.1, page 21. The user can work at the level of subset of correlation matrices (each group of random variables has its own submatrix of correlation coefficients) or at the global level (all random variables resulting to a large correlation matrix – “All variables”). Statistical correlation among the variables is imposed using simulated annealing algorithm (or by other methods) in subsequent step. The correlation is illustrated graphically during interactive input: the active item is highlighted in an upper window (Fig. A.6), the positive definiteness is checked. Note,

that the simulated annealing applied consequently does not require this strong requirement (theoretically described in Part 3, section 3.4.2). Since the knowledge on full correlation structure is usually very poor (and the user can face problems to input a correlation matrix which is positive definite) this feature can be considered to be an advantage from such practical point of view.

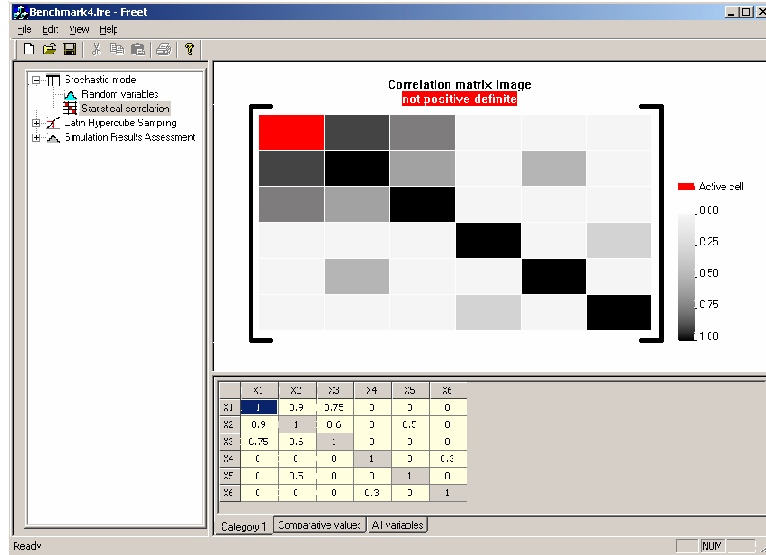


Figure A.6: Window Statistical Correlation

The result of this step is the defined set of input parameters for computational model – the random vector consisting of input variables.

A.4 Response or limit state function definition

A.4.1 FREET M-version

The analyzed response/limit state function is defined completely outside as subroutine written in C++, FORTRAN or other programming languages. This subroutine has to be compiled into DLL. The structure of an DLL program unit should follow prescribed convention. We provide here self-explanatory example for simple function

$$G(\mathbf{X}) = \sum_i X_i \quad (\text{A.1})$$

Program units in C++ and FORTRAN are shown in figs. A.7 and A.8 respectively. Note the difference in indexing: $X_1=\text{input}[0]$, $X_2=\text{input}[1]$, $X_3=\text{input}[2]$, etc. in C++ and $X_1=\text{input}(1)$, $X_2=\text{input}(2)$, $X_3=\text{input}(3)$, etc. in FORTRAN. Note, that the number of random variables in DLL function must correspond with number of random variables defined in “Stochastic model”. This is fully the responsibility of an user, FREET cannot check this fundamental requirement.

A.4.2 FREET A-version

ATENA computational model of nonlinear fracture mechanics for concrete is integrated fully using specially developed software environment called SARA Studio developed by Červenka Consulting company in Prague. It enables communication between FREET and ATENA software. SARA Studio is described fully in different documentation, here only basic concept is outlined.

Response variable is selected at the level of ATENA deterministic model. It is associated with definition of monitoring points and assigned quantities. Response function represents ATENA computational modeling — response is a quantity at monitoring point. Typically it is a peak load of load deflection

```
#include "math.h"

_declspec(dllexport) double __stdcall XlimitC(int *num,double *input){
    double ret=0;

    //Calculates sum of the values
    for(int i=0;i<*num;i++)ret+=input[i];
    return ret;
}
```

Figure A.7: The structure of external program unit in C++

```
real*8 function XlimitF(num,input)
    !DEC$ ATTRIBUTES DLLEXPORT::XlimitF
    integer*4 num,i
    real*8 input(*)

    ! Calculates sum of the values
    do i=1,num
        XlimitF=XlimitF+input(i)
    enddo

end function XlimitF
```

Figure A.8: The structure of external program unit in FORTRAN

diagram or maximum deflection or maximum crack width. Variables at monitoring points represent responses and they are transferred into FREET software.

Response variables from ATENA can be evaluated statistically in part “Simulation results assessment” including sensitivity analysis. For reliability analysis, these response variables have to be combined with additionally defined comparative values defined as additional variables in “Stochastic model”. Number of values associated with monitoring points can be combined with number of comparative values. It enables definition of limit state functions representing ultimate and serviceability limit states. This combination is described in details in section A.6.

A.5 Sampling

A.5.1 General data

Latin hypercube samples are prepared first, samples are reordered by simulated annealing approach (or any other approach, section 3.2 and 3.3) in order to match required correlation matrix as close as possible, see Fig. A.9 or 3.6. Basic parameter — number of simulations of LHS is on input here. Random input parameters are generated according to their PDF using Monte Carlo type simulation and generated realizations of random parameters are used as inputs for analyzed function (computational model). The solution is performed repeatedly and results (structural responses) are saved. Three alternatives of sampling scheme can be selected (sampling type): LHS – probabilistic means (preferable alternative), LHS – probabilistic median or crude Monte Carlo. For the information about sampling alternatives see section 3.2.

Simulated annealing (sec. 3.3, p. 26) is used as the most universal and robust technique to impose statistical correlation. A heuristic time prediction is included; the estimation is rough and the real time needed for correlation treatment may differ. Parameters of simulated annealing are estimated as suitable defaults however, user can change them. The process of the imposing of statistical correlation can be stopped using the button “Stop Sampling”. The window with information about the achieved accuracy

(deviations of elements in correlation matrix is controlled – desired and obtained) is displayed after simulated annealing process, see Fig. A.10.

The result of this step is the table of random realization of random variables which exhibits statistical correlation as close as possible to prescribed correlation matrix. Note, that in case of very small number of simulations (e.g. tens), imposition of prescribed correlation is difficult and maximum deviation in “Reached correlation” window can be high.

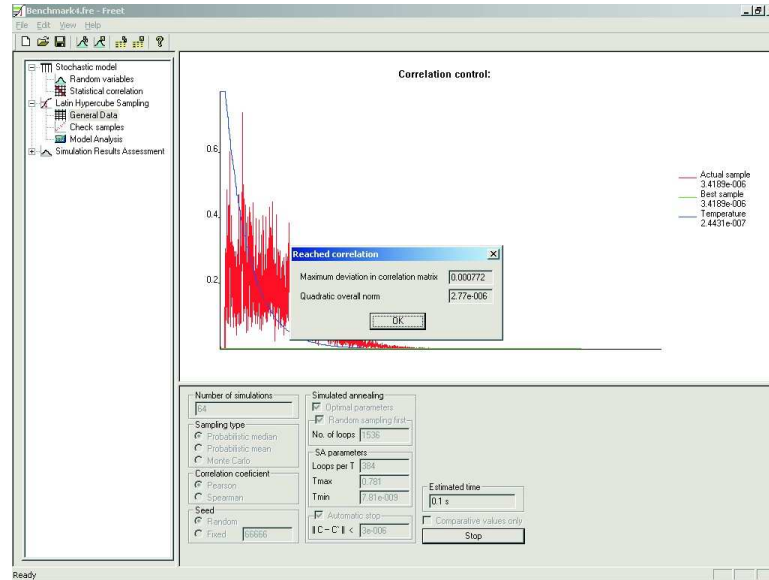


Figure A.9: Imposing of statistical correlation, see figure 3.6

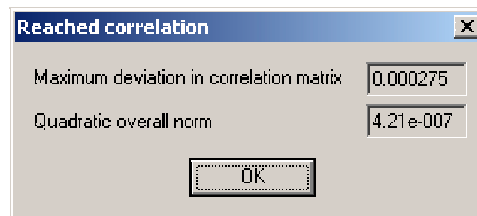


Figure A.10: Information about the achieved accuracy

A.5.2 Check of the samples

The aim of this entry is to have the possibility to check the results of sampling scheme applied to random variables before running repetitive calculation. Achieved correlation matrix, after simulated annealing is visualized in lower triangular part of correlation matrix, upper triangle contains desired correlation. If user clicks on diagonal, upper part window will show associated sampled variable, see Fig. A.11. If an user’s click is targeted to correlation coefficient out of diagonal, the image of sampled values is shown where correlation is clearly visible, figure A.12 or figures 3.2 and 3.3 (pp. 24–25).

A.5.3 Model analysis

Repetitive calculations of response/limit state functions is started when the user activates this button. The process is monitored and after all random simulations are completed the results are transferred back into FREET software.

M-version: Analyzed user-defined function defined in the DLL function unit is repeatedly solved. FREET will require to input name of DLL function which contains response/limit state function as is

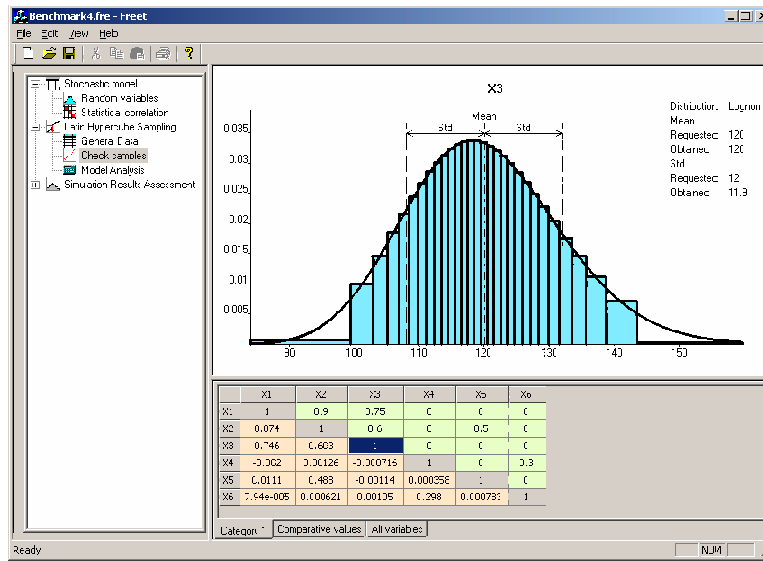


Figure A.11: Window “Check samples” – sampled marginal variable

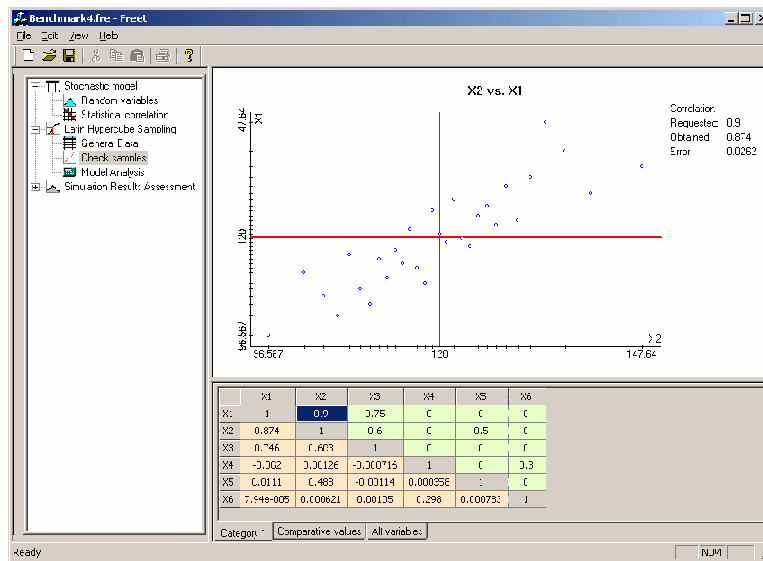


Figure A.12: Window “Check samples” – sampled pair of variables (correlation check)

described in section A.4.1. The user has to use double-click on “New Model Function” definition. The name of internal functions programmed in DLL function is indicated on the screen (Exported functions), see Fig. A.13. Button “Run Model Analysis” starts the real simulation process.

Note, that not only one DLL function can be defined here. FREET allows to define several functions here and in consequent step – simulation – treat them simultaneously. Every function will use the same set of randomly generated parameters. The user should take into account the overall time of whole simulation in case of computationally demanding response/limit state functions.

A-version: All solutions of nonlinear fracture mechanics analysis with randomized inputs are performed via SARA Studio environment and output files of ATENA outputs are saved. Responses associated with monitoring points are transferred into FREET after ending simulation process.

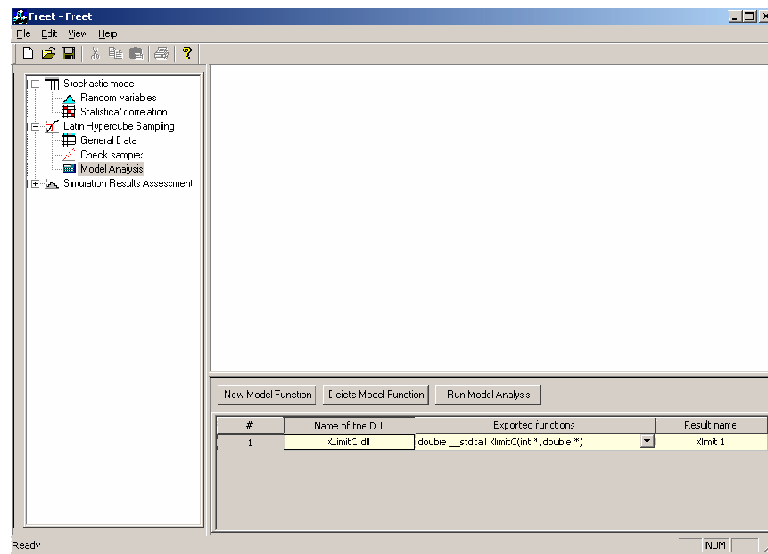


Figure A.13: Input of DLL function window

A.6 Simulation results assessment

A.6.1 Histograms

After simulation process successfully finishes, the resulting set of structural responses can be statistically evaluated. The results are: histogram, mean value, variance, coefficient of skewness and empirical probability density function of structural response. This basic statistical assessment is visualized through the window Histograms, see Fig. A.14. Theoretical models of PDF are treated using a standard Kolmogorov-Smirnov test in order to describe the most suitable models from the group of available models. The most suitable model (with the highest significance level) is listed at the top.

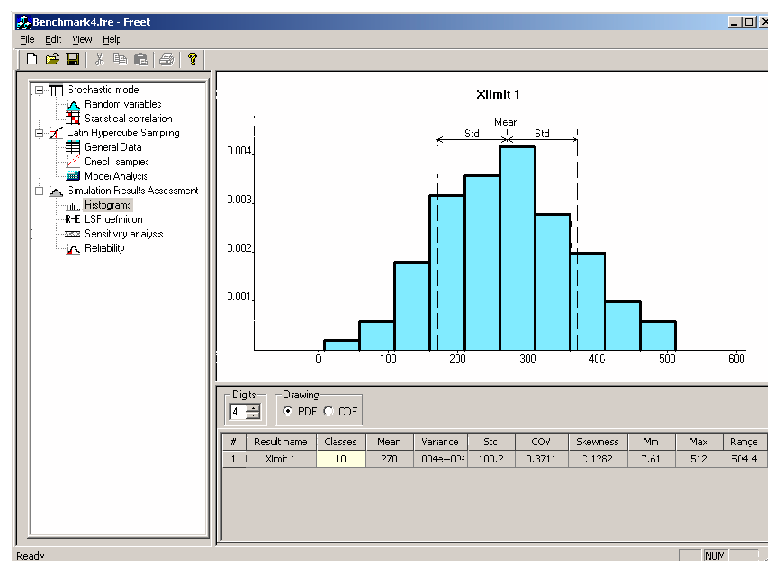


Figure A.14: Basic statistical assessment – histogram and statistical characteristics

A.6.2 Limit state function definition

The window is designed for the definition of a limit state function by combination of response variable obtained via simulation and comparative values. Usual type of combination is in the form (see Fig. 2.1, page 10)

$$Z = R - E \quad (\text{A.2})$$

where R is a response and E action of loading (carrying capacity limit state).

For serviceability limit state the form is just opposite (comparative value – response, e.g. allowable maximum deflection – real deflection).

The concept of all possibilities of combinations of response monitor variables and comparative values using basic algebraic operations (+, –, /) to define any basic form. Standard pictures of PDF of R and E are illustratively shown including safety margin Z , see Fig. A.15.

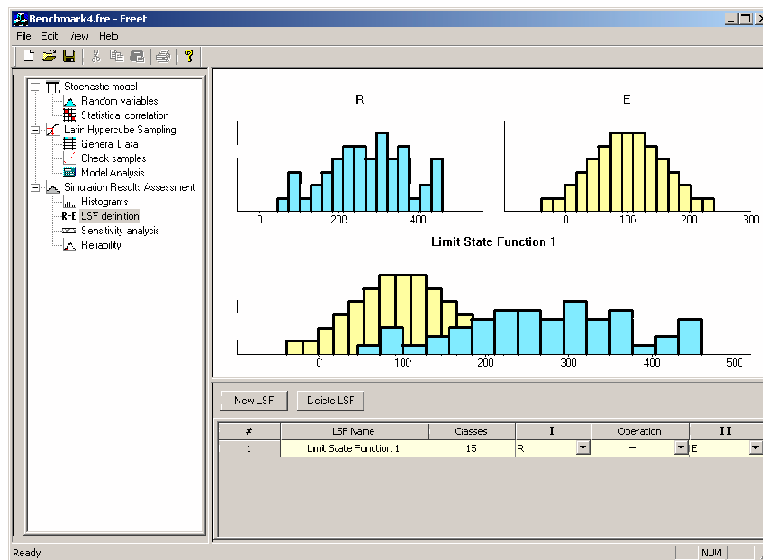


Figure A.15: Response R , action of loading E , safety margin $Z = R - E$

A.6.3 Sensitivity analysis

The window “Sensitivity analysis” shows the importance of random variables. Nonparametric rank-order correlation coefficients are calculated between all random input variables and response variables. Positive and negative sensitivity is shown in separate columns. There are two ways of graphical representation – cartesian and parallel coordinates representations. Parallel coordinate representation provides an insight into analyzed problem. Random variables are ordered with respect of the sensitivity expressed by nonparametric rank-order correlation coefficient. Positive and negative sensitivity is shown in Fig. A.16 and in Fig. A.17 (parallel coordinates) and in Fig. A.18 and Fig. A.19 (cartesian coordinates).

Note 1: When the user assess this relative measure of sensitivity it is necessary to take into account the signs of input random variables considered in Stochastic model. Therefore an option to change the sign of variable (x^{-1}) is included here.

Note 2: “What-if-study” known as deterministic sensitivity analysis can be done easily by FREET. To study absolute influence of a specific, we can consider it as random variable with rectangular distribution (other variables are deterministic). Sensitivity window in cartesian coordinates will provide just functional relationship between variables, varying between upper and lower limits of rectangular distribution, and response variable, see Fig. A.20.

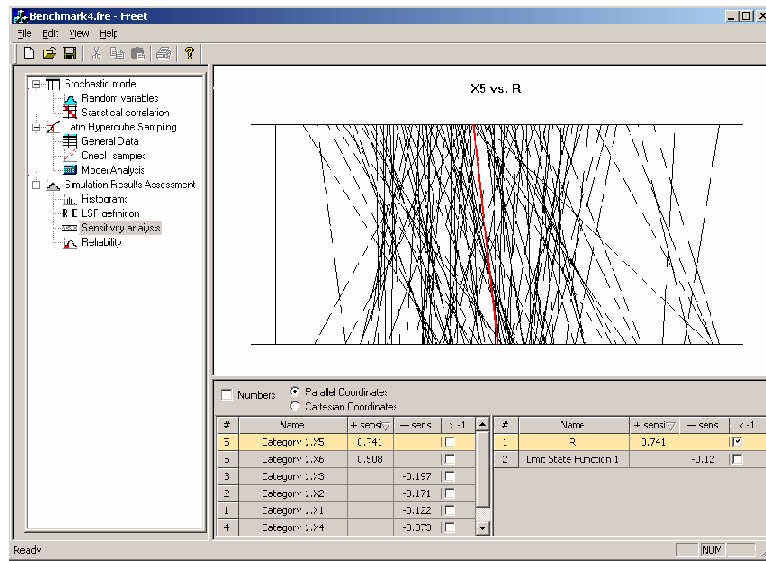


Figure A.16: Window Sensitivity Analysis – positive sensitivity (parallel coordinates)

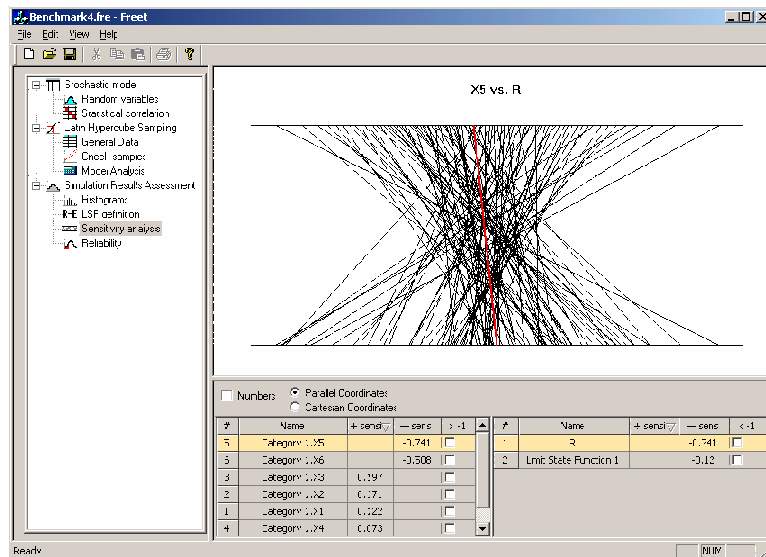


Figure A.17: Window Sensitivity Analysis – negative sensitivity (parallel coordinates)

A.6.4 Reliability analysis

Histogram of safety margin as specified in limit state function definition is visualized. The aim of this window is to provide an estimation of theoretical failure probability (and reliability index respectively).

Following alternatives are implemented:

- Cornell’s reliability index and corresponding failure probability based on normal probability distribution for safety margin;
- failure probability estimation based on the selection of the most suitable theoretical model for PDF of safety margin (curve fitting approach);
- calculation of failure probability based on classical frequency definition of probability, N_f/N_{Sim} , where N_f is number of realizations resulting in a failure (negative limit state function) and N_{Sim} is total number of simulations. Note, that this alternative can be used only for very large number of

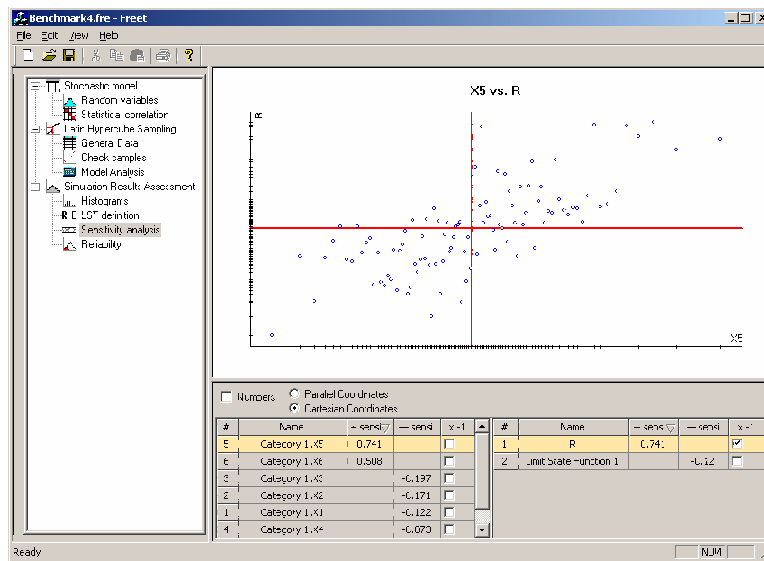


Figure A.18: Window Sensitivity Analysis – positive sensitivity (cartesian coordinates)

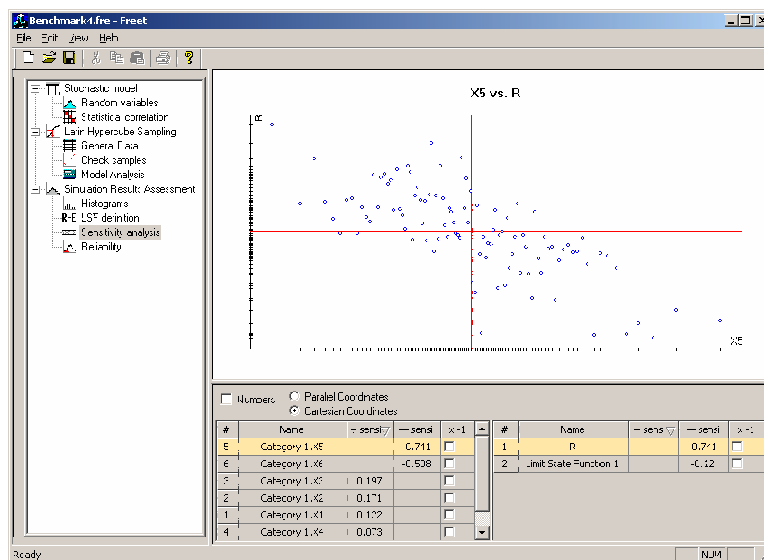


Figure A.19: Window Sensitivity Analysis – negative sensitivity (cartesian coordinates)

simulations estimating high failure probabilities. Software FREET is generally designed for small numbers of simulations, this classical Monte Carlo based estimation of failure probability is included here only for reference studies.

A.7 Software ATENA

The non-linear finite element program ATENA was designed for realistic numerical simulation of behavior, damage and failure of concrete and reinforced concrete structures (Margoldová et al., 1998). ATENA is able to reflect all the essential features of concrete behavior in tension as well as in compression, including non-linear fracture mechanics. It employs advanced material models and efficient solution strategies, tools for FE discretization etc. (Cervenka and Pukl, 2003). ATENA is conceptually object oriented, written in MS Visual C++, and based on MS-Windows environment. ATENA offers user-friendly graphical interface, which enables an efficient solving of practical engineering problems. It offers an excellent

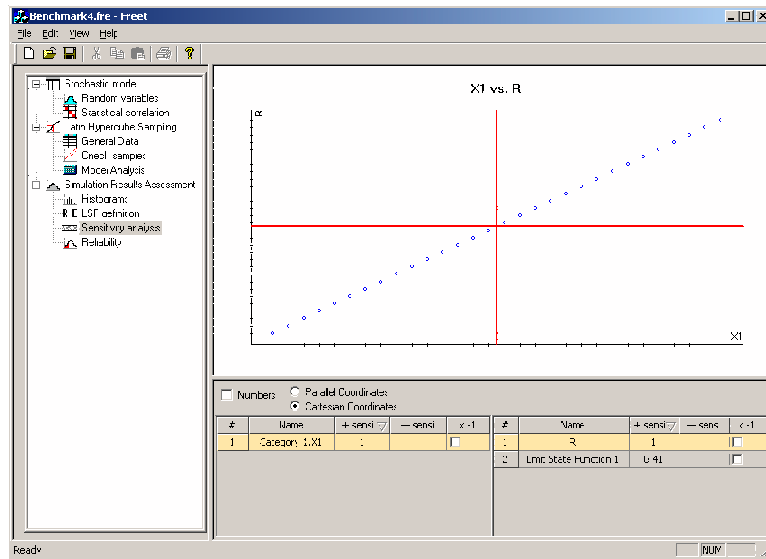


Figure A.20: “What-if-study” using sensitivity analysis window

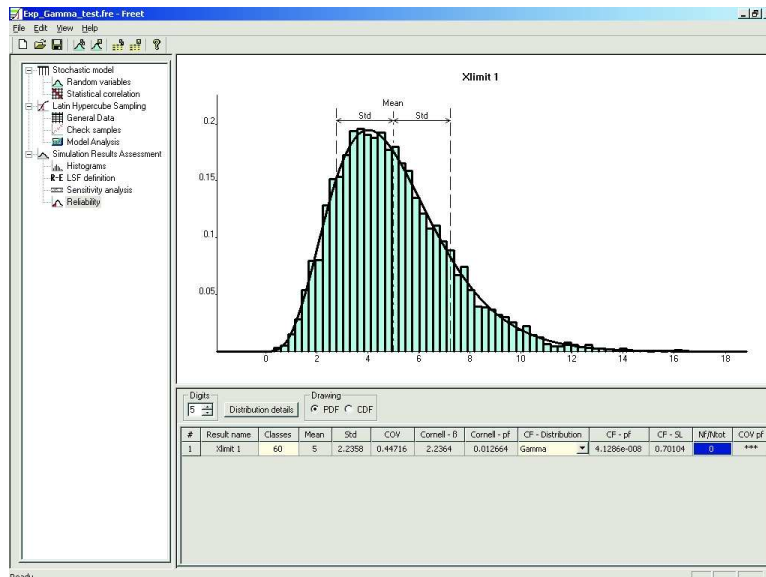


Figure A.21: Curve fitting and estimators of failure probability p_f

support during all stages of the non-linear FE-analysis - preparation of input data, analysis run-time (see Fig. A.22), and evaluation of the obtained results.

Fracture is one of the most important features of concrete behavior with a significant non-linear effect. Tensile cracking model in ATENA is based on the smeared crack approach, which replaces the discrete cracks, occurring in real concrete structures, by strain localization in a continuous displacement field. Concrete fracture in 2D is covered by unique “SBETA material model” of non-linear fracture mechanics based on fracture energy (best with an exponential softening law derived experimentally by Hordijk (1991)). Another efficient model available is the microplane model M4 due to Bažant et al. (2000).

The objectivity of the finite element solution is assured by crack band approach of Bažant and Oh (1983) – the descending branch of the stress-strain relationship is adjusted according to the finite element size and mesh orientation in SBETA model or more generally, the strains are divided into elastic and inelastic part according to the prescribed crack band width.

The hierarchical, multilevel layered structure of ATENA (see Fig. A.23) enabled an effective inte-

gration of the probabilistic software FREET using COM-interface communication. User interaction is supported also for data-exchange ASCII files. The direct communication between ATENA graphical user environment (GUE) and FREET graphical user interface enables employment of ATENA GUI during the stochastic analysis and ensures full compatibility of data information with the deterministic ATENA analysis.

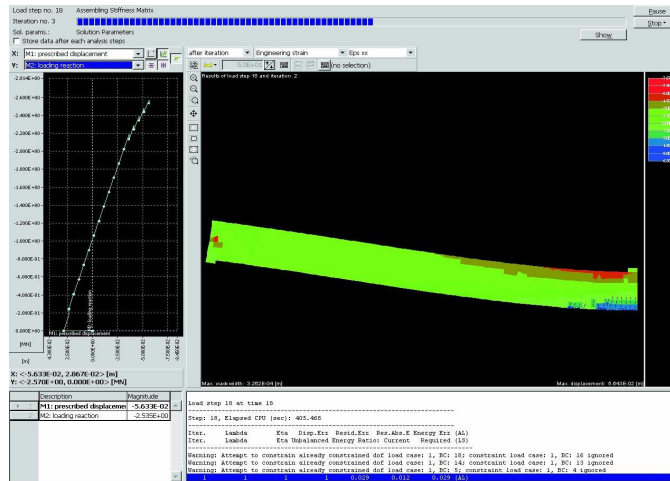


Figure A.22: ATENA run-time interactive graphical window

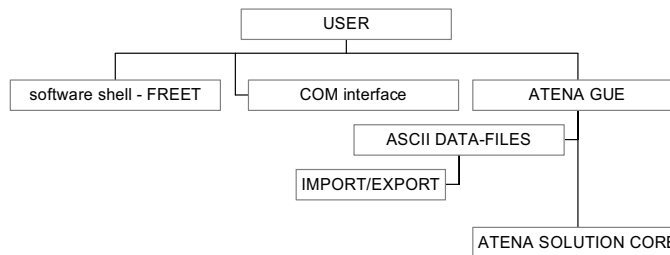


Figure A.23: Hierarchical structure of ATENA

A.8 Conclusions

1. Efficient methods of statistical and sensitivity analysis are described and implemented in a multipurpose probabilistic software FREET. The FREET software development and its recent applications are documented. This software is opened to analysis of any particular computational problem and generally can be used especially in case of computationally intensive problems based on non-linear FEM. The ability of used statistical techniques based on LHS method to estimate efficiently statistical parameters of response using only small number of samples is an advantage of the approach. The software is designed in the form suitable for a relatively easy assessment of any user-defined computational problem. It can be applied without serious difficulties even to realistic computationally demanding reliability problems. This is very important in case of non-linear analysis which is computationally rather demanding, and number of samples should be minimized as much as possible.
2. Software FREET was integrated with non-linear fracture mechanics commercial software ATENA for advanced analysis of concrete and reinforced concrete structures. This complex system enables to use the stochastic non-linear analysis and reliability assessment consistently in a homogeneous user-friendly environment, which is an important precondition for the use in practice.

3. The approach is general and can be applied for basic statistical analysis of computationally intensive (e.g. fracture mechanics) problems. The aim of stochastic calculation could be the estimation of reliability of the structure using statistical characteristics of response. Sensitivity analysis can help to estimate which parameters plays the major role in the structural response and should be recognized well.
4. These new exciting efforts are advancing beyond strict boundaries of design codes and attempt to treat in a combined manner the material non-linearity and reliability. The change of engineering thinking together with economical consequences can be expected in near future.

A.9 Available probability distributions in FREET

This section overviews the probability distribution functions available in the software FREET and programmed by author.

1. Deterministic

2. Normal (Gaussian)

Parameters (2):

- Scale “Std” $\sigma : \sigma > 0$ (Standard deviation)
- Location “Mean” $\mu : -\infty \leq \mu \leq +\infty$ (mean value)

Probability density function

$$f_X(x) = \frac{e^{-\frac{1}{2} \left(\frac{X - \mu}{\sigma} \right)^2}}{\sigma \sqrt{2\pi}} ; \quad -\infty \leq X \leq +\infty$$

3. Log-Normal

Parameters (3):

- Scale “lambda” λ
- Shape “zeta” $\zeta : \zeta > 0$
- Location “bound” $s : -\infty < s < \infty$ (left bound, a shift)

Probability density function:

$$f_X(x) = \frac{1}{\zeta(x-s)\sqrt{2\pi}} e^{-\frac{1}{2} \left[\frac{\ln(x-s) - \lambda}{\zeta} \right]^2} ; \quad s \leq X \leq +\infty$$

4. Log-Normal (2 par)

Parameters (2):

- Scale “lambda” λ
- Shape “zeta” $\zeta : \zeta > 0$

Probability density function:

$$f_X(x) = \frac{1}{\zeta x \sqrt{2\pi}} e^{-\frac{1}{2} \left[\frac{\ln(x) - \lambda}{\zeta} \right]^2} ; \quad s \leq X \leq +\infty$$

5. Weibull-min (EVT III, 3 par)

Parameters (3):

- Scale “w” $w : w > s$
- Shape “m” $m : m > 0$
- Location “bound” $s : -\infty < s < \infty$ (left bound, a shift)

Probability density function:

$$f_X(x) = \frac{m}{(w-s)} \left(\frac{x-s}{w-s}\right)^{m-1} e^{-\left(\frac{x-s}{w-s}\right)^m} = m (w-s)^{-m} (x-s)^{m-1} e^{-\left(\frac{x-s}{w-s}\right)^m} ; s \leq X \leq +\infty$$

6. Weibull-min (EVT III, 2 par)

Parameters (2):

- Scale “w” $w : w > 0$
- Shape “m” $m : m > 0$

Probability density function:

$$f_X(x) = \frac{m}{w} \left(\frac{x}{w}\right)^{m-1} e^{-\left(\frac{x}{w}\right)^m} = m (w)^{-m} (x)^{m-1} e^{-\left(\frac{x}{w}\right)^m} ; 0 \leq X \leq +\infty$$

7. Weibull-max (EVT III, 3 par)

Parameters (3):

- Scale “w” $w : w < s$
- Shape “m” $m : m > 0$
- Location “bound” $s : -\infty < s < \infty$ (right bound, a shift)

Probability density function:

$$f_X(x) = \frac{m}{s-w} \left(\frac{s-x}{s-w}\right)^{m-1} e^{-\left(\frac{s-x}{s-w}\right)^m} ; -\infty \leq X \leq s$$

8. Weibull-max (EVT III, 2 par)

Parameters (2):

- Scale “w” $w : w < 0$
- Shape “m” $m : m > 0$

Probability density function:

$$f_X(x) = \frac{-m}{w} \left(\frac{x}{w}\right)^{m-1} e^{-\left(\frac{x}{w}\right)^m} ; -\infty \leq X \leq 0$$

9. Rayleigh

Parameters (2):

- Scale “beta” $\beta : 0 < \beta$
- Location (shift) “bound” $\varepsilon : -\infty < \varepsilon < \infty$

Probability density function:

$$f_X(x) = \frac{(x-\varepsilon)}{\beta} e^{-\frac{1}{2}\left(\frac{x-\varepsilon}{\beta}\right)^2} ; \varepsilon \leq X \leq +\infty$$

10. Exponential

Parameters (2):

- Scale “lambda” $\lambda : \lambda > 0$
- Location “bound” $\varepsilon : -\infty < \varepsilon < \infty$ (Standard Exponential Distribution $\varepsilon = 0$)

Probability density function:

$$f_X(x) = \lambda e^{\lambda(\varepsilon - x)} \quad ; \quad \varepsilon \leq X \leq \infty$$

11. Laplace

Parameters (2):

- Scale “lambda” $\lambda : \lambda > 0$
- Location “Mean” $\varepsilon : -\infty < \varepsilon < \infty$ (Standard Laplace Distribution $\varepsilon = 0$)

Probability density function:

$$f_X(x) = \frac{\lambda}{2} e^{-\lambda |X - \varepsilon|} \quad ; \quad -\infty \leq X \leq \infty$$

12. Rectangular (Uniform)

Parameters (2):

- Location “a” $a : -\infty < a$
- Location “b” $b : a < b < +\infty$

Probability density function:

$$f_X(x) = \frac{1}{b - a} \quad ; \quad a \leq X \leq b$$

13. Triangular

Parameters (3):

- Location “a” $a : -\infty < a$
- Location “b” $b : b > a$
- Location “c” $c : a \leq c \leq b$

Probability density function:

$$f_X(x) = \begin{cases} \frac{2(x-a)}{(b-a)(c-a)}, & a \leq X \leq c; \\ \frac{2(b-x)}{(b-a)(b-c)}, & c < X \leq b; \end{cases}$$

14. Pareto

Parameters (2):

- Location, Scale “k” $k : k > 0$
- Shape “a” $a : a > 0$

Probability density function:

$$f_X(x) = \frac{a}{k} \left(\frac{k}{x} \right)^{a+1} = \frac{a \cdot k^a}{x^{a+1}} \quad ; \quad k \leq X \leq +\infty$$

15. Logistic

Parameters (2):

- Scale “beta” $\beta : \beta > 0$
- Location “alpha” $\alpha : -\infty \leq \alpha \leq +\infty$ (mean value)

Probability density function:

$$f_X(x) = \frac{\exp\left(\frac{\alpha - x}{\beta}\right)}{\beta \left[1 + \exp\left(\frac{\alpha - x}{\beta}\right)\right]^2} ; \quad -\infty \leq X \leq +\infty$$

16. Half-Normal

Parameters (2):

- Scale “beta” $\beta : \beta > 0$
- Location “bound” $\varepsilon : -\infty \leq \varepsilon \leq +\infty$

Probability density function:

$$f_X(x) = \frac{2}{\beta} \varphi\left(\frac{x - \varepsilon}{\beta}\right) ; \quad \varepsilon \leq X \leq +\infty$$

where $\varphi(\cdot)$ is standard normal distribution function (density)

17. Gumbel-min (EVT I)

Parameters (2):

- Shape “beta” $\beta : \beta > 0$
- Location “mode” $s : -\infty < s < \infty$ (modus)

Probability density function:

$$f_X(x) = \frac{1}{\beta} \exp\left[\frac{x - s}{\beta} - \exp\left(\frac{x - s}{\beta}\right)\right] = f_Y(y) = \frac{1}{\beta} e^y \cdot e^{-e^y} ; \quad -\infty \leq X \leq +\infty$$

where $Y(X) = (X - s)/\beta$ (for the standard form)

18. Gumbel-max (EVT I)

Parameters (2):

- Shape “beta” $\beta : \beta > 0$
- Location “mode” $s : -\infty < s < \infty$ (modus)

Probability density function:

$$f_X(x) = \frac{1}{\beta} \exp\left[\frac{s - x}{\beta} - \exp\left(\frac{s - x}{\beta}\right)\right] = f_Y(y) = \frac{1}{\beta} e^y \cdot e^{-e^y} ; \quad -\infty \leq X \leq +\infty$$

where $Y(X) = (s - X)/\beta$ (for the standard form)

19. Gamma

Parameters (3):

- Shape “gamma” $\gamma : \gamma > 0$
- Scale “beta” $\beta : \beta > 0$
- Location “bound” $\varepsilon : -\infty < \varepsilon < +\infty$

Probability density function:

$$f_X(x) = \frac{\left(\frac{x-\varepsilon}{\beta}\right)^{(\gamma-1)} \cdot e^{\left(-\frac{x-\varepsilon}{\beta}\right)}}{\beta \Gamma(\gamma)} = \frac{y^{(\gamma-1)} \cdot e^{-y}}{\beta \Gamma(\gamma)} ; \quad \varepsilon \leq X \leq +\infty$$

where $Y(X) = (X - \varepsilon)/\beta$

20. **Gamma** (2 par)

Parameters (2):

- Shape “gamma” $\gamma : \gamma > 0$
- Scale “beta” $\beta : \beta > 0$

Probability density function:

$$f_X(x) = \frac{\left(\frac{x}{\beta}\right)^{(\gamma-1)} \cdot e^{\left(-\frac{x}{\beta}\right)}}{\beta \Gamma(\gamma)} = \frac{y^{(\gamma-1)} \cdot e^{-y}}{\beta \Gamma(\gamma)} ; \quad 0 \leq X \leq +\infty$$

where $Y(X) = X/\beta$

Bibliography

- Alzebedeh, K., Al-Ostaz, A., Jasiuk, I., Ostoja-Starzewski, 1998. Fracture of random matrix-inclusion composites: Scale effects and statistics. *International Journal of Solids Structures* 35 (19), 2537–2566.
- Ayyub, B. M., Lai, K. L., 1989. Structural reliability assessment using Latin Hypercube Sampling. In: Ang, A. H.-S., Shinozuka, M., Schuëller, G. (Eds.), *ICoSSaR '89, the 5th International Conference on Structural Safety and Reliability*. Vol. 2. ASCE, San Francisco, CA, USA, pp. 1177–1184.
- Bažant, Z. P., Li, Z., 1995. Modulus of rupture: Size effect due to fracture initiation in boundary layer. *Journal of Structural Engineering* 121 (4), 739–746.
- Bažant, Z. P., Li, Z., 1996. Discussion to paper “Fracture mechanics approach to evaluation of flexural strength of concrete” by Rokugo, K., Uchida, Y., Katoh, H. and Koyanagi, W. *ACI Materials Journal* 93 (5), 507–510.
- Bažant, Z. P., 1984. Size effect in blunt fracture: Concrete, rock, metal. *Journal of Engineering Mechanics, ASCE* 110, 518–535.
- Bažant, Z. P., 1986. Mechanics of distributed cracking. *Appl. Mech. Reviews ASME* 39, 675–705.
- Bažant, Z. P., 1997. Scaling of quasibrittle fracture: Asymptotic analysis. *Int. Journal of Fracture* 83 (1), 19–40.
- Bažant, Z. P., 1998a. Size effect in tensile and compression fracture of concrete structures: Computational modeling and design. In: Mihashi, H., Rokugo, K. (Eds.), *3rd Int. Conf., FraMCoS-3 Fracture Mechanics of Concrete Structures*. Aedificatio Publishers, Freiburg, Germany, Gifu, Japan, pp. 1905–1922.
- Bažant, Z. P., 1998b. Statistical and fractal aspects of size effect in quasibrittle structures: Conspectus of recent results. In: Shiraishi, N., Shinozuka, M., Wen, Y. (Eds.), *ICoSSaR '97, the 7th International Conference on Structural Safety and Reliability*. Vol. 2. Rotterdam Balkema, Kyoto, Japan.
- Bažant, Z. P., 1999a. Size effect. *International Journal of Solids and Structures* 200 (37), 69–80, special issue of invited review articles on *Solid Mechanics* edited by G.J. Dvorak for U.S. Nat. Comm. on Theor. and Appl. Mech., publ. as a book by Elsevier Science, Ltd.
- Bažant, Z. P., 1999b. Size effect on structural strength: a review. *Archives of Applied Mechanics (Ingenieur-Archiv, Springer Verlag)*, (75th Anniversary Issue) 69, 703–725, reprinted with updates in *Handbook of Materials Behavior*, J. Lemaitre, ed., Academic Press, San Diego 2001, Vol. 1, 30–68.
- Bažant, Z. P., 2001. Size effects in quasibrittle fracture: Apercu of recent results. In: de Borst et al, R. (Ed.), *4th Int. Conference FraMCoS – Fracture Mechanics of Concrete and Concrete Structures*. A.A Balkema Publishers, Lisse, Cachan, France, pp. 651–658.
- Bažant, Z. P., 2002a. Probabilistic modeling of quasibrittle fracture and size effect. In: Corotis, R., Schuëller, G., Shinozuka, M. (Eds.), *ICoSSaR '01 the 8th International Conference on Structural Safety and Reliability*. A.A.Balkema Publishers, Netherlands; Swets & Zeitinger Publishing, Newport Beach, California.
- Bažant, Z. P., 2002b. *Scaling of Structural Strength*. Hermes Penton Science (Kogan Page Science).

- Bažant, Z. P., 2003. Energetic and statistical size effects in fiber composites and sandwich structures. A precis of recent progress. In: Hui, D. (Ed.), 10th Int. Conf. on Composites/Nano Engineering (ICCE-10, July). University of New Orleans, USA, pp. 869–872.
- Bažant, Z. P., 2004. Probability distribution of energetic-statistical size effect in quasibrittle fracture. Probabilistic Engineering Mechanics, In Press, Corrected Proof, Available online 20 November 2003.
- Bažant, Z. P., Belytschko, T. B., Chang, T.-P., 1984. Continuum model for strain softening. Journal of Engineering Mechanics, ASCE 110, 1666–1692.
- Bažant, Z. P., Caner, F. C., Carol, I., D., A. M., Akers, S. A., 2000. Microplane model M4 for concrete: I. Formulation with work-conjugate deviatoric stress. Journal of Engineering Mechanics, ASCE 126 (9), 971–980.
- Bažant, Z. P., Chen, E.-P., 1997. Scaling of structural failure. Applied Mechanics Reviews ASME 50 (10), 593–627, transl. in *Advances in Mechanics* (China), Vol. 20, No. 3.
- Bažant, Z. P., Kazemi, M. T., 1990. Determination of fracture energy, process zone length and brittleness number from size effect, with application to rock and concrete. International Journal of Fracture 44, 111–131.
- Bažant, Z. P., Novák, D., 2000a. Energetic-statistical size effect in quasi-brittle failure at crack initiation. ACI Materials Journal 97 (3), 381–392.
- Bažant, Z. P., Novák, D., 2000b. Probabilistic nonlocal theory for quasi-brittle fracture initiation and size effect I: Theory. Journal of Engineering Mechanics 126 (2), 166–174.
- Bažant, Z. P., Novák, D., 2000c. Probabilistic nonlocal theory for quasi-brittle fracture initiation and size effect II: Application. Journal of Engineering Mechanics 126 (2), 175–185.
- Bažant, Z. P., Novák, D., 2001. Proposal for standard test of modulus of rupture of concrete with its size dependence. Journal of ACI 98 (1), 79–87.
- Bažant, Z. P., Novák, D., 2003. Stochastic models for deformation and failure of quasibrittle structures: Recent advances and new directions. In: Bičanič, N., de Borst, R., Mang, H., Meschke, G. (Eds.), Computational modelling of concrete structures (Euro-C 2003). A.A. Balkema Publishers, Lisse, St. Johann in Pongau, Austria, pp. 583–598.
- Bažant, Z. P., Novák, D., Vořechovský, M., Pang, S. D., 2004a. Stochastic crack band model for quasibrittle failure. Journal of Engineering Mechanics, in submission process.
- Bažant, Z. P., Oh, B.-H., 1983. Crack band theory for fracture of concrete. Materials and Structures (RILEM, Paris) 16, 155–177.
- Bažant, Z. P., Pang, S. D., Vořechovský, M., Novák, D., Pukl, R., 2004b. Statistical size effect in quasibrittle materials: Computation and extreme value theory. In: Li, V. C., Willam, K. J., Leung, C. K. Y., Billington, S. L. (Eds.), 5th Int. Conference FraMCoS – Fracture Mechanics of Concrete and Concrete Structures. Vol. 1. Ia-FraMCoS, Vail, Colorado, USA, pp. 189–196.
- Bažant, Z. P., Planas, J., 1998. Fracture and Size Effect in Concrete and Other Quasibrittle Materials. CRC Press, Boca Raton Florida and London.
- Bažant, Z. P., Vořechovský, M., Novák, D., 2004c. Superimposition of deterministic-energetic and statistical size effects in quasibrittle failure at crack initiation. Journal of Engineering Mechanics, submitted for possible publication.
- Bažant, Z. P., Vořechovský, M., Novák, D., 2005. Role of deterministic and statistical length scales in size effect for quasibrittle failure at crack initiation. In: ICoSSaR '05 the 9th International Conference on Structural Safety and Reliability. Rome, Italy, in preparation.
- Bažant, Z. P., Xi, Y., 1991. Statistical size effect in quasibrittle structures: II. Nonlocal theory. ASCE Journal of Engineering Mechanics 117 (11), 2623–2640.

- Bergmeister, K., Strauss, A., Eichinger, E. M., Kolleger, J., Novák, D., Pukl, R., Červenka, V., 2002. Structural analysis and safety assessment of existing concrete structures, session 11. In: The first fib Congres. Osaka, Japan, pp. 47–54.
- Beyerlein, I. J., Phoenix, S. L., 1996. Comparison of shear-lag theory and continuum fracture mechanics for modeling fiber and matrix stresses in an elastic cracked composite lamina. *International journal of Solids and Structures* 33 (18), 2543–2574.
- Beyerlein, I. J., Phoenix, S. L., 1997. Stress profiles and energy release rates around fiber breaks in a lamina with propagating zones matrix yielding and debonding. *Composites Science and Technology* 57, 869–885.
- Bogdanoff, J. L., Kozin, F., 1987. Effect of length on fatigue life of cables. *Journal of Engineering Mechanics* 113 (6), 925–940.
- Bogdanoff, J. L., Kozin, F., 1989. Effect of length on fatigue life of long thin continuous components. *Journal of Engineering Mechanics* 115 (7), 1441–1457.
- Bouchaud, J.-P., Potters, M., 2000. *Theory of financial risks*. Cambridge University Press.
- Bourgund, U., Bucher, C. G., 1986. A code for importance sampling procedure using design points - ISPUd - a user's manual. Tech. Rep. Report No. 8-86., Institute of Engineering Mechanics, Innsbruck University.
- Brenner, C. E., 1991. Stochastic finite element methods (Literature review). Tech. Rep. Internal Working Report, No. 35-91, Institute of Engineering Mechanics, University of Innsbruck, Austria.
- Breysse, D., 1990. Probabilistic formulation of damage evolution law of cementitious composites. *Journal of Engineering Mechanics, ASCE* 116 (7), 1389–1410.
- Breysse, D., Fokwa, D., 1992. Influence of disorder of the fracture process of mortar. In: Bažant, Z. P. (Ed.), 1st Int. Conf., FraMCoS: Fracture Mechanics of Concrete Structures. Elsevier, London, Breckenridge, Colorado, USA, pp. 536–541.
- Breysse, D., Fokwa, D., Drahý, F., 1994. Spatial variability in concrete: Nature, Structure, and Consequences. *JApplied Mechanics Reviews, ASME* 47 (1), 184–196.
- Breysse, D., Renaudin, P., 1996. On the influence of local disorder on size effect. In: Carpinteri, A. (Ed.), *Size-Scale Effects in the Failure Mechanisms of Materials and Structures*, IUTAM Symp. held in 1994. London, Politecnico di Torino, Italy, pp. 187–199.
- Bucher, C. G., 1988. Adaptive sampling - An iterative fast Monte-Carlo procedure. *Journal of Structural Safety* 5 (2), 119–126.
- Bucher, C. G., Bourgund, U., 1987. Efficient use of response surface methods. Tech. Rep. No. 9-87, Institute of Engineering Mechanics, Innsbruck University.
- Bucher, C. G., Ebert, M., 2000. Load carrying behavior of prestressed bolted steel flanges considering random geometrical imperfections. In: 8th ASCE Specialty Conference on Probabilistic Mechanics and Structural Reliability, PMC 2000 (CDROM Proc.). ASCE, Notre Dame, USA.
- Beyerlein, I. J., Phoenix, S. L., 1997. Statistics of fracture for an elastic notched composite lamina containing Weibull fibers, part I: Features from Monte-Carlo simulation. *Engineering Fracture Mechanics* 57 (2/3), 241–265.
- Carmeliet, J., 1994. On stochastic descriptions for damage evaluation in quasi-brittle materials. In: Kusters, G., Hendriks, M. (Eds.), *DIANA Computational Mechanics*.
- Carmeliet, J., Hens, H., 1994. Probabilistic nonlocal damage model for continua with random field properties. *Journal of Engineering Mechanics, ASCE* 120 (10), 2013–2027.

- Carpinteri, A., Chiaia, B., Ferro, G., 1994. Multifractal scaling law for the nominal strength variation of concrete structures. In: Mihashi, M., Okamura, H., zant, Z. B. (Eds.), *Int. Workshop on Size Effect in Concrete Structures*, Japan Concrete Institute International Workshop. E & FN Spon London-New York, Sendai, Japan, pp. 193–206.
- Carpinteri, A., Chiaia, B., Ferro, G., 1995. Size effects on nominal tensile strength of concrete structures: Multifractality of material ligaments and dimensional transition from order to disorder. *Materials and Structures* 28 (7), 311–317.
- Castillo, E., 1988. *Extreme value theory in engineering*. Academic Press, Inc. (London) LTD.
- Cervenka, V., 2000. Simulating a response. *Concrete Engineering International* 4 (4), 45–49.
- Cervenka, V., Pukl, R., 1994. SBETA analysis of size effect in concrete structures. In: Mihashi, M., Okamura, H., zant, Z. B. (Eds.), *Int. Workshop on Size Effect in Concrete Structures*, Japan Concrete Institute International Workshop. E & FN Spon London-New York, Sendai, Japan, pp. 271–281.
- Cervenka, V., Pukl, R., 2003. ATENA - Computer program for nonlinear finite element analysis of reinforced concrete structures. Tech. rep., Červenka Consulting, Prague, Czech Republic, program documentation (Theory and User's guide).
- Cervenka, V., Pukl, R., 2004. SARA. Tech. rep., Červenka Consulting, Prague, Czech Republic, Program Documentation (User's guide).
- Chudoba, R., Vořechovský, M., Konrad, M., 2004. Stochastic modeling of multi-filament yarns I: Random properties within the cross section and size effect. *Journal of Engineering Mechanics*, submitted to.
- Coleman, B. D., 1958. On the strength of classical fibres and fibre bundles. *Journal of the Mechanics and Physics of Solids* 7, 60–70.
- Cornell, C. A., 1969. A probability-based structural code. *Journal of the American Concrete Institute* 66 (12), 974–985.
- Curbach, M., 2002. Arbeits- und Ergebnisbericht zum Sonderforschungsbereich 532 'Textile Bewehrung zur Bautechnischen Verstärkung und Instandsetzung' für die Periode II/1999 bis I/2002. Tech. Rep. SFB528, Technical University Dresden.
- Curbach, M., Hegger, J. (Eds.), 2001. *Textilbeton - 1. Fachkollquium der Sonderforschungsbereiche 528 und 532*. RWTH Aachen.
- Daniels, H. E., 1945. The statistical theory of the strength of bundles of threads. *Proc. Royal Soc. (London)* 183A, 405–435.
- de Borst, R., Carmeliet, J., 1996. Stochastic approaches for damage evolution in local and non-local continua. In: Carpinteri, A. (Ed.), *Size-Scale Effects in the Failure Mechanism of Materials and Structures*. E & FN Spon, London, Newport Beach, California, pp. 242–257.
- Der Kiureghian, A., Ke, J.-B., 1988. The stochastic finite element method in structural reliability. *Probabilistic Engineering Mechanics* 3 (2), 83–91.
- Enevoldsen, I., 2001. Experience with probabilistic-based assessment of bridges. *Structural Engineering International* 11 (4), 251–260.
- Epstein, B., 1948. Statistical aspects of fracture problems. *Journal of Applied Physics* 19, 140–147.
- Fisher, R. A., Tippett, L. H. C., 1928. Limiting forms of the frequency distribution of the largest and smallest member of a sample. *Proc., Cambridge Philosophical Society* 24, 180–190.
- Florian, A., 1992. An efficient sampling scheme Updated Latin Hypercube Sampling. *Probabilistic Engineering Mechanics* 2 (7), 123–130.

- Frantziskonis, G. N., 1998. Stochastic modeling of heterogeneous materials – A process for analysis and evaluation of alternative formulations. *Mechanics of Materials* 27, 165–175.
- Fréchet, M., 1927. Sur la loi de probabilité de l' écart maximum. *Ann. Soc. Polon. Math.*, Cracow 6, 93.
- Freudenthal, A. M., 1956a. Physical and statistical aspects of fatigue. *Advance in Applied Mechanics* 4, 117–157.
- Freudenthal, A. M., 1956b. Safety and the probability of structural failure. *Transactions* 121, 1327–1397.
- Freudenthal, A. M., 1963. Safety of mechanical systems. In: Bogdanoff, J. L., Kozin, F. (Eds.), *First Symposium on Engineering Applications of Random Function Theory and Probability 1962*. John Wiley and Sons, New York and London, Purdue University, p. 149.
- Freudenthal, A. M., 1968. Statistical approach to brittle fracture. In: Liebowitz, H. (Ed.), *Chpt 6 in Fracture*. Vol. 2. Academic Press, pp. 591–619.
- Freudenthal, A. M., Garrets, J. M., Shinozuka, M., 1966. The analysis of structural safety. *Journal of the Structural Division* 92 (ST1), 267–325.
- Freudenthal, A. M., Gumbel, E. J., 1953. On the statistical interpretation of fatigue tests. *Proc., Cambridge Philosophical Society (London)* A 21, 309–332.
- Ghanem, R. G., Spanos, P. D., 1991. *Stochastic Finite Elements: A Spectral Approach*. Springer-Verlag.
- Gnedenko, B. V., 1943. Sur la distribution limite du terme maximum d'une série aléatoire. *Annals of Mathematics*, 2nd Ser 44 (3), 423–453.
- Gries, T., Royé, A., 2003. Three-dimensional reinforcement structures for thin walled components. In: Curbach, M. (Ed.), *2nd Colloquium on Textile Reinforce Structures (CTRS2)*. Dresden, Germany, pp. 513–524.
- Grigoriu, M., 1982/1983. Methods for approximate reliability analysis. *Journal of Structural Safety* 1, 155–165.
- Grigoriu, M., 1983. Reliability of chain and ductile-parallel systems. *Journal of Engineering Mechanics* 109 (5), 1175–1188.
- Grigoriu, M., 1990. Reliability analysis of dynamic daniels systems with local load-sharing rule. *Journal of Engineering Mechanics* 116 (12), 2625–2642.
- Gumbel, E. J., 1958. *Statistics of extremes*. Columbia University Press, New York.
- Gutiérrez, M. A., de Borst, R., 1999. Deterministic and stochastic analysis of size effects and damage evaluation in quasi-brittle materials. *Archive of Applied Mechanics* 69, 655–676.
- Gutiérrez, M. A., de Borst, R., 2002. Deterministic and probabilistic material length-scales and their role in size-effect phenomena. In: Corotis, R., Schuëller, G., Shinozuka, M. (Eds.), *ICoSSaR '01 8th International Conference on Structural Safety and Reliability*. A.A.Balkema Publishers, Netherlands; Swets & Zeitinger, Newport Beach, California, pp. 129–136.
- Harlow, D. G., Phoenix, S. L., 1978a. The chain-of-bundles probability model for the strength of fibrous materials I: Analysis and conjectures. *Journal Composite Materials* 12, 195–214.
- Harlow, D. G., Phoenix, S. L., 1978b. The chain-of-bundles probability model for the strength of fibrous materials II: A numerical study of convergence. *Journal of Composite Materials* 12, 314–335.
- Hasofer, A. M., Lind, N. C., 1974. Exact and invariant second-moment code format. *Journal of the Engineering Mechanics Division, ASCE* 100 (EM1) (1), 111–121.
- Hegger, J., 2002. *Arbeits- und Ergebnisbericht zum Sonderforschungsbereich 532 'Textilbewehrter Beton: Grundlagen für die Entwicklung einer neuartigen Technologie' für die Periode II/1999 bis I/2002*. Tech. Rep. SFB532, Aachen University.

- Hidalgo, R. C., Moreno, Y., Kun, F., Hermann, H. J., 2002. Fracture model with variable range of interaction. *Physical review E* 65, 1–8.
- Hillerborg, A., Modéer, M., Petersson, P. E., 1976. Analysis of crack formation and crack growth in concrete by means of fracture mechanics and finite elements. *Cem. Concr. Res.* 6, 773–782.
- Hohenbichler, M., 1983. Resistance of large brittle parallel systems. In: ICASP 4, International Conference on Applications of Statistics and Probability in Soil and Structural Engineering. University of Firenze, Italy, pp. 1301–1312.
- Hohenbichler, M., Rackwitz, R., 1981. Non-normal dependent vectors in structural safety. *Journal of Engineering Mechanics, ASCE* 107 (6), 1227–1238.
- Hohenbichler, M., Rackwitz, R., 1983. Reliability of parallel systems under imposed uniform strain. *Journal of Engineering Mechanics* 109 (3), 896–907.
- Hordijk, D. A., 1991. Local approach to fatigue of concrete. Ph.D. thesis, Delft University of Technology, Delft, The Netherlands, ISBN 90-9004519-8.
- Huntington, D. E., Lyrantzis, C. S., 1998. Improvements to and limitations of Latin Hypercube Sampling. *Probabilistic Engineering Mechanics* 13 (4), 245–253.
- Ibnabdeljalil, M., Curtin, W. A., 1997. Strength and reliability of fiber-reinforced composites: localized load sharing and associated size-effects. *International Journal of Solids Structures* 34 (21), 2649–2668.
- Iman, R. C., Conover, W. J., 1980. Small sample sensitivity analysis techniques for computer models with an application to risk assessment. *Communications in Statistics: Theory and Methods* A9 (17), 1749–1842.
- Iman, R. C., Conover, W. J., 1982. A distribution free approach to inducing rank correlation among input variables. *Communications in Statistics* B11, 311–334.
- Iman, R. L., Shortencarier, M. J., 1984. A FORTRAN 77 program and user's guide for the generation of Latin Hypercube and random samples for use with computer models. Tech. Rep. NUREG/CR-3957 Report, U.S. Nuclear Regulatory Commission, SAND83-2365.
- Jirásek, M., Bažant, Z. P., 2002. *Inelastic Analysis of Structures*. John Wiley and Sons, Chichester.
- Kala, Z., Novák, D., Vořechovský, M., 2001. Probabilistic nonlinear analysis of steel frames focused on target reliability of Eurocodes. In: Corotis, R., Schuëller, G., Shinozuka, M. (Eds.), *ICoSSaR '01 8th International Conference on Structural Safety and Reliability*. A.A.Balkema Publishers, Netherlands, Newport Beach, California, USA, p. 146.
- Keramat, M., Kielbasa, R., 1997. Efficient average quality index of estimation of integrated circuits by Modified Latin Hypercube Sampling Monte Carlo (MLHSMC). In: *IEEE International Symposium on Circuits and Systems*. Hong Kong.
- Kleiber, M., Hien, T. D., 1992. *The Stochastic Finite Element Method*. John Willey & Sons Ltd, New York.
- Koide, H., Akita, H., Tomon, M., 1998. Size effect on flexural resistance due to bending span of concrete beams. In: Mihashi, H., Rokugo, K. (Eds.), *3rd Int. Conf., FraMCoS-3 Fracture Mechanics of Concrete Structures*. Aedificatio Publishers, Freiburg, Germany, Gifu, Japan, pp. 2121–2130.
- Koide, H., Akita, H., Tomon, M., 2000. Probability model of flexural resistance on different lengths of concrete beams. In: Melchers, R. E., Stewart, M. G. (Eds.), *ICASP 8, International Conference on Applications of Statistics and Probability in Civil Engineering*. Vol. 2. Balkema, Rotterdam, Sydney, Australia 1999, pp. 1053–1057.
- Krajcinovic, D., Silva, M. A. G., 1982. Statistical aspects of the continuous damage theory. *International Journal of Solids Structures* 18 (7), 551–562.

- Kubanová, J., Linda, B., 2002. Confidence intervals based on bootstrap methods. In: Kmeř, S., Miron, P. (Eds.), VII International Scientific Conference, Section 1: Applied mathematics. Technical University of Košice, Košice, Slovak Republic, pp. 35–40.
- Kun, F., Zapperi, S., Herrmann, H. J., 2000. Damage in fiber bundle models. *The European Physical Journal B* (17), 269–279.
- Laarhoven, P. J., Aarts, E. H., 1987. *Simulated Annealing: Theory and Applications*. D. Reidel Publishing Company, Holland.
- Lehký, D., Matesová, D., Novák, D., Teplý, B., Veselý, V., Vořechovský, M., 2003. Stochastic analysis, fracture mechanics and pre-stressed concrete members. In: Konvalinka, P., Máca, J. (Eds.), CTU Reports 1 Vol 7, 2003: Contribution to Computational and Experimental Investigation of Engineering Materials and Structures. Dedicated to Zdeněk Bittnar on the occasion of his 60th birthday. Czech Technical University in Prague, Faculty of Civil Engineering, Prague, Czech Republic, pp. 111–120.
- Lehký, D., Novák, D., 2002. Statistical size effect of concrete in uniaxial tension. In: Schießl, P., Gebbeken, N., Keuser, M., Zilch, K. (Eds.), 4th International Ph.D. Symposium in Civil Engineering. Vol. 1. Millpress, Rotterdam, Munich, Germany, <http://www.phd.bv.tum.de>, pp. 435–444.
- Lehký, D., Vořechovský, M., 2002. Generování náhodných polí: Teorie a aplikace. In: 4th Scientific PhD international workshop. Brno University of Technology, pp. CD-ROM.
- Levy, M., Salvadori, M., 1992. *Why buildings fall down?* W.W. Norton, New York.
- Li, K. S., Lumb, P., 1985. Reliability analysis by numerical integration and curve fitting. *Journal of Structural Safety* 3, 29–36.
- Liu, P., Der Kiureghian, A., 1986. Multivariate distribution models with prescribed marginals and covariances. *Probabilistic Engineering Mechanics* 1 (2), 105–111.
- Liu, W. K., Belytschko, T., Lua, Y. J., 1995. *Probabilistic Structural Mechanics Handbook: Theory and Industrial Applications*, 4th Edition. Springer Verlag, New York, Texas, USA.
- Loève, M., 1977. *Probability theory*, 4th Edition. Springer Verlag, New York.
- Madsen, H. O., Krenk, S., Lind, N. C., 1986. *Methods of Structural Safety*. Prentice Hall, Englewood Cliffs.
- Mahesh, S., Phoenix, S. L., Beyerlein, I. J., 2002. Strength distributions and size effects for 2D and 3D composites with Weibull fibers in an elastic matrix. *International Journal of Fracture* 115, 41–85.
- Margoldová, J., Červenka, V., Pukl, R., 1998. Applied brittle analysis. *Concrete Engineering International* 8 (2), 65–69.
- Mariotte, E., 1686. *Traité du mouvement des eaux*. Engl. transl. by J. T. Desvaguliers, London (1718), posthumously edited by M. de la Hire, also *Mariotte's collected works*, 2nd ed., The Hague (1740).
- Marston, C., Cabbitas, B., Adams, J., 1997. The effect of fibre sizing on fibres and bundle strength in hybrid glass carbonfibre composites. *Journal of Materials Science* 32, 1415–1423.
- Mazars, J., 1982. Probabilistic aspects of mechanical damage in concrete structures. In: Sih, G. (Ed.), *Conf. on Fracture Mech. Technol. Appl. to Mat. Evaluation and Struct. Design*. Melbourne, Australia, pp. 657–666.
- Mazars, J., Pijaudier-Cabot, G., Saouridis, C., 1991. Size effect and continuous damage in cementitious materials. *International Journal of Fracture* 51, 159–173.
- McCartney, L. N., Smith, R. L., 1983. Statistical theory of the strength of fiber bundles. *Journal of Applied Mechanics* 50, 601–608.

- McKay, M. D., Conover, W. J., Beckman, R. J., 1979. A comparison of three methods for selecting values of input variables in the analysis of output from a computer code. *Technometrics* 21, 239–245.
- Mihashi, H., Izumi, M., 1977. A stochastic theory for concrete fracture. *Cement and Concrete Research*, Pergamon Press 7, 411–422.
- Nataf, A., 1962. Détermination des distributions de probabilités dont les marges sont donnés. *Comptes Rendus de L'Académie des Sciences* 225, 42–43.
- Novák, D., Bažant, Z. P., Vořechovský, M., 2003a. Computational modeling of statistical size effect in quasibrittle structures. In: Der Kiureghian, A., Madanat, S., Pestana, J. M. (Eds.), *ICASP 9, International Conference on Applications of Statistics and Probability in Civil Engineering*. Millpress, Rotterdam, San Francisco, USA, pp. 621–628.
- Novák, D., Kijawatworawet, W., 1990. A comparison of accurate advanced simulation methods and Latin Hypercube Sampling method with approximate curve fitting to solve reliability problems. Tech. Rep. Internal Working Report No. 34 - 90, Institute of Engineering Mechanics, University of Innsbruck, Austria.
- Novák, D., Lawanwisut, W., Bucher, C., 2000. Simulation of random fields based on orthogonal transformation of covariance matrix and Latin Hypercube Samplings. In: G. I. Schuëller P. D. Spanos Der Kiureghian, M., Pestana (Eds.), *International Conference on Monte Carlo Simulation MC 2000*. Swets & Zeitlinger, Lisse (2001), Monaco, Monte Carlo, pp. 129–136.
- Novák, D., Pukl, R., Rusina, R., M. Vořechovský, M., Červenka, V., 2002a. Statistical, sensitivity and reliability assessment of computationally intensive problems: Nonlinear fracture mechanics analysis. In: Menčík, J. (Ed.), *Reliability and Diagnostic of Transport Structures and Means 2002*, First International Conference. University of Pardubice, Pardubice, Czech Republic, pp. 252–260.
- Novák, D., Pukl, R., Červenka, V., Vořechovský, M., Rusina, R., Lehký, D., 2005. Stochastic nonlinear fracture mechanics finite element analysis of concrete structures. In: *ICoSSaR '05 the 9th International Conference on Structural Safety and Reliability*. Rome, Italy, in preparation.
- Novák, D., Pukl, R., Vořechovský, M., Rusina, R., Červenka, V., 2002b. Feasible structural reliability assessment of computationally intensive problems - nonlinear FEM analysis. In: *1st International ASRANet Colloquium*. Glasgow, Scotland.
- Novák, D., Rusina, R., Vořechovský, M., 2002c. Freet - software pro pravděpodobnostní posudky výpočtově náročných problémů mechaniky kontinua. In: *Reliability of Structures, 3rd International Conference*, Faculty of Civil Engineering, Ostrava University of Technology. Academy of Sciences – Institute of Theoretical and Applied Mechanics of the ASCR Prague, Ostrava, Czech Republic, pp. 71–74.
- Novák, D., Stoyanoff, S., Herda, H., 1995. Error assessment for wind histories generated by autoregressive method. *Structural safety* 17 (1), 121–125.
- Novák, D., Teplý, B., Keršner, Z., 1998. The role of Latin Hypercube Sampling method in reliability engineering. In: Shiraishi, N., Shinozuka, M., Wen, Y. K. (Eds.), *ICoSSaR '97, the 7th International Conference on Structural Safety and Reliability*. Vol. 2. Rotterdam Balkema, Kyoto, Japan, pp. 403–409.
- Novák, D., Teplý, B., Keršner, Z., Vořechovský, M., 2004. FREET. Tech. rep., Institute of Engineering Mechanics, Faculty of Civil Engineering, Brno University of Technology / Červenka Consulting, Praha, Czech Republic, program documentation – Part 1 – Theory.
- Novák, D., Teplý, B., Shiraishi, N., 1993. Sensitivity analysis of structures: A review. In: *CIVIL COMP '93*. Edinburgh, Scotland, pp. 201–207.
- Novák, D., Vořechovský, M., 2004. Error assessment of random fields simulation for stochastic finite element method. *Probabilistic Engineering Mechanics*, in submission process.

- Novák, D., Vořechovský, M., Pukl, R., Červenka, V., 2001. Statistical nonlinear analysis - size effect of concrete beams. In: de Borst, R., Mazars, J., Pijaudier-Cabot, G., van Mier, J. G. M. (Eds.), 4th Int. Conference FraMCoS – Fracture Mechanics of Concrete and Concrete Structures. Swets & Zeitlinger, Lisse, Cachan, France, pp. 823–830.
- Novák, D., Vořechovský, M., Rusina, R., 2003b. Small-sample probabilistic assessment - FREET software. In: Der Kiureghian, A., Madanat, S., Pestana, J. M. (Eds.), ICASP 9, International Conference on Applications of Statistics and Probability in Civil Engineering. Millpress, Rotterdam, San Francisco, USA, pp. 91–96.
- Novák, D., Vořechovský, M., Rusina, R., Lehký, D., Teplý, B., Keršner, Z., 2002d. FREET – *F*easible *R*eliability *E*ngineering *E*fficient *T*ool. Tech. rep., Institute of Engineering Mechanics, Faculty of Civil Engineering, Brno University of Technology / Červenka Consulting, Praha, Czech Republic, program documentation.
- Olsson, J., Sandberg, G. E., 2002. Latin Hypercube Sampling for Stochastic Finite Element Analysis. *Journal of Engineering Mechanics*, ASCE 128 (1), 121–125, technical note.
- Otten, R. H. J. M., Ginneken, L. P. P. P., 1989. *The Annealing Algorithm*. Kluwer Academic Publishers, USA.
- Patterson, H. D., 1954. The errors of lattice sampling. *Journal of the Royal Statistical Society B* 16, 140–149.
- Peirce, F. T., 1926. Theorems on the strength of long and of composite specimens. *Journal of the Textile Institute* 17, 355–368.
- Perla, J., Vořechovský, M., 2003. Využití programu FEAT při rekonstrukcích. In: *Statika 2003*. Hotel Myslivna, Brno.
- Petersson, P.-E., 1981. Crack growth and development of fracture zone in plain concrete and similar materials. Tech. Rep. TVBM-1006, Division of Building Materials, Lund Institute of Technology, Lund, Sweden.
- Phoenix, S. L., 1978a. The random strength of series-parallel structures with load sharing among members. *Probabilistic Mechanics*, 91–95.
- Phoenix, S. L., 1978b. Stochastic strength and fatigue of fiber bundles. *International Journal of Fracture* 14 (3), 327–344.
- Phoenix, S. L., Beyerlein, I. J., 2000. Distribution and size scalings for strength in a one-dimensional random lattice with load redistribution to nearest and next nearest neighbors. *Physical Review E* 62 2, 1622–1645.
- Phoenix, S. L., Ibnabdeljalil, M., Hui, C. Y., 1997. Size effects in the distribution for strength of brittle matrix fibrous composites. *International Journal of Solids and Structures* 34 (5), 545–568.
- Phoenix, S. L., Smith, R., 1983. A comparison of probabilistic techniques for the strength of fibrous materials under local load-sharing among fibers. *International Journal of Solids and Structures* 196, 479–496.
- Pijaudier-Cabot, G. and Bažant, Z. P., 1987. Nonlocal damage theory. *Journal of Engineering Mechanics*, ASCE 113 (10), 1512–1533.
- Pukl, R., Eligehausen, R., Červenka, V., 1992. Computer simulation of pullout test of headed anchors in a state of plane-stress. In: Gerstle, W., Bažant, Z. P. (Eds.), *Concrete design based on fracture mechanics*. ACI SP-134, Detroit, Michigan, USA, pp. 79–100.
- Pukl, R., Novák, D., Bergmeister, K., 2003a. Reliability assessment of concrete structures. In: Bičanič, N., de Borst, R., Mang, H., Meschke, G. (Eds.), *Computational modelling of concrete structures (Euro-C 2003)*. A.A. Balkema Publishers, Lisse, St. Johann in Pongau, Austria, pp. 793–803.

- Pukl, R., Novák, D., Vořechovský, M., Rusina, R., Červenka, V., 2001. Stochastická nelineární analýza betonových konstrukcí. In: Betonářské Dny 2001 (Concrete Days 2001). ČBZ, Pardubice, Czech Republic, pp. 136–141.
- Pukl, R., Strauss, A., Novák, D., Červenka, V., Bergmeister, K., 2003b. Probabilistic-based assessment of concrete structures using non-linear fracture mechanics. In: Der Kiureghian, A., Madanat, S., Pestana, J. M. (Eds.), ICASP 9, International Conference on Applications of Statistics and Probability in Civil Engineering. Millpress, Rotterdam, San Francisco, USA.
- Roelfstra, P. E., H., S., Wittmann, F. H., 1985. Rle béton numérique. *Materials and Structures* 18, 327–335.
- Rokugo, K., Uchida, Y., Katoh, H., Koyanagi, W., 1995. Fracture mechanics approach to evaluation of flexural strength of concrete. *ACI Materials Journal* (Selected translation from Japan Concrete Institute) 92 (5), 561–566.
- Rosenblatt, M., 1952. Remarks on multivariate analysis. *Annals of Statistics* 23, 470–472.
- Rubenstein, R. Y., 1981. *Simulation and the Monte Carlo method*. John Wiley & Sons, New York, New Press, Oxford.
- Sabnis, G. M., Mirza, S. M., 1979. Size effects in model concretes? *J. of Struct. Div. - ASCE* 106, 1007–1020.
- Saibel, E., 1969. Size effect in fracture. In: *Int. Conf. on Structure, Solid Mechanics and Engineering Design in Civil Engineering Materials*. Vol. Part 1. ČBZ, Southampton, pp. 125–130.
- Schneider, J., 1996. *Introduction to Safety and Reliability of Structures*. IABSE, GED, ETH, Zurich.
- Schuëller, G. I., 1998. Structural reliability — recent advances. (Freudenthal lecture). In: Shiraishi, N., Shinozuka, M., Y.K., W. (Eds.), ICoSSaR '97, the 7th International Conference on Structural Safety and Reliability. Vol. I. Balkema, Rotterdam, Kyoto, Japan, pp. 3–35.
- Schuëller, G. I., Bucher, C. G., Bourgund, U., Ouypornprasert, W., 1989. On efficient computational schemes to calculate structural failure probabilities. *Probabilistic Engineering Mechanics* 4 (1), 10–18.
- Schuëller, G. I., Bucher, C. G., J., P. H., 1990. Computational methods in stochastic structural dynamics. In: *EURODYN'90*. Germany.
- Schuëller, G. I., Stix, R., 1987. A critical appraisal of methods to determine failure probabilities. *Journal of Structural Safety* 4 (4), 293–309.
- Segal, I., 1938. Fiducial distribution of several parameters with applications to a normal system. *Proceedings of Cambridge Philosophical Society* 34, 41–47.
- Shinozuka, M., 1972. Probabilistic modeling of concrete structures. *ASCE Journal of Engineering Mechanics* 98 (EM6), 1433–1451.
- Smith, R. L., 1982. The asymptotic distribution of a series-parallel system with equal load-sharing. *The Annals of Probability* 10 (1), 137–171.
- Smith, R. L., Phoenix, S. L., 1981. Asymptotic distributions for the failure of fibrous materials under series-parallel structure and equal load-sharing. *Journal of Applied Mechanics* 48, 75–82.
- Spanos, P. D., Ghanem, R. G., 1989. Stochastic finite element expansion for random media. *Journal of Engineering Mechanics* 115 (5), 1035–1053.
- Tippett, L. H. C., 1925. On the extreme individuals and the range of samples. *Biometrika* 17, 364–387.
- Van Vliet, M. R. A., Van Mier, J. G. M., 1998. Experimental investigation of size effect in concrete under uniaxial tension. In: Mihashi, H., Rokugo, K. (Eds.), 3rd Int. Conf., FraMCoS-3 Fracture Mechanics of Concrete Structures. Aedificatio Publishers, Freiburg, Germany. D-79104, Gifu, Japan, pp. 1923–1936.

- Van Vliet, M. R. A., Van Mier, J. G. M., 2000. Size effect of concrete and sandstone. *Heron* 45 (2), 91–108.
- Vanmarcke, E. H., Shinozuka, M., Nakagiri, S., Schuëller, G. I., Grigoriu, M., 1986. Random fields and stochastic finite elements. *Structural Safety* (3), 143–166.
- Veselý, V., Keršner, Z., Stibor, M., Vořechovský, M., 2002. Efektivní hodnota lomové houževnatosti z krychle se zářezy (Effective fracture toughness on notched cubes). In: Kmeť, S., Křištofovič, V. (Eds.), VII International Scientific Conference, Section 9: Structural Mechanics. Košice (Medzev), Slovak Republic, pp. 300–304.
- Vořechovský, M., 2000a. K problematice výpočtu spolehlivosti u nelineárních úloh mechaniky kontinua (On reliability calculations of nonlinear continuum mechanics problems). Master's thesis, Institute of Structural Mechanics, Faculty of Civil Engineering, Brno University of Technology, Brno, Czech Republic.
- Vořechovský, M., 2000b. Probabilistic analysis of steel frames focused on design concept of Eurocodes. In: Workshop 3RE (on CD ROM). Institute of Structural mechanics, FCE, BUT Brno, Brno, Czech Republic.
- Vořechovský, M., 2001a. Modelování vlivu velikosti na pevnost v tahu za ohybu u betonových nosníků (Modeling size effect on modulus of rupture of concrete beams). In: 3rd Scientific international PhD workshop. Brno University of Technology, Faculty of Civil Engineering, Brno, Czech Republic, pp. 145–148.
- Vořechovský, M., 2001b. Možnosti využití lomové mechaniky v kombinaci se stochastickými metodami při modelování vlivu velikosti. In: Stibor, M. (Ed.), Problémy lomové mechaniky (Problems of Fracture Mechanics). Brno University of Technology, Academy of Sciences - Institute of physics of materials of the ASCR, pp. 93–97.
- Vořechovský, M., 2001c. Pravděpodobnostní posouzení ocelové konstrukce podle EC 1 (probabilistic assessment of steel structure according to the Eurocode 1). In: 3rd Scientific international PhD workshop. Brno University of Technology, Faculty of Civil Engineering, Brno, Czech Republic, pp. 141–144.
- Vořechovský, M., 2002a. FEM simulace předpjatých nosníků a jejich statistické zpracování. In: 4th Scientific PhD international workshop. Brno University of Technology, pp. CD-ROM.
- Vořechovský, M., 2002b. Lomově-mechanické parametry betonu jako vzájemně korelovaná náhodná pole. In: Stibor, M. (Ed.), Problémy lomové mechaniky II (Problems of Fracture Mechanics II). Brno University of Technology, Academy of Sciences - Institute of physics of materials of the ASCR, pp. 84–90.
- Vořechovský, M., 2002c. Možnosti a vylepšení simulační metody LHS. In: 4th Scientific PhD international workshop. Brno University of Technology, pp. CD-ROM.
- Vořechovský, M., 2002d. Nové úpravy simulační metody Latin Hypercube Sampling a možnosti využití. In: Stibor, M. (Ed.), Problémy modelování. Brno University of Technology, Faculty of Civil Engineering VŠB-TUO, Ostrava, Czech Republic, pp. 83–90.
- Vořechovský, M., 2003. Application of extreme value theory for size effect of concrete structures. In: 5th Scientific international PhD workshop. Brno University of Technology, Faculty of Civil Engineering, Brno, Czech Republic, CD-ROM proc.
- Vořechovský, M., 2004a. Comparison of stability and accuracy of numerical simulation methods for simulation of statistics of extremes. Probabilistic Engineering Mechanics, under preparation.
- Vořechovský, M., 2004b. Simulation of cross correlated random fields by series expansion methods. Structural safety, submitted to.
- Vořechovský, M., 2004c. Stabilita a konvergence numerických metod při simulaci extrémních hodnot rozdělení. In: PPK 2004 Pravděpodobnost porušování konstrukcí. Brno University of Technology, Faculty of Civil Engineering & Ústav aplikované mechaniky Brno, s.r.o. & Asociace strojních inženýrů & TERIS, a.s., pobočka Brno, Brno, Czech Republic.

- Vořechovský, M., 2004d. Statistical alternatives of combined size effect on nominal strength for structures failing at crack initiation. In: Stibor, M. (Ed.), *Problémy lomové mechaniky IV (Problems of Fracture Mechanics IV)*. Brno University of Technology, Academy of Sciences - Institute of physics of materials of the ASCR, pp. 99–106.
- Vořechovský, M., Bažant, Z. P., Novák, D., 2005. Procedure of statistical size effect prediction for crack initiation problems. In: *ICF XI 11th International Conference on Fracture*. Turin, Italy, in preparation.
- Vořechovský, M., Chudoba, R., 2004a. Stochastic modeling of multi-filament yarns II: Random properties over the length and size effect. *Journal of Engineering Mechanics*, submitted for possible publication.
- Vořechovský, M., Chudoba, R., 2004b. Stochastické modelování mnohovláknitých svazků pro vyztužení betonu. In: *PPK 2004 Pravděpodobnost porušování konstrukcí*. Brno University of Technology, Faculty of Civil Engineering & Ústav aplikované mechaniky Brno, s.r.o. & Asociace strojních inženýrů & TERIS, a.s., pobočka Brno, Brno, Czech Republic.
- Vořechovský, M., Chudoba, R., 2005. Statistical length scale for micromechanical model of multifilament yarns and size effect on strength. In: *ICoSSaR '05 the 9th International Conference on Structural Safety and Reliability*. Rome, Italy, in preparation.
- Vořechovský, M., Kala, Z., 2001. Nevyrovnanost pravděpodobnosti poruchy podle konceptu EC 1 (Unbalanced reliability using concept of Eurocode 1). In: *Reliability of Structures, 2nd International Conference*, Faculty of Civil Engineering, Ostrava University of Technology. Academy of Sciences – Institute of Theoretical and Applied Mechanics of the ASCR Prague, Ostrava, Czech Republic, pp. 141–144.
- Vořechovský, M., Novák, D., 2001. Probability of failure using reliability design concept of Eurocodes. In: *TRANSCOM '2001 – 4th European Conference of Young Research and Science Workers in Transport and Telecommunications*. EDIS Press, Žilina, Slovak Republic.
- Vořechovský, M., Novák, D., 2002. Correlated random variables in probabilistic simulation. In: Schießl, P., Gebbeken, N., Keuser, M., Zilch, K. (Eds.), *4th International Ph.D. Symposium in Civil Engineering*. Vol. 2. Millpress, Rotterdam, Munich, Germany, <http://www.phd.bv.tum.de>, pp. 410–417.
- Vořechovský, M., Novák, D., 2003a. Efficient random fields simulation for stochastic FEM analyses. In: Bathe, K. J. (Ed.), *2nd M.I.T. Conference on Computational Fluid and Solid Mechanics*. Elsevier Science Ltd., Oxford, UK, Cambridge, USA, pp. 2383–2386.
- Vořechovský, M., Novák, D., 2003b. Statistical correlation in stratified sampling. In: Der Kiureghian, A., Madanat, S., Pestana, J. M. (Eds.), *ICASP 9, International Conference on Applications of Statistics and Probability in Civil Engineering*. Millpress, Rotterdam, San Francisco, USA, pp. 119–124.
- Vořechovský, M., Novák, D., 2004. Modeling statistical size effect in concrete by the extreme value theory. In: Walraven, J., Blaauwendraad, J., Scarpas, T., Snijder, B. (Eds.), *5th International Ph.D. Symposium in Civil Engineering*. Vol. 2. A.A. Balkema Publishers, London, Delft, The Netherlands, pp. 867–875.
- Vořechovský, M., Novák, D., 2005. Simulation of random fields for stochastic finite element analyses. In: *ICoSSaR '05 the 9th International Conference on Structural Safety and Reliability*. Rome, Italy, in preparation.
- Vořechovský, M., Novák, D., Pukl, R., Červenka, V., 2000. Modelování vlivu velikosti nosníku na jeho únosnost prostředky nelineární lomové mechaniky — SBETA/ATENA. In: *Betonářské Dny 2000 (Concrete Days 2000)*. ČBZ, Pardubice, Czech Republic, pp. 375–379.
- Vořechovský, M., Novák, D., Rusina, R., 2002a. A new efficient technique for samples correlation in Latin Hypercube Sampling. In: Kmeť, S., Miron, P. (Eds.), *VII International Scientific Conference, Section 1: Applied Mathematics*. Technical University of Košice, Košice, Slovak Republic, pp. 102–108.
- Vořechovský, M., Pukl, R., Veselý, V., Červenka, V., Rusina, R., 2002b. Statistical nonlinear analysis of concrete structures. In: Dhir, R., Jones, M. R., Zheng, L. (Eds.), *International Congress on Challenges of Concrete Construction, Seminar 3*. Dundee, Scotland, pp. 217–226.

- Vořechovský, M., Červenka, V., 2002. ATENA 2D - Uživatelský manuál. Tech. rep., Červenka Consulting, Prague, Czech Republic.
- Vořechovský, M., Veselý, V., Pukl, R., 2002c. Statistical nonlinear analysis of concrete structures. In: Kmeť, S., Křištofovič, V. (Eds.), VII International Scientific Conference, Section 9: Structural Mechanics. Technical University of Košice, Košice (Medzev), Slovak Republic, pp. 308–313.
- Waarts, P. H., 2001. Structural reliability in Diana. Tech. Rep. No. 1: 14-15, Diana Newsletter.
- Wegman, E. J., 1990. Hyperdimensional data analysis using parallel coordinates. *Journal of the American Statistical Association* 85 (411), 664–675.
- Weibull, W., 1939a. The phenomenon of rupture in solids. *Royal Swedish Institute of Engineering Research (Ingenioersvetenskaps Akad. Handl.)*, Stockholm 153, 1–55.
- Weibull, W., 1939b. A statistical theory of the strength of materials. *Royal Swedish Institute of Engineering Research (Ingenioersvetenskaps Akad. Handl.)*, Stockholm 151.
- Weibull, W., 1949. A statistical representation of fatigue failures in solids. *Proc., Roy. Inst. Of Techn.* (27).
- Weibull, W., 1951. A statistical distribution function of wide applicability. *Journal of Applied Mechanics, ASME* 18, 292–297.
- Weibull, W., 1956. Basic aspects of fatigue. In: *Colloquium on Fatigue*. Springer-Verlag, Berlin, Stockholm, Sweden, pp. 289–298.
- Yamazaki, F., Shinozuka, M., 1990. Simulation of stochastic fields by statistical preconditioning. *Journal of Engineering Mechanics* 116 (2), 268–287.
- Yamazaki, F., Shinozuka, M., Dasgupta, G., 1988. Neumann expansion for stochastic finite element analysis. *Journal of Engineering Mechanics* 114 (8), 1335–1354.
- Zhang, J., Ellingwood, B., 1994. Orthogonal series expansion of random fields in reliability analysis. *Journal of Engineering Mechanics* 120 (12), 2660–2677.
- Zhang, J., Ellingwood, B., 1995. Error measure for reliability studies using reduced variable set. *Journal of Engineering Mechanics* 121 (8), 935–937.
- Zhou, S. J., Curtin, W. A., 1995. Failure of fiber composites: A lattice green function model. *Acta Metalurgica Material* 43 (8), 3093–3104.

Curriculum Vitae

Personal data

Miroslav Vořechovský
Institute of Structural Mechanics
Faculty of Civil Engineering
Brno University of Technology
Veveří 95
635 00 Brno
Czech Republic

Tel.: (+ 420) 5 41 14 73 70
E- Mail: Vorechovsky.M@fce.vutbr.cz
<http://www.fce.vutbr.cz/STM/vorechovsky.m>

Born on February 07, 1977 in Brno, Czech Republic
single, Czech nationality

Education

- 09/1995–06/2000 Master's degree "Ing." (equiv C-Eng or MSc) Brno University of Technology, Brno, Czech Republic Thesis: "On reliability calculations of problems of nonlinear continuum mechanics" (in Czech)
- 09/2000–now Ph.D. candidate, Brno University of Technology, Brno, Czech Republic. Preliminary Dissertation: "Stochastic Fracture Mechanics and Size Effect" (in English)

Awards, honors and scholarships

- 6/2000 Award of Dean, Brno University of Technology
- 6/2000 Diploma thesis Award, Brno University of Technology
- 6/2000 Award of Chancellor, Brno University of Technology
- 01/2001 Doctoral scholarship, Hlávka foundation, Prague
- 05/2001 Electricité de France, Conference Stipend of Excellence, FraMCoS, France, Paris, 2001
- 04/2002 Award of Josef Hlávka foundation, Prague
- 05/2002 Travel stipend for conference in Scotland, Dundee
- 9/2002–6/2003 *Preciosa* scholarship
- 09/2002 A good paper award at the 4th International Ph.D. Symposium in Civil Engineering, Munich, Germany
- 05/2003 M.I.T. Young Researcher Fellowship (award), 2nd M.I.T. Conference, Boston, USA
- 06/2003 *Cerra award*, ICASP 9 conference, San Francisco, USA
- 09/2003–03/2004 Fulbright Doctoral Fellowship, Northwestern University, Evanston, USA

Specialization, research interests

Nonlinear fracture mechanics with focus on stochastic aspects. Size effects, scaling in structures. Efficient methods of reliability engineering, mathematical statistics (random variables, random fields and processes, extreme value theories) connected with nonlinear fracture mechanics methods (behavior of quasibrittle materials). Stochastic optimization techniques, structural safety and reliability, stochastic computational mechanics, random fields, Genetic algorithms, Monte Carlo simulation techniques, modeling of concrete structures mechanics, size effect of structures. Programming and software development.

Memberships, activities

- since 09/2000 member of FRAMCoS society (**FR**acture **M**echanics of **C**oncrete **S**tructures)
- since 01/2004 member of ASCE (American Society of Civil Engineers)
- 1997–1999 Academic senate and Branch convocation - section Structures and transportation constructions
- 09/2000 Member of Local Organizing Committee: Workshop *3RE*, Institute of Structural mechanics TUB together with Institute of Structural Mechanics, Weimar
- 02/2001 Chairman of section, Member of Local Organizing Committee: Brno University of Technology, Faculty of Civil Engineering, 3rd Scientific PhD international workshop.

International cooperation

- Prof. Z. P. Bažant Northwestern University, Evanston, Illinois, USA: stochastic fracture mechanics of quasibrittle materials
- Dr. R. Chudoba, Technical University of Aachen (RWTH Aachen), Germany: stochastic fracture mechanics of textile reinforced concrete, computational mechanics
- Dr. G. Cusatis, Technical University in Milano, Italy: micromechanical models of concrete (lattice and microplane modeling)

Teaching experience

- 09/2000–06/2004 Institute of Structural Mechanics, Faculty of Civil Engineering, Brno University of Technology, Brno, Czech Republic:
Elasticity & Plasticity
Reliability of structures
Structural Analysis I

Participation in Research projects

- 1997–2004 Theory, reliability and mechanism of damage statically and dynamically stressed structures. Project of the Czech Ministry of Education CEZ: J22/98:261100007.
- 1997–2002 Material models of concrete for the assessment of severe accidents in nuclear industry. Project of Grant Agency of Czech republic GACR 103/97/K003.
- 2000–2002 Risk assessment of structures - the loss of load-bearing capacity and serviceability of thin-walled structures, Project of the Grant Agency of Czech republic GACR 103/00/0603
- 2002–2004 Nonlinear Fracture Mechanics of Concrete with Utilization of Stochastic Finite Elements and Random Fields. Project of the Grant Agency of Czech republic GACR 103/02/1030
- 2001–2003 SARA: Structural Analysis and Reliability Assessment, International project of Brno University of Technology (Czech Republic), BOKU Vienna (Austria), Cervenka Consulting Prague (Czech Republic), TU Vienna (Austria), and University Trento (Italy).
- 2004–now Model identification and optimization at material and structural levels. Project of the Grant Agency of Czech republic GACR 103/04/2092
- 01/2003–03/2003 Grant of German Science Foundation (DFG) in the framework of the Collaborative Research Center 532.
- 03/2004–04/2004 U.S. National Science Foundation under grant CMS-9713944 to Northwestern University NU (Prof. Z.P. Bažant)

Student research competitions

- 1997 session Applied Physics: Thermal dependence measuring of modulus of elasticity of special structural materials using dynamic methods. (Awarded by 1st prize)

- 1998 session Structural Mechanics: Price optimization of deteriorated RC structure in time. (Awarded by 1st price)
- 2000 in session Structural Mechanics: Application of reliability methods at monitoring of size effect on carrying capacity of concrete structures
- 2000 in session Structural Mechanics: Probabilistic nonlinear analysis of steel frames focused on reliability level according to Eurocodes. (Awarded by 1st price)

Professional stays, visiting positions

- 4/2001 PhD course Elastic and Inelastic Analysis of Heterogeneous Materials. Certificate of Attendance from Czech university in Prague, Faculty of Civil Engineering, Department of Structural Mechanics
- 07/2001–08/2001 summer school (two-week course) Advanced Studies in Structural Engineering and CAE, 9th European Summer Academy 2001. Certificate of Attendance from Bauhaus University Weimar, Germany, Civil & Structural Engineering. Passed final oral examination with the mark A (ECTS Grade) and therefore credited with 7 ECTS credits
- 08/2001–09/2001 Professional 6-week training IAESTE, Croatia, Zagreb. The Dalekovod Company. Focus on Antennae towers, transmission lines (steel structures); Foundations of structures (concrete structures and soil mechanics)
- 01/2003–03/2003 Visiting research position in Aachen, Germany. Invited lectures. Cooperation on development of methodology and software for consideration of stochastic aspects in failures of Textile Reinforced Concrete
- 04/2003–05/2003 Visiting research position in Aachen, Germany. Invited lectures. Cooperation on development of methodology and software for consideration of stochastic aspects in failures of Textile Reinforced Concrete
- 06/2003–07/2003 Visiting research position at Prof. Z.P. Bažant: Northwestern University, Evanston, IL, USA
- 08/2003 Fulbright preacademic training, University of Philadelphia, USA
- 8/2003–04/2004 Visiting research position (Fulbright scholarship) at Prof. Z.P. Bažant: Northwestern University, Evanston, IL, USA (extension supported by NSF grants to Prof. Z.P. Bažant)

Related experience, positions

- 2001–present Faculty of Civil Engineering, Brno University of Technology, Czech republic. Staff.
- 08/2004 JAPE projekt, sro. Structural design and computations. Consultant.
- 2001–now IT Technologies: Programming within the project SARA (reliability software FREET).

Languages Czech – native language, English and Slovak – speak fluently and read/write with high proficiency, Russian – basics of language

Computer skills

Operating systems MS Windows®, MS DOS®, Linux
 Languages C++, FORTRAN 77, Pascal, BASIC, HTML
 Applications MS Office®, Corel-DRAW, SBETA/ATENA, L^AT_EX, XEmacs, ANSYS, NEXIS

Interests Music, Sport

Brno, July 20, 2004

List of published papers

Invited seminars, lectures

- (1l) Vořechovský, M., Applied stochastic fracture mechanics and size effect, Lecture given at RWTH Aachen, Germany.
- (2l) Vořechovský, M., Chudoba, R. and Konrad, M., Determination of material characteristics of multi-filament yarns: Phenomena, Experiments, Models and their relations. Lecture given at RWTH Aachen, Germany.
- (3l) Vořechovský, M., Numerické stanovení materiálových charakteristik mnoho-vláknových svazků Lecture given at Brno University of Technology, Institute of Structural Mechanics, Czech Republic.
- (4l) Vořechovský, M., Material characteristics of composite structure: multi-filament yarns and textile reinforced concrete. Lecture given at Northwestern University, Evanston, USA.
- (5l) Vořechovský, M., 2004d. Statistical alternatives of combined size effect on nominal strength for structures failing at crack initiation. Lecture given at the Academy of Sciences - Institute of physics of materials of the ASCR, pp. 99–106.

Papers in Refereed Journals

- (1j) Vořechovský, M., 2004b. *Simulation of cross correlated random fields by series expansion methods*. Structural safety, submitted to.
- (2j) Bažant, Z. P., Vořechovský, M., Novák, D., 2004c. *Superimposition of deterministic-energetic and statistical size effects in quasibrittle failure at crack initiation*. Journal of Engineering Mechanics, ASCE, submitted for possible publication.
- (3j) Chudoba, R., Vořechovský, M., Konrad, M., 2004. *Stochastic modeling of multi-filament yarns I: Random properties within the cross section and size effect*. Journal of Engineering Mechanics, ASCE, submitted to.
- (4j) Vořechovský, M., Chudoba, R., 2004a. *Stochastic modeling of multi-filament yarns II: Random properties over the length and size effect*. Journal of Engineering Mechanics, ASCE, submitted for possible publication.
- (5j) Bažant, Z. P., Novák, D., Vořechovský, M. and Pang, S. D., 2004a. Stochastic crack band model for quasibrittle failure. Journal of Engineering Mechanics, in submission process.
- (6j) Novák, D., Vořechovský, M., 2004. Error assessment of random fields simulation for stochastic finite element method. Probabilistic Engineering Mechanics, in submission process.
- (7j) Vořechovský, M., 2004a. *Comparison of stability and accuracy of numerical simulation methods for simulation of statistics of extremes*. Probabilistic Engineering Mechanics, under preparation.

Papers at Refereed Foreign Conferences

- (1z) Novák, D., Vořechovský, M., Pukl, R. and Červenka, V., 2001. Statistical nonlinear analysis - size effect of concrete beams. In: de Borst, R. et al. (Eds.), 4th Int. Conference FraMCoS – Fracture Mechanics of Concrete and Concrete Structures. Swets & Zeitlinger, Lisse. Cachan, France, pp. 823–830.

- (2z) Kala, Z., Novák, D., Vořechovský, M., 2001. Probabilistic nonlinear analysis of steel frames focused on target reliability of Eurocodes. In: Corotis, R. et al. (Eds.), ICoSSaR '01– 8th International Conference on Structural Safety and Reliability. A.A.Balkema Publishers, Netherlands. Newport Beach, California, USA, p. 146.
- (3z) Vořechovský, M., Novák, D., 2001. Probability of failure using reliability design concept of Eurocodes. In: TRANSCOM '2001 – 4th European Conference of Young Research and Science Workers in Transport and Telecommunications. EDIS Press, Žilina, Slovak Republic.
- (4z) Veselý, V., Keršner, Z., Stibor, M., Vořechovský, M., 2002. Efektivní hodnota lomové houževnatosti z krychle se zářezy (Effective fracture toughness on notched cubes). In: Kmeť, S. and Křištofovič, V. (Eds.), VII International Scientific Conference, Section 9: Structural Mechanics. Košice (Medzev), Slovak Republic, pp. 300–304.
- (5z) Vořechovský, M., Veselý, V. and Pukl, R., 2002c. Statistical nonlinear analysis of concrete structures. In: Kmeť, S. and Křištofovič, V. (Eds.), VII International Scientific Conference, Section 9: Structural Mechanics. Technical University of Košice, Košice (Medzev), Slovak Republic, pp. 308–313.
- (6z) Vořechovský, M., Novák, D. and Rusina, R., 2002a. A new efficient technique for samples correlation in Latin Hypercube Sampling. In: Kmeť, S. and Miron, P. (Eds.), VII International Scientific Conference, Section 1: Applied Mathematics. Technical University of Košice, Košice, Slovak Republic, pp. 102–108.
- (7z) Novák, D., Pukl, R., Vořechovský, M., Rusina, R. and Červenka, V., 2002b. Feasible structural reliability assessment of computationally intensive problems - nonlinear FEM analysis. In: 1st International ASRANet Colloquium. Glasgow, Scotland.
- (8z) Vořechovský, M., Pukl, R., Veselý, V., Červenka V. and Rusina, R., 2002b. Statistical nonlinear analysis of concrete structures. In: Dhir, R., Jones, M. R., Zheng, L. (Eds.), International Congress on Challenges of Concrete Construction, Seminar 3. Dundee, Scotland, pp. 217–226.
- (9z) Vořechovský, M., Novák, D., 2002. Correlated random variables in probabilistic simulation. In: Schiebl, P. et al. (Eds.), 4th International Ph.D. Symposium in Civil Engineering. Vol. 2. Millpress, Rotterdam. Munich, Germany, pp. 410–417. Awarded paper.
- (10z) Vořechovský, M., Novák, D., 2003a. Efficient random fields simulation for stochastic FEM analyses. In: Bathe, K. (Ed.), 2nd M.I.T. Conference on Computational Fluid and Solid Mechanics. Elsevier Science Ltd., Oxford, UK. Cambridge, USA, pp. 2383–2386. Awarded paper.
- (11z) Novák, D., Vořechovský, M., Rusina, R., 2003b. Small-sample probabilistic assessment - FREET software. In: Der Kiureghian, A. et al. (Eds.), ICASP 9, International Conference on Applications of Statistics and Probability in Civil Engineering. Millpress, Rotterdam, San Francisco, USA, pp. 91–96.
- (12z) Vořechovský, M. and Novák, D., 2003b. Statistical correlation in stratified sampling. In: Der Kiureghian, A. et al. (Eds.), ICASP 9, International Conference on Applications of Statistics and Probability in Civil Engineering. Millpress, Rotterdam. San Francisco, USA, pp. 119–124.
- (13z) Novák, D., Bažant, Z. and Vořechovský, M., 2003a. Computational modeling of statistical size effect in quasibrittle structures. In: Der Kiureghian, A. et al. (Eds.), ICASP 9, International Conference on Applications of Statistics and Probability in Civil Engineering. Millpress, Rotterdam. San Francisco, USA, pp. 621–628.
- (14z) Bažant, Z. P., Pang, S. D., Vořechovský, M., Novák, D. and Pukl, R., 2004b. Statistical size effect in quasibrittle materials: Computation and extreme value theory. In: Li, V. C. et al. (Eds.), 5th Int. Conference FraMCoS – Fracture Mechanics of Concrete and Concrete Structures. Vol. 1. Ia-FraMCoS. Vail, Colorado, USA, pp. 189–196.
- (15z) Vořechovský, M. and Novák, D., 2004. Modeling statistical size effect in concrete by the extreme value theory. In: Walraven, J. et al. (Eds.), 5th International Ph.D. Symposium in Civil Engineering. Vol. 2. A.A. Balkema Publishers, London. Delft, The Netherlands, pp. 867–875.
- (16z) Vořechovský, M., Bažant, Z. P. and Novák, D., 2005. Procedure of statistical size effect prediction for crack initiation problems. In: ICF XI 11th International Conference on Fracture. Turin, Italy, in preparation.

- (17z) Vořechovský, M. and Chudoba, R., 2005. Statistical length scale for micromechanical model of multifilament yarns and size effect on strength. In: ICoSSaR '05 the 9th International Conference on Structural Safety and Reliability. Rome, Italy, in preparation.
- (18z) Novák, D., Pukl, R., Červenka, V., Vořechovský, M., Rusina, R. and Lehký, D., 2005. Stochastic nonlinear fracture mechanics finite element analysis of concrete structures. In: ICoSSaR '05 the 9th International Conference on Structural Safety and Reliability. Rome, Italy, in preparation.
- (19z) Vořechovský, M. and Novák, D., 2005. Simulation of random fields for stochastic finite element analyses. In: ICoSSaR '05 the 9th International Conference on Structural Safety and Reliability. Rome, Italy, in preparation.
- (20z) Bažant, Z. P., Vořechovský, M. and Novák, D., 2005. Role of deterministic and statistical length scales in size effect for quasibrittle failure at crack initiation. In: ICoSSaR '05 the 9th International Conference on Structural Safety and Reliability. Rome, Italy, in preparation.

Papers at Refereed Domestic Conferences

- (1c) Vořechovský, M., 2000b. Probabilistic analysis of steel frames focused on design concept of Eurocodes. In: Workshop 3RE (on CD ROM). Institute of Structural mechanics, FCE, BUT Brno, Brno, Czech Republic.
- (2c) Vořechovský, M., Novák, D., Pukl, R., Červenka, V., 2000. Modelování vlivu velikosti nosníku na jeho únosnost prostředky nelineární lomové mechaniky — SBETA/ATENA. In: Betonářské Dny 2000 (Concrete Days 2000). ČBZ, Pardubice, Czech Republic, pp. 375–379.
- (3c) Vořechovský, M., 2001a. Modelování vlivu velikosti na pevnost v tahu za ohybu u betonových nosníků (Modeling size effect on modulus of rupture of concrete beams). In: 3rd Scientific international PhD workshop. Brno University of Technology, Faculty of Civil Engineering, Brno, Czech Republic, pp. 145–148.
- (4c) Vořechovský, M., 2001c. Pravděpodobnostní posouzení ocelové konstrukce podle EC 1 (Probabilistic assessment of steel structure according to the Eurocode 1). In: 3rd Scientific international PhD workshop. Brno University of Technology, Faculty of Civil Engineering, Brno, Czech Republic, pp. 141–144.
- (5c) Vořechovský, M., Kala, Z., 2001. Nevyrovnanost pravděpodobnosti poruchy podle konceptu EC 1 (Unbalanced reliability using concept of Eurocode 1). In: Reliability of Structures, 2nd International Conference, Faculty of Civil Engineering, Ostrava University of Technology. Academy of Sciences – Institute of Theoretical and Applied Mechanics of the ASCR Prague, Ostrava, Czech Republic, pp. 141–144.
- (6c) Vořechovský, M., 2001b. Možnosti využití lomové mechaniky v kombinaci se stochastickými metodami při modelování vlivu velikosti. In: Stibor, M. (Ed.), Problémy lomové mechaniky (Problems of Fracture Mechanics). Brno University of Technology, Academy of Sciences - Institute of physics of materials of the ASCR, pp. 93–97.
- (7c) Pukl, R., Novák, D., Vořechovský, M., Rusina, R. and Červenka, V., 2001. Stochastická nelineární analýza betonových konstrukcí. In: Betonářské Dny 2001 (Concrete Days 2001). ČBZ, Pardubice, Czech Republic, pp. 136–141.
- (8c) Vořechovský, M., 2002d. Nové úpravy simulační metody Latin Hypercube Sampling a možnosti využití. In: Stibor, M. (Ed.), Problémy modelování. Brno University of Technology, Faculty of Civil Engineering VŠB-TUO, Ostrava, Czech Republic, pp. 83–90.
- (9c) Vořechovský, M., 2002c. Možnosti a vylepšení simulační metody LHS. In: 4rd Scientific PhD international workshop. Brno University of Technology, pp. CD-ROM.
- (10c) Vořechovský, M., 2002a. FEM simulace předpjatých nosníků a jejich statistické zpracování. In: 4rd Scientific PhD international workshop. Brno University of Technology, CD-ROM.
- (11c) Lehký, D. and Vořechovský, M., 2002. Generování náhodných polí: Teorie a aplikace. In: 4rd Scientific PhD international workshop. Brno University of Technology, CD-ROM.

- (12c) Novák, D., Rusina, R. and Vořechovský, M., 2002c. Freet - software pro pravděpodobnostní posudky výpočtově náročných problémů mechaniky kontinua. In: Reliability of Structures, 3rd International Conference, Faculty of Civil Engineering, Ostrava University of Technology. Academy of Sciences – Institute of Theoretical and Applied Mechanics of the ASCR Prague. Ostrava, Czech Republic, pp. 71–74.
- (13c) Vořechovský, M., 2002b. Lomově-mechanické parametry betonu jako vzájemně korelovaná náhodná pole. In: Stibor, M. (Ed.), Problémy lomové mechaniky II (Problems of Fracture Mechanics II). Brno University of Technology, Academy of Sciences - Institute of physics of materials of the ASCR, pp. 84–90.
- (14c) Novák, D., Pukl, R., Rusina, R., M. Vořechovský, M. and Červenka, V., 2002a. Statistical, sensitivity and reliability assessment of computationally intensive problems: Nonlinear fracture mechanics analysis. In: Menčík, J. (Ed.), Reliability and Diagnostic of Transport Structures and Means 2002, First International Conference. University of Pardubice, Pardubice, Czech Republic, pp. 252–260.
- (15c) Vořechovský, M., 2003. Application of extreme value theory for size effect of concrete structures. In: 5th Scientific international PhD workshop. Brno University of Technology, Faculty of Civil Engineering, Brno, Czech Republic, CD-ROM proc.
- (16c) Lehký, D., Matesová, D., Novák, D., Teplý, B., Veselý, V. and Vořechovský, M., 2003. Stochastic analysis, fracture mechanics and pre-stressed concrete members. In: Konvalinka, P., Máca, J. (Eds.), CTU Reports 1 Vol 7, 2003: Contribution to Computational and Experimental Investigation of Engineering Materials and Structures. Dedicated to Zdeněk Bittnar on the occasion of his 60th birthday. Czech Technical University in Prague, Faculty of Civil Engineering, Prague, Czech Republic, pp. 111–120.
- (17c) Perla, J. and Vořechovský, M., 2003. Využití programu FEAT při rekonstrukcích. In: Statika 2003. Hotel Myslivna, Brno, Czech Republic.
- (18c) Vořechovský, M., 2004d. Statistical alternatives of combined size effect on nominal strength for structures failing at crack initiation. In: Stibor, M. (Ed.), Problémy lomové mechaniky IV (Problems of Fracture Mechanics IV). Brno University of Technology, Academy of Sciences - Institute of physics of materials of the ASCR, pp. 99–106.
- (19c) Vořechovský, M. and Chudoba, R., 2004b. Stochastické modelování mnohovláknitých svazků pro vyztužení betonu. In: PPK 2004 Pravděpodobnost porušování konstrukcí. Brno University of Technology, Faculty of Civil Engineering & Ústav aplikované mechaniky Brno, s.r.o. & Asociace strojních inženýrů & TERIS, a.s., pobočka Brno, Brno, Czech Republic.
- (20c) Vořechovský, M., 2004c. Stabilita a konvergence numerických metod při simulaci extrémních hodnot rozdělení. In: PPK 2004 Pravděpodobnost porušování konstrukcí. Brno University of Technology, Faculty of Civil Engineering & Ústav aplikované mechaniky Brno, s.r.o. & Asociace strojních inženýrů & TERIS, a.s., pobočka Brno, Brno, Czech Republic.

Technical report, software manuals

- (1r) Vořechovský, M. and Červenka, V., 2002. ATENA 2D - Uživatelský manuál. Červenka Consulting, Prague, Czech Republic.
- (2r) Novák, D., Vořechovský, M., Rusina, R., Lehký, D., Teplý, B. and Keršner, Z., 2002d. FREET – Feasible REliability Engineering Efficient Tool. Institute of Engineering Mechanics, Faculty of Civil Engineering, Brno University of Technology / ČervenkaConsulting, Praha, Czech Republic, program documentation (Czech Translation).
- (3r) Novák, D., Teplý, B., Keršner, Z. and Vořechovský, M., 2004. FREET. Tech. rep., Institute of Engineering Mechanics, Faculty of Civil Engineering, Brno University of Technology / ČervenkaConsulting, Praha, Czech Republic, program documentation – Part 1 – Theory.

Diploma thesis

- (1t) Vořechovský, M., 2000a. K problematice výpočtu spolehlivosti u nelineárních úloh mechaniky kontinua (On reliability calculations of nonlinear continuum mechanics problems). Master's thesis, Institute of Structural Mechanics, Faculty of Civil Engineering, Brno University of Technology, Brno, Czech Republic.